Charles University in Prague
Faculty of Science

Ph.D. study program: Inorganic Chemistry

RNDr. Jiří Tauchman

Phosphinoferrocene Conjugates of Selective Amino Acids

Fosfinoferrocenové konjugáty vybraných aminokyselin

Ph.D. Thesis

Supervisor: Prof. RNDr. Petr Štěpnička, Ph.D.

Prague, 2012

Declaration

I declare that this Thesis is my own original work except as cited in the references. The Thesis has not been submitted, or is being concurrently submitted, for any other degree.

Prague, 1.6.2012

Jiří Tauchman

The work presented in this dissertation Thesis was financially supported by the Grant Agency of Charles University in Prague (grant no. 58009), by the Ministry of Education, Youth and Sport of the Czech Republic (project no. MSM0021620857) and also by the bilateral Swiss-Czech Scientific Exchange Program (Sciex) NMS-CH (project no. 10.133).

Abstract

A series of chiral phosphinoferrocene amides was prepared by the condensation either of 1'-(diphenylphosphino)ferrocene-1-carboxylic acid (Hdpf) or its planar-chiral 1,2-isomers and amino acid methyl esters in the presence of peptide coupling agents. The resulting phosphinoamides were tested as ligands in Cu-catalyzed asymmetric conjugate additions of diethylzinc to chalcones and in Pd-mediated asymmetric allylic substitution reactions of 1,3-diphenylallyl acetate with the respective nucleophile (alkylation, amination and etherification). The catalytic tests were focused on an optimization of the reaction parameters (solvent, temperature, base, metal/ligand ratio) and on survey of various substrates. Compounds based on Hdpf proved to be better ligands in both catalytic reactions than their planar chiral analogues. In order to rationalize the influence of the ligand structure on the reaction course and also to interpret the catalytic results, several model complexes were prepared and structurally characterized.

Other three series of non-chiral complexes were prepared from the corresponding (η^6-arene)ruthenium(II) precursor and Hdpf-glycine conjugates; the neutral complexes of the type [(arene)$RuCl_2$(Hdpf-Gly(R)-κ*P*)] (arene = benzene, *p*-cymene, hexamethyl-benzene; R = OMe, NH_2, OH) as well as two series of mono- and dicationic complexes resulting from the substitution of the Ru-bound chloro ligands by acetonitrile, which were isolated as $[PF_6]^-$ salts. These complexes proved to be highly active pre-catalyst for oxidation of secondary alcohols to the corresponding ketones with *t*-BuOOH in water.

Finally, a new type of ferrocene-based amino acid conjugate, 2-[(methoxycarbonyl)methyl]-2-aza[3]ferrocenophane, was designed and obtained by the condensation reaction of 1,1'-bis(hydroxymethyl)ferrocene and glycine methyl ester. The aza[3]ferrocenophane was subsequently reacted with 2,4,6-trinitrophenol to afford the corresponding picrate.

All newly prepared compounds were fully characterized by multinuclear NMR, MS and IR spectroscopy, elemental analysis and the crystal structures of several representatives were determined by X-ray crystallography. In addition, electrochemical properties of the mentioned ruthenium complexes and the aza[3]ferrocenophane were studied by cyclic voltammetry.

Keywords: Amino Acids, Phosphinoferrocene ligands, Amides, Asymmetric catalysis, Conjugate addition, Allylic substitution, oxidation, Copper, Palladium, Ruthenium.

Abstrakt

Série chirálních amidů byla připravena reakcí 1'-(difenylfosfino)ferrocene-1-karboxylové kyseliny nebo jejích planárně chirálních 1,2-izomerů s methylestery aminokyselin v přítomnosti činidel používaných v peptidové syntéze. Získané fosfinoamidy byly testovány jako ligandy v mědí katalyzované enantioselektivní konjugované adici diethylzinku na chalkony a v enantioselektivních allylových substitučních reakcí (alkylace, aminace a etherifikace) 1,3-difenylallyl acetátu s odpovídajícími nukleofily. Katalytické testy zahrnovaly optimalizaci reakčních parametrů jako je např. volba rozpouštědla, reakční teploty, báze a poměr ligandu a kovu. Donory odvozené od Hdpf prokázaly lepší katalytické vlastnosti v obou reakcích než jejich planárně chirální analoga. Rovněž bylo připraveno a strukturně charakterizováno několik modelových komplexů s těmito ligandy za účelem vysvětlení katalytických výsledků a objasnění vlivu struktury ligandu.

Reakcemi (η^6-aren)ruthenatých prekurzorů a příslušného Hdpf-glycinového konjugátu byly dále připraveny tři série achirálních komplexů: neutrální komplexy typu [(aren)$RuCl_2$(Hdpf-Gly(R)-κ*P*)] (aren = benzen, *p*-cymen, hexamethylbenzen; R = OMe, NH_2, OH) a také příslušné mono- a dikationtové komplexy připravené substitucí chloro ligadů acetonitrilem. Tyto nabité částice byly izolovány jako $[PF_6]^-$ soli. Získané ruthenaté komplexy se prokázaly být účinnými prekatalyzátory pro oxidace sekundárních alkoholů pomocí *t*-BuOOH na příslušné ketony prováděné ve vodě.

Kondenzací 1,1'-bis(hydroxymethyl)ferrocenu a glycin methylesteru byl dále získán nový typ ferrocenového konjugátu s aminokyselinou, 2-[(methoxykarbonyl)-methyl]-2-aza[3]ferrocenofan. Následná reakce tohoto aza[3]ferrocenofanu s 2,4,6-trinitrofenolem poskytla příslušný pikrát.

Všechny nově připravené sloučeniny byly charakterizovány vícejadernou NMR, MS a IR spektroskopií a elementární analýzou. Pro několik zástupců byla také pomocí rentgenostrukturní analýzy zjištěna krystalová struktura v pevné fázi. Elektrochemické vlastnosti ruthenatých komplexů a aza[3]ferrocenofanu byly navíc studovány cyklickou voltametrií.

Klíčová slova: Aminokyseliny, fosfinoferrocenové ligandy, amidy, enantioselektivní katalýza, konjugovaná adice, allylová substituce, oxidace, měď, palladium, ruthenium.

Acknowledgement

Shortly after beginning of my chemistry studies at the Faculty of Science, Charles University in Prague, prof. RNDr. Petr Štěpnička, Ph.D. has offered me to join his research group. With a pleasure, I have accepted this invitation. Although more than eight years passed since that time, I have never regretted my decision. I would like to express my sincere and immense thanks to Petr. I am grateful for his guidance and for all scientific and research experiences, which I could learn during our collaboration.

I am also obliged to other members of tutor's group for an inspiring and friendly atmosphere, especially my classmate RNDr. Jiří Schulz. Furthermore, I would like to thank Dr. Ivana Císařová for X-ray measurements. Special thanks are also to Professor Georg Süss-Fink and his colleagues in Neuchâtel where I spent fruitful six months.

Last but not at least, I want to thank my friends, family and my girlfriend who supported me greatly during the work and writing of this Thesis.

Table of Contens

1 Abbreviations

Ac	acetyl
Boc	*tert*-(butyloxy)carbonyl
BOP	benzotriazol-1-yloxy-tris(dimethylamino)phosphonium hexafluorophosphate
BSA	*N*,*O*-bis(trimethylsilyl)acetamide
CIC	*N*-cyclohexyl-*N'*-isopropylcarbodiimide
cod	η^2:η^2-cycloocta-1,5-diene
Cys	cysteine
DCC	*N,N'*-dicyclohexylcarbodiimide
DIC	*N,N'*-diisopropylcarbodiimide
EDC	*N*-ethyl-*N'*-[(3-dimethylamino)propyl]carbodiimide
ee	enantiomeric excess
EEDQ	*N*-ethoxycarbonyl-2-ethoxy-1,2-dihydroquinoline
fc	ferrocene-1,1'-diyl
Fmoc	(9-fluorenylmethyloxy)carbonyl
Gly	glycine
Hdpf	1´-(diphenylphosphino)-1-ferrocenecarboxylic acid
HOAt	1-hydroxy-7-azabenzotriazole
HOBt	1-hydroxybenzotriazole
HODbht	3,4-dihydro-3-hydroxy-4-oxo-1,2,3-benzotriazine
i-Pr	isopropyl
PEG	poly(ethylene glycol)
PG	protecting group
Ph	phenyl
SAMP	(*S*)-1-amino-2-methoxymetylpyrrolidine
TBTU	*O*-(benzotriazol-1-yl)-1,1,3,3,-tetramethyluronium tetrafluoroborate
t-Bu	*tert*-butyl
TOF	turnover frequency: mol product/(mol catalyst × reaction time)
TON	turnover number: mol product/mol catalyst
UBI	peptide ubiquicidin
Z	(benzyloxy)carbonyl

2 Introduction

2.1 Catalysis

Catalysis, one of the most attractive chemical phenomenon, has become an indispensable tool in chemical laboratories and industry. Life would not even exist without catalysis, since each cell is a complex catalytic factory using very efficient biocatalytic reactions. Catalysis has been defined by Berzelius[1] as a process by which rates of chemical reactions are altered upon the addition of a substance (the catalyst) that is not itself changed during the course of chemical reaction. Catalysts alter activation energy needed to perform a certain chemical reaction and thus affect the reaction rate of a particular chemical process. In turn, this allows to favor one of several possible chemical transformations and to improve the overall selectivity or to perform the reaction under more convenient reaction conditions (typically at lower temperatures). As the result, catalysis helps in making chemical reactions more efficient, less environmentally demanding and more economic and thus plays an important role in developing sustainable approaches to social, economic, and industrial development. From an academical viewpoint, investigations into catalytic processes represent a challenging research area with a high practical relevance.

Molecular chirality is an important characteristic in the pharmaceutical, agrochemical, flavor and fragrance industry and research because it affects biological activities and functions of compounds. Typical example represents limonene (**1** in Scheme 1); the more common (*R*)-strereoisomer possesses a strong smell of orange, while (*S*)-strereoisomer has a piney, turpentine-like odor.[2] It has been also shown for many

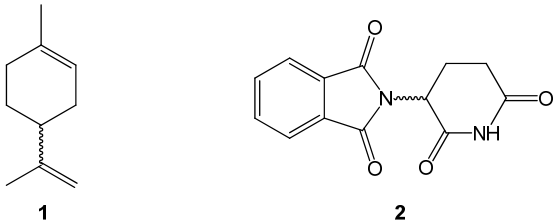

1 2

Scheme 1 (*RS*)-limonene (**1**) and (*RS*)-thalidomide (**2**).

pharmaceuticals that only one enantiomer exerts the desired activity, whereas the other is either totally inactive or even toxic. The Thalidomide (**2** in Scheme 1) tragedy is well known and led to much stricter testing being introduced for drug and pesticide licensing.[3]

There are several possible methods for obtaining enantiomerically pure materials. However, catalytic asymmetric synthesis has played a significant role because of its atom efficiency and wide applications.

The importance and practical relevance of catalysis as one of the most perspective areas of contemporary chemical research is reflected by the fact that several recent Nobel Prizes in chemistry have been awarded in this area. In 2001, the Royal Swedish Academy of Science has decided to award W. S. Knowles[4a] and R. Noyori[4b] for their work on asymmetric catalyzed hydrogenation reactions and K. B. Sharpless[4c] for his work on asymmetric oxidation reactions. The Nobel Prize for chemistry in 2005 was given to R. Grubbs,[5a] R. Schrock[5b] and Y. Chauvin.[5c] These laureates have been rewarded for their contribution to the development of metathesis reactions in which carbon-carbon double bonds are broken and formed catalytically. More recently, in 2010 three researches, R. F. Heck, E. Negishi, A. Suzuki, shared Nobel Prize in chemistry for the development of palladium-catalyzed cross-coupling reactions, which found manifold use in organic synthesis both at laboratory and industrial scales.[6]

During the second half of the 20th century, transition metals have come to play an important role in organic chemistry and this has led to the discovery of a large number of transition metal-catalyzed reactions for creating organic molecules. Transition metals possess a unique ability to activate various organic compounds and, through this activation, they can catalyze the formation or breaking of chemical bonds. Ligands around the central metal atom can profoundly change catalytic performance of a metal ion through their steric and electronic or, usually, a combination of both effects. These effects are common for all classes of ligands regardless of their structure. Aryl- and alkyl-substituted tertiary phosphines are among the most common ligands studied and practically used in catalysis. The possibility of almost limitless variation of the substituents at the phosphorus atom has made phosphines extremely popular ligands in organometallic and coordination chemistry and their complexes accordingly found extensive applications in catalysis. Tuning the ligand properties by means of the attached substituents was many times used to improve the efficiency and selectivity of transition metal-mediated reactions.

2.2 Phosphine-Functionalized Amino Acid Amides

Natural and unnatural amino acids are among the most readily available sources of enantiomerically pure chiral compounds (chiral pool) and thus represent an important class of building blocks for organic and organometallic synthesis. The term "functionalized amino acid amide" used as a title for this sub-chapter stands for amides derived from amino acids having additional phosphine functional group(s), which facilitate(s) coordination of these compounds to (soft) metal centers and change their donor properties.

A simultaneous presence of hard and soft donor atoms according to the R. G. Pearson's Hard and Soft Acids and Bases theory[7] and chemical variability of the amide group enables amino acid based-phosphinoamide ligands to coordinate to almost any metal ion and to bind in diverse coordination modes. Phosphinoamides are typical representatives of the so-called hybrid ligands,[8] which in some cases are able to coordinate in hemilable fashion.[9] Soft metals usually used in catalysis are bound firmly to ligand's phosphine group while the other (hard donor group) remains free or coordinates only weakly. Hemilable ligands can thus provide open coordination sites at the metal during reactions that are masked in the resting state, which results in relative stabilization of reactive intermediates. This has a particular impact on the catalytic performance of phosphinoamide ligands since the metal–oxygen (nitrogen) dative bond can be cleaved by the substrate and formed again after the product of the catalytic process is released from the coordination sphere of the metal ion. Furthermore, the presence of polar amino acid moiety makes phosphino-amino acid amides and their complexes more soluble in polar solutions and can even allow for performing catalytic reaction in water.

Several techniques have been developed to prepare amidophosphines. These methods are usually based on the construction of amide bond(s) from suitable (sometimes protected) precursor(s). Synthetic protocols for amidation reactions often rely on the methods developed for peptide synthesis.[10] Thus, the major synthetic approach for the preparation of amino acid-based phosphino-carboxamides is represented by conjugation of protected amino acids or peptides with phosphinocarboxylic acids in the presence of carbodimides (DCC, EDC, CIC, DIC) (Scheme 2). Additives such as *N*-hydroxy heterocyclic derivatives (HOBt, HOAt, HODhbt) increase the efficiency of these carbodiimide-mediated reactions and suppress the formation of undesired, relatively stable intermediate *N*-acylurea **4**. The beneficial effect of *N*-hydroxy derivatives is attributed to

its ability to protonate *O*-acylisourea **3** as the primary product. The active esters involved in these amidation reactions can be generated either *in situ* or some of them (typically substituted phenyl esters) can be purified, isolated and stored before the amidation reaction and then subsequently reacted with an amine to afford the desired amide. The use of alternative coupling agents such as phosphonium (BOP), uronium reagent (HBTU) or EEDQ (Scheme 3) are also reported in literature.[10]

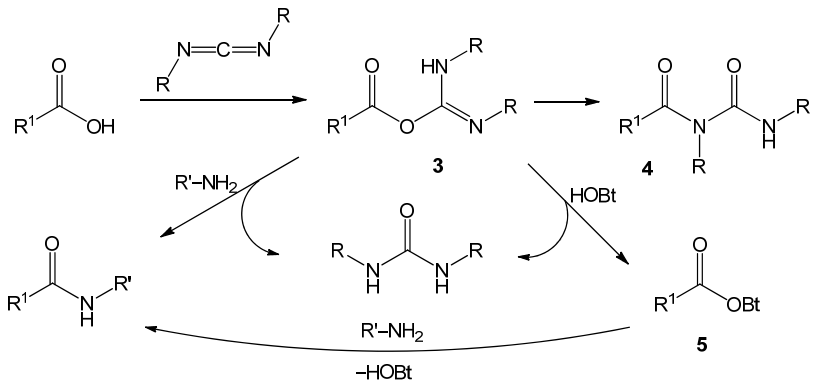

Scheme 2 Carbodiimide-mediated amide coupling.

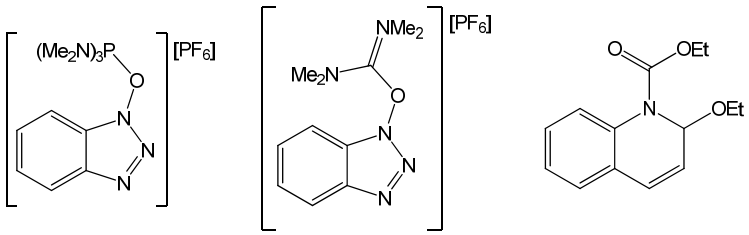

Scheme 3 Other commonly used coupling agents.

Other notable synthetic route to amino acid phosphinoamides involves palladium-catalyzed cross-coupling reactions of aryl halides with phosphines, typically with diphenylphosphine ($HPPh_2$)[11] (**A**, Scheme 4), and with (trimethylstannyl)- or (trimethylsilyl)diphenylphosphine ($RPPh_2$, where R = $SnMe_3$ or $SiMe_3$).[12] In addition, there were reported nucleophilic phosphination reactions of secondary phosphines with halogen-modified protected amino acids proceeding without any transition metal catalyst.[13] In another synthetic approach functionalized α-phosphino amino acids are obtained by one-pot three-component reaction of primary amines, diphenylphosphine and glyoxylic acid[14] (**B**, Scheme 4). Yet another noteworthy synthetic method is based on Mannich reaction of

amino acid ester hydrochlorides, formaldehyde and secondary phosphine to give *N*,*N*-bis(phosphinomethyl) amino acid derivatives[15] (**C**, Scheme 4).

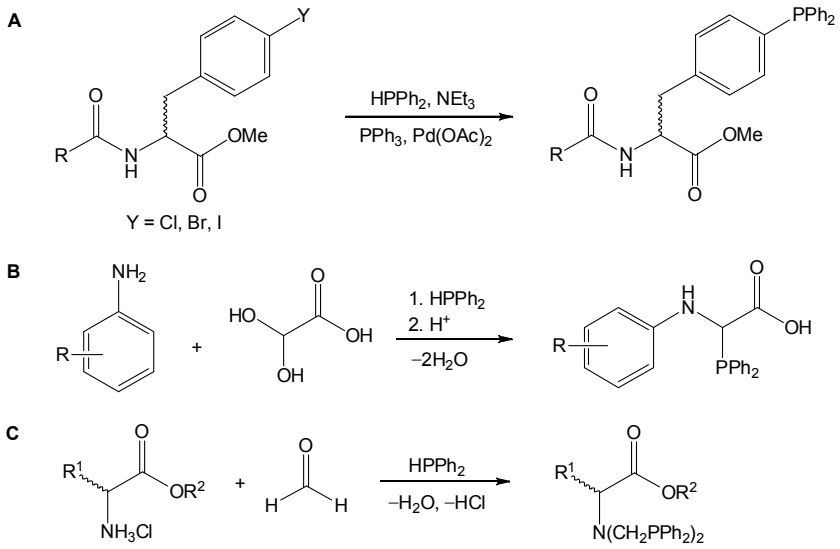

Scheme 4 General synthetic routes towards amino acid phosphinoamides.

3 Catalytic Applications of Amino Acid Phosphinocarboxamides

Phosphinoamides derived from amino acids have found numerous practical applications. These donors have proven extremely versatile ligands for coordination chemistry and for various transition metal-catalyzed transformations, especially for asymmetric ones.[16] Besides, a number of phosphinoamides have been designed and synthesized for a potential use as multifunctional chelator agents for ^{99m}Tc- and ^{188}Re-based radiopharmaceuticals.[16]

3.1 Rhodium-Catalyzed Asymmetric Hydrogenation

The first homogeneous transition metal-catalyzed asymmetric reaction, Rh-catalyzed asymmetric hydrogenation, was reported by Noyori in 1966.[17] At almost the same time, Knowles[18] and Horner[19] independently discovered that prochiral olefins are asymmetrically hydrogenated in the presence of Wilkinson's catalyst modified by a chiral monophosphine. Nowadays, asymmetric hydrogenations utilizing molecular hydrogen to reduce prochiral olefins, ketones and imines have become one of the most efficient

methods for the preparation of chiral compounds both in research laboratories and industrial plants.[20]

Several phosphino-carboxamide derivatives were developed from proline, which was found to be a good entry to such compounds. Already in 1976, the first proline based-amido diphosphines **8** were synthesized by Achiwa from L-hydroxyproline (Scheme 5).[21] Hydrogenation experiments with substituted cinnamic acids as benchmark substrates revealed remarkable effect of triethylamine additive on the selectivity of the catalyzed reaction, particularly in the case of diphosphine **6**. Promising catalytic results led to the preparation of further *N*-acyl derivatives.[22] The family of proline amidophosphines was further extended toward ligands bearing either different phosphine groups[23] or acyl moieties derived from *N*-protected amino acids.[24] In addition, rhodium complexes of these amidophosphines have been studied in solution with NMR techniques for better understanding of their coordination behavior and factors influencing the course of the catalyzed reactions.[25]

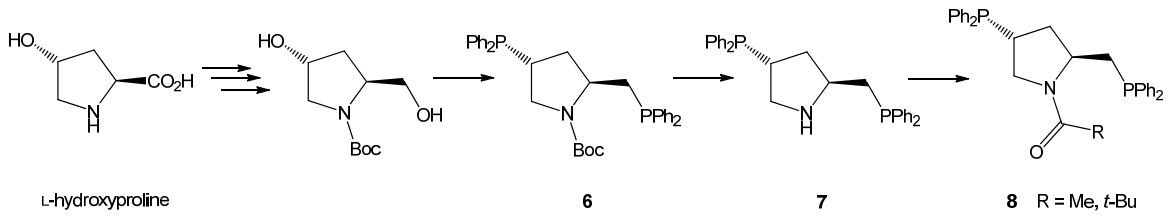

Scheme 5 Synthetic route to **8** starting from L-hydroxyproline.

Achiwa *et al*. have also synthesized polymer-supported chiral ligand **7** by the reaction of **7** with 4-vinylbenzoyl chloride and co-polymerization of the resulting *N*-(4-vinylbenzoyl)-**8** with 2-hydroxyethyl methacrylate in the presence azobis(isobutyronitrile).[26] Later on, ligand **8** was immobilized over several water-soluble polymers and applied to asymmetric Rh-catalyzed hydrogenations in aqueous reaction media.[27]

Carbodiimide protocol for the synthesis of phosphine-carboxamides was firstly used by Joó and Trócsányi in 1982.[28] Conjugation of (diphenylphosphino)acetic acid and L-amino acid esters in the presence DCC afforded chiral ligands **9**–**11** (Scheme 6), that were tested in Rh-catalyzed hydrogenation of acetophenone and styrene. The authors have observed improvements in the reaction rate and selectivity upon adding water to the catalytic system. Condensation reaction of 3-(diphenylphosphino)benzoic acid and an

alanine-valine dipeptide resulted in novel phosphine ligands **12** (Scheme 6). These amides were found to be suitable for the formation of chelating donors via self-assembly by means of hydrogen bonding interactions between the peptidyl side chains.[29]

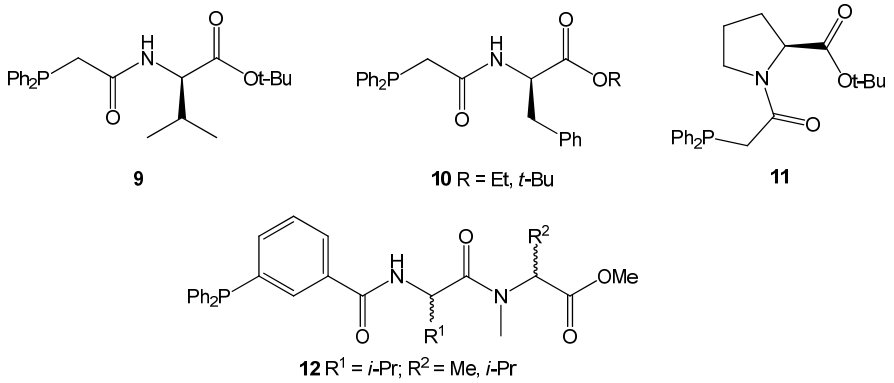

9 **10** R = Et, *t*-Bu **11**

12 R^1 = *i*-Pr; R^2 = Me, *i*-Pr

Scheme 6 Selected amino acid-based phosphine ligands.

Gilbertson *et al*. have prepared phosphinylated amino acid building blocks derived from L-alanine[30] (**13**) and L-proline[31] (**14**, Scheme 7) aiming at incorporation of these units into peptides. After desulfuration with Raney nickel, the resulting peptide-based diphosphines efficiently coordinated Rh(I) ions. Phenylalanine amidophosphines **15** (Scheme 7) were synthesized from L-tyrosine via the palladium-catalyzed phosphinylation of the respective aryl triflates. This phosphinylation method could be also used to modify peptides possessing hydroxyaryl groups.[32] The resulting peptides differing by the number and type of amino acids bearing various phosphine groups have been examined in transition metal-catalyzed hydrogenation reactions.[33]

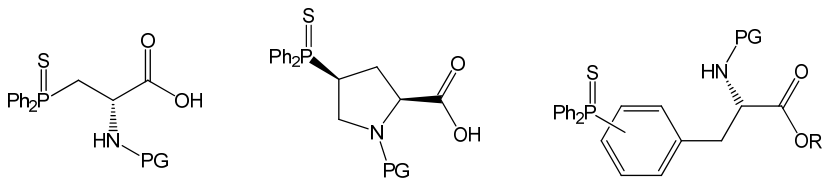

13 **14** PG = Fmoc or Boc; R = Me or CH_2Ph **15**

Scheme 7 Functionalized amino acid based-building blocks for peptide modifications.

3.2 Palladium-Catalyzed Asymmetric Allylic Alkylation

Generation of carbon centers whose absolute stereochemistry can by controlled by alkylation reactions still represents a major challenge for synthetic chemists. The palladium-catalyzed asymmetric allylic alkylation has been demonstrated to be useful in the synthesis of valuable small molecules as well as complex natural products.[34] Many attractive mixed donors, potentially capable of forming chelates have been extensively exploited in these reactions. These ligands induce an electronic differentiation of allylic termini in (π-allyl)palladium intermediates and thus provide the necessary bias for the reaction to proceed selectively.[35]

Indeed, the Gilbertson's library of peptide-derived phosphine ligands (see above) has been further extended and used in Pd-catalyzed asymmetric allylic alkylation affording moderate enantiomeric excess.[36] For a summarizing article concerning the chemistry of peptide-containing phosphine amino acids, see reference.[37]

A new methodology for the solid-phase synthesis of peptide-based phosphine ligands has been developed by Meldal.[38] Peptides possessing either primary or secondary amine groups have been synthesized according to the usual solid-phase protocol and then reacted with (diphenylphosphino)methanol to afford *N*-(diphenylphosphino)methyl- or *N*,*N*-bis[(diphenylphosphino)methyl]-substituted peptides. In another work, a series of *P,S*-ligands bearing a cysteine-derived amino acid resulted from the same procedure as developed for the preparation of phosphine-functionalized peptide.[39] These synthetic peptides were evaluated as ligands in palladium complexes and tested in asymmetric allylic alkylation reactions to afford only a poor selectivity.

A C_2-symmetric chiral diphosphine ligand **17**[40] was obtained by Morimoto from aminophosphine **16**, which was prepared from L-valine in five steps (Scheme 8).[41] The family of **17**-type ligands was further extended and the compounds were evaluated in asymmetric allylic substitution of both cyclic and acyclic substrates with an excellent enantioselectivity.[42] Ligand **18** (Scheme 8) and its chalcogeno-derivatives have been synthesized[43] in order to use the concept of fluorous biphasic catalysis.[44] A catalyst bearing fluorinated ligand is dissolved in fluorous solvent, whereas the substrate remains in organic phase. If the resulting biphasic system is warmed, the catalytic reaction occurs under homogeneous conditions. Once the reaction is complete the two phases are readily

separated at lower temperature, allowing easy separation of organic phase (product) from fluorous phase (catalyst) by simple decantation.

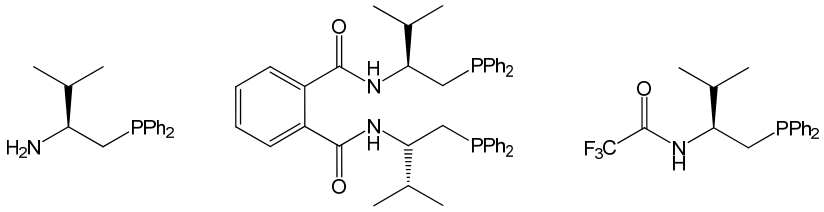

16 **17** **18**

Scheme 8 Amidophosphines derived from L-valine.

Phosphinoamides **19–21** (Scheme 9) were obtained from 2-(diphenylphosphino)benzoic acid and various chiral amines.[45] The naphthyl analogue **22** (Scheme 9) was synthesized in three steps; amidation of 2-hydroxy-1-naphthoate followed by triflation and nickel-catalyzed phosphinylation. Ligands **19–22** were studied in asymmetric allylic alkylation of 1,3-diphenylallyl acetate with moderate to good enantioselectivities. The L-proline-based amide performed best (94% *ee*).

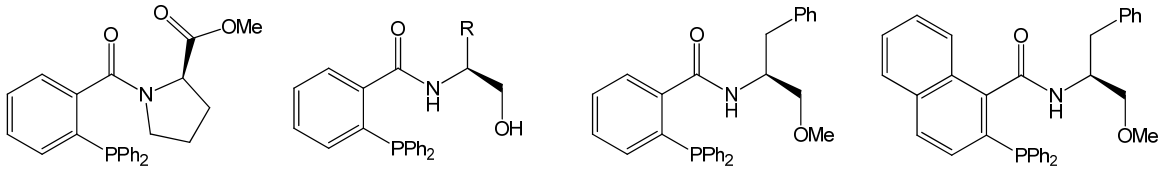

19 **20** R = Ph, CH_2Ph **21** **22**

Scheme 9 Chiral phosphino-carboxamide ligands studied in asymmetric allylic alkylations.

3.3 Copper-Catalyzed Asymmetric Conjugate Addition

Asymmetric conjugate addition of organometallic reagents to α,β-unsaturated compounds is another basic method in synthetic chemists' repertoire for the construction of C–C bonds. This is mainly due to the broad scope of donors and acceptors that can be employed in this reaction. The nucleophiles can be carbon or heteroatom based (H, O, S, Se, N, P, Si), whereas the diversity in acceptors arises due to the many possible activating groups that can be appended to the double bond (ketones, aldehydes, esters, amides, nitriles, nitro, sulfonates, sulfoxides, phosphanes, etc.). Conjugate addition reactions have been used as key steps in the synthesis of numerous biologically active compounds.[46]

Breit[47] *et al*. and Hoveyda[48] *et al*. independently reported peptides containing one to three L- or D-valine units (**23**–**25**, Scheme 10). These ligands were obtained by carbodiimide-mediated coupling of valine methyl ester with Z-protected valine. Deprotection of the Z-group through hydrogenolysis was followed by amidation with the third amino acid or by 2-(diphenylphosphino)benzoic acid. In conjugate addition of diethylzinc to cyclohexanone the best enantiomeric induction was achieved with compound **24** (97% *ee*). In addition, Cu/**24** catalyst showed a high catalytic activity in asymmetric addition of diethylzinc to several α′-oxy enone templates.[49] New *P,N*-ligands (**26**–**29**, Scheme 10) derived from valinol and prolinol have been developed for the asymmetric Cu-catalyzed conjugate addition of diethylzinc to unsaturated ketones.[50] The donors possessing tertiary amide group proved to be superior to their secondary amide counterparts.

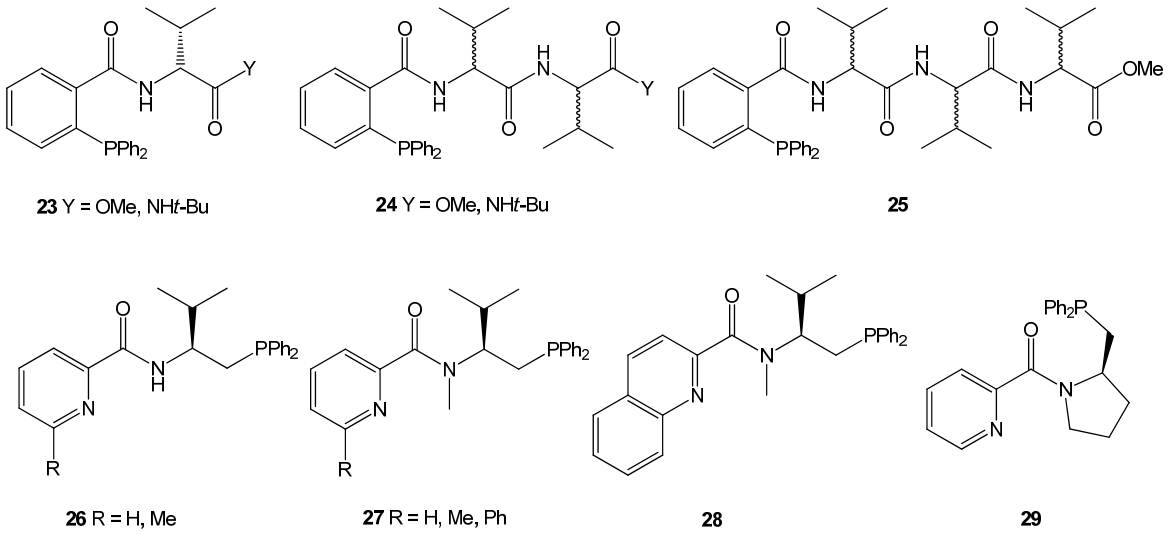

Scheme 10 Phosphino-based amino acid amides designed for used in Cu-catalyzed asymmetric conjugate addition.

3.4 Other Applications to Asymmetric Catalysis

Stille *et al*. utilized a polymer support to immobilize homogeneous catalysts for Rh-catalyzed hydrogenation[27] (see above). A similar approach was used to prepare polymers containing a chiral chelating phosphine by co-polymerization of **8** (R = vinyl) either with 2-hydroxyethyl methacrylate/ethylene dimethacrylate or with styrene/divinylbenzene,

respectively.[51] Pt(II) complexes prepared from these polymers in the presence of stannous chloride catalyzed asymmetric hydroformylation of a variety of prochiral olefins.

Since the unique catalytic performance was demonstrated in the asymmetric allylic alkylations, ligand **17**, its isomer derived from 1,2-disubstituted benzene and diphosphine **30** (Scheme 11) were further applied to another type of asymmetric catalysis, rhodium-catalyzed asymmetric hydrosilylations affording chiral alcohols from prochiral carbonyl compounds.[42a] Phosphine-functionalized peptides of the general structure **31** (Scheme 11) were found to be suitable candidates for the envisioned self-assembly process. The work of Breit *et al*. presents a perspective interface between the protein design and supramolecular catalysis for the design of *β*-sheet mimetics and screening of libraries of self-organizing supramolecular catalysts. The Rh-catalyzed hydroformylation of styrene was chosen as an initial test reaction to explore the potential of the self-assembled peptide-based ligands in catalysis.[52]

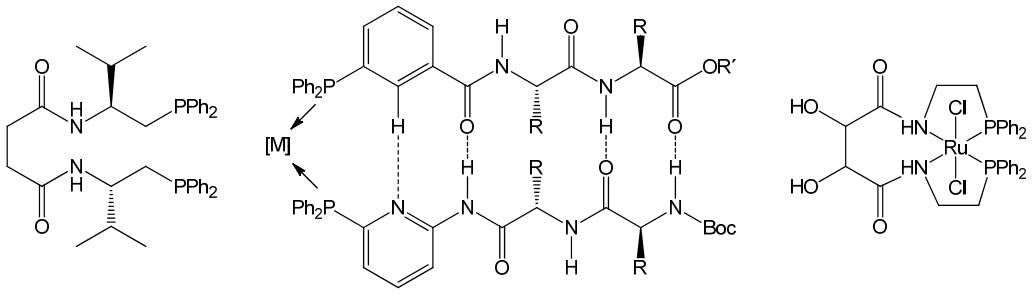

Scheme 11

Finally, complex **32** (Scheme 11) was tested in asymmetric transfer hydrogenation of several aryl–alkyl ketones employing 2-propanol as a hydrogen source. In particular, catalytic asymmetric transfer hydrogenation using 2-propanol has been shown to be an elegant and economic reduction method due to the cheap hydrogen source employed and the avoidance of high pressure equipment.[53] Unfortunately, complex **32** bearing two hydroxy groups achieved only poor conversion and enantioselectivity.[54] A series of **13**-type compounds containing multifunctional alanine-based phosphine differing by the protection group at the nitrogen atom (Scheme 7) were shown to be good organocatalysts for asymmetric [3 + 2]-cycloaddition of allenic esters and enones.[55]

4 Applications of Amino Acid Phosphinoamides in Medicinal Chemistry

The ^{99m}Tc nuclear isotope is widely used for medicinal imaging due to its nearly ideal nuclear characteristic; suitable half-life and optimal emission energy of γ rays. The practical use of ^{99m}Tc for regular imaging is also facilitated by the ready availability of this isotope from the ^{99}Mo/^{99m}Tc generator. Technetium-tagged radiopharmaceuticals are compounds, for which the targeting moiety (e.g., peptide, hormone) is labeled with ^{99m}Tc, either directly or by means of a bifunctional chelate, and the ^{99m}Tc essentially reaches the target site as a passenger. A bifunctional chelate is a multidentate ligand, which has appropriate ligating groups for coordination to the metal and also contains a functional group for covalent attachment to the targeting moiety.[56] For this purpose several phosphino-based amino acids or peptides have been developed. Non-radioactive rhenium metal ion is utilized for model coordination studies, since the lanthanide contraction ensures that the complexes of both elements are very similar in terms of their physical characteristic. In addition, $^{186/188}$Re radioactive isotopes are suitable for therapeutic use by means of β-irradiation.[56a,57] One of the most important prerequisites in the design of new classes of ligands for technetium/rhenium-based diagnostic and therapeutic agents is the development of stable complexes with these metals and the elucidation of their structure.

As the first example of phosphine derived peptide for biomedicine application, *N*-[*N*-(3-(diphenylphosphino)propionyl)glycyl]-L-(*S*)-benzylcysteine methyl ester (H_2**33** Scheme 12), was developed in 1995.[58] This potentially tetradentate ligand containing the *PNNS* donor atom set was synthesized by coupling of 3-(diphenylphosphino)propionic acid with protected Gly-L-Cys dipeptide. Reaction of H_2**33** with [$ReOCl_3(PPh_3)_2$], a common source of $[ReO]^{3+}$ moiety, smoothly led to complex **35** (Scheme 12).[58] Complex **35** was structurally characterized and treated with potassium hydroxide to afford a hydroxo complex [ReO(OH)(**33**-κ^4*P,N,N,S*)].[59] In contrast, reaction of [$ReOCl_3(PPh_3)_2$] with the corresponding free acid H_3**34** (Scheme 12) gave rise to two products: [ReOCl(H**34**-κ^4*P,N,N,S*)] similar to **35** with non-coordinated protonated carboxylic group and [ReO(H_2O)(**34**-κ^4*P,N,N,O*)], where the ligand is coordinated via carboxylic group instead of the sulfur atom.[59] Donors H_2**33** and H_3**34** were studied in ^{99m}Tc labeling experiments

with model peptide (tetragastrin, cholecystokinin-fragment). The peptide was conjugated to the ligand chelator by active ester chemistry, either before or after radiolabeling.[60]

The coordination reactions of the related ligand MeH_3**36** (Scheme 12) were performed with either $[ReOCl_3(PPh_3)_2]$ or $PPh_4[ReOCl_4]$ as the starting materials in equimolar quantities. Both reactions produced the same final mixture of two isomers [ReO(Me**36**-κ^4*P,N,N,S*)] in 1:1 ratio.[61] Acid H_4**37** (Scheme 12) and its ester MeH_3**36** were labeled with ^{99m}Tc at neutral pH, leading to neutral pentacoordinated complexes [^{99m}TcO(H**37**-κ^4*P,N,N,S*)] and [^{99m}TcO(Me**37**-κ^4*P,N,N,S*)]. In addition, saponification of complex molecule bearing the ester function afforded [^{99m}TcO(H**37**-κ^4*P,N,N,S*)], thus confirming the availability of the carboxylic group localized outside the coordination sphere.[62]

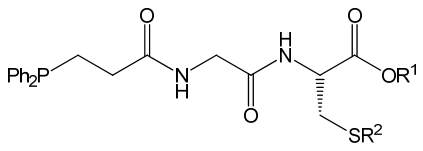

R^1/R^2 =

Me/CH_2Ph	H_2**33**
H/CH_2Ph	H_3**34**
Me/H	MeH_3**36**
H/H	H_4**37**

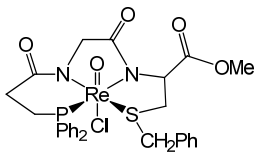

35

Scheme 12 Phosphinoamides designed for biomedicine used and an example of rhenium complex with these ligands.

A PEG-supported ligand H_4**37** was obtained by standard peptide coupling of PEG-NH_2 and free carboxylic group in H_4**37** in order to avoid the use of an external reducing agent during the ^{99m}Tc-labeling process. The labeling was based on a supramolecular assembly of the PEG-H_4**37** conjugates in aqueous solution to yield micelles that favor the reduction and coordination of technetium. However, the labeling did not affect the polymer behavior of PEG.[63] Recently, the H_4**37**-PEG-UBI conjugate was prepared, labeled with ^{99m}Tc and studied as a candidate for clinical imaging of infection.[64]

Other chelate ligands **38** (Scheme 13) were synthesized from 2-(diphenylphosphino)aniline and the corresponding carboxylic acid, and reacted with Re(V) precursors. The reaction of both tritylated and non-tritylated donors with $[ReOCl_3(PPh_3)_2]$ gave the same expected neutral complex [ReO(**38**-κ^4*P,N,N,S*)]. A neutral and diamagnetic species, [ReN(**38b**-κ^4*P,N,N,S*)], was isolated during the complexation of **38b** with $[ReNCl_2(PPh_3)_2]$.[65] Liu and co-workers reported a lysin-containing chelator with hydrazine

group derived either from 2- or 4-(diphenylphosphino)benzoic acid (**39** in Scheme 13) for the ^{99m}Tc complexes. The free hydrazine group in **39** was found to be unstable and, therefore, 2-sulfonatobenzaldehyde hydrazone was used as the protecting group.[66] Finally, several monodentate functionalized phosphines (**40** in Scheme 13) were prepared and utilized for coordination of rhenium tricarbonyl species with a dithiocarbamate auxiliary ligand.[67]

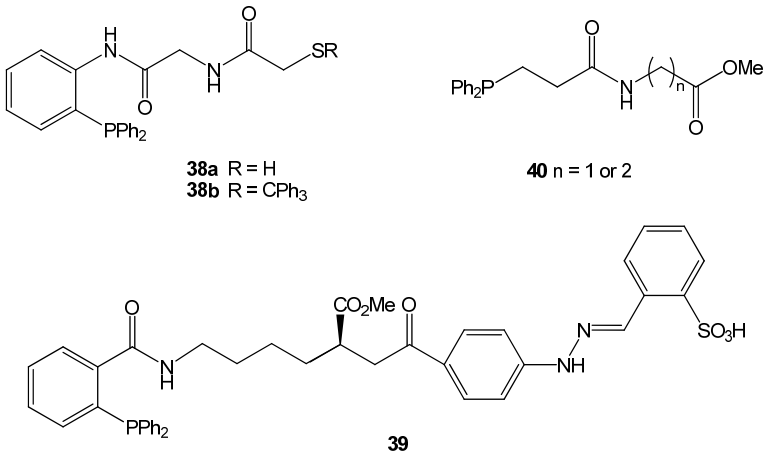

Scheme 13 Selected ligands prepared for coordination of rhenium/technecium ion.

5 Ferrocene

Sixty years ago a new iron-containing compound $C_{10}H_{10}Fe$ with high and unexpected stability was independently reported by two different groups.[68,69] The structure of this organometallic compound was at first wrongly proposed featuring an iron atom bonded to the cyclopentadienyl rings via σ-bonds (**41** in Scheme 14). The correct structure of bis(cyclopentadienyl)iron with ten equivalent Fe–C bonds (**42** in Scheme 14) was put forward in two independent publications by Fischer and Pfab[70] and by Wilkinson *et al.*[71] The discovery of ferrocene and elucidation of its unique sandwich structure prompted the development of modern organometallic chemistry.

Ferrocenes have played an important role in many areas of synthetic, material and medicinal chemistry.[72] Among organometallic compounds, ferrocenes are characterized by remarkably high thermal and chemical stability, display electron transfer properties due to the ferrocene/ferrocenium redox couple and are prone to a wealth of relatively easy derivatization methods. The unique combination of conformational flexibility resulting

from facile rotation of the aromatic rings and a relatively rigid cylindrical shape favoring the mutually coplanar orientation of the cyclopentadienyl rings has resulted in many particular "structure-based" applications of ferrocene derivatives.

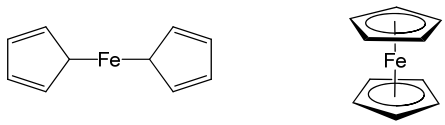

41 42

Scheme 14 Ferrocene: the wrong structure proposed originally (**41**) and the correct formulation (**42**).

Another attractive feature of ferrocene is the possibility of preparing chiral derivatives. Chirality can be introduced simply by attaching a chiral substituent or by the generation and manipulation of α-stereogenic centers. The hydrazone **43** readily prepared from ferrocenecarboxaldehyde and chiral 2-(methoxymethyl)-1-pyrrolidinamine, undergoes highly diastereoselective (>99:1) addition of a number of alkyl lithium reagents to give hydrazines **44**. Reductive N–N bond cleavage with Raney nickel affords (*R*)-1-ferrocenylalkylamides **45** with ~90% *ee* (Scheme 15).[73] Asymmetric reduction of ferrocenyl ketones **46**, which are easily accessible by Friedel-Crafts acylation of ferrocene, is another attractive route for the synthesis of chiral α-ferrocenyl alcohols **47** with excellent enantiomeric excesses ~90% (Scheme 15).[74]

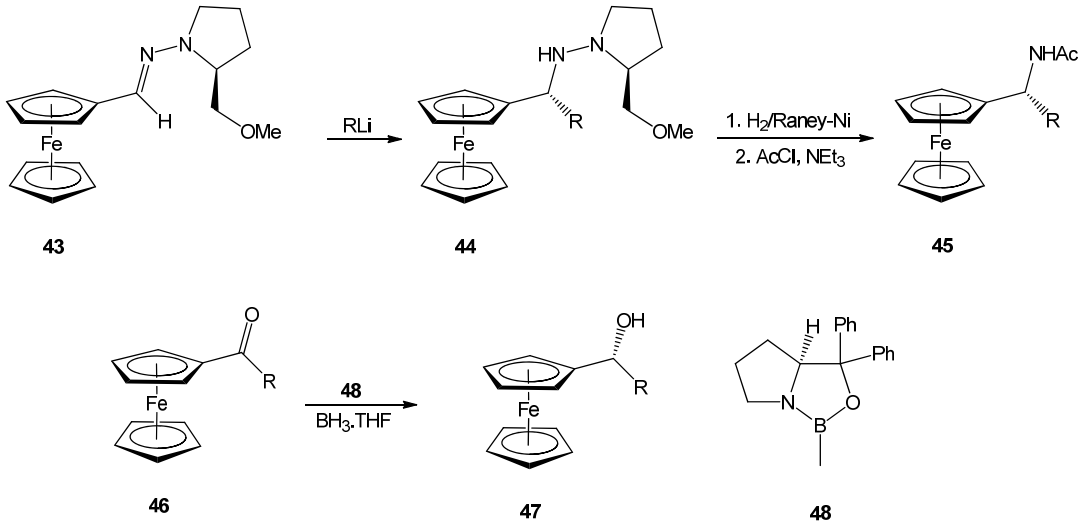

43 44 45

46 47 48

Scheme 15 Generation of center chirality in ferrocene compounds.

More interestingly, the presence of a chiral substituent containing suitably located donor atom on the cyclopentadienyl ring directs lithiation to the adjacent position in stereoselective manner. Reaction of the resulting lithio-intermediate with an electrophile affords in planar-chiral 1,2-disubstituted ferrocene derivatives. The diastereoselective *ortho*-lithiation reaction was developed by Hayashi and Kumada[75] using enantiomerically pure *N*,*N*-dimethyl-1-ferrocenylethylamine (Ugi-amine, Scheme 16).[76] Chiral sulfoxides,[77] cyclic acetals,[78] oxazolines,[79] SAMP hydrazones[80] etc. have been also utilized as the other *ortho*-directing. In combination, the use of chiral *ortho*-directing groups evolved into a method of choice for the preparation ferrocene donors possessing both planar and central chirality.

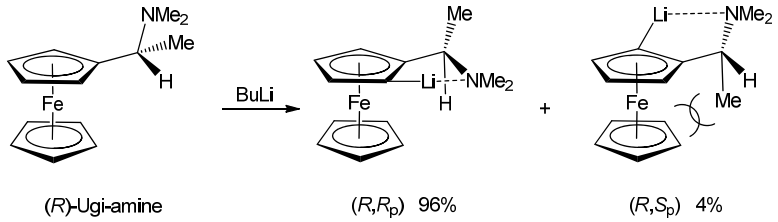

Scheme 16 Diastereoselective *ortho*-lithiation of Ugi's-amine.

Phosphinoferrocenes are the most frequently studied and practically utilized ferrocene ligands. Up to now, tremendous progress has been made in the design of phosphinoferrocenes and the related *P,N*-donors, with decisive stimulus coming from a search for new highly active catalysts for organic transformations. A brief mention must be made of the symmetrical diphosphine 1,1'-bis(diphenylphosphino)ferrocene (dppf, Scheme 17). Dppf can coordinate to a number of metals, acting as a monodentate, chelating or bridging ligand. Dppf as a catalyst component has found wide applications in various carbon–carbon cross-coupling reactions, hydrogenation, hydroformylation and hydrosilylation reactions.[81]

Chiral phosphinoferrocenes constitute a fundamentally important class of chiral ligands for transition metal-catalyzed stereoselective synthesis. The most popular Josiphos-type ligands[82] (Scheme 17) have been applied in four industrial scale processes and several others are on pilot stage.[83] Wide catalytic utilization of dppf and successful industrial applications of Josiphos-type ligands are one of the reasons for this area to develop very rapidly.

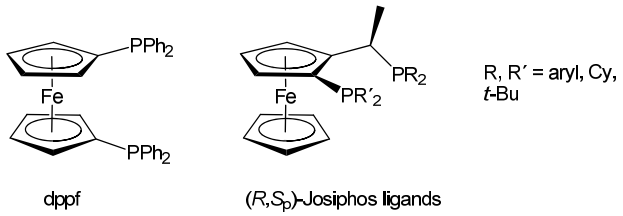

Scheme 17 Representative ferrocene ligands.

5.1 Non-Chiral Phosphinoferrocene Carboxamides

Phosphinoferrocene-carboxamides bearing simple and functional substituents at the amide nitrogen have been typically prepared via amide coupling of the respective phosphinocarboxylic acid (or its activated derivatives) and amines (see Scheme 2). An alternative synthetic route was devised for the preparation of simple amides **49** based on the reaction of 1´-(diphenylphosphino)-1-lithioferrocene generated *in situ* by lithiation of 1´-(diphenylphosphino)-1-bromoferrocene (PPh_2fcBr) and isocyanates (Scheme 18).[84]

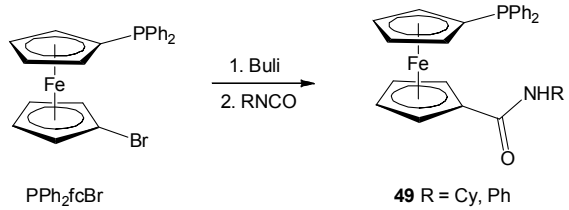

Scheme 18 Prepation of simple phosphinoferrocene amides.

Most likely the first phosphinoferrocene carboxamide was synthesized in 1999 by the reaction of 1,1´-bis(chlorocarbonyl)ferrocene with two equivalents of (3-aminopropyl)diphenylphosphine. The resulting diphosphine-amide **50** (Scheme 19) was coordinated as a chelate donor toward several metal ions (Mo, Cr, Rh and Ru).[85] A number of amides were synthesized from 1´-(diphenylphosphino)-1-ferrocenecarboxylic acid (Hdpf)[86] by Štěpnička and co-workers. Amides **51** (Scheme 19) served as valuable building blocks for organometallic synthesis, allowing access to unique *P*-chelated tungsten and chromium carbene complexes.[87] Recently, were reported versatile ligands **52**–**54** (Scheme 19), whose donor properties can be tuned through changing the substitution patterns at the pyridyl ring and the length of the spacer. These ligands showed high structural variability in palladium, mercury and cadmium complexes.[88] Compounds **52**, **53**

and **55**[89] were demonstrated to be able to ligate palladium in a relatively rare *trans-P,N*- or *trans-P,P*-chelating fashion.[90] In addition, these donors proved to be good catalyst components for Suzuki-Miyaura cross-coupling reactions of aryl bromides and phenylboronic acid to give the corresponding biphenyls.[88a,89] Recently, the archetypal primary amide derived from Hdpf was synthesized together with the related carbohydrazide **56** (Scheme 19), which was further converted via standard condensation reactions to several phosphinoferrocene heterocycles.[91]

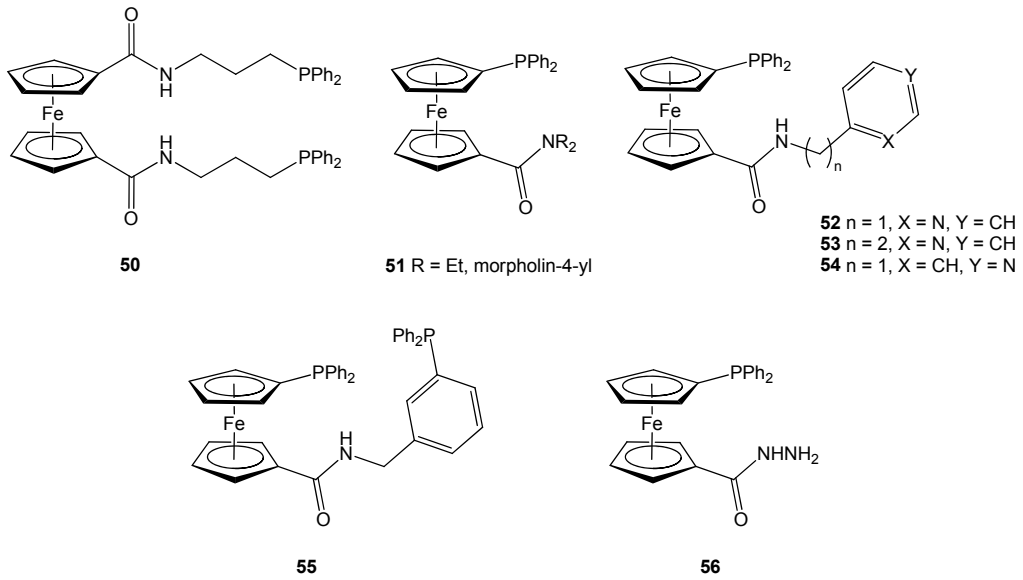

Scheme 19 Representatives of ferrocene-based phosphino-carboxamides.

In order to perform catalytic reactions in water and in biphasic water–organic solvent mixtures, two series of highly polar phosphinoferrocene amidoalcohols **57**[92a] and amidosulfonates **58**[92b] were designed (Scheme 20). The solid-state structures of the ligands and their palladium complexes revealed complicated hydrogen-bonded arrays. Palladium complexes with these ligands were tested as defined pre-catalyst for Pd-catalyzed Suzuki-Miyaura cross-coupling reactions and for Pd-catalyzed cyanation of aryl bromides with $K_4[Fe(CN)_6]\cdot 3H_2O$ in aqueous reaction media. Ligand **57a**, its chalcogenide derivatives and platinum and palladium complexes [MCl_2(**57a**-κ*P*)] (M = *trans*-Pd, *trans*-Pt and *cis*-Pt) were further evaluated for anticancer activity.[93]

Attention was also paid to the use of dendritic and star-shaped molecules as supporting scaffolds for catalyst systems. The resulting multifunctional catalysts often reacted as their parent counterparts, but could be easily recovered and subsequently

recycled. Homogeneous but supported dendrimer-like catalysts were synthesized by amidation of Hdpf with the appropriate amines and used in Pd-mediated Suzuki-Miyaura and Heck reaction of butyl acrylate with bromobenzene to give butyl cinnamate.[94]

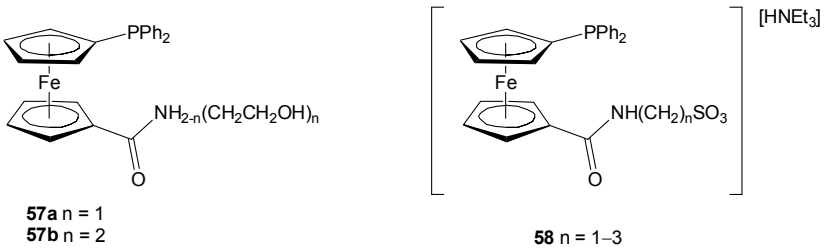

Scheme 20 Polar phosphinoferrocenyl amides.

The first phosphinoferrocene-carboxamides bearing glycine-based pendant groups have been obtained by the conjugation of Hdpf with glycine esters. Donor **59** was further modified both in the amino acids pendant via transformation of the terminal ester group to primary amide **60** or to free acid **61** or, and at the phosphine moiety by oxidation to the corresponding phosphine oxide **62** or phosphine sulfide **63** (Scheme 21). Hdpf-GlyOMe **59**

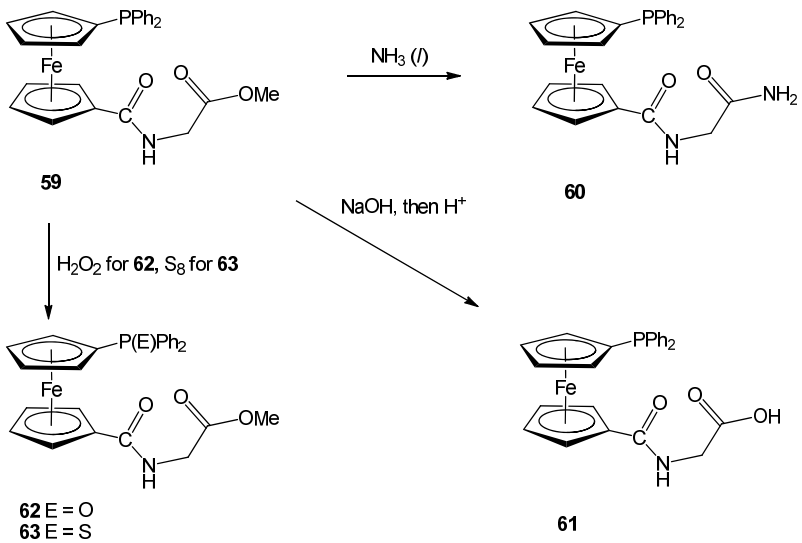

Scheme 21 Synthesis of Hdpf-Gly derivatives.

was firstly studied as a ligand in palladium complexes to demonstrate its versatile coordination. It was shown that such donor can simply coordinate via their phosphine function or can form *P,O*- and (after the removal of the amide proton) anionic *P,N*-chelates (see complexes **64**–**66** in Scheme 22). In addition, compounds **59**–**61** were reacted with

[$PdCl_2$(cod)] or $Na_2[PdCl_4]$ to afford the respective (mostly solvated) bis-phosphine complexes *trans*-[$PdCl_2$(L-κ*P*)$_2$] (L = **59**–**61**). Catalytic properties of the Hdpf-Gly conjugates **59**–**61** have been demonstrated in palladium-catalyzed Suzuki cross-coupling reaction performed in aqueous solution.[95]

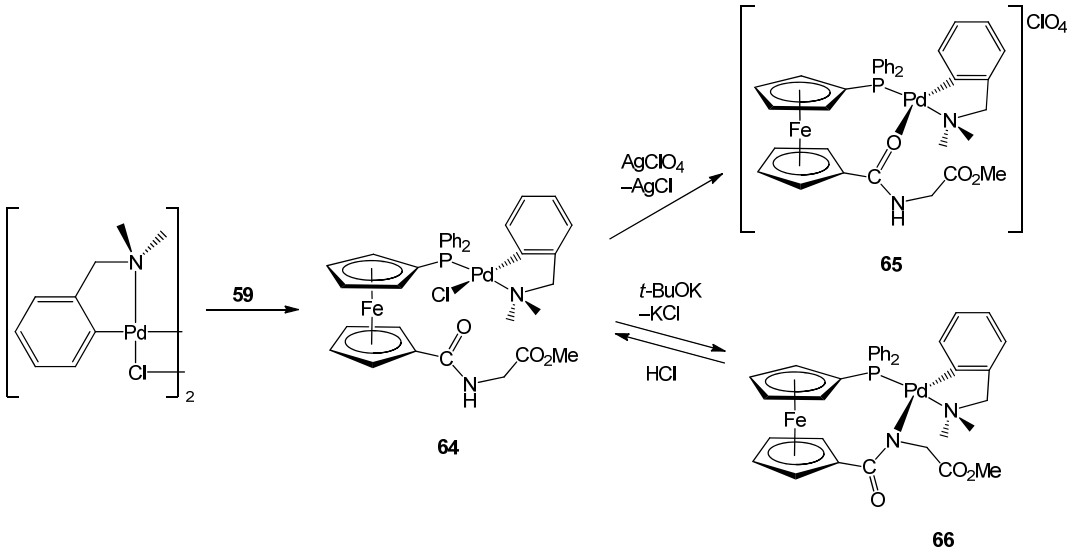

Scheme 22 Coordination versatility of ligand **59** in palladium complexes **64**–**66**.

5.2 Chiral Phosphinoferrocene Amides

Planar-chiral amides **67** (Scheme 23) were obtained in several steps from enantiomerically pure ferrocenyl sulfoxide via diastereoselective *ortho*-lithiation and Pd-catalyzed Suzuki-Miyaura cross-coupling reaction. The compounds were tested as catalytic components in asymmetric copper-mediated conjugate addition with moderated to good *ee*'s.[96] A series of phosphinoferrocene ligands with secondary and tertiary amide groups **68** (Scheme 23) have been prepared from the appropriate (phosphinoferrocenyl)amines and an acid chloride or anhydride. As ligands, these compounds were evaluated in asymmetric Pd-catalyzed allylic alkylation and showed high conversion and enantioselectivity (99% *ee*) after optimization of the catalytic conditions.[97]

Development of novel (phosphino)ferrocenecarboxylic acids and utilization of these compounds and their derivatives as organometallic synthons and catalyst components have attracted much attention in last decade.[98,99] Štěpnička and co-workers have prepared a number of phosphinoferrocene amides via amide coupling of the respective phosphinoferrocene acids and appropriate amines.[99,100] Amides presented in Scheme 24,

and their complexes were tested in asymmetric Pd-catalyzed allylic alkylation reaction. Catalytic tests revealed that ligands derived from Hdpf bearing only central chirality at the amide nitrogen **69** afforded racemic products, whereas their 1,2-isomers **70** possessing either planar chirality or combined planar and central chirality elements achieved 90% *ee* under optimized conditions. In contrast, lower *ee*'s were attained with amides **71** as compared to amides **70**, which can be accounted for their particular ligating properties. Ligands **71** coordinate to palladium as symmetric *P,P*-chelates and, hence, do not provide sufficient electronic differentiation of the allylic termini such in complexes with amides **70**, which form *P,O*-chelates.

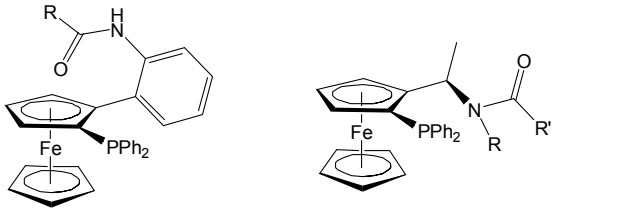

67 R = *t*-Bu, 2-pyridyl

68 R = H, Me, Ph, CH_2Ph
R' = Me, Et, *t*-Bu, Ph, O*t*-Bu

Scheme 23 Chiral ferrocenylphosphines with secondary and tertiary amide groups.

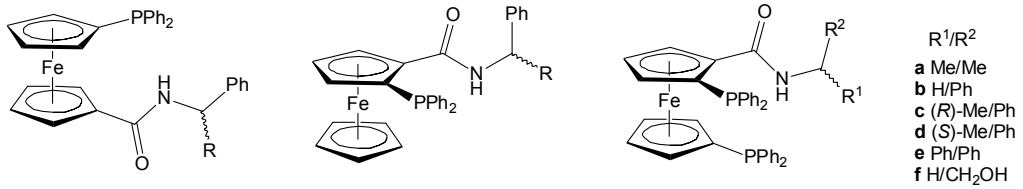

69 R = (*S*)-Me, (*R*)-Me

(S_p)-**70** R = H, (*S*)-Me, (*R*)-Me

(R_p)-**71a-f**

Scheme 24 Chiral ferrocenylamides derived from (phosphino)ferrocenecarboxylic acids.

Another series of chiral amides bearing up to three (S_p)-2-(diphenylphosphino)ferrocene-1-yl moieties at the periphery (Scheme 25) were prepared via similar procedure as the previously mentioned amides **69**–**71**. Palladium catalysts based on these ligands promoted asymmetric allylic alkylation of symmetrical substrate 1,3-diphenylprop-2-en-1-yl with *in situ* generated malonate anion. Whereas the enantioselectivity varied only slightly with the ligand structure (~88% *ee*), the conversion achieved with **72**–**74** changed with the size of these ligands, being lower with the larger donors.[101]

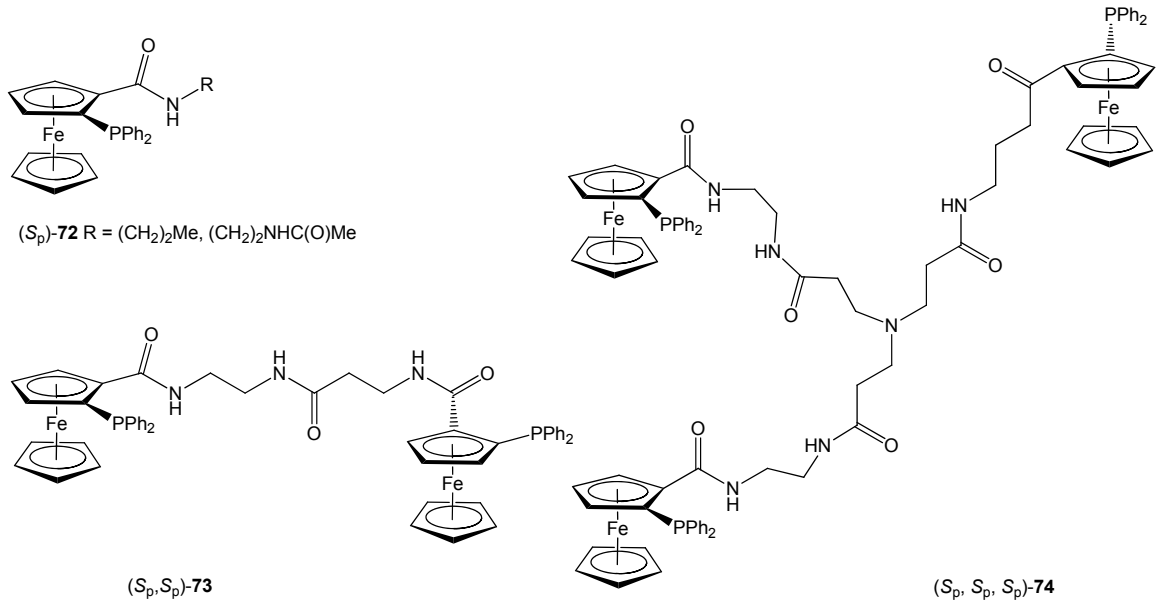

Scheme 25 Planar-chiral amides bearing (S_p)-2-(diphenylphosphino)ferrocene-1-yl moieties.

6 Aims of the Thesis

With the respect to my previous work focused on the preparation, coordination chemistry and catalytic utilization of phosphinoferrocene amino acid conjugates, the non-chiral Hdpf-Gly amides[95] (see page 26), the aim of the presented Thesis was to extend the scope of these donors toward chiral representatives resulting from other (chiral) amino acids. The series of structurally related phosphinoferrocene-carboxamides was designed to incorporate compounds featuring either a chirality center in the amino acid chain or a chirality plane, as well as their analogues combining both chirality elements (Scheme 26).

After the preparation and characterization of such a library of new amino acid amides, the next objective was to evaluate the catalytic potential of these donors in practically useful asymmetric catalytic processes. Considering the presence of *P*-, *N*- and *O*-donor atoms, the ligands were tested as catalytic components in transition metal-mediated reactions catalyzed either by copper, palladium or ruthenium that are readily coordinated by these donors.

Several attempts to interpret catalytic results were made aiming at the nature of putative reaction intermediates and structural factors governing the reaction course. For this purpose, several model complexes were synthesized and structurally characterized usually featuring Hdpf-GlyOMe (**59**) as the model achiral donor.

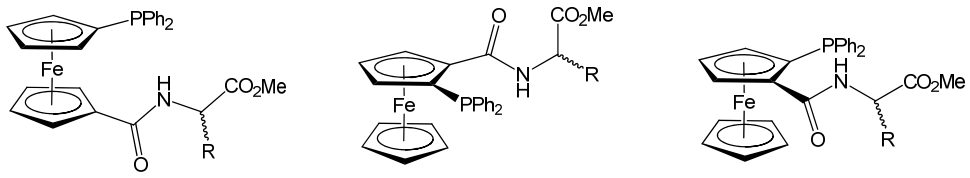

R =
H, (*S*)-Me, (*R*)-Me, (*S*)-$CHMe_2$, (*R*)-$CHMe_2$, (*S*)-CH_2Ph, (*R*)-CH_2Ph

R =
(S_p)-H, (S,S_p)-Me, (R,S_p)-Me, (S,S_p)-$CHMe_2$, (R,S_p)-$CHMe_2$, (S,S_p)-CH_2Ph, (R,S_p)-CH_2Ph, (S,S_p)-CH_2CHMe_2, (S,S,S_p)-$CH(Me)CH_2Me$

R =
(S,R_p)-Me

Scheme 26 Series of (diphenylphosphino)ferrocene amino acid conjugates presented in this Thesis.

7 Concise Summary of Results and Discussion

As the first part on my Ph.D. Thesis (Appendix 1), novel amidophosphine ligands were prepared via standard amide coupling protocol either from 1′-(diphenylphosphino)-ferrocene-1-carboxylic acid (Hdpf)[86] or its 1,2-planar chiral isomers ((S_p)-**75** and (R_p)-**75**)[102] and from the respective amino acid methyl esters in the presence of EDC/HOBt as the commonly used amide coupling agents (Scheme 27).

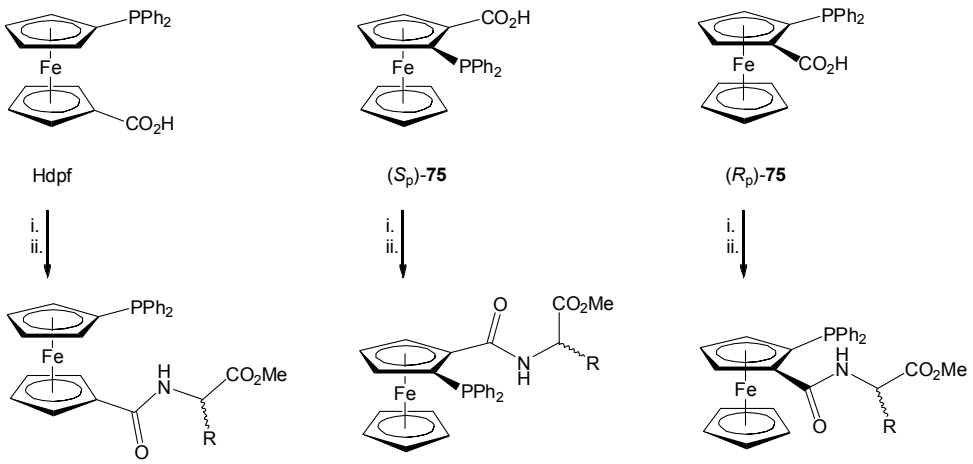

R		R		R	
59	H	(S_p)-**79**	(S_p)-H	(S,R_p)-**83**	(S,R_p)-Me
(S)-**76**	(S)-Me	(S,S_p)-**80**	(S,S_p)-Me		
(R)-**76**	(R)-Me	(R,S_p)-**80**	(R,S_p)-Me		
(S)-**77**	(S)-$CHMe_2$	(S,S_p)-**81**	(S,S_p)-$CHMe_2$		
(R)-**77**	(R)-$CHMe_2$	(R,S_p)-**81**	(R,S_p)-$CHMe_2$		
(S)-**78**	(S)-CH_2Ph	(S,S_p)-**82**	(S,S_p)-CH_2Ph		
(R)-**78**	(R)-CH_2Ph	(R,S_p)-**82**	(R,S_p)-CH_2Ph		

Scheme 27 Library of the prepared phosphinoferrocene carboxamides. Legend: (i) EDC/HOBt, (ii) $[H_3NCH(R)CO_2Me]Cl/NEt_3$.

Whereas amides derived from L-amino acids were obtained in very high yields for all phosphinoferrocene acids, reaction of D-amino acids with (S_p)-**75** did not reach completion and small amounts of the intermediary active ester 1-hydroxybenzotriazolyl (S_p)-2-(diphenylphosphino)ferrocene-1-carboxylate was also isolated, very likely due to a structural mismatch.

As a next step, these newly prepared ligands were evaluated in asymmetric copper-catalyzed 1,4-conjugate addition of diethylzinc to *trans*-chalcones **84** affording chiral ketones **85** (Scheme 28). The pre-catalysts were formed *in situ* from a copper salt and the respective ligand. Attention was firstly paid to an optimization of the reaction conditions in

terms of the copper salts, solvent and the Cu/L ratio (see Appendix 1 for complete results). The initial screening reactions were performed with ligand (*S*)-**76**.

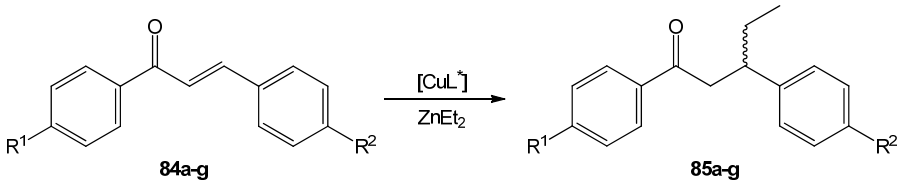

Scheme 28 Asymmetric Cu-catalyzed conjugate addition of $ZnEt_2$ to chalcones.

All catalytic reactions afforded either pure products **85a**-**g** or their mixture with the starting chalcone in the case of incomplete conversion. In addition, the crude reaction mixtures usually contained traces of 1,3,5-triphenyl-2-(1-phenylpropyl)pentane-1,5-dione (**86**). This side-product, formed presumably from an intermediate zinc enolate (Scheme 29), preferentially crystallized from the product mixture and was structurally characterized.

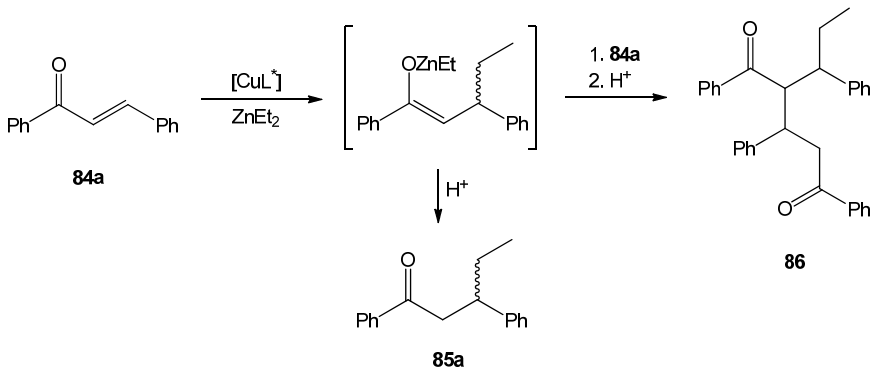

Scheme 29 Plausible reaction pathway leading to the side-product **86**.

After the optimization of reaction parameters, the influence of ligand structure on the reaction course was established (Table 1). The utilization of donors derived from Hdpf generally resulted in good levels of conversion and enantioselectivity. A positive effect of the size of the amino acid substituent on the enantioselectivity was observed (the bulkier amino acid pendant, the better results). The best results were obtained with the valine derivatives (*S*)-**77** and (*R*)-**77** affording the alkylation product with complete conversion at 0 °C within 4 h and with 84% *ee*. On the other hand, the planar-chiral phosphines proved to be poor ligands with the exception of amide (S_p)-**79** possessing only planar chirality and bearing the least bulky amino acid substituent. This is rather unexpected, particularly in

view of successful utilization of the related planar- and *C*-chiral ferrocenyl ligands in Pd-mediated asymmetric allylic alkylation[100] and Cu-catalyzed asymmetric conjugate addition.[46f,j]

Table 1 Influence of the ligand structure in Cu-mediated conjugate addition.[a]

Entry	Ligand	Conversion (%)	*ee* (%) [Configuration]
1	(*S*)-**76**	98	70 [*R*]
2	(*R*)-**76**	97	68 [*S*]
3	(*S*)-**77**	100	83 [*R*]
4	(*R*)-**77**	100	84 [*S*]
5	(*S*)-**78**	92	79 [*R*]
6	(*R*)-**78**	91	80 [*S*]
7	(S_p)-**79**	86	72 [*S*]
8	(*S*,S_p)-**80**	20	39 [*S*]
9	(*R*,S_p)-**80**	14	12 [*S*]
10	(*S*,R_p)-**83**	13	11 [*R*]
11	(*S*,S_p)-**81**	10	9 [*S*]
12	(*R*,S_p)-**81**	32	13 [*S*]
13	(*S*,S_p)-**82**	16	8 [*S*]
14	(*R*,S_p)-**82**	23	3 [*S*]

[a] Reaction conditions: **84a** (0.5 mmol), $ZnEt_2$ (0.75 mmol), $(CuOTf)_2 \cdot PhMe$ (7.5 μmol, 3.0 mol.-% Cu), ligand (18 μmol, i.e. 3.6 mol.-%), CH_2Cl_2 (3 mL), reaction temperature/time 0 °C/4 h. The results are averages of two independent runs.

With the most efficient ligand (*S*)-**77** another series of catalytic tests was performed in order to elucidate a possible influence of the reaction temperature and to test the related substrates **84b-g** (Table 2). Lowering of the reaction temperature to –40 °C slightly decreased the reaction rate and, surprisingly, had a negative effect on enantioselectivity. On the other hand, reaction performed at 20 °C afforded the alkylation product with 87% *ee*. The influence of chalcone substituents in positions 4 and 4' can be expected to be limited to an electronic effect. Indeed, the alkylation of all substituted chalcones was

complete within 4 h in the presence of Cu/(*S*)-**77** catalyst and produced the respective alkylation products with similar stereoselectivity (*ee* = 83–90%).

Table 2 Influence of the reaction temperature and chalcone substituent.[a]

Entry	Substrate	T (°C) (t (h))	Conversion (%)	ee (%) [Configuration]
1	**84a**	+40 °C (4)	100	82 [*R*]
2	**84a**	+20 °C (4)	100	87 [*R*]
3	**84a**	0 °C (4)	100	83 [*R*]
4	**84a**	–20 °C (4)	100	79 [*R*]
5	**84a**	–40 °C (4)	41	70 [*R*]
6	**84a**	–40 °C (23)	100	64 [*R*]
7	**84b**	0 °C (4)	100	90[b]
8	**84c**	0 °C (4)	100	87[b]
9	**84d**	0 °C (4)	100	90[b]
10	**84e**	0 °C (4)	100	89[b]
11	**84f**	0 °C (4)	100	83[b]
12	**84g**	0 °C (4)	100	85[b]

[a] For reaction conditions, see Table 1, footnote *a*. Ligand (*S*)-**77** (18 μmol) was performed in all reactions. [b] The configuration was not determined.

In order to interpret the catalytic results, interaction of the copper(I) triflate and **59** as a model donor was studied in solution and in the solid-state. Mass, ^{1}H and ^{31}P NMR spectra were recorded for a mixture copper(I) triflate and **59** at the molar ratio 1:0.9 showing presence of two species and at 1:2 ratio affording only one product. Addition of hexane to a solution of $Cu(OTf)_2 \cdot PhMe$ and **59** (Cu/L = 1:1) afforded yellow crystals of solvated complex [Cu(**59**-κ^2*P*,*O*)$_2$](TfO), which was structurally characterized. The crystal structure demonstrated that chelate coordination of **59**-type donor brings the ligand's chirality into proximity of the catalytically active metal center. Taken together, the data suggest an equilibrium mixture of cationic species of the type $[CuL_n]^+$ (n = 0–2) formed upon the addition of phosphinoamide ligands to copper(I) triflate. The $[CuL_2]^+$ cation is probably the most stable (isolable), whereas $[CuL]^+$ appears to be a likely precursor to the catalytically active species.

The second contribution (Appendix 2) focused on the catalytic utilization of the extensive series of chiral ligands (Scheme 27) and their complexes in Pd-catalyzed allylic substitution reactions. In the view of our previous results, two more phosphinoferrocene amides-based Hdpf were synthesized (according the same procedure as in Scheme 27) bearing sterically encumbered amino acid pendants from L-leucine and L-isoleucine methyl esters (Scheme 30).

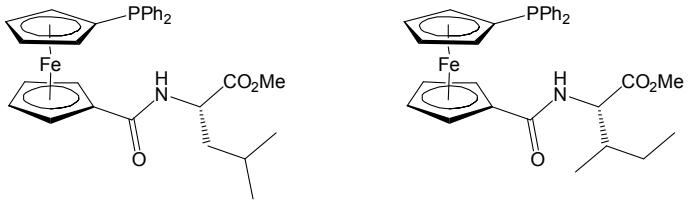

(*S*)-**87** (*S*,*S*)-**88**

Scheme 30 Phosphinoferrocene amides (*S*)-**87** and (*S*,*S*)-**88**.

The catalytic potential of all chiral donors was then examined in palladium-mediated allylic alkylation of 1,3-diphenylallyl acetate **89** with a nucleophile generated *in situ* from dimethyl malonate and a base (Scheme 31). The pre-catalysts were also generated *in situ* from $[Pd(\mu\text{-}Cl)(\eta^3\text{-}C_3H_5)]_2$ and the respective ligand. The initial screening reactions were performed with the simple chiral representatives (S_p)-**79** and (*S*)-**76** in order to optimize reaction parameters (solvent, base, additive, Pd/L ratio, temperature). In addition, another allylic substrate (1,3-diphenylallyl ethyl carbonate), and malonate ester (di-*tert*-butyl malonate) were included in testing (for all catalytic results see Appendix 2).

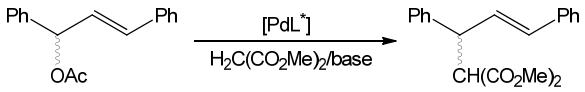

89 **90**

Scheme 31 Asymmetric allylic alkylation catalyzed by [Pd/L].

Having established the optimal reaction conditions (solvent, base, additive, Pd/L ratio), the whole series of ligands was firstly assessed in allylic alkylation (Table 3). Among the donors derived from Hdpf, the highest conversion and enantioselectivity was achieved with (*S*)-**76** as the ligand bearing the smallest substituent in the amino acid pendant. Ligands possessing relatively bulkier groups afforded significantly worse enantiomeric excesses. The situation among the planar-chiral amides proved more

complicated mostly because the chirality elements may combine in a matched or a mismatched manner. Yet again, the best results were obtained with the ligand containing the least sterically demanding glycine pendant, (S_p)-**79**.

Table 3 Survey of the ligands in the Pd-catalyzed allylic alkylation.[a]

Entry	Ligand	Conversion (%)	*ee* (%) [Configuration]
1	(*S*)-**76**	100	85 [*S*]
2	(*R*)-**76**	100	84 [*R*]
3	(*S*)-**77**	23	24 [*S*]
4	(*R*)-**77**	25	26 [*R*]
5	(*S*)-**78**	56	67 [*S*]
6	(*R*)-**78**	92	66 [*R*]
7	(*S*)-**87**	93	65 [*S*]
8	(*S*,*S*)-**88**	53	11 [*S*]
9	(S_p)-**79**	81	85 [*R*]
10	(*S*,S_p)-**80**	55	52 [*R*]
11	(*R*,S_p)-**80**	34	83 [*R*]
12	(*S*,R_p)-**83**	43	85 [*S*]
13	(*S*,S_p)-**81**	80	60 [*R*]
14	(*R*,S_p)-**81**	12	57 [*R*]
15	(*S*,S_p)-**82**	51	65 [*R*]
16	(*R*,S_p)-**82**	15	58 [*R*]

[a] Reaction conditions: **89** (0.25 mmol), dimethyl malonate (0.75 mmol), BSA (0.75 mmol), $[Pd(\mu\text{-}Cl)(\eta^3\text{-}C_3H_5)]_2$ (6.3 μmol, i.e. 5.0 mol.-%), ligand (12.5 μmol, i.e. 5.0 mol.-%), CH_2Cl_2 (3 mL), room temperature, reaction time 24 h. The results are averages of two independent runs.

The most catalytic active ligand (*S*)-**76** was further studied in allylic substitution using *N*- and *O*-nucleophiles (Scheme 32). Allylic amination of **89** with benzylamine in the presence of BSA gave only racemic product **91** (96% conversion after 2 days). When the reaction was carried out without any base added, it gave only a poor enantioselectivity and conversion (13% *ee*, 29% conversion after 2 days). A related etherification reaction with

benzyl alcohol either in the presence of base or with no added base did not proceed at all (Scheme 32).

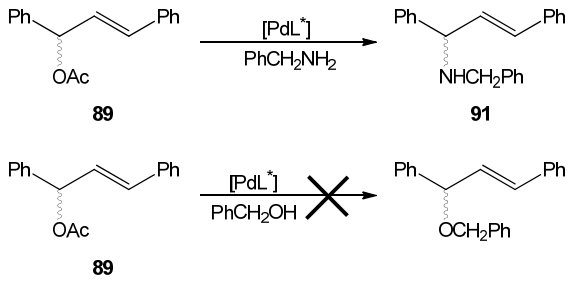

Scheme 32 Other tested Pd-catalyzed allylic substitution reactions.

Unfortunately, repeated attempts to synthesize well-defined (solid) (η^3-1,3-diphenylallyl)palladium complexes from (*S*)-**76** failed. Thus, we decided to study the reactions in a similar system featuring the achiral model ligand **59** in a solution by NMR and electrospray mass techniques (for details see Appendix 2).

Since subsequent attempts to prepare crystalline materials either from [(η^3-$Ph_2C_3H_3$)PdCl(**59**)] or [(η^3-$Ph_2C_3H_3$)Pd(**59**)]ClO_4 were also unsuccessful, we focused on (η^3-methallyl)palladium complexes containing ligand **59** (Scheme 33). A bridge cleavage reaction between dimeric palladium precursor **92** and **59** cleanly afforded complex **94**. Halide removal from dimer **92** in acetonitrile yielded solvento complex **93**, from which cationic complexes **95** and **96** were obtained after addition of one or two molar equivalents

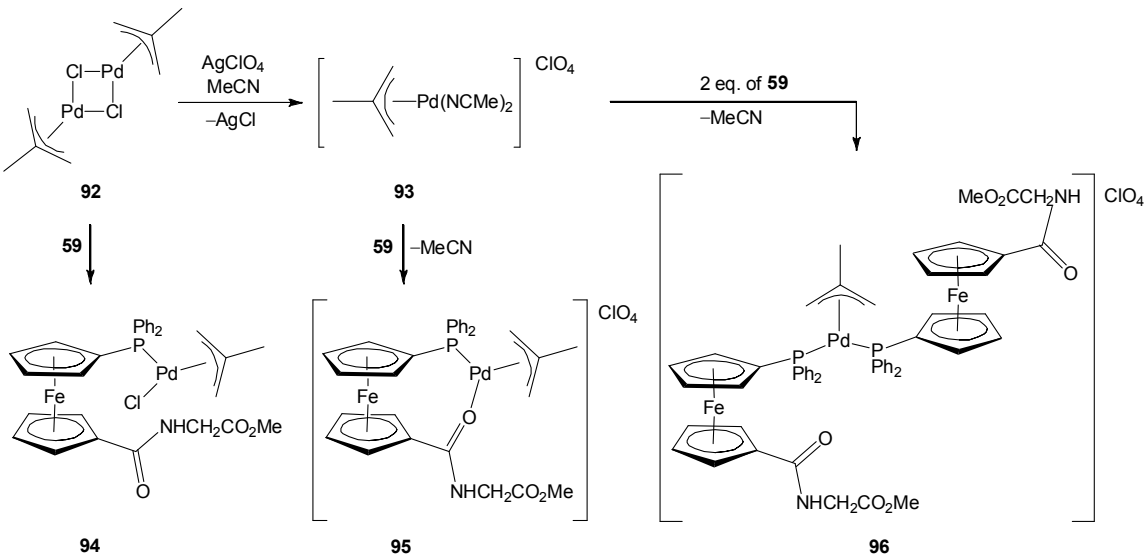

Scheme 33 Preparation of model (η^3-methallyl)palladium complexes featuring ligand **59**.

of ligand **59**. All synthesized complexes were characterized by the standard spectroscopic methods and the molecular structures of **93**–**95** were determined by single-crystal X-ray crystallography. This model coordination study expectedly demonstrated that the amidophosphine ligands coordinate the soft palladium(II) ion preferentially via their soft *P*-donor site. However, at 1:1 ligand-to-metal ratio they form *P*,*O*-chelates. It is the chelate coordination that plays a key role in determining catalytic efficacy of these donors as it brings chirality of the ligand into proximity to the catalytically active metal ion.

The subsequent work (Appendix 3) was focused on the preparation of three series of (η^6-arene)Ru(II) complexes (Scheme 34) containing the previously described Hdpf-Gly conjugates[95] (**59**–**61**). The diruthenium precursors [(η^6-arene)$RuCl_2$]$_2$ reacted smoothly with **59** yielding the bridge cleavage products **97a-c**, in which the ferrocene ligands coordinated as *P*-monodentate donors. The related neutral complex **98b** was obtained from bis-amide **60** by a similar procedure. In contrast, attempts to synthesize complex **99b** from the free acid **61** failed due to the side reaction and problems with isolation of **99b** from the reaction mixture. Subsequent halide removal from **97a-c** with two equivalents of Ag[PF_6] in acetonitrile solution afforded bis-acetonitrile complexes **101a-c** as hexafluorophosphate salts. The monocationic complexes **100a-c** were obtained by reaction of ligand **59** with the

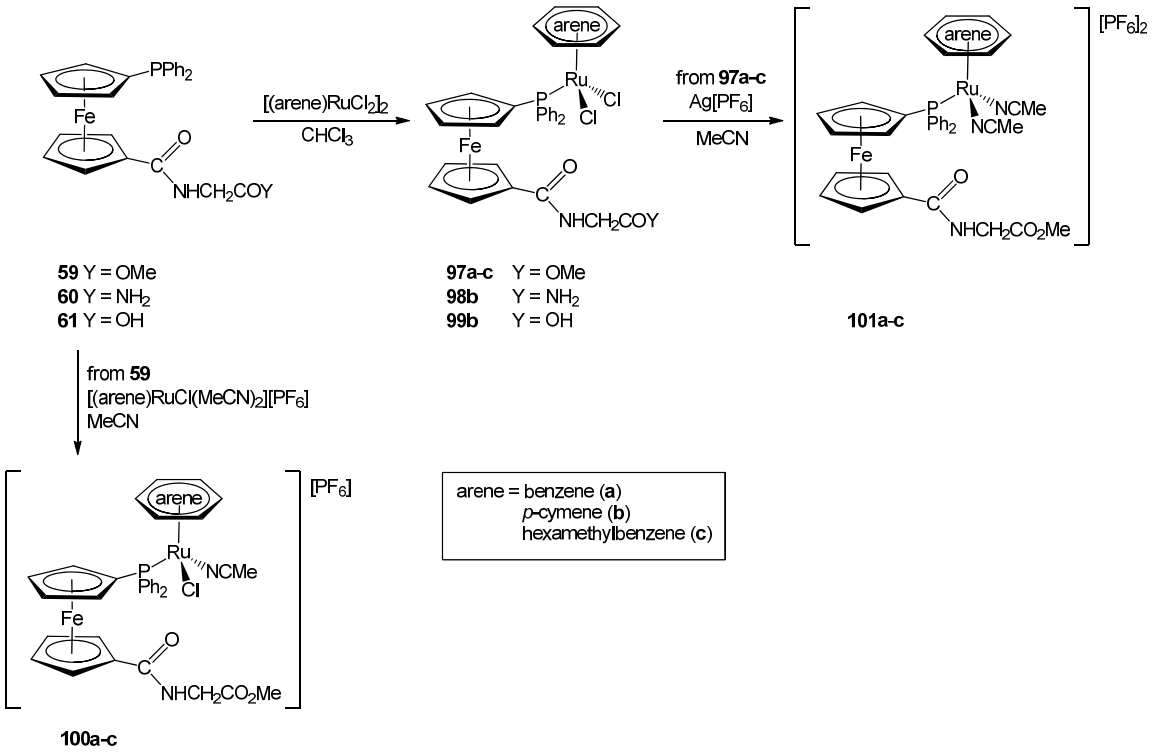

Scheme 34 Preparation of (η^6-arene)Ru(II)-complexes with ferrocene amido-phosphines.

respective solvento complex [(η^6-arene)RuCl(MeCN)$_2$][PF_6] via displacement of the coordinated acetonitrile. Alternative synthetic routes to complexes **100b** and **101b** have been also studied (see Appendix 3).

The Ru(II) complexes were characterized by spectroscopic techniques (multinuclear NMR, MS and IR), elemental analysis and the crystal structures of two representatives (**97b** and **101b**) were determined by X-ray crystallography. In addition, the electrochemical properties of the complexes were studied by cyclic voltammetry at a Pt-disc electrode.

All arene-ruthenium complexes possessing the ferrocenyl donors were further tested as defined pre-catalysts in the oxidation of secondary alcohols to ketones, which is another important reaction both for laboratory syntheses and industry.[103] The most easily accessible ruthenium-iron compound **97b** was firstly used to find optimal catalytic conditions for the oxidation of 1-phenylethanol **102** as a model substrate with *t*-BuOOH in pure water (Scheme 35, for complete results see Appendix 3). Oxidation proceeded even at very low catalyst loading (66% conversion after 5 h with 0.001 mol.-% of this Ru catalyst). The complete conversion of starting alcohols was reached within 24 h.

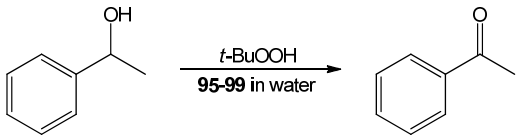

102 **103**

Scheme 35 Oxidation of 1-phenylethanol to acetophenone with *t*-BuOOH.

As a next step, the whole series of (η^6-arene)ruthenium complexes was evaluated in oxidation 1-phenylethanol 102 **to acetophenone** 103 **with substrate to catalyst ratio of 100 000:1 (**

Table 4). The most active catalyst **97b** showed an excellent catalytic turnover frequency of 13 200 h^{-1}, whereas oxidation reaction under the same conditions without the presence of Ru-catalyst did not proceed at all. The conversions were complete for all catalysts in 24 h but, on the other hand, the conversions after 5 h were found to depend on the structure of the pre-catalysts (conversion between 28%–66%). This observation could reflect easy of the conversion of the defined pre-catalysts into the true catalytically active species.

Table 4 Catalytic activity of ruthenium–iron complexes.[a]

Entry	Catalyst	Conversion after 5 h/24 h (%)	TON after 24 h	TOF after 5 h (h^{-1})
1	**97a**	30/99	99 000	6 000
2	**97b**	66/100	100 000	13 200
3	**97c**	45/100	100 000	9 000
4	**98b**	41/99	99 000	8 200
5	**100a**	61/100	100 000	12 200
6	**100b**	53/99	99 000	10 600
7	**100c**	61/100	100 000	12 200
8	**101a**	35/100	100 000	7 000
9	**101b**	38/99	99 000	7 600
10	**101c**	28/100	100 000	5 600
11	none	0/0	0	0

[a] Reaction conditions: **102** (1.0 mmol), *t*-BuOOH (4.0 mmol), catalyst (0.01 μmol; i.e. 0.001 mol.-%), water (4 mL), room temperature, reaction time 5 or 24 h.

Following work was concerned with a kinetic study and possible dependence of turnover number on pH of the reaction mixture (Figure 1). The best results were obtained at pH ca. 5.5-7.0. This may indicate that aquation reaction plays an important role and that an aqua complex might be a real entry to the catalytic cycle. The kinetic study did not demonstrate a significant induction period. Moreover, time dependence of the conversion was in a good accordance with (pseudo) first–order kinetics.

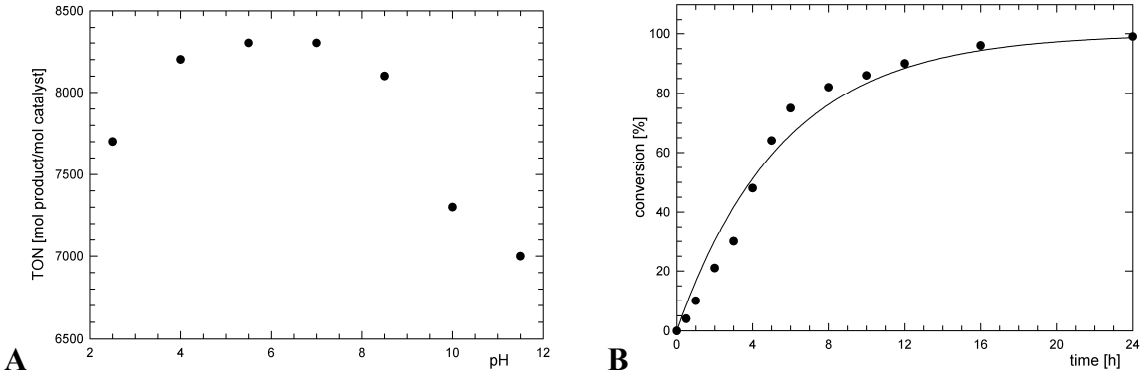

Figure 1 pH dependence of TON (A) and kinetic profile (B) for oxidation of **102** with *t*-BuOOH catalyzed by **97b**.

Catalyst **97b** was then tested for oxidation **102** in various organic solvent or in their biphasic mixtures with water and also with various oxidizing agents replacing *t*-BuOOH (see Appendix 3). However, all catalytic results were considerably worse. Finally, catalytic study included tests of various secondary alcohols (Table 5). Complex **97b** showed at 0.001 mol.-% loading excellent catalytic properties for most substrates, the exception being 1-(4-methoxyphenyl)-, sterically hindered 1-(2-bromophenyl)ethanol and aliphatic secondary alcohols.

Table 5 Oxidation of various secondary alcohols in the presence of catalyst **97b**.[a]

Entry	Substrate	Product	Conversion after 5 h/24 h (%)	Isolated yield (%)
1	1-phenylethanol	acetophenone	66/100	93
2	1-(4-fluorophenyl)ethanol	4´-fluoroacetophenone	46/99	92
3	1-(4-chlorophenyl)ethanol	4´-chloroacetophenone	53/100	90
4	1-(4-bromoophenyl)ethanol	4´-bromoacetophenone	67/100	91
5	1-(4-methylphenyl)ethanol	4´-metnylacetophenone	62/99	90
6	1-(4-methoxyphenyl)ethanol	4´-methoxyacetophenone	44/70	n.d.
7	1-(3-bromophenyl)ethanol	3´-bromoacetophenone	47/99	92
8	1-(2-bromophenyl)ethanol	2´-bromoacetophenone	8/35	n.d.
9	1-(2-naphthyl)ethanol	2´-acetonaphthone	53/100	91
10	1-cyclohexanol	hexahydroacetophenone	13/36	n.d.
11	diphenylmethanol	benzophenone	77/100	94
12	1-indanol	1-indanone	67/99	90
13	1-tetralol	1-tetralone	61/99	89
14	cyclohexanol	cyclohexanone	14/55	n.d
15	2-butanol	2-butanone	8/29	n.d.

[a] For reaction conditions, see Table 4, footnote *a*.

The last article included in this Thesis deals with the preparation of new ferrocene-containing amino acid (Appendix 4). While seeking for an alternative synthetic method affording ferrocene-based amino acid conjugates, we have applied the procedure reported by Osakada.[104] Compound **105** was thus obtained by condensation reaction of diol **104**

with glycine methyl ester catalyzed by $[RuCl_2(PPh_3)_3]$ at 170 °C in *N*-methylpyrrolidone (Scheme 36). Apart from **105**, a small amount of 2-oxa[3]ferrocenophane (dehydration product of the starting **102**) was also isolated. Conjugate **105** was characterized by the conventional spectroscopic methods, elemental analysis and its crystal structure was determined by X-ray analysis. Electrochemical properties were studied by cyclic voltammetry. Subsequent alkylation reaction of compound **105** with an excess of methyl iodide yielded only the starting unreacted conjugate **105**. On the other hand, treatment of **105** with 2,4,6-trinitrophenol afforded defined crystalline picrate **106** (Scheme 36).

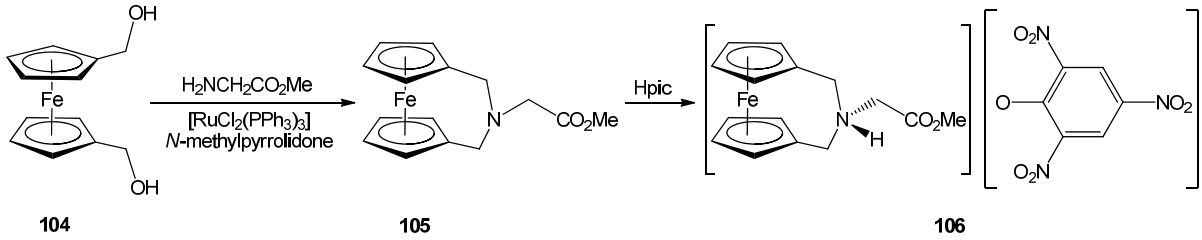

104 105 106

Scheme 36 Preparation of aza[3]ferrocenophane **105** and its picrate salt **106** (Hpic = 2,4,6-trinitrophenol).

8 Conclusion

Amide coupling of 1'-(diphenylphosphino)ferrocene-1-carboxylic acid (Hdpf) or its planar-chiral 1,2-isomers with amino acid methyl esters as common chiral pool molecules smoothly affords novel phosphinoferrocene-carboxamides in extensive series. These easy-to-synthesize compounds were characterized by standard techniques (NMR, IR, MS) and the crystal structure of one representative was determined by X-ray crystallography.

A library of structurally related amidophosphines combining chirality at the ferrocene fragment with that of the amino acid moiety were utilized as ligands in Cu-mediated asymmetric additions of diethylzinc to chalcones. Donors derived from Hdpf were found to be better catalyst components than their 1,2-counterparts. According to the data available from the coordination study of model glycine donor and Cu precursor in solution and in the solid-state, it is the chelate coordination, which determines catalytic efficiency by bringing the chirality from the amino acid side chain to the proximity of catalytically active metal center, while the ligand remains firmly bound through the phosphine group.

The phosphinoferrocene ligands were further successfully tested in palladium-catalyzed asymmetric allylic alkylation of 1,3-diphenylallyl acetate with dimethyl malonate. The Hdpf derivatives showed again better results then the respective 1,2-counterparts. On the other hand, these ligands performed only poorly in the related allylic amination or did not produce any substitution product in the etherification reaction. The model coordination study expectedly confirmed hybrid nature of these ligands. Amido-phosphines preferentially coordinate palladium(II) via their soft phosphor-donor site. However, at 1:1 metal-to-ligand ratio they form chelates (*P*,*O*- or *P*,*N*-). The coordination of two different atom leads to an electronic differentiation of allylic termini in the plausible (η^3-allyl)palladium reaction intermediates. At 1:2 metal-to-ligand ratio, a bis(phosphine) complex is formed where the amino acid chirality is located far from the metal center. This explains why Hdpf-based ligands at this Pd/L ratio produced only racemic alkylation products. The situation with 1,2-isomers is more complicated. Donors groups are situated closer to each other, which may result in sterically crowded intermediates and a diminished preference for a single reaction intermediate.

Heterobimetallic Fe(II)-Ru(II) complexes were easily obtained from (η^6-arene)precursors and the respective glycine-ferrocene conjugates. These complexes were

characterized by multinuclear NMR, IR, MS spectroscopy, elemental analysis and the structure of two representatives was established by single-crystal X-ray diffraction analysis. The coordination study demonstrated that phosphino-carboxamides coordinate to (η^6-arene)ruthenium species strictly in monodentate fashion via the *P*-donor site. The resulting complexes served as highly active pre-catalysts for catalytic oxidation of secondary alcohols with *t*-BuOOH in aqueous media. The oxidation reaction proceed cleanly and rapidly even at catalyst-to-metal ratio 1:100 000. Additional, electrochemical studies on these complexes revealed an electronic communication between the metal centers.

Finally, a new type of amino acid-ferrocene conjugate was synthesized by condensation of 1,1'-bis(hydroxymethyl)ferrocene and glycine methyl ester. The resulting 2-[(methoxycarbonyl)methyl]-2-aza[3]ferrocenophane was structurally characterized. The cyclic voltammogram of this compound displayed single one-electron reversible oxidation.

9 References

1 M. W. Roberts, *Catal. Lett.* **2000**, *67*, 1.

2 For basic informations, see <*http://en.wikipedia.org/wiki/Limonene*> (retrieved on May 20, 2012).

3 FDA'S policy statement for the development of new stereoisomeric drugs, *Chirality* **1992**, *4*, 338.

4 Nobel lectures: (a) W. S. Knowless, *Angew. Chem. Int. Ed.* **2002**, *41*, 1998. (b) R. Noyori, *Angew. Chem. Int. Ed.* **2002**, *41*, 2008. (c) K. B. Sharpless, *Angew. Chem. Int. Ed.* **2002**, *41*, 2024.

5 Nobel lectures: (a) R. H. Grubbs, *Angew. Chem. Int. Ed.* **2006**, *45*, 3760. (b) R. R. Schrock, *Angew. Chem. Int. Ed.* **2006**, *45*, 3748. (c) Y. Chauvin, *Angew. Chem. Int. Ed.* **2006**, *45*, 3740.

6 Nobel lectures: (a) A. Suzuki, *Angew. Chem. Int. Ed.* **2011**, *50*, 6722. (b) E. Negishi, *Angew. Chem. Int. Ed.* **2011**, *50*, 6738.

7 (a) R. G. Pearson, *J. Am. Chem. Soc.* **1963**, *85*, 3533. (b) R. G. Pearson, *J. Chem. Educ.* **1968**, *45*, 581. (c) R. G. Pearson, *J. Chem. Educ.* **1968**, *45*, 643.

8 J. C. Jeffrey, T. B. Rauchfuss, *Inorg. Chem.* **1979**, *18*, 2658.

9 (a) A. Bader, E. Lindner, *Coord. Chem. Rev.* **1991**, *108*, 27. (b) P. Braunstein, F. Naud, *Angew. Chem. Int. Ed.* **2001**, *40*, 680.

10 (a) S.-Y. Han, Y.-A. Kim, *Tetrahedron* **2004**, *60*, 2447. (b) A. El-Faham, F. Albericio, *Chem. Rev.* **2011**, *111*, 6557.

11 (a) O. Herd, A. Hessler, M. Hingst, M. Tepper, O. Stelzer, *J. Organomet. Chem.* **1996**, *522*, 69. (b) D. J. Brauer, M. Hingst, K. W. Kottsieper, C. Liek, T. Nickel, M. Tepper, O. Stelzer, W. S. Sheldrick, *J. Organomet. Chem.* **2002**, *645*, 14. (c) H. B. Kraatz, A. Pletsch, *Tetraheron: Asymmetry* **2000**, *11*, 1617.

12 S. E. Tunney, J. K. Stille, *J. Org. Chem.* **1987**, *52*, 748.

13 (a) D. J. Brauer, S. Schenk, S. Rossenbach, M. Tepper, O. Stelzer, T. Häusler, W. S. Sheldrick, *J. Organomet. Chem.* **2000**, *598*, 116. (b) D. J. Brauer, K. W. Kottsieper, S. Schenk, O. Stelzer, *Z. Anorg. Allg. Chem.* **2001**, *627*, 1151.

14 (a) J. Heinicke, N. Peulecke, P. G. Jones, *Chem. Commun.* **2005**, *262*. (b) J. Lach, C.-Y. Guo, M. K. Kindermann, P. G. Jones, J. Heinicke, *Eur. J. Org. Chem.* **2010**, 1176.

15 (a) K. Kellner, A. Tzschach, Z. Nagy-Magos, L. Markó, *J. Organomet. Chem.* **1980**, *193*, 307. (b) K. Kellner, W. Hanke, *J. Organomet. Chem.* **1987**, *326*, C9.

16 P. Štěpnička, *Chem. Soc. Rev.* **2012**, *41*, 4273.

17 H. Nozaki, H. Takaya, S. Moriuti, R. Noyori, *Tetrahedron* **1968**, 24, 3655.

18 W. S. Knowles, M. J. Sabacky, *Chem. Commun.* **1968**, 1445.

19 L. Horner, H. Siegel, H. Büthe, *Angew. Chem. Int. Ed.* **1968**, *7*, 942.

20 (a) W. Tank, X. Zhang, *Chem. Rev.* **2003**, *103*, 3029. (b) W. Zhang, Y. Chi, X. Zhang, *Acc. Chem. Res.* **2007**, *40*, 1278. (c) J.-H. Xie, S.-F. Zhu, Q.-L. Zhou, *Chem. Rev.* **2011**, *111*, 1713. (d) D.-S. Wang, Q.-A. Chen, S.-M. Lu, Y.-G. Zhou, *Chem. Rev.* **2012**, *112*, 2557.

21 K. Achiwa, *J. Am. Chem. Soc.* **1976**, *98*, 8265.

22 (a) K. Achiwa, *Chem. Lett.* **1977**, 777. (b) K. Achiwa, T. Kogure, I. Ojima, *Chem. Lett.* **1978**, 297. (c) K. Achiwa, *Chem. Lett.* **1978**, 561. (d) H. Takeda, T. Tachinami, S. Hosokawa, M. Aburatani, K. Inoguchi, K. Achiwa, *Chem. Pharm. Bull.* **1991**, *39*, 2706.

23 (a) H. Takahashi, T. Morimoto, K. Achiwa, *Chem. Lett.* **1987**, 855. (b) S. Sakubara, H. Takahashi, H. Takeda, K. Achiwa, *Chem. Pharm. Bull.* **1995**, *43*, 738.

24 I. Ojima, T. Kogure, N. Yoda, T. Suzuki, M. Yatabe, T. Tanaka, *J. Org. chem.* **1982**, *47*, 1329.

25 (a) K. Achiwa, Y. Ohga, Y. Iitaka, *Chem. Lett.* **1979**, 865. (b) I. Ojima, T. Kogure, *Chem. Lett.* **1979**, 641. (c) I. Ojima, T. Kogure, N. Yoda, *J. Org. Chem.* **1980**, *45*, 4728.

26 K. Achiwa, *Chem. Lett.* **1978**, 905.

27 (a) G. L. Baker, S. J. Fritschel, J. R. Stille, J. K. Stille, *J. Org. Chem.* **1981**, *46*, 2954. (b) G. L. Baker, S. J. Fritschel, J. K. Stille, *J. Org. Chem.* **1981**, *46*, 2960. (c) M. T. Zarka, O. Nuyken, R. Weberskirch, *Chem. Eur. J.* **2003**, *9*, 3228. (d) N. Ishizuka, M. Togashi, M. Inoue, S. Enomoto, *Chem. Pharm. Bull.* **1987**, *35*, 1686.

28 F. Joó, E. Trócsányi, *J. Organomet. Chem.* **1982**, *231*, 63.

29 A. C. Laungani, B. Breit, *Chem. Commun.* **2008**, 844.

30 S. R. Gilbertson, G. Chen, M. McLounghlin, *J. Am. Chem. Soc.* **1994**, *116*, 4481.

31 (a) S. R. Gilbertson, R. V. Pawlick, *Angew. Chem. Int. Ed.* **1996**, *35*, 902. (b) S. J. Greenfield, S. R. Gilbertson, *Synthesis* **2001**, 2337.

32 S. R. Gilbertson, G. W. Starkey, *J. Org. Chem.* **1996**, *61*, 2922.

33 (a) S. R. Gilbertson, X. Wang, *Tetrahedron Lett.* **1996**, *37*, 6475. (b) S. R. Gilbertson, X. Wang, G. S. Hoge, C. A. Klug, J. Schaefer, *Organometallics* **1996**, *15*, 4678. (c) S. R. Gilbertson, X. Wang, *Tetrahedron* **1999**, *55*, 11609. (d) S. R. Gilbertson, X. Wang, *J. Org. Chem.* **1996**, *61*, 434.

34 (a) T. Hayashi in *Catalytic Asymmetric Synthesis*, ed. I. Ojima, ch. 7.1, pp. 325-365, VCH, New York 1993. (b) B. M. Trost, D. L. Van Vranken, *Chem. Rev.* **1996**, *96*, 395. (c) B. M. Trost, M. L. Crawley, *Chem. Rev.* **2003**, *103*, 2921. (d) I. G. Rios, A. Rosas-Hernandez, E. Martin, *Molecules* **2011**, *16*, 970.

35 B. M. Trost, M. R. Machacek, A. Aponick, *Acc. Chem. Res.* **2006**, *39*, 747.

36 (a) S. R. Gilbertson, S. E. Collibee, A. Agarkov, *J. Am. Chem. Soc.* **2000**, *122*, 6522. (b) S. R. Gilbertson P. Lan, *Org. Lett.* **2001**, *3*, 2237. (c) A. Agarkov, E. W. Uffman, S. R. Gilbertson, *Org. Lett.* **2003**, *5*, 2091. (d) S. J. Greenfield, A. Agarkov, S. R. Gilbertson, *Org. Lett.* **2003**, *5*, 3069. (e) A. Agarkov, S. J. Greenfield, T. Ohishi, S. E. Collibee, S. R. Gilbertson, *J. Org. Chem.* **2004**, *69*, 8077. (f) S. R. Gilbertson, S. Yamada, *Tetrahedron Lett.* **2004**, *45*, 3917. (g) A. Agarkov, S. R. Gilbertson, *Tetraheron Lett.* **2005**, *46*, 181.

37 A. Agarkov, S. Greenfield, D. Xie, R. Pawlick, G. Starkey, S. R. Gilbertson, *Biopolymers* **2006**, *84*, 48.

38 C. A. Christensen, M. Meldal, *Chem. Eur. J.* **2005**, *11*, 4121.

39 C. A. Christensen, M. Meldal, *J. Comb. Chem.* **2007**, *9*, 79.

40 A. Saitoh, M. Misawa, T. Morimoto, *Tetrahedron: Asymmetry* **1999**, *10*, 1025.

41 A. Saitoh, T. Morimoto, K. Achiwa, *Tetrahedron: Asymmetry* **1997**, *8*, 3567.

42 (a) A. Saitoh, T. Uda, T. Morimoto, *Tetrahedron: Asymmetry* **1999**, *10*, 4501. (b) A. Saitoh, K. Achiwa, K. Tanaka, T. Morimoto, *J. Org. Chem.* **2000**, *65*, 4227. (c) A. Saitoh, T. Uda, T. Morimoto, *Tetrahedron: Asymmetry* **2000**, *11*, 4049.

43 J. A. Sehnem, P. Milani, V. Nascimento, L. H. Andrade, L. Dorneles, A. L. Braga, *Tetrahedron: Asymmetry* **2010**, *21*, 997.

44 I. T. Horváth, J. Rábai, *Science* **1994**, *266*, 72.

45 (a) Y.-H. Lee, Y. K. Kim, J.-H. Son, K. H. Ahn, *Bull. Korean Chem. Soc.* **2003**, *24*, 225. (b) V. R. Marinho, A. I. Rodrigues, A. J. Burke, *Tetrahedron: Asymmetry* **2008**,

19, 454. (c) T. Mino, K. Kashihara, M. Yamashita, *Tetrahedron: Asymmetry* **2001**, *12*, 287.

46 (a) B. E. Rossiter, N. M. Swingle, *Chem. Rev.* **1992**, *92*, 771. (b) M. P. Sibi, S. Manyem, *Tetrahedron* **2000**, *56*, 8033. (c) N. Krause, A. Hoffmann-Röder, *Synthesis* **2001**, 171. (d) B. L. Feringa, R. Naasz, R. Imbos, L. A. Arnold in *Modern Organocopper Chemistry*, ed. N. Krause, ch. 7, pp. 224-258, Wiley-VCH, Weinheim, 2002. (e) A. Alexakis, C. Benhaim, *Eur. J. Org. Chem.* **2002**, 3221. (f) F. López, A. J. Minnaard, B. L. Feringa, *Acc. Chem. Res.* **2007**, *40*, 179. (g) A. Alexakis, J. E. Bäckvall, N. Krause, O. Pàmies, M. Diéguez, *Chem. Rev.* **2008**, *108*, 2796. (h) S. R. Harutyunyan, T. den Hartog, K. Geurts, A. J. Minnaard, B. L. Feringa, *Chem. Rev.* **2008**, *108*, 2824. (i) T. Jerphagnon, M. G. Pizzuti, A. J. Minnaard, B. L. Feringa, *Chem. Soc. Rev.* **2009**, *38*, 1039.

47 B. Breit, A. C. Laungani, *Tetrahedron: Asymmetry* **2003**, *14*, 3823.

48 A. W. Hird, A. H. Hoveyda, *Angew. Chem. Int. Ed.* **2003**, *42*, 1276.

49 J. M. García, A. González, B. G. Kardak, J. M. Odriozola, M. Oiarbide, J. Razkin, C. Palomo, *Chem. Eur. J.* **2008**, *14*, 8768.

50 (a) A. V. Malkov, J. B. Hand, P. Kočovský, *Chem. Commun.* **2003**, 1948. (b) T. Morimoto, Y. Yamaguchi, M. Suzuki, A. Saitoh, *Tetraheron Lett.* **2000**, *41*, 10025.

51 (a) J. K. Stille, G. Parrinello, *J. Mol. Catal.* **1983**, *21*, 203. (b) G. Parrinello, J. K. Stille, *J. Am. Chem. Soc.* **1987**, *109*, 7122.

52 A. C. Laungani, J. M. Slattery, I. Krossing, B. Breit, *Chem. Eur. J.* **2008**, *14*, 4488.

53 S. Gladiali, E. Alberico, *Chem. Soc. Rev.* **2006**, *35*, 226.

54 M. Quirmbach, J. Holz, V. I. Tatarov, A. Börner, *Tetrahedron* **2000**, *56*, 775.

55 B. J. Cowen, S. J. Miller, *J. Am. Chem. Soc.* **2007**, *129*, 10988.

56 (a) J. R. Dilworth, S. J. Parrott, *Chem. Soc. Rev.* **1998**, *27*, 43. (b) S. S. Jurisson, J. D. Lydon, *Chem. Rev.* **1999**, *99*, 2205. (c) S. Liu, D. S. Edwards, *Chem. Rev.* **1999**, *99*, 2235. (d) Y. Arano, *J. Nucl. Radiochem. Sci.* **2005**, *6*, 177.

57 B. Lambert, J. M. H. de Klerk, *Nucl. Med. Commun.* **2006**, *27*, 223.

58 M. Santimaria, T. Maina, U. Mazzi, M. Nicolini, *Inorg. Chim. Acta* **1995**, *240*, 291.

59 M. Santimaria, U. Mazzi, S. Gatto, A. Dolmella, G. Bandoli, M. Nicolini, *J. Chem. Soc., Dalton, Trans.* **1997**, 1765.

60 M. Santimaria, D. Blok, R. I. J. Feitsma, U. Mazzi, E. K. J. Pauwels, *Nucl. Med. Biol.* **1999**, *26*, 251.

61 R. Visentin, R. Rossin, M. C. Giron, A. Dolmella, G. Bandoli, U. Mazzi, *Inorg. Chem.* **2003**, *42*, 950.

62 R. Visentin, M. C. Giron, M. Bello, U. Mazzi, *Nucl. Med. Biol.* **2004**, *31*, 655.

63 R. Visentin, G. Pasut, F. M. Veronese, U. Mazzi, *Bioconjugate Chem.* **2004**, *15*, 1046.

64 L. Meléndez-Alafort, A. Nadali, G. Pasut, E. Zangoni, R. De Caro, L. Cariolato, M. C. Giron, I. Castagliuolo, F. M. Veronese, U. Mazzi, *Nucl. Med. Biol.* **2009**, *36*, 57.

65 L. Latapie, J. Le Gal, B. Hamaoui, J. Jaud, M. Gressier, E. Benoist, *Polyhedron* **2007**, *26*, 5185.

66 A. Purohit, S. Liu, D. Casebier, D. S. Edwards, *Bioconjugate Chem.* **2003**, *14*, 720.

67 M. Riondato, D. Camporese, D. Martín, J. Suades, A. Alvarez-Larena, U. Mazzi, *Eur. J. Inorg. Chem.* **2005**, 4048.

68 T. J. Kealy, P. L. Pauson, *Nature* **1951**, *168*, 1039.

69 S. A. Miller, J. A. Tebboth, J. F. Tremaine, *J. Chem. Soc., Dalton Trans.* **1952**, 632.

70 E. O. Fischer, W. Pfab, *Z. Naturforsch.* **1952**, *7b*, 377.

71 G. Wilkinson, M. Rosenblum, M. C. Whiting, R. B. Woodward, *J. Am. Chem. Soc.* **1952**, *74*, 2125.

72 (a) *Ferrocenes: Ligands, Materials and Biomolecules*, ed. P. Štěpnička, Wiley, Chichester, 2008. (b) *Ferrocenes: Homogeneous Catalysis, Organic Synthesis, Materials Science*, eds. A. Togni, T. Hayashi, VCH, Weinheim, 1995.

73 D. Enders, R. Lochtman, G. Raabe, *Synlett* **1996**, 126.

74 J. Wright, L. Frambes, P. Reeves, *J. Organomet. Chem.* **1994**, *476*, 215.

75 T. Hayashi, K. Yamamoto, M. Kumada, *Tetrahedron Lett.* **1974**, *15*, 4405.

76 D. Marquarding, H. Klusacek, G. Gokel, P. Hoffmann, I. Ugi, *J. Am. Chem. Soc.* **1970**, *92*, 5389.

77 F. Rebière, O. Riant, L. Ricard, H. B. Kagan, *Angew. Chem. Int. Ed.* **1993**, *32*, 568.

78 O. Riant, O. Samuel, H. B. Kagan, *J. Am. Chem. Soc.* **1993**, *115*, 5835.

79 (a) T. Sammakia, H. A. Latham, D. R. Schaad, *J. Org. Chem.* **1995**, *60*, 10. (b) C. J. Richards, A. W. Mulvaney, *Tetrahedron: Asymmetry* **1996**, *7*, 1419

80 D. Enders, R. Peters, R. Lochtman, J. Runsink, *Synlett* **1997**, 1462.

81 (a) G. P. Sollot, J. L. Snead, S. Portnoy, W. R. Peterson Jr., H. E. Mertwoy *U. S. Dept. Com., Office Tech. Serv., PB Rep.* **1965**, vol. II, pp. 441-452; *Chem. Abstr.* **1965**, *63*, 18174. (b) For comprehensive reviews on dppf chemistry, see: S. W. Chien, T. S. A. Hor, *The Coordination and Homogeneous Catalytic Chemistry of 1,1'-Bis(diphenylphophino)ferrocene and its Chalcogenide derivatives* in ref. 72a, ch. 2, pp. 33-116. (c) T. J. Colacot *Platinum Met. Rev.* **2001**, *45*, 22. (d) G. Bandoli, A. Dolmella *Coord. Chem. Rev.* **2000**, *209*, 161. (e) K.-S. Gan, T. S. A. Hor, *1,1'-Bis(diphenylphophino)ferrocene – Coordination Chemistry, Organic Syntheses, and Catalysis* in ref. 72b, ch. 1, pp. 3-104.

82 A. Togni, C. Breutel, A. Schnyder, F. Spindler, H. Landert, A. Tijani, *J. Am. Chem. Soc.* **1994**, *116*, 4062.

83 H-U. Blaser, W. Chen, F. Camponovo, A. Togni, *Chiral 1,2-Disubstituted Ferrocene Diphosphines for Asymmetric Catalysis* in ref. 72a, ch. 6, pp.205-235.

84 P. Štěpnička, H. Solařová, M. Lamač, I. Císařová, *J. Organomet. Chem.* **2010**, *695*, 2423.

85 J. E. Kingston, L. Ashford, P. D. Beer, M. G. B. Drew, *J. Chem. Soc., Dalton, Trans.* **1999**, 251.

86 J. Podlaha, P. Štěpnička, J. Ludvík, I. Císařová, *Organometallics* **1996**, *15*, 543.

87 L. Meca, D. Dvořák, J. Ludvík, I. Císařová, P. Štěpnička, *Organometallics* **2004**, *23*, 2541.

88 (a) J. Kühnert, M. Dušek, J. Demel, H. Lang, P. Štěpnička, *Dalton Trans.* **2007**, 2802. (b) J. Kühnert, I. Císařová, M. Lamač, P. Štěpnička, *Dalton Trans.* **2008**, 2454.

89 P. Štěpnička, M. Krupa, M. Lamač, I. Císařová, *J. Organomet. Chem.* **2009**, *694*, 2987.

90 (a) C. A. Bessel, P. Aggarwal, *Chem. Rev.* **2001**, *101*, 1031. (b) Z. Freixa, P. W. N. M. van Leeuwen, *Coord. Chem. Rev.* **2008**, *252*, 1755.

91 P. Štěpnička, H. Solařová, I. Císařová, *J. Organomet. Chem*. **2011**, *696*, 3727.

92 (a) J. Schulz, I. Císařová, P. Štěpnička, *J. Organomet. Chem.* **2009**, *694*, 2519. (b) J. Schulz, I. Císařová, P. Štěpnička, *Organometallics* **2012**, *31*, 729.

93 (a) J. Schulz, A. K. Renfrew, I. Císařová, P. J. Dyson, P. Štěpnička, *Appl. Organomet. Chem.* **2010**, *24*, 392.

94 J. Kühnert, M. Lamač, J. Demel, A. Nicolai, H. Lang, P. Štěpnička, *J. Mol. Catal. A: Chem.* **2008**, *285*, 41.

95 J. Tauchman, I. Císařová, P. Štěpnička, *Organometallics* **2009**, *28*, 3288.

96 J. F. Jensen, I. Søtofte, H. O. Sørensen, M. Johannsen, *J. Org. Chem.* **2003**, *68*, 1258.

97 N. W. Boaz, J. A. Ponasik, S. E. Large, S. D. Debenham, *Tetrahedron: Asymmetry* **2004**, *15*, 2151.

98 P. Štěpnička, *Eur. J. Inorg. Chem.* **2005**, 3787.

99 (a) M. Lamač, I. Císařová, P. Štěpnička, *Eur. J. Inorg. Chem.* **2007**, 2274. (b) M. Lamač, I. Císařová, P. Štěpnička, *New J. Chem.* **2009**, *33*, 1549.

100 M. Lamač, J. Tauchman, I. Císařová, P. Štěpnička, *Organometallics* **2007**, *26*, 5042.

101 M. Lamač, J. Tauchman, S. Dietrich, I. Císařová, H. Lang, P. Štěpnička, *Appl. Organomet. Chem.* **2010**, *24*, 326.

102 (a) P. Štěpnička, *New J. Chem.* **2002**, *26*, 567. (b) B. Breit, D. Breuninger, *Synthesis* **2005**, 2782.

103 *Comprehensive Organic Transformations*, R. C. Larock, VCH, New York, 1999.

104 K. Osakada, T. Sakano, M. Horie, Y. Suzaki, *Coord. Chem. Rev.* **2006**, *250*, 1012.

10 List of Appendices

1) J. Tauchman, I. Císařová, P. Štěpnička: "Chiral Phosphanylferrocene-carboxamides with Amino Acid Pendant Groups as Ligands for Cu-Mediated Asymmetric Conjugate Additions of Diethylzinc to Chalcones – Structural Characterisation of Precursors to the Cu Catalyst." *Eur. J. Org. Chem.* **2010**, 4276.

2) J. Tauchman, I. Císařová, P. Štěpnička: "Chiral phosphinoferrocene carboxamides with amino acid substituents as ligands for Pd-catalysed asymmetric allylic substitutions. Synthesis and structural characterisation of catalytically relevant Pd complexes." *Dalton Trans.* **2011**, *40*, 11748.

3) J. Tauchman, B. Therrien, G. Süss-Fink, P. Štěpnička: "Heterodinuclear Arene Ruthenium Complexes Containing a Glycine-Derived Phosphinoferrocene Carboxamide: Synthesis, Molecular Structure, Electrochemistry, and Catalytic Oxidation Activity in Aqueous Media." *Organometallics* **2012**, *31*, 3985.

4) J. Tauchman, P. Štěpnička: "Preparation and structural characterisation of a novel ferrocene–amino acid conjugate." *Inorg. Chem. Commun.* **2010**, *13*, 14.

10.1 Appendix 1

J. Tauchman, I. Císařová, P. Štěpnička: "Chiral Phosphanylferrocene-carboxamides with Amino Acid Pendant Groups as Ligands for Cu-Mediated Asymmetric Conjugate Additions of Diethylzinc to Chalcones – Structural Characterisation of Precursors to the Cu Catalyst." *Eur. J. Org. Chem.* **2010**, 4276.

DOI: 10.1002/ejoc.201000480

Chiral Phosphanylferrocenecarboxamides with Amino Acid Pendant Groups as Ligands for Cu-Mediated Asymmetric Conjugate Additions of Diethylzinc to Chalcones – Structural Characterisation of Precursors to the Cu Catalyst

Jiří Tauchman,[a] Ivana Císařová,[a] and Petr Štěpnička*[a]

Keywords: Phosphanylferrocene ligands / Amino acids / Amides / Copper / Asymmetric synthesis / Conjugate addition

A series of chiral phosphanylferrocenecarboxamides was prepared by treatment of either 1′-(diphenylphosphanyl)-ferrocene-1-carboxylic acid (Hdpf) or its planar-chiral 1,2-isomers with amino acid methyl esters in the presence of peptide coupling agents. The compounds were characterised by spectroscopic methods, and the crystal structure of one representative was determined by X-ray diffraction. Catalytic testing of these donors in Cu-catalysed asymmetric conjugate additions of diethylzinc to chalcones revealed that the reaction outcomes were highly sensitive to the ligand structure and the reaction conditions (copper source and solvent), whereas the chalcone substituents (Me, MeO, or Cl in positions 4 or 4′) had a less pronounced influence. Compounds based on Hdpf proved to be better ligands than their planar-chiral analogues. Under optimised conditions, the reaction with L-valine–Hdpf conjugate, (*S*)-$Ph_2PfcCONHCH(CHMe_2)$-CO_2Me (fc = ferrocene-1,1′-diyl) and unsubstituted chalcone gave the alkylation product with complete conversion (20 °C/4 h) and in 87 % *ee*. The catalytic behaviour of the amidophosphane ligands was correlated to the results of a model coordination study and the crystal structure of $[Cu(Ph_2PfcCONHCH_2CO_2Me)_2](CF_3SO_3)\cdot 2CHCl_3$.

Introduction

Asymmetric conjugate additions of carbon nucleophiles to acceptor-activated double bonds represent an attractive tool for the stereoselective formation of C–C bonds. Their practical implementation was recently facilitated by the discovery of metal-catalysed processes that allow for controlled use of highly reactive organometals and require the presence of only catalytic amounts of a metal precursor and a chiral ligand.[1]

In this regard, copper-mediated conjugate additions of diorganozinc reagents to α,β-unsaturated ketones have attracted particular synthetic interest and have dominated the field since their discovery in the 1990s.[2] This is very probably due to the efficient acceleration of this reaction through the use of Cu/L* catalysts (typically generated in situ), allowing in turn for fine-tuning of the course of the reaction. In addition, organozinc reagents react rather selectively and tolerate a variety of functional groups,[3] which further broadens the field of application of these reactions. On the other hand, careful attention has to be paid to the design of chiral donors for any enantioselective variant of these reactions because the chiral ligands are the only source of chirality in this process and thus have crucial impact on the reaction outcomes.[1]

During our studies on phosphanylferrocenecarboxamides,[4,5] we noticed that these donors have a structural similarity with some ligands utilised (though with varying success) in conjugate additions of organometals. Prominent examples of such ligands, combining phosphane and carboxamide moieties, are Trost's chiral bis(amide) (**A** in Scheme 1),[6] some C- and axial-chiral amidophosphanes

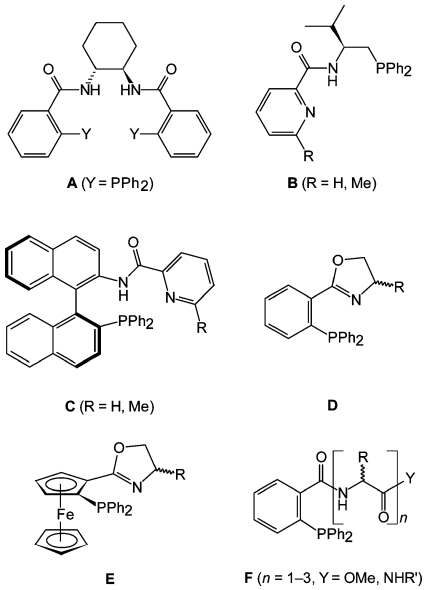

Scheme 1.

[a] Department of Inorganic Chemistry, Faculty of Science, Charles University in Prague,
Hlavova 2030, 12840 Prague, Czech Republic
Fax: +420-221-951-253
E-mail: stepnic@natur.cuni.cz

Supporting information for this article is available on the WWW under http://dx.doi.org/10.1002/ejoc.201000480.

(e.g., **B** and **C**),[7] phosphanyloxazolines (**D** and **E**)[8] and, mainly, the highly versatile amino-acid- and peptide-based phosphanes [**F**; R and chirality depend on the amino acid(s) used].[9,10]

In view of this similarity and of the successful applications of phosphanylferrocene ligands in asymmetric conjugate additions,[1,6,11] we decided to extend our work directed towards the design, coordination properties and catalytic utilisation of phosphanylferrocene–glycine donors Ph_2P-fcC(O)NHCH$_2$C(O)Y (fc = ferrocene-1,1′-diyl; Y = OH, OMe, NH_2)[4a] to their chiral analogues. Here we describe the preparation of a library of phosphanylferrocenecarboxamides with stereogenic carbon atoms in their amide side chains and/or planar chirality at their ferrocene units, together with the results of their testing as ligands for copper-catalysed asymmetric conjugate additions of diethylzinc to chalcones.

Results and Discussion

Synthesis and Characterisation of the Ligands

The series of amino acid amides (Scheme 2) was designed to incorporate compounds featuring either a chirality centre in the amino acid or a chirality plane, as well as their analogues with combined chirality. Accordingly, the amides were prepared from 1′-(diphenylphosphanyl)ferrocene-1-carboxylic acid (Hdpf)[12] or its planar-chiral isomers (S_p)- and (R_p)-**1**,[13] and from glycine or C-chiral (L- or D-)amino acids. Amino acid methyl esters, which were used throughout this study in order to avoid undesired reactions at the carboxyl group, were generated in situ from the corresponding hydrochlorides – [H_3NCH(R)CO$_2$Me]Cl (R = H, Me, *i*Pr, and CH$_2$Ph) – and triethylamine.

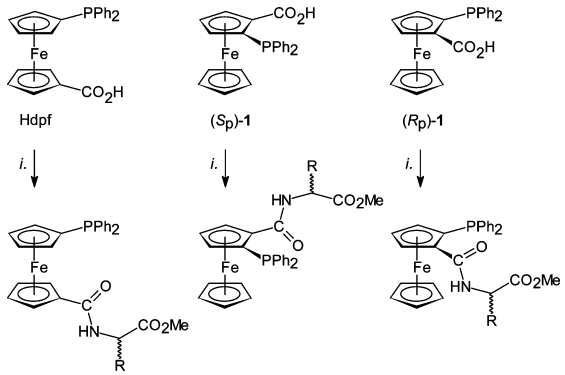

Scheme 2. Preparation of the amidophosphane ligands **2**–**9**. Reagents and conditions: (i) 1-hydroxybenzotriazole and *N*-[3-(dimethylamino)propyl]-*N*′-ethylcarbodiimide in dry dichloromethane (0 °C/30 min); then addition of an [H_3NCH(R)CO$_2$Me]Cl/NEt$_3$/CH$_2$Cl$_2$ mixture and stirring at room temp. overnight.

All amides were obtained by standard amide coupling in the presence of 1-hydroxybenzotriazole and a carbodiimide reagent[14] and were isolated by column chromatography, typically in the forms of orange amorphous solids. It should be noted that, whereas the reactions with L-amino acids proceeded with excellent yields for all phosphanylcarboxylic acids, those involving (S_p)-**1** *and* D-amino acids did not reach completion, with limited amounts of the intermediate active ester 1-hydroxybenzotriazolyl (S_p)-2-(diphenylphosphanyl)ferrocene-1-carboxylate [(S_p)-**10**] also being isolated. This can be explained by a chirality mismatch, resulting in steric crowding and making the coupling reaction more difficult.

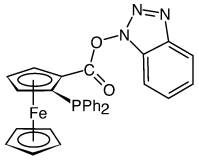

(S_p)-**10**

The presence of amide and ester moieties in **3**–**9** is manifested in their IR spectra through the strong bands due to $\nu_{C=O}$ (ester; 1740–1751 cm^{-1}), amide I (1624–1656 cm^{-1}) and amide II (1517–1532 cm^{-1}) vibrations. In addition to signals attributable to the functional substituents, ^{1}H NMR spectra of the Hdpf-based amides each displayed eight resonances due to diastereotopic ferrocene protons, whereas compounds derived from the acid **1** each showed a sharp singlet and three characteristic multiplets of the unsubstituted C_5H_5 ring and the C_5H_3 protons, respectively. Notably, the signals of the amide protons and the CH (or CH$_2$) groups bonding to the amide nitrogen atom in the planar-chiral amides were observed as ^{31}P-coupled multiplets (confirmed by ^{1}H{^{31}P} NMR). This interaction, resulting in relatively high coupling constants (ca. 13 Hz for the NH protons), seems to reflect the mutual orientation of the interacting moieties and possible N–H···P contacts (vide infra).

The ^{13}C{^{1}H} NMR spectra confirmed the formulation by combining the signals of the PPh_2-substituted ferrocene units and the amide pendants, with two C=O resonances being of particular diagnostic value (Hdpf-based compounds: $\delta_C \approx 170$ ppm for CONH and $\delta_C \approx 173$ ppm for CO$_2$Me; compounds based on **1**: $\delta_C = 170.6$–173.7 ppm for CO$_2$Me, and a ^{31}P-coupled doublet at $\delta_C \approx 170$ ppm for CONH). Finally, the ^{31}P{^{1}H} NMR spectra displayed single resonances at $\delta_P \approx -17$ ppm for the Hdpf derivatives and at $\delta_P \approx -20$ ppm for their planar-chiral analogues.

Circular dichroism (CD) spectra of isomeric amides bearing alanine pendants (Figure 1) show several Cotton effects in the regions of ferrocene d–d and CT transitions.[15] The spectra of (*R*)- and (*S*)-**3** demonstrate the expected enantiomeric relationship. Those of the planar-chiral isomers suggest a dominant contribution of planar chirality to the CD response.

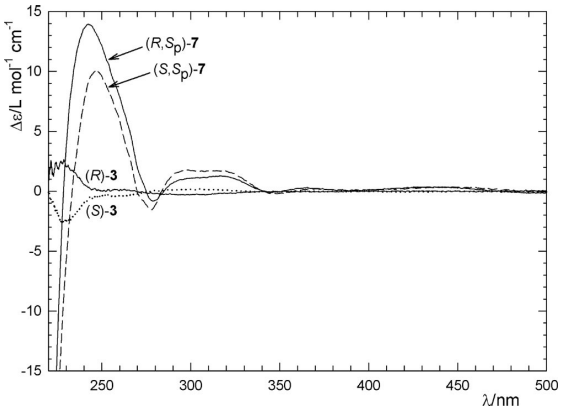

Figure 1. CD spectra of the isomeric compounds (*S*)-**3** (dotted line), (*R*)-**3**, (S,S_p)-**7** (dashed line) and (R,S_p)-**7** ($c \approx 1$ mM in MeOH).

In addition to the spectroscopic characterisation, the crystal structure of (S,S_p)-**9** (Figure 2) was determined, corroborating both the expected connectivity and chirality. The geometric data for (S,S_p)-**9** compare well with those for the achiral donor **2**[4a] and for amides prepared from the acid (S_p)-**1**.[4g] The ferrocene cyclopentadienyl rings (Cp) in (S,S_p)-**9** are practically coplanar and assume a near-to-eclipsed conformation. However, the substituents are bonded somewhat asymmetrically. Whereas the P–C2–C1/C3 angles differ by less than 2°, the difference in the C11–C1–C2/C5 angles is 10.5°, because the C1–C11 bond is bent away from the PPh_2 group. This bending occurs without any notable torsion, however, as indicated by the P–C2–C1–C11 angle of 2.5(2)°. The amide group (C11,O1,N) is nearly coplanar with its parent Cp ring [dihedral angle 5.4(2)°] and is oriented with the N–H bond pointing towards the phosphorus atom.[16]

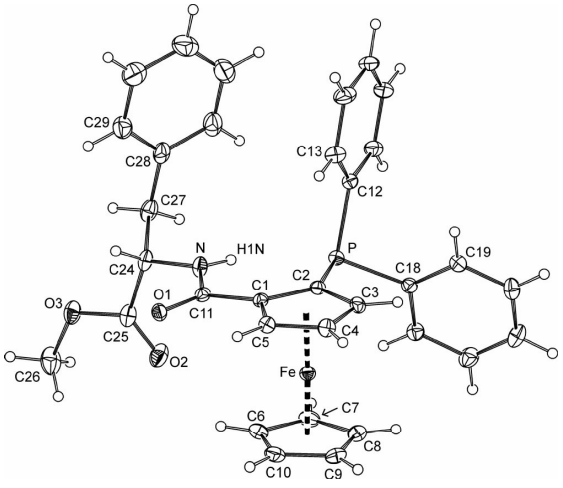

Figure 2. PLATON[17] plot of the molecular structure of (S,S_p)-**9** showing displacement ellipsoids with 30% probability. Selected distances [Å] and angles [°]: Fe–Cg1 1.6421(7), Fe–Cg2 1.6527(7), ∠Cp1,Cp2 2.84(9); C1–C11 1.492(2), C11–O1 1.228(2), C11–N 1.350(2), N–C24 1.449(2), C24–C25 1.520(2), C25–O2 1.196(2), C25–O3 1.342(2), O3–C26 1.451(3), C24–C27 1.537(2), C27–C28 1.512(3), C2–P 1.817(2), P–C12 1.830(1), P–C18 1.833(2); O1–C11–N 121.8(1), C11–N–C24 120.5(1), O2–C25–O3 124.3(2), C25–O3–C26 115.7(1), C–P–C angles 101.84(7)–103.13(7). Definitions: Cp1 = C(1–5), Cp2 = C(6–10); Cg1 and Cg2 are the corresponding ring centroids.

Catalytic Tests

The catalytic potential of the amidophosphane ligands was examined in the copper-catalysed conjugate addition of diethylzinc to *trans*-chalcone (**11a**) to give the ketone **12a** (Scheme 3). The initial screening reactions were performed with (*S*)-**3**, possessing only central chirality. Particular attention was paid to finding the optimal reaction conditions (Table 1).

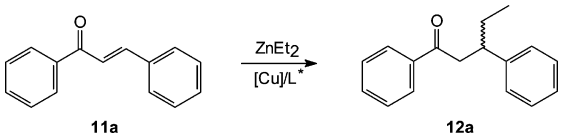

Scheme 3. Conjugate addition of diethylzinc to chalcone (**11a**) to give **12a**.

All reactions proceeded cleanly, affording either pure alkylation product or, in cases of incomplete conversion, its mixtures with unreacted chalcone. No 1,3-diphenylpent-1-en-3-ol, the product of direct attack of diethylzinc on the carbonyl group, was detected. However, the crude reaction mixtures typically contained traces of 1,3,5-triphenyl-2-(1-phenylpropyl)pentane-1,5-dione (**13**). This compound, presumably arising from a side-reaction of an intermediate zinc enolate (Scheme 4),[18] was found to crystallise preferentially from the product mixture and was structurally characterised (see the Supporting Information). The amounts of isolated pure alkylation products were always high: a 91% yield of analytically pure **12a**, for instance, was isolated by flash column chromatography from the reaction presented as Entry 1 in Table 1 (conversion 98%).

The results summarised in Table 1 demonstrate that the reaction course (conversion and *ee*) changes strongly both with the metal source and with the solvent. In donor media the reaction became slow (in MeCN it stopped entirely) and less selective. However, even the similar halogenated solvents proved to give different results (cf. Entries 1, 10, 11). On the other hand, the initial oxidation state of copper did not play any important role, whereas the counterions (Entries 1, 3–8), possibly influencing the solubility (etc.) of the copper source, had a pronounced impact. The selectivity was also strongly affected by the Cu/L ratio (Entries 1 and 2). Out of the conditions tested, the combination of a catalyst prepared in situ from $(CuOTf)_2$·PhMe (3 mol-% Cu)

Table 1. Initial optimisation of the reaction conditions with the ligand (*S*)-**3**.[a]

Entry	Metal salt	Solvent	*T* [°C] (*t* [h])	Conversion [%]	*ee* [%][c]
1	$(CuOTf)_2$·PhMe	CH_2Cl_2	0 (4)	98	+70
2	$(CuOTf)_2$·PhMe[b]	CH_2Cl_2	0 (4)	92	+20
3	$Cu(OTf)_2$	CH_2Cl_2	0 (4)	94	+57
4	CuCl	CH_2Cl_2	0 (4)	91	+39
5	CuBr	CH_2Cl_2	0 (4)	87	+40
6	CuI	CH_2Cl_2	0 (4)	79	+35
7	$CuBr·SMe_2$	CH_2Cl_2	0 (4)	40	+33
8	$Cu_2(OAc)_4·2H_2O$	CH_2Cl_2	0 (4)	93	+35
9	$(CuOTf)_2$·PhMe	PhMe	0 (4)	98	+38
10	$(CuOTf)_2$·PhMe	$CHCl_3$	0 (4)	81	+64
11	$(CuOTf)_2$·PhMe	$(ClCH_2)_2$	0 (4)	75	+48
12	$(CuOTf)_2$·PhMe	*t*BuOMe	0 (4)	100	+49
13	$(CuOTf)_2$·PhMe	Et_2O	0 (4)	100	+42
14	$(CuOTf)_2$·PhMe	THF	0 (4)	57	+13
15	$(CuOTf)_2$·PhMe	$(MeOCH_2)_2$	0 (4)	10	+8
16	$(CuOTf)_2$·PhMe	MeCN	0 (4)	0	–

[a] All reactions were carried out with **11a** (0.50 mmol) and diethylzinc (0.75 mmol, 1 M heptane solution) in the presence of 15 μmol of "copper" (3.0 mol-%) and 18 μmol of ligand (*S*)-**3** (3.6 mol-%), in 3 mL of the solvent stated. The results are averages of two independent runs. [b] Reaction performed at Cu/L = 1:2.4 (molar ratio). [c] *ee* = {[(*R*)] – [(*S*)]}/{[(*R*)] + [(*S*)]}; positive values indicate that the (*R*) isomer dominates.

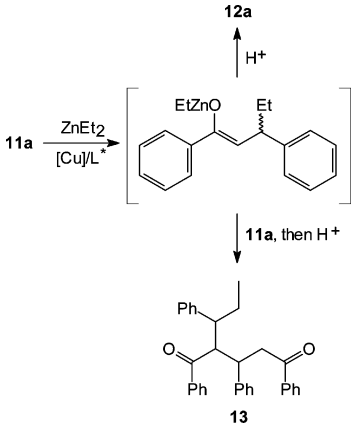

Scheme 4. Plausible reaction pathway leading to the side-product **13**.

Table 2. Survey of the ligands.[a]

Entry	Ligand	*T* [°C] (*t* [h])	Conversion [%]	*ee* [%][c]
1	(*S*)-**3**	0 (4)	98	+70
2	(*R*)-**3**	0 (4)	97	–68
3	(*S*)-**4**	0 (4)	100	+83
4	(*R*)-**4**	0 (4)	100	–84
5	(*S*)-**5**	0 (4)	92	+79
6	(*R*)-**5**	0 (4)	91	–80
7	(S_p)-**6**	0 (4)	86	–72
8	(S_p)-**6**[b]	0 (4)	87	–59
9	(*S*,S_p)-**7**	0 (4)	20	–39
10	(*R*,S_p)-**7**	0 (4)	14	–12
11	(*S*,R_p)-**7**	0 (4)	13	+11
12	(*S*,S_p)-**8**	0 (4)	10	–9
13	(*R*,S_p)-**8**	0 (4)	32	–13
14	(*S*,S_p)-**9**	0 (4)	16	–8
15	(*R*,S_p)-**9**	0 (4)	23	–3

[a] All reactions were carried out with **11a** (0.50 mmol) and diethylzinc (0.75 mmol, 1 M heptane solution) in the presence of $(CuOTf)_2$·PhMe (7.5 μmol, 3.0 mol-% Cu) and ligand (*S*)-**3** (18 μmol, 3.6 mol-%) in CH_2Cl_2 (3 mL). The results are averages of two runs. [b] Reaction performed at Cu/L molar ratio = 1:2.4. [c] *ee* = {[(*R*)] – [(*S*)]}/{[(*R*)] + [(*S*)]}.

and 1.2 equiv. of ligand in dichloromethane as the solvent gave the best results and was therefore used in all subsequent reactions.

Having established the optimal reaction conditions, we continued with the assessment of the influence of the ligand structure on the reaction course (Table 2). The application of all of the Hdpf-based ligands (Entries 1–6) resulted in good levels of conversion and enantioselectivity. However, a distinct positive effect of the size of the amino acid substituent on the *ee* was noted: ligands bearing bulkier groups gave better results. Accordingly, the best results were obtained with the valine-based donors (*S*)-**4** and (*R*)-**4**, which gave rise to active catalysts affording the alkylation products with complete conversion at 0 °C within 4 h and with *ee* values of +83 or –84% depending on the configurations of the amino acid chirality centres.

Quite unexpectedly, the planar chiral amides proved to be rather poor ligands, with the single exception of the sterically least congested (S_p)-**6** (Entry 7). No improvement was observed when the amount of ligand was increased to 2.4 equiv. (Entry 8). This is rather surprising in view of the high efficiency of the related (non-amino acid) ligands in Pd-catalysed asymmetric allylic alkylations[4g,5] and of the successful application of C- *and* planar-chiral ferrocenediyldiphosphanes in Cu-catalysed conjugate additions of Grignard reagents to enones.[1f,1j]

Another series of catalytic tests was performed with ligand (*S*)-**4** in order to establish possible effects of the reaction temperature and chalcone substituents. The former parameter was varied in the model system involving **11a**. For

the latter purpose, six additional substituted chalcones **11b**–**g** were included in the testing, each bearing a substituent (Cl, Me, or MeO) in the 4- or 4′-position, where its influence can be expected to be limited mainly to electronic effects (Scheme 5).

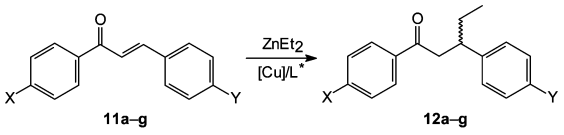

X/Y = H/H (**a**), H/Me (**b**), Me/H (**c**), H/MeO (**d**), MeO/H (**e**), H/Cl (**f**), Cl/H (**g**)

Scheme 5. Conjugate additions of diethylzinc to ring-substituted chalcones.

As indicated by the results in Table 3, the lowering of the reaction temperature to –20 °C did not decrease the reaction rates (conversion) considerably but, surprisingly, had a negative effect on enantioselectivity.[19] At –40 °C the reactions became not only rather slow but also even less selective (Entries 5 and 6). On the other hand, the alkylation performed at 20 °C was complete within 4 h and produced **12a** with 87% *ee* (Entry 2). An increase in the reaction temperature by another 20 °C (Entry 1) finally led to a lower *ee* value.

Table 3. Influence of the reaction temperature and remote substituents.[a]

Entry	Substrate	*T* [°C] (*t* [h]]	Conversion [%]	*ee* [%][c]
1	**11a**	+40 (4)	100	+82
2	**11a**	+20 (4)	100	+87
3[b]	**11a**	0 (4)	100	+83
4	**11a**	–20 (4)	100	+79
5	**11a**	–40 (4)	41	+70
6	**11a**	–40 (23)	100	+64
7	**11b**	0 (4)	100	(90)[d]
8	**11c**	0 (4)	100	(87)[d]
9	**11d**	0 (4)	100	(90)[d]
10	**11e**	0 (4)	100	(89)[d]
11	**11f**	0 (4)	100	(83)[d]
12	**11g**	0 (4)	100	(85)[d]

[a] The reactions were performed with the corresponding chalcone (0.50 mmol) and diethylzinc (0.75 mmol, 1 M heptane solution) in the presence of $(CuOTf)_2$·PhMe (7.5 μmol, 3.0 mol-% Cu) and ligand (*S*)-**4** (18 μmol, 3.6 mol-%) in dry CH_2Cl_2 (3 mL). The results are averages of two independent runs. [b] This entry from Table 2 is included for comparison. [c] *ee* = {[(*R*)] – [(*S*)]}/{[(*R*)] + [(*S*)]}. [d] The configuration was not determined.

Previous studies on the influence of remote substituents in conjugate additions to chalcones had given diverse results.[20] In the present case, the introduction of a substituent at the 4- or 4′-position in the substrate (Table 3, Entries 3 and 7–12) influenced the stereoselectivity only marginally, irrespective of the point of attachment. Nonetheless, the substrates with electron-donating groups (Me and MeO) consistently afforded better results than those bearing chlorine as an electron-withdrawing substituent.

Coordination Study

In attempts to interpret the catalytic results, the interaction of copper(I) triflate with **2** as a model donor in solution and in the solid state was studied. ^1H and $^{31}P\{^1H\}$ NMR spectra recorded in CD_2Cl_2 for a mixture of **2** and $(CuOTf)_2$·PhMe at a Cu/L molar ratio of 1:0.9 indicated the presence of two species with chemical shifts δ_P = –10.8 and –4.2 ppm (Figure 3). The signal due to free ligand (δ_P = –17.1 ppm) was not observed. With a change in the Cu/L ratio to 1:2 the high-field signal became dominant (δ_P = –11.0 ppm), and a minor resonance tentatively attributed to ligand phosphane oxide[4a] appeared (δ_P = +32.2 ppm). Electrospray mass spectra of both mixtures revealed the presence of ions attributable to $[\mathbf{2} + H]^+$ (*m*/*z* = 486), $[\mathbf{2} + Na]^+$ (*m*/*z* = 508), $[\mathbf{2} + K]^+$ (*m*/*z* = 524), $[\mathbf{2} + Cu]^+$ (*m*/*z* = 548) and $[(\mathbf{2})_2 + Cu]^+$ (*m*/*z* = 1033).

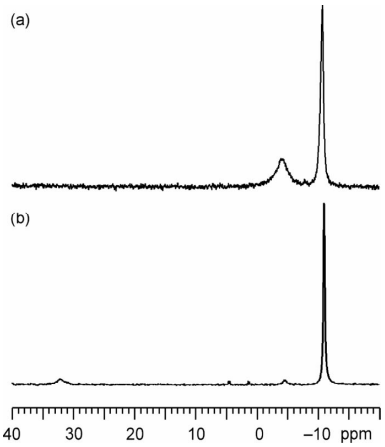

Figure 3. $^{31}P\{^1H\}$ NMR spectra of $(CuOTf)_2$·PhMe/**2** mixtures as recorded in CD_2Cl_2 at 25 °C and (a) 1:0.9, or (b) 1:2 Cu/L molar ratios.

Addition of hexane to a solution of $(CuOTf)_2$·PhMe and **2** (Cu/L = 1:1, *sic!*) in CH_2Cl_2 afforded yellow crystals of the solvated complex $[Cu(\mathbf{2})_2](TfO)$. Unfortunately, these crystals readily decomposed by desolvation, and the determined structure suffered from severe disorder. With a change in the solvent to $CHCl_3$, the same complex was isolated as a slightly more stable $CHCl_3$ solvate, $[Cu(\mathbf{2})_2](TfO)$·$2CHCl_3$ (**14**). Even in this case, the solvent and the counterion are disordered in the solid state, but the better quality and higher stability of the crystals allowed for the collection of good-quality diffraction data and, consequently, for obtaining a reliable structural model.

A view of the cation in the structure of **14** is shown in Figure 4 (for a "full" view, see the Supporting Information). Selected geometric data are presented in Table 4. The copper(I) ion is surrounded by two phosphorus atoms and two *amide* oxygen atoms making up a distorted tetrahedron. The Cu–donor distances are quite uniform and somewhat longer than those reported for a Cu^I complex with a doubly $(2\text{-}Ph_2PC_6H_4)NHCOCH_2$-functionalised calix[4]arene

forming an identical donor set.[21] On the other hand, the interligand angles span a rather wide range (ca. 85–124°) and clearly reflect steric demands of the donor moieties: the O11–Cu–O21 angle is the most acute, whereas the P1–Cu–P2 angle represents the maximum.

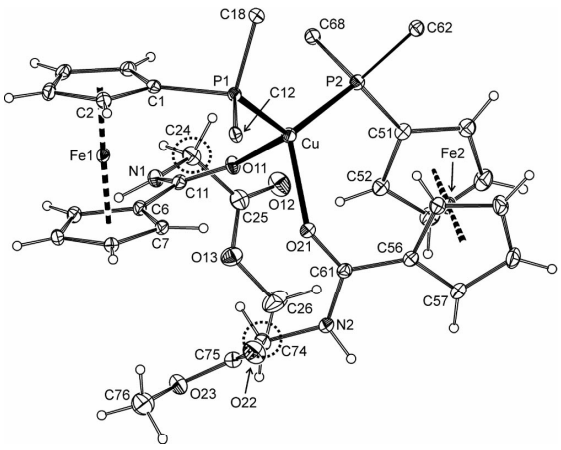

Figure 4. PLATON[17] plot of the cation in the structure of **14** showing atom labelling. (Note: The ligand "molecules" are labelled analogously. Atomic labels for "ligand 2" are obtained by adding 50 for the carbon atoms or by changing the first digit to 2 for other heavy atoms.) Displacement ellipsoids correspond to 20% probability level. For clarity, only pivotal carbon atoms in the phenyl rings and one orientation of the disordered phenyl ring C(62–67) are shown. Carbon atoms that are stereogenic (i.e., substituted) in *chiral* ligands are circled (C24 and C74).

Table 4. Selected distances [Å] and angles [°] for the cation in the structure of complex **14**.[a]

Cu–P1	2.244(1)	Cu–P2	2.275(1)
Cu–O11	2.201(2)	Cu–O21	2.135(2)
P1–Cu–P2	124.38(4)	O11–Cu–O21	84.72(9)
P1–Cu–O11	113.74(8)	P2–Cu–O21	115.77(8)
P1–Cu–O21	113.52(8)	P2–Cu–O11	94.98(7)
C11–O11	1.251(4)	C61–O21	1.248(3)
C11–N1	1.332(5)	C61–N2	1.326(3)
O11–C11–N1	120.7(4)	O21–C61–N2	122.0(2)
C25–O12	1.197(6)	C75–O22	1.198(5)
C25–O13	1.327(5)	C75–O23	1.337(5)
Fe–Cg^P(1)	1.642(2)	Fe–Cg^P(2)	1.640(2)
Fe–Cg^C(1)	1.646(2)	Fe–Cg^C(2)	1.642(2)
∡Cp^P(1),Cp^C(1)	4.2(2)	∡Cp^P(2),Cp^C(2)	1.5(2)
τ(1)	69.5	τ(2)	68.4
ϕ(1)	16.0(5)	ϕ(2)	15.0(3)

[a] Definitions: Cp^P and Cp^C are PPh_2- and amide-substituted Cp rings, respectively; Cg^P and Cg^C denote their ring centroids; τ(1/2) = torsion angles C(1/51)–Cg^P(1/2)–Cg^C(1/2)–C(6/56); ϕ = dihedral angles of the Cp^C and amide planes (N1–C11–O11 and N2–C61–O21).

The geometry of the ferrocene units in **14** is regular (cf. Fe–Cg distances and tilt angles). The chelate coordination of **2** is facilitated by a synclinal eclipsed orientation of the donor substituents (cf. ideal value: τ = 72°) and by an inclination of the amide oxygen atom towards the copper atom (see ϕ angles). Notably, the amide C=O distances in **14** are only very slightly elongated in relation to that found for uncoordinated $Ph_2PfcCONHCH_2CO_2tBu$ [1.235(2) Å].[4a]

The complex was also characterised in solution. The NMR spectra recorded for [Cu(**2**)$_2$](OTf) generated in situ indicate that the O,P-coordination remains intact, showing the ^{31}P NMR signal ($\Delta\delta_P \approx +6$ ppm) and the amide resonance [$\Delta\delta_C$(CONH) ≈ +2 ppm] shifted to lower fields. Furthermore, IR spectra of a solid sample suggest a coordinated C=O group (the amide $\nu_{C=O}$ band is shifted by ca. 40 cm^{-1} to lower energies vs. that of free **2**; the ester $\nu_{C=O}$ band remains practically unaffected) and corroborate the presence of the triflate anion (strong bands at 1165–1295 and 1029 cm^{-1}).[22] Electrospray mass spectra confirm the formulation, showing the [Cu(**2**)$_2$]$^+$ ion at m/z = 1033 with the corresponding accurate mass and isotopic patterns.

Conclusions

Phosphanylferrocenecarboxamides with amino acid pendant groups, readily available in extensive libraries from phosphanylferrocenecarboxylic acids and amino acids as a common chiral pool, were shown to be efficient ligands for copper-catalysed asymmetric conjugate additions of diethylzinc to chalcones. In the series of ligands tested, the donors based on Hdpf proved to be superior to their planar-chiral 1,2-counterparts, providing both high reactivity and enantioselectivity under convenient reaction conditions. The alkylation of unsubstituted chalcone (**11a**) in the presence of L-valine–Hdpf conjugate (*S*)-**4**, for instance, afforded the alkylation product with 100% conversion (20 °C/4 h; 3 mol-% Cu) and 87% *ee*. With **11d** as the substrate, the same catalytic system also achieved the highest selectivity (*er* 95:5 at 0 °C/4 h).

The particular combination of hard and soft donor atoms allows the phosphanyl amides to bind (principally) to both metal atoms involved in the reaction (Cu and Zn) and to act as O,P-chelate ligands. It is the chelate coordination that plays a key role in determining catalytic efficacy, because it results in the formation of rigid structures and brings the ligand's chirality into proximity to the catalytically active metal centre. Furthermore, the data suggest that the addition of the phosphanyl amide ligands to copper(I) triflate affords an equilibrium mixture of cationic species of the type [CuL_n]$^+$ (n = 0–2), the exact composition of which changes with the Cu/L molar ratio. Whereas the [CuL_2]$^+$ cation is probably the most stable (isolable), the [CuL]$^+$ species appears to be a likely precursor to the catalytically active species. On the other hand, the available data do not allow for any conclusion with regard to the nature of the true catalytic species or substrate–catalyst interactions.

Experimental Section

Materials and Methods: All syntheses were performed under argon and with exclusion of direct daylight. Hdpf,[12a] (S_p)-**1**,[13a] (R_p)-**1**,[13b] **2**[4a] and **11b**–**g**[23] were prepared by literature procedures.

Amino acid methyl ester hydrochlorides – $[H_3NCH(R)CO_2Me]Cl$ (R = H, Me, *i*Pr, CH_2Ph) – were obtained by treatment of the amino acid in question with methanol and thionyl chloride (see the Supporting Information).[24] The racemic ketones **12a**–**g** used for optimisation of the HPLC conditions were synthesised as described in the literature.[25] Anhydrous acetonitrile and *t*BuOMe were purchased from Fluka. Other solvents (Lach-Ner) were dried by standing over appropriate drying agents (CH_2Cl_2, $CHCl_3$, and $ClCH_2CH_2Cl$: K_2CO_3; diethyl ether, 1,2-dimethoxyethane, THF, and toluene: sodium) and distilled under argon. Other chemicals were obtained from commercial sources (Fluka, Aldrich, Alfa) and were used as received. NMR spectra were measured with a Varian UNITY Inova 400 spectrometer (^1H, 399.95; ^{13}C, 100.58; ^{31}P, 161.90 MHz) at 298 K. Chemical shifts (δ/ppm) are given relative to internal tetramethylsilane (^1H and ^{13}C) or to external 85% aqueous H_3PO_4 (^{31}P). IR spectra were recorded with a Nicolet 7600 FTIR spectrometer (Thermo Fisher Scientific) in the 400–4000 cm^{-1} range. Electron impact mass spectra (EI MS), including high-resolution (HR) measurements, were performed with a GCT Premier (Waters) spectrometer. Electrospray mass spectra (ESI MS) were obtained with an Esquire 3000 (Bruker; low resolution) or an LTQ Orbitrap XL instrument (Thermo Fisher Scientific; high resolution). CD spectra were recorded with a JASCO J-815 spectrometer (ca. 1 mM solutions in methanol, d = 1 mm). Optical rotations were determined with an Autopol III (Rudolph Research) automatic polarimeter at room temperature.

Preparation of the Ligands

General Procedure for the Preparation of Amides 2–9: A two-necked flask fitted with a gas inlet and containing a stirrer bar was charged with the appropriate acid (1.0 equiv.) and 1-hydroxybenzotriazole (HOBt, 1.2 equiv.). The reaction vessel was flushed with argon and sealed with a septum. Dry dichloromethane (10 mL per 1.0 mmol of the acid) was introduced, and the mixture was stirred for 5 min in an ice bath. Neat *N*-[3-(dimethylamino)propyl]-*N*′-ethylcarbodiimide (EDC, 1.2 equiv.) was added, and the reaction mixture was stirred in an ice bath for another 30 min. Another mixture, prepared separately by mixing the corresponding amino acid methyl ester hydrochloride (1.2 equiv.), dry triethylamine (ca. 1.4 equiv.) and dichloromethane (10 mL per 1.0 mmol of the hydrochloride), was then introduced. After stirring at room temperature overnight, the reaction mixture was washed successively with aqueous citric acid (10%), saturated $NaHCO_3$ and brine. The organic layer was dried with $MgSO_4$, and the solvents were removed under vacuum. The residue was purified by column chromatography on silica gel with dichloromethane/methanol (20:1) as the eluent. In the cases of (*R*,S_p)-**6**, (*R*,S_p)-**7** and (*R*,S_p)-**8**, the crude reaction product was contaminated with unreacted (S_p)-**10**. This ester was easily separated from the amide (major component) by column chromatography on silica gel (dichloromethane/methanol, 50:1).

1-(Diphenylphosphanyl)-1′-{*N*-[(*S*)-1-(methoxycarbonyl)ethyl]carbamoyl}ferrocene [(*S*)-3]: The General Procedure, starting with Hdpf (414 mg, 1.0 mmol), HOBt (165 mg, 1.20 mmol), EDC (0.21 mL, 1.20 mmol), (*S*)-$[H_3NCH(CH_3)CO_2Me]Cl$ (170 mg, 1.20 mmol) and Et_3N (0.20 mL, 1.42 mmol), afforded the amide (*S*)-**3** as an orange solid (474 mg, 95%). $[\alpha]_D$ = +10 (c = 0.5, $CHCl_3$).^1H NMR ($CDCl_3$): δ = 1.47 (d, $^3J_{H,H}$ = 7.2 Hz, 3 H, CH_3CH), 3.75 (s, 3 H, OMe), 4.09 (dq, J = 1.2, 3.2 Hz, 1 H, fc), 4.21 (m, 2 H, fc), 4.24 (dq, J = 1.2, 3.2 Hz, 1 H, fc), 4.44 (dt, J = 1.2, 2.4 Hz, 1 H, fc), 4.47 (dt, J = 1.2, 2.4 Hz, 1 H, fc), 4.55 (dt, J = 1.3, 2.6 Hz, 1 H, fc), 4.62 (dt, J = 1.3, 2.6 Hz, 1 H, fc), 4.69 (p, $^3J_{H,H}$ = 7.3 Hz, 1 H, CH_3CH), 6.31 (d, $^3J_{H,H}$ = 7.4 Hz, 1 H, NH), 7.30–7.41 (m, 10 H, PPh_2) ppm. $^{13}C\{^1H\}$ NMR ($CDCl_3$): δ = 18.57 (CH_3CH), 48.01 (CH_3CH), 52.42 (OMe), 69.50 (*C*H fc), 71.76 (d, $J_{P,C}$ = 1 Hz, *C*H fc), 71.82 (d, $J_{P,C}$ = 1 Hz, *C*H fc), 72.90 (d, $J_{P,C}$ = 4 Hz, *C*H fc), 73.05 (d, $J_{P,C}$ = 4 Hz, *C*H fc), 74.30 (d, $J_{P,C}$ = 13 Hz, *C*H fc), 74.44 (d, $J_{P,C}$ = 15 Hz, *C*H fc), 75.97 (*C*CONH fc), 128.26 (d, $^3J_{P,C}$ = 7 Hz, *C*H PPh_2), 128.70 (*C*H PPh_2), 128.72 (*C*H PPh_2), 133.36 (d, $^2J_{P,C}$ = 3 Hz, *C*H PPh_2), 133.55 (d, $^2J_{P,C}$ = 3 Hz, *C*H PPh_2), 138.35 (d, $^1J_{P,C}$ = 10 Hz, C_{ipso} PPh_2), 138.49 (d, $^1J_{P,C}$ = 10 Hz, C_{ipso} PPh_2), 169.53 (CONH), 173.65 (CO_2Me) ppm; the signal due to *C*P of fc was not found. $^{31}P\{^1H\}$ NMR ($CDCl_3$): δ = –17.0 (s) ppm. IR (Nujol): $\tilde{\nu}_{max}$ = 3325 (s, ν_{NH}), 1743 (vs., ν_{CO}), 1632 (vs., amide I), 1530 (vs., amide II), 1305 (s), 1266 (w), 1214 (m), 1193 (m), 1175 (m), 1161 (m), 1055 (w), 1027 (m), 834 (w), 743 (s), 697 (s), 569 (w), 488 (m), 451 (w) cm^{-1}. EI MS: m/z (%) = 499 (15) $[M]^{+\cdot}$, 412 (5) $[M - CH(Me)CO_2Me]^+$, 321 (4) $[Fe(C_5H_4PPh_2)O]$, 305 (2), 279 (9), 256 (5), 201 (9) $[Ph_2PO]^+$, 183 (5) $[Ph_2P - 2\ H]^+$, 167 (8), 149 (30), 129 (5), 111 (5), 105 (11), 83 (100), 73 (10) $[CH_2CO_2Me]^+$, 69 (24), 57 (32). HR MS: calcd. for $C_{27}H_{26}NO_3PFe$ 499.0999; found 499.1008.

1-(Diphenylphosphanyl)-1′-{*N*-[(*R*)-1-(methoxycarbonyl)ethyl]carbamoyl}ferrocene [(*R*)-3]: The above procedure, starting with Hdpf (207 mg, 0.50 mmol), HOBt (82 mg, 0.60 mmol), EDC (0.11 mL, 0.60 mmol), (*R*)-$[H_3NCH(CH_3)CO_2Me]Cl$ (97 mg, 0.69 mmol) and Et_3N (0.11 mL, 0.80 mmol), gave the amide (*R*)-**3** as an orange solid (225 mg, 90%). The NMR spectroscopic data for (*R*)-**3** were identical to those of the corresponding (*S*) isomer. $[\alpha]_D$ = –9 (c = 0.5, $CHCl_3$).

1-(Diphenylphosphanyl)-1′-{*N*-[(*S*)-1-(methoxycarbonyl)-2-methylprop-1-yl]carbamoyl}ferrocene [(*S*)-4]: The General Procedure, starting with Hdpf (414 mg, 1.0 mmol), HOBt (170 mg, 1.26 mmol), EDC (0.22 mL, 1.20 mmol), (*S*)-$[H_3NCH(CHMe_2)CO_2Me]Cl$ (203 mg, 1.21 mmol) and Et_3N (0.21 mL, 1.49 mmol), provided (*S*)-**4** as an orange solid (496 mg, 94%). $[\alpha]_D$ = –5 (c = 0.5, $CHCl_3$). ^1H NMR ($CDCl_3$): δ = 0.97 (d, $^3J_{H,H}$ = 6.8 Hz, 3 H, $CHMe_2$), 1.0 (d, $^3J_{H,H}$ = 6.8 Hz, 3 H, $CHMe_2$), 2.24 (d of sept, $^3J_{H,H}$ = 4.9, 6.8 Hz, 1 H, C*H*Me_2), 3.72 (s, 3 H, OMe), 4.11 (dq, J = 1.2, 3.1 Hz, 1 H, fc), 4.22 (m, 2 H, fc), 4.25 (dq, J = 1.2, 3.1 Hz, 1 H, fc), 4.43 (dt, J = 1.2, 2.4 Hz, 1 H, fc), 4.47 (dt, J = 1.2, 2.4 Hz, 1 H, fc), 4.55 (dt, J = 1.5, 2.2 Hz, 1 H, fc), 4.60 (dt, J = 1.5, 2.3 Hz, 1 H, fc), 4.66 (dd, $^3J_{H,H}$ = 4.9, 8.8 Hz, 1 H, NHC*H*), 6.25 (d, $^3J_{H,H}$ = 8.7 Hz, 1 H, NH), 7.29–7.41 (m, 10 H, PPh_2) ppm. $^{13}C\{^1H\}$ NMR ($CDCl_3$): δ = 17.99 ($CHMe_2$), 19.21 ($CHMe_2$), 31.17 (*C*HMe_2), 52.15 (OMe), 56.98 (NHCH), 69.25 (*C*H fc), 69.69 (d, $J_{P,C}$ = 1 Hz, *C*H fc), 71.79 (d, $J_{P,C}$ = 1 Hz, *C*H fc), 71.83 (d, $J_{P,C}$ = 1 Hz, *C*H fc), 72.92 (d, $J_{P,C}$ = 3 Hz, *C*H fc), 73.12 (d, $J_{P,C}$ = 4 Hz, *C*H fc), 74.13 (d, $J_{P,C}$ = 13 Hz, *C*H fc), 74.43 (d, $J_{P,C}$ = 15 Hz, *C*H fc), 76.25 (*C*CONH fc), 128.24 (2 × d, $^3J_{P,C}$ = 7 Hz, *C*H PPh_2), 128.68 (*C*H PPh_2), 128.74 (*C*H PPh_2), 133.34 (d, $^2J_{P,C}$ = 7 Hz, *C*H PPh_2), 133.54 (d, $^2J_{P,C}$ = 7 Hz, *C*H PPh_2), 138.30 (d, $^1J_{P,C}$ = 9 Hz, C_{ipso} PPh_2), 138.49 (d, $^1J_{P,C}$ = 9 Hz, C_{ipso} PPh_2), 169.99 (CONH), 172.72 (CO_2Me) ppm; the *C*P of fc was not found. $^{31}P\{^1H\}$ NMR ($CDCl_3$): δ = –17.1 (s) ppm. IR (neat): $\tilde{\nu}_{max}$ = 3335 (m, ν_{NH}), 1742 (vs., ν_{CO}), 1652 (vs., amide I), 1521 (vs., amide II), 1434 (s), 1309 (m), 1259 (w), 1193 (m), 1163 (s), 1093 (w), 1067 (w), 1027 (m), 999 (w), 833 (m), 744 (s), 697 (s), 492 (m), 451 (w) cm^{-1}. EI MS: m/z (%) = 527 (26) $[M]^{+\cdot}$, 496 (3) $[M - OMe]^+$, 412 (41) $[M - CH(CHMe_2)CO_2Me]^+$, 397 (4) $[M - NHCH(CHMe_2)CO_2Me]^+$, 321 (20) $[Fe(C_5H_4PPh_2)O]$, 305 (6), 250 (4), 226 (4), 201 (29) $[Ph_2PO]^+$, 183 (7) $[Ph_2P - 2\ H]^+$, 171 (9), 121 (5) $[Fe(C_5H_5)]^+$, 83 (100). HR MS: calcd. for $C_{29}H_{30}NO_3PFe$ 527.1313; found 527.1300.

1-(Diphenylphosphanyl)-1′-{*N*-[(*R*)-1-(methoxycarbonyl)-2-methylprop-1-yl]carbamoyl}ferrocene [(*R*)-4]: When treated according to

the General Procedure, Hdpf (207 mg, 0.50 mmol), HOBt (81 mg, 0.60 mmol), EDC (0.10 mL, 0.60 mmol), (*R*)-[$H_3NCH(CHMe_2)CO_2Me$]Cl (117 mg, 0.70 mmol) and Et_3N (0.11 mL, 0.80 mmol) afforded (*R*)-**4** as an orange solid (251 mg, 95%). The NMR spectroscopic data for (*R*)-**4** were identical with those for (*S*)-**4**. $[a]_D$ = +4 (*c* = 0.5, $CHCl_3$).

1-(Diphenylphosphanyl)-1′-{*N*-[(*S*)-1-(methoxycarbonyl)-2-phenylethyl]carbamoyl}ferrocene [(*S*)-5]: The amide (*S*)-**5** was prepared according to the General Procedure from Hdpf (414 mg, 1.0 mmol), HOBt (169 mg, 1.25 mmol), EDC (0.22 mL, 1.25 mmol), (*S*)-[$H_3NCH(CH_2Ph)CO_2Me$]Cl (262 mg, 1.21 mmol) and Et_3N (0.20 mL, 1.42 mmol), and was isolated as an orange solid (541 mg, 94%). $[a]_D$ = –3 (*c* = 0.5, $CHCl_3$). ^1H NMR ($CDCl_3$): δ = 3.13 (dd, $^3J_{H,H}$ = 7.1, $^2J_{H,H}$ = 14.0 Hz, 1 H, CH_2Ph), 3.22 (dd, $^3J_{H,H}$ = 5.6, $^2J_{H,H}$ = 14.0 Hz, 1 H, CH_2Ph), 3.72 (s, 3 H, OMe), 3.96 (dq, *J* = 1.2, 3.1 Hz, 1 H, fc), 4.15 (dq, *J* = 1.2, 3.2 Hz, 1 H, fc), 4.17 (m, 2 H, fc), 4.28 (dt, *J* = 1.2, 2.4 Hz, 1 H, fc), 4.34 (dt, *J* = 1.2, 2.4 Hz, 1 H, fc), 4.45 (dt, *J* = 1.3, 2.6 Hz, 1 H, fc), 4.54 (dt, *J* = 1.3, 2.6 Hz, 1 H, fc), 4.99 (ddd, $^3J_{H,H}$ = 5.5, 7.1, 7.9 Hz, 1 H, NHC*H*), 6.18 (d, $^3J_{H,H}$ = 7.9 Hz, 1 H, N*H*CH), 7.18–7.35 (m, 15 H, CH_2Ph + PPh_2) ppm. $^{13}C\{^1H\}$ NMR ($CDCl_3$): δ = 37.96 (*C*H_2Ph), 52.33 (OMe), 52.91 (NH*C*H), 64.06 (*C*H fc), 69.68 (d, $J_{P,C}$ = 1 Hz, *C*H fc), 71.80 (d, $J_{P,C}$ = 1 Hz, *C*H fc), 71.82 (d, $J_{P,C}$ = 1 Hz, *C*H fc), 72.84 (d, $J_{P,C}$ = 4 Hz, *C*H fc), 73.07 (d, $J_{P,C}$ = 4 Hz, *C*H fc), 74.07 (d, $J_{P,C}$ = 13 Hz, *C*H fc), 74.41 (d, $J_{P,C}$ = 15 Hz, *C*H fc), 75.96 (*C*CONH fc), 127.18 (*C*H CH_2Ph), 128.19 (d, $^3J_{P,C}$ = 1 Hz, *C*H PPh_2), 128.26 (d, $^3J_{P,C}$ = 2 Hz, *C*H PPh_2), 128.66 (*C*H PPh_2), 128.67 (*C*H CH_2Ph), 128.71 (*C*H PPh_2), 129.21 (*C*H CH_2Ph), 133.34 (d, $^2J_{P,C}$ = 10 Hz, *C*H PPh_2), 133.53 (d, $^2J_{P,C}$ = 10 Hz, *C*H PPh_2), 136.11 (*C*$_{ipso}$ CH_2Ph), 138.30 (d, $^1J_{P,C}$ = 9 Hz, *C*$_{ipso}$ PPh_2), 138.47 (d, $^1J_{P,C}$ = 9 Hz, *C*$_{ipso}$ PPh_2), 169.70 (CONH), 172.28 (*C*O_2Me) ppm; the signal due to *C*P of fc was not found. $^{31}P\{^1H\}$ NMR ($CDCl_3$): δ = –17.2 (s) ppm. IR (Nujol): $\tilde{\nu}_{max}$ = 3325 (s, ν_{NH}), 1743 (vs., ν_{CO}), 1633 (vs., amide I), 1532 (vs., amide II), 1305 (m), 1216 (m), 1196 (m), 1161 (m), 1094 (w), 1027 (s), 834 (m), 743 (vs), 698 (vs), 491 (s) cm^{-1}. EI MS: *m*/*z* (%) = 575 (48) $[M]^{+\cdot}$, 544 (5) $[M - OMe]^+$, 516 (5) $[M - CO_2Me]^+$, 412 (100) $[M - CH(CH_2Ph)CO_2Me]^+$, 397 (12) $[M - NHCH(CH_2Ph)CO_2Me]^+$, 374 (37) $[M - Ph_2PO]^+$, 321 (69) $[Fe(C_5H_4PPh_2)O]^+$, 305 (28), 264 (27), 226 (14), 201 (81) $[Ph_2PO]^+$, 183 (20) $[Ph_2P - 2H]^+$, 171 (33), 133 (13), 121 (32) $[Fe(C_5H_5)]^+$, 109 (15), 93 (33), 65 (25). HR MS: calcd. for $C_{33}H_{30}NO_3PFe$ 575.1313; found 575.1319.

1-(Diphenylphosphanyl)-1′-{*N*-[(*R*)-1-(methoxycarbonyl)-2-phenylethyl]carbamoyl}ferrocene [(*R*)-5]: Treatment of Hdpf (207 mg, 0.50 mmol), HOBt (81 mg, 0.60 mmol), EDC (0.10 mL, 0.60 mmol), (*R*)-[$H_3NCH(CH_2Ph)CO_2Me$]Cl (151 mg, 0.70 mmol) and Et_3N (0.11 mL, 0.80 mmol) according to the General Procedure provided (*R*)-**5** as an orange solid (280 mg, 97%). The NMR spectroscopic data for (*R*)-**5** were identical to those for (*S*)-**5**. $[a]_D$ = +3 (*c* = 0.5, $CHCl_3$).

(S_p)-1-(Diphenylphosphanyl)-2-{*N*-[(methoxycarbonyl)methyl]carbamoyl}ferrocene [(S_p)-6]: The above procedure, starting with (S_p)-Hpfc (414 mg, 1.0 mmol), HOBt (163 mg, 1.20 mmol), EDC (0.21 mL, 1.20 mmol), ($H_3NCH_2CO_2Me$)Cl (151 mg, 1.20 mmol) and Et_3N (0.20 mL, 1.42 mmol), yielded the amide (S_p)-**6** as an orange solid (354 mg, 73%). $[a]_D$ = –177 (*c* = 0.5, $CHCl_3$). ^1H NMR ($CDCl_3$): δ = 3.75 (s, 3 H, OMe), 3.87 (m, 1 H, C_5H_3), 3.95 (ddd, $J_{P,H}$ = 0.8, $^3J_{H,H}$ = 4.9, $^2J_{H,H}$ = 18.2 Hz, 1 H, NHCH_2), 4.18 (s, 5 H, C_5H_5), 4.30 (ddd, $J_{P,H}$ = 1.3, $^3J_{H,H}$ = 6.2, $^2J_{H,H}$ = 18.2 Hz, 1 H, NHCH_2), 4.49 (dt, *J* = 0.5, 2.6 Hz, 1 H, C_5H_3), 5.16 (dt, *J* = 1.6, 2.6 Hz, 1 H, C_5H_3), 7.10–7.65 (m, 10 H, PPh_2), 7.73 (apparent dt, $J_{P,C} \approx 12$, $^3J_{H,H} \approx 6$ Hz, 1 H, NH) ppm. $^{13}C\{^1H\}$ NMR ($CDCl_3$): δ = 41.31 ($NHCH_2$), 52.22 (OMe), 70.97 (*C*H C_5H_5), 71.75 (*C*H C_5H_3), 73.41 (d, $J_{P,C}$ = 2 Hz, *C*H C_5H_3), 74.61 (d, $J_{P,C}$ = 4 Hz, *C*H C_5H_3), 75.48 (d, $^1J_{P,C}$ = 11 Hz, *C*P C_5H_3), 79.82 (d, $^2J_{P,C}$ = 20 Hz, *C*CONH C_5H_3), 128.21 (*C*H PPh_2), 128.24 (d, $^3J_{P,C}$ = 7 Hz, *C*H PPh_2), 128.37 (d, $^3J_{P,C}$ = 7 Hz, *C*H PPh_2), 129.71 (*C*H PPh_2), 131.98 (d, $^2J_{P,C}$ = 17 Hz, *C*H PPh_2), 135.22 (d, $^2J_{P,C}$ = 21 Hz, *C*H PPh_2), 136.15 (d, $^1J_{P,C}$ = 6 Hz, *C*$_{ipso}$ PPh_2), 138.18 (d, $^1J_{P,C}$ = 7 Hz, *C*$_{ipso}$ PPh_2), 170.61 (*C*O_2Me), 170.73 (d, $^3J_{P,C}$ = 4 Hz, CONH) ppm. $^{31}P\{^1H\}$ NMR ($CDCl_3$): δ = –20.2 (s) ppm. IR (Nujol): $\tilde{\nu}_{max}$ = 3330 (m, ν_{NH}), 1750 (vs., ν_{CO}), 1640 (vs., amide I), 1532 (vs., amide II), 1434 (vs), 1410 (w), 1366 (s), 1279 (m), 1199 (s), 1178 (s), 1107 (m), 1094 (w), 1019 (m), 1003 (m), 987 (w), 940 (w), 844 (w), 821 (m), 744 (s), 698 (s), 563 (w), 486 (s), 463 (w) cm^{-1}. EI MS: *m*/*z* (%) = 485 (40) $[M]^{+\cdot}$, 454 (5) $[M - OMe]^+$, 420 (100) $[M - C_5H_5]^+$, 412 (58) $[M - CH_2CO_2Me]^+$, 397 (8) $[M - NHCH_2CO_2Me]^+$, 362 (35), 346 (26), 291 (14), 226 (13), 201 (90) $[Ph_2PO]^+$, 183 (21) $[Ph_2P - 2H]^+$, 170 (38), 152 (11), 121 (45) $[Fe(C_5H_5)]^+$, 55 (15). HR MS: calcd. for $C_{26}H_{24}NO_3PFe$ 485.0843; found 485.0834.

(S_p)-1-(Diphenylphosphanyl)-2-{*N*-[(*S*)-1-(methoxycarbonyl)ethyl]carbamoyl}ferrocene [(*S*,S_p)-7]: The General Procedure, starting with (S_p)-**1** (414 mg, 1.0 mmol), HOBt (163 mg, 1.20 mmol), EDC (0.21 mL, 1.20 mmol), (*S*)-[$H_3NCH(CH_3)CO_2Me$]Cl (170 mg, 1.20 mmol) and Et_3N (0.20 mL, 1.42 mmol), afforded the amide (*S*,S_p)-**7** (orange solid; 379 mg, 76%). $[a]_D$ = –176 (*c* = 0.5, $CHCl_3$). ^1H NMR ($CDCl_3$): δ = 1.29 (d, $^3J_{H,H}$ = 7.3 Hz, 3 H, CH_3CH), 3.80 (s, 3 H, OMe), 3.80 (dt, *J* = 1.2, 2.8 Hz, 1 H, C_5H_3), 4.21 (s, 5 H, C_5H_5), 4.46 (dt, *J* = 0.5, 2.6 Hz, 1 H, C_5H_3), 4.63 (dp, $^3J_{H,H}$ = 7.3, $J_{P,H}$ = 2.1 Hz, 1 H, CH_3CH), 5.14 (dt, *J* = 1.6, 2.6 Hz, 1 H, C_5H_3), 7.13–7.60 (m, 10 H, PPh_2), 7.82 (dd, $^3J_{H,H}$ = 7.7, $J_{P,C}$ = 12.9 Hz, 1 H, NH) ppm. $^{13}C\{^1H\}$ NMR ($CDCl_3$): δ = 17.87 (*C*H_3CH), 48.04 (CH_3CH), 52.35 (OMe), 70.96 (*C*H C_5H_5), 71.51 (*C*H C_5H_3), 73.41 (d, $J_{P,C}$ = 2 Hz, *C*H C_5H_3), 74.55 (d, $J_{P,C}$ = 2 Hz, *C*H C_5H_3), 75.57 (d, $^1J_{P,C}$ = 10 Hz, *C*P C_5H_3), 79.83 (d, $^2J_{P,C}$ = 20 Hz, *C*CONH C_5H_3), 128.33 (d, $^3J_{P,C}$ = 6 Hz, *C*H PPh_2), 128.41 (d, $^3J_{P,C}$ = 5 Hz, *C*H PPh_2), 128.47 (*C*H PPh_2), 129.71 (*C*H PPh_2), 132.20 (d, $^2J_{P,C}$ = 18 Hz, *C*H PPh_2), 135.07 (d, $^2J_{P,C}$ = 21 Hz, *C*H PPh_2), 135.77 (d, $^1J_{P,C}$ = 6 Hz, *C*$_{ipso}$ PPh_2), 137.65 (d, $^1J_{P,C}$ = 7 Hz, *C*$_{ipso}$ PPh_2), 170.00 (d, $^3J_{P,C}$ = 4 Hz, CONH), 173.78 (*C*O_2Me) ppm. $^{31}P\{^1H\}$ NMR ($CDCl_3$): δ = –20.0 (s) ppm. IR (Nujol): $\tilde{\nu}_{max}$ = 3290 (w, ν_{NH}), 1742 (vs., ν_{CO}), 1652 (vs., amide I), 1521 (vs., amide II), 1434 (vs), 1340 (w), 1309 (w), 1264 (m), 1215 (m), 1195 (s), 1165 (m), 1107 (m), 1094 (w), 1069 (w), 1001 (m), 985 (w), 845 (w), 819 (m), 744 (vs), 697 (vs), 545 (w), 498 (s), 484 (s), 456 (m) cm^{-1}. EI MS: *m*/*z* (%) = 499 (26) $[M]^{+\cdot}$, 468 (4) $[M - OMe]^+$, 434 (66) $[M - C_5H_5]^+$, 412 (73) $[M - CH(Me)CO_2Me]^+$, 397 (8) $[M - NHCH(Me)CO_2Me]^+$, 374 (42), 346 (43), 291 (10), 226 (10), 201 (100) $[Ph_2PO]^+$, 183 (18) $[Ph_2P - 2H]^+$, 170 (37), 152 (6), 133 (8), 121 (38) $[Fe(C_5H_5)]^+$, 115 (6), 100 (6), 83 (38), 77 (8), 56 (17). HR MS: calcd. for $C_{27}H_{26}NO_3PFe$ 499.0999; found 499.0981.

(S_p)-1-(Diphenylphosphanyl)-2-{*N*-[(*R*)-1-(methoxycarbonyl)ethyl]carbamoyl}ferrocene [(*R*,S_p)-7]: The amide (*R*,S_p)-**7** was prepared as described above, from (S_p)-**1** (207 mg, 0.50 mmol), HOBt (81 mg, 0.60 mmol), EDC (0.11 mL, 0.60 mmol), (*R*)-[$H_3NCH(CH_3)CO_2Me$]Cl (84 mg, 0.60 mmol) and Et_3N (0.10 mL, 0.71 mmol). Isolation by column chromatography afforded (*R*,S_p)-**7** as an orange solid (170 mg, 68%). Some (S_p)-**10** was also isolated. Analytical data for (*R*,S_p)-**7**. $[a]_D$ = –153 (*c* = 0.5, $CHCl_3$). ^1H NMR ($CDCl_3$): δ = 1.46 (d, $^3J_{H,H}$ = 7.2 Hz, 3 H, CH_3CH), 3.60 (s, 3 H, OMe), 3.81 (m, 1 H, C_5H_3), 4.16 (s, 5 H, C_5H_5), 4.45 (dt, *J* = 0.5, 2.6 Hz, 1 H, C_5H_3), 4.71 (dp, $^3J_{H,H}$ = 7.3, $J_{P,H}$ = 1.5 Hz, 1 H, CH_3CH), 5.06 (dt, *J* = 1.4, 2.8 Hz, 1 H, C_5H_3), 7.14–7.60 (m, 11

H, N*H* + P*Ph*$_2$) ppm. ^{13}C{^{1}H} NMR ($CDCl_3$): δ = 18.75 (*C*H$_3$CH), 48.19 (CH$_3$*C*H), 52.21 (OMe), 70.92 (*C*H C$_5$H$_5$), 71.42 (*C*H C$_5$H$_3$), 73.05 (d, $J_{P,C}$ = 2 Hz, *C*H C$_5$H$_3$), 74.53 (d, $J_{P,C}$ = 5 Hz, *C*H C$_5$H$_3$), 76.25 (d, $^1J_{P,C}$ = 12 Hz, *C*P C$_5$H$_3$), 80.24 (d, $^2J_{P,C}$ = 18 Hz, *C*CONH C$_5$H$_3$), 128.18 (*C*H PPh$_2$), 128.21 (d, $^3J_{P,C}$ = 6 Hz, *C*H PPh$_2$), 128.31 (d, $^3J_{P,C}$ = 7 Hz, *C*H PPh$_2$), 129.54 (*C*H PPh$_2$), 132.18 (d, $^2J_{P,C}$ = 18 Hz, *C*H PPh$_2$), 135.19 (d, $^2J_{P,C}$ = 21 Hz, *C*H PPh$_2$), 136.65 (d, $^1J_{P,C}$ = 9 Hz, *C*$_{ipso}$ PPh$_2$), 138.50 (d, $^1J_{P,C}$ = 7 Hz, *C*$_{ipso}$ PPh$_2$), 169.71 (d, $^3J_{P,C}$ = 4 Hz, CONH), 173.33 (*C*O$_2$Me) ppm. ^{31}P{^{1}H} NMR ($CDCl_3$): δ = –20.0 (s) ppm. IR (Nujol): $\tilde{\nu}_{max}$ = 3325 (w, ν_{NH}), 1746 (vs., ν_{CO}), 1624 (vs., amide I), 1521 (vs., amide II), 1265 (w), 1193 (m), 1155 (s), 1106 (w), 1050 (w), 1002 (w), 909 (w), 819 (m), 743 (vs), 698 (vs), 489 (s), 466 (w) cm^{-1}. EI MS: *m*/*z* (%) = 499 (21) [M]$^{+\cdot}$, 468 (5) [M – OMe]$^+$, 434 (69) [M – C$_5$H$_5$]$^+$, 412 (64) [M – CH(Me)CO$_2$Me]$^+$, 397 (8) [M – NHCH(Me)CO$_2$Me]$^+$, 374 (38), 346 (33), 291 (8), 247 (8), 226 (8), 201 (84) [Ph$_2$PO]$^+$, 183 (14) [Ph$_2$P – 2 H]$^+$, 170 (25), 149 (21), 121 (36) [Fe(C$_5$H$_5$)]$^+$, 111 (19), 97 (34), 81 (44), 69 (95), 57 (100). HR MS: calcd. for $C_{27}H_{26}NO_3PFe$ 499.0999; found 499.1010.

(*R*$_p$)-1-(Diphenylphosphanyl)-2-{*N*-[(*S*)-1-(methoxycarbonyl)ethyl]-carbamoyl}ferrocene [(*S*,*R*$_p$)-7]: The amide (*R*,*S*$_p$)-**7** was prepared as described above, from (*R*$_p$)-**1** (69 mg, 0.17 mmol), HOBt (27 mg, 0.20 mmol), EDC (0.03 mL, 0.20 mmol), (*S*)-[H$_3$NCH(CH$_3$)CO$_2$Me]Cl (30 mg, 0.22 mmol) and Et$_3$N (0.03 mL, 0.25 mmol). Yield: 52 mg (63%) of an orange solid. The NMR spectroscopic data were identical to those for (*R*,*S*$_p$)-**7**. [*a*]$_D$ = +156 (*c* = 0.5, $CHCl_3$).

(*S*$_p$)-1-(Diphenylphosphanyl)-2-{*N*-[(*S*)-1-(methoxycarbonyl)-2-methylprop-1-yl]carbamoyl}ferrocene [(*S*,*S*$_p$)-8]: The General Procedure, with (*S*$_p$)-**1** (207 mg, 0.50 mmol), HOBt (81 mg, 0.60 mmol), EDC (0.11 mL, 0.60 mmol), (*S*)-[H$_3$NCH(CHMe$_2$)CO$_2$Me]Cl (101 mg, 0.60 mmol) and Et$_3$N (0.10 mL, 0.71 mmol), yielded the amide (*S*,*S*$_p$)-**8** as an orange solid (198 mg, 75%). [*a*]$_D$ = –195 (*c* = 0.5, $CHCl_3$). ^{1}H NMR ($CDCl_3$): δ = 0.64 (d, $^3J_{H,H}$ = 6.9 Hz, 3 H, CH*Me*$_2$), 0.83 (d, $^3J_{H,H}$ = 6.9 Hz, 3 H, CH*Me*$_2$), 2.17 (dsept, $^3J_{H,H}$ = 4.5, 6.9 Hz, 1 H, C*H*Me$_2$), 3.77 (m, 1 H, C$_5$H$_3$), 3.80 (s, 3 H, OMe), 4.22 (s, 5 H, C$_5$H$_5$), 4.47 (t, *J* = 2.6 Hz, 1 H, C$_5$H$_3$), 4.63 (ddd, $J_{P,H}$ = 2.2, $^3J_{H,H}$ = 4.9, 8.8 Hz, 1 H, NHC*H*), 5.20 (dt, *J* = 1.5, 2.7 Hz, 1 H, C$_5$H$_3$), 7.11–7.60 (m, 10 H, PPh$_2$), 7.88 (dd, $J_{P,H}$ = 13.6, $^3J_{H,H}$ = 8.7 Hz, 1 H, NH) ppm. ^{13}C{^{1}H} NMR ($CDCl_3$): δ = 17.60 (d, $^7J_{P,C}$ = 2 Hz, CH*Me*$_2$), 18.85 (CH*Me*$_2$), 30.66 (*C*HMe$_2$), 52.11 (OMe), 57.43 (NHCH), 70.91 (*C*H C$_5$H$_5$), 71.63 (*C*H C$_5$H$_3$), 73.83 (d, $J_{P,C}$ = 2 Hz, *C*H C$_5$H$_3$), 74.57 (d, $J_{P,C}$ = 4 Hz, *C*H C$_5$H$_3$), 74.83 (d, $^1J_{P,C}$ = 9 Hz, *C*P C$_5$H$_3$), 80.08 (d, $^2J_{P,C}$ = 18 Hz, *C*CONH C$_5$H$_3$), 128.31 (d, $^3J_{P,C}$ = 6 Hz, *C*H PPh$_2$), 128.36 (*C*H PPh$_2$), 128.41 (d, $^3J_{P,C}$ = 9 Hz, *C*H PPh$_2$), 129.81 (*C*H PPh$_2$), 132.07 (d, $^2J_{P,C}$ = 17 Hz, *C*H PPh$_2$), 135.22 (d, $^2J_{P,C}$ = 21 Hz, *C*H PPh$_2$), 135.56 (d, $^1J_{P,C}$ = 6 Hz, *C*$_{ipso}$ PPh$_2$), 137.40 (d, $^1J_{P,C}$ = 6 Hz, *C*$_{ipso}$ PPh$_2$), 170.70 (d, $^3J_{P,C}$ = 4 Hz, CONH), 172.86 (*C*O$_2$Me) ppm. ^{31}P{^{1}H} NMR ($CDCl_3$): δ = –20.0 (s) ppm. IR (neat): $\tilde{\nu}_{max}$ = 3315 (m, ν_{NH}), 1740 (vs., ν_{CO}), 1653 (vs., amide I), 1517 (vs., amide II), 1310 (m), 1274 (w), 1193 (m), 1160 (m), 1107 (w), 1028 (m), 1001 (m), 845 (w), 820 (m), 743 (s), 697 (s), 543 (w), 484 (s) cm^{-1}. EI MS: *m*/*z* (%) = 527 (31) [M]$^{+\cdot}$, 496 (3) [M – OMe]$^+$, 462 (100) [M – C$_5$H$_5$]$^+$, 412 (64) [M – CH(CHMe$_2$)CO$_2$Me]$^+$, 402 (51), 397 (10) [M – NHCH(CHMe$_2$)CO$_2$Me]$^+$, 346 (43), 303 (7), 291 (6), 247 (6), 226 (10), 201 (85) [Ph$_2$PO]$^+$, 183 (15) [Ph$_2$P – 2 H]$^+$, 170 (28), 149 (11), 121 (30) [Fe(C$_5$H$_5$)]$^+$, 97 (10), 83 (14), 73 (20), 55 (39). HR MS: calcd. for $C_{29}H_{30}NO_3PFe$ 527.1313; found 527.1306.

(*S*$_p$)-1-(Diphenylphosphanyl)-2-{*N*-[(*R*)-1-(methoxycarbonyl)-2-methylprop-1-yl]carbamoyl}ferrocene [(*R*,*S*$_p$)-8]: The General Procedure, starting with (*S*$_p$)-**1** (207 mg, 0.50 mmol), HOBt (81 mg, 0.60 mmol), EDC (0.11 mL, 0.60 mmol), (*R*)-[H$_3$NCH(CHMe$_2$)CO$_2$Me]Cl (101 mg, 0.60 mmol) and Et$_3$N (0.10 mL, 0.71 mmol), afforded amide (*R*,*S*$_p$)-**8** (orange solid; 169 mg, 64%). Some unreacted (*S*$_p$)-**10** was also isolated. Analytical data for (*R*,*S*$_p$)-**8**. [*a*]$_D$ = –151 (*c* = 0.5, $CHCl_3$). ^{1}H NMR ($CDCl_3$): δ = 1.03 (d, $^3J_{H,H}$ = 6.9 Hz, 3 H, CH*Me*$_2$), 1.06 (d, $^3J_{H,H}$ = 6.9 Hz, 3 H, CH*Me*$_2$), 2.27 (dsept, $^3J_{H,H}$ = 4.8, 6.8 Hz, 1 H, C*H*Me$_2$), 3.43 (s, 3 H, OMe), 3.85 (m, 1 H, C$_5$H$_3$), 4.13 (s, 5 H, C$_5$H$_5$), 4.46 (dt, *J* = 0.5, 2.6 Hz, 1 H, C$_5$H$_3$), 4.63 (ddd, $J_{P,H}$ = 2.0, $^3J_{H,H}$ = 4.8, 8.6 Hz, 1 H, NHC*H*), 5.15 (dt, *J* = 1.6, 3.0 Hz, 1 H, C$_5$H$_3$), 7.12–7.60 (m, 11 H, N*H* + P*Ph*$_2$) ppm. ^{13}C{^{1}H} NMR ($CDCl_3$): δ = 18.10 (CH*Me*$_2$), 19.31 (CH*Me*$_2$), 30.88 (*C*HMe$_2$), 51.71 (OMe), 57.56 (NHCH), 70.80 (*C*H C$_5$H$_5$), 71.59 (*C*H C$_5$H$_3$), 73.64 (d, $J_{P,C}$ = 2 Hz, *C*H C$_5$H$_3$), 74.50 (d, $J_{P,C}$ = 4 Hz, *C*H C$_5$H$_3$), 75.45 (d, $^1J_{P,C}$ = 11 Hz, *C*P C$_5$H$_3$), 80.72 (d, $^2J_{P,C}$ = 20 Hz, *C*CONH C$_5$H$_3$), 128.16 (*C*H PPh$_2$), 128.19 (d, $^3J_{P,C}$ = 6 Hz, *C*H PPh$_2$), 128.33 (d, $^3J_{P,C}$ = 9 Hz, *C*H PPh$_2$), 129.68 (*C*H PPh$_2$), 132.06 (d, $^2J_{P,C}$ = 17 Hz, *C*H PPh$_2$), 135.24 (d, $^2J_{P,C}$ = 21 Hz, *C*H PPh$_2$), 136.26 (d, $^1J_{P,C}$ = 7 Hz, *C*$_{ipso}$ PPh$_2$), 138.26 (d, $^1J_{P,C}$ = 7 Hz, *C*$_{ipso}$ PPh$_2$), 170.24 (d, $^3J_{P,C}$ = 4 Hz, CONH), 172.01 (*C*O$_2$Me) ppm. ^{31}P{^{1}H} NMR ($CDCl_3$): δ = –20.0 (s) ppm. IR (neat): $\tilde{\nu}_{max}$ = 3305 (m, ν_{NH}), 1745 (vs., ν_{CO}), 1656 (vs., amide I), 1525 (vs., amide II), 1435 (vs), 1311 (m), 1267 (m), 1206 (m), 1161 (m), 1107 (w), 1093 (w), 1069 (w), 1027 (m), 1003 (m), 823 (s), 752 (vs), 699 (vs), 666 (w), 646 (w), 613 (w), 501 (s), 485 (s), 461 (m) cm^{-1}. EI MS: *m*/*z* (%) = 527 (26) [M]$^{+\cdot}$, 496 (10) [M – OMe]$^+$, 481 (10), 462 (27) [M – C$_5$H$_5$]$^+$, 412 (18) [M – CH(CHMe$_2$)CO$_2$Me]$^+$, 402 (16), 397 (4) [M – NHCH(CHMe$_2$)CO$_2$Me]$^+$, 346 (11), 201 (23) [Ph$_2$PO]$^+$, 183 (7) [Ph$_2$P – 2 H]$^+$, 170 (8), 165 (16), 149 (13), 121 (12) [Fe(C$_5$H$_5$)]$^+$, 97 (22), 83 (100), 69 (53), 57 (81). HR MS: calcd. for $C_{29}H_{30}NO_3PFe$ 527.1313; found 527.1321.

(*S*$_p$)-1-(Diphenylphosphanyl)-2-{*N*-[(*S*)-1-(methoxycarbonyl)-2-phenylethyl]carbamoyl}ferrocene [(*S*,*S*$_p$)-9]: Treatment of (*S*$_p$)-**1** (207 mg, 0.50 mmol), HOBt (81 mg, 0.60 mmol), EDC (0.11 mL, 0.60 mmol), (*S*)-[H$_3$NCH(CH$_2$Ph)CO$_2$Me]Cl (131 mg, 0.61 mmol) and Et$_3$N (0.10 mL, 0.71 mmol) according to the General Procedure gave (*S*,*S*$_p$)-**9** as an orange solid (204 mg, 71%). Single crystals suitable for X-ray diffraction analysis were grown from acetone/diethyl ether at +4 °C. [*a*]$_D$ = –198 (*c* = 0.5, $CHCl_3$). ^{1}H NMR ($CDCl_3$): δ = 3.02 (dd, $^3J_{H,H}$ = 7.6, $^2J_{H,H}$ = 14.0 Hz, 1 H, C*H*$_2$Ph), 3.12 (dd, $^3J_{H,H}$ = 5.2, $^2J_{H,H}$ = 14.0 Hz, 1 H, C*H*$_2$Ph), 3.78 (s, 3 H, OMe), 3.86 (m, 1 H, C$_5$H$_3$), 4.09 (s, 5 H, C$_5$H$_5$), 4.46 (dt, *J* = 1.0, 2.6 Hz, 1 H, C$_5$H$_3$), 4.95 (dddd, $J_{P,H}$ = 2.3, $^3J_{H,H}$ = 5.3, 7.7, 7.7 Hz, 1 H, NHC*H*), 5.14 (dt, *J* = 1.6, 2.7 Hz, 1 H, C$_5$H$_3$), 6.96–7.61 (m, 15 H, CH$_2$*Ph* + P*Ph*$_2$), 7.91 (dd, $^3J_{H,H}$ = 7.8, $J_{P,H}$ = 12.8 Hz, 1 H, N*H*CH) ppm. ^{13}C{^{1}H} NMR ($CDCl_3$): δ = 37.97 (*C*H$_2$Ph), 52.27 (OMe), 53.86 (NH*C*H), 70.90 (*C*H C$_5$H$_5$), 71.89 (*C*H C$_5$H$_3$), 73.64 (d, $J_{P,C}$ = 2 Hz, *C*H C$_5$H$_3$), 74.62 (d, $J_{P,C}$ = 4 Hz, *C*H C$_5$H$_3$), 75.02 (d, $^1J_{P,C}$ = 11 Hz, *C*P C$_5$H$_3$), 79.97 (d, $^2J_{P,C}$ = 20 Hz, *C*CONH C$_5$H$_3$), 126.77 (*C*H CH$_2$Ph), 128.08 (*C*H PPh$_2$), 128.24 (d, $^3J_{P,C}$ = 5 Hz, *C*H PPh$_2$), 128.35 (*C*H CH$_2$Ph), 128.35 (d, $^3J_{P,C}$ = 9 Hz, *C*H PPh$_2$), 129.16 (*C*H CH$_2$Ph), 129.81 (*C*H PPh$_2$), 131.85 (d, $^2J_{P,C}$ = 17 Hz, *C*H PPh$_2$), 135.36 (d, $^2J_{P,C}$ = 21 Hz, *C*H PPh$_2$), 136.14 (d, $^1J_{P,C}$ = 6 Hz, *C*$_{ipso}$ PPh$_2$), 136.17 (*C*$_{ipso}$ CH$_2$Ph), 138.36 (d, $^1J_{P,C}$ = 6 Hz, *C*$_{ipso}$ PPh$_2$), 170.34 (d, $^3J_{P,C}$ = 4 Hz, CONH), 172.54 (*C*O$_2$Me) ppm. ^{31}P{^{1}H} NMR ($CDCl_3$): δ = –20.6 (s) ppm. IR (Nujol): $\tilde{\nu}_{max}$ = 3290 (w, ν_{NH}), 1751 (vs., ν_{CO}), 1647 (vs., amide I), 1524 (s, amide II), 1410 (w), 1308 (m), 1269 (m), 1217 (m), 1203 (w), 1193 (m), 1153 (m), 1106 (m), 1090 (w), 1034 (w), 999 (w), 985 (w), 845 (w), 818 (w), 747 (s), 699 (s), 502 (m), 484 (s), 457 (w) cm^{-1}. EI MS: *m*/*z* (%) = 575 (23) [M]$^{+\cdot}$, 544 (5) [M – OMe]$^+$, 510 (27) [M – C$_5$H$_5$]$^+$, 450 (31), 412 (74) [M – CH(CH$_2$Ph)CO$_2$Me]$^+$, 397 (11) [M – NHCH(CH$_2$Ph)CO$_2$Me]$^+$, 374 (12) [M – Ph$_2$PO]$^+$, 346 (44), 291 (14), 226 (12), 201 (100) [Ph$_2$PO]$^+$, 183 (20) [Ph$_2$P –

2 H]$^+$, 170 (35), 133 (8), 121 (42) [Fe(C_5H_5)]$^+$, 91 (25), 69 (9), 57 (14). HR MS: calcd. for $C_{33}H_{30}NO_3PFe$ 575.1313; found 575.1295.

(S_p)-1-(Diphenylphosphanyl)-2-{*N*-[(*R*)-1-(methoxycarbonyl)-2-phenylethyl]carbamoyl}ferrocene [(*R*,S_p)-9]: Treatment of (S_p)-**1** (207 mg, 0.50 mmol), HOBt (81 mg, 0.60 mmol), EDC (0.11 mL, 0.60 mmol), (*R*)-[H_3NCH(CH_2Ph)CO_2Me]Cl (129 mg, 0.60 mmol) and Et_3N (0.10 mL, 0.71 mmol) according to the General Procedure gave the amide (*R*,S_p)-**9** (orange solid; 178 mg, 62%) and also some (S_p)-**10**. $[a]_D$ = –125 (*c* = 0.5, $CHCl_3$). ^{1}H NMR ($CDCl_3$): δ = 3.10 (dd, $^3J_{H,H}$ = 8.3, $^2J_{H,H}$ = 14.1 Hz, 1 H, C*H*$_2$Ph), 3.27 (dd, $^3J_{H,H}$ = 5.2, $^2J_{H,H}$ = 14.1 Hz, 1 H, C*H*$_2$Ph), 3.45 (s, 3 H, OMe), 3.81 (m, 1 H, C_5H_3), 3.90 (s, 5 H, C_5H_5), 4.41 (dt, *J* = 0.5, 2.6 Hz, 1 H, C_5H_3), 5.01 (m, 2 H, NHC*H* + C_5H_3), 7.11–7.56 (m, 16 H, N*H*CH + CH_2*Ph* + P*Ph*$_2$) ppm. ^{13}C{^{1}H} NMR ($CDCl_3$): δ = 37.97 (*C*H$_2$Ph), 52.05 (OMe), 53.57 (NH*C*H), 70.80 (*C*H C_5H_5), 71.58 (*C*H C_5H_3), 73.04 (d, $J_{P,C}$ = 4 Hz, *C*H C_5H_3), 74.44 (d, $J_{P,C}$ = 4 Hz, *C*H C_5H_3), 75.82 (d, $^1J_{P,C}$ = 11 Hz, *C*P C_5H_3), 80.04 (d, $^2J_{P,C}$ = 20 Hz, *C*CONH C_5H_3), 127.17 (*C*H CH_2Ph), 128.12 (*C*H PPh$_2$), 128.14 (d, $^3J_{P,C}$ = 10 Hz, *C*H PPh$_2$), 128.32 (d, $^3J_{P,C}$ = 7 Hz, *C*H PPh$_2$), 128.73 (*C*H CH_2Ph), 129.32 (*C*H CH_2Ph), 129.65 (*C*H PPh$_2$), 132.05 (d, $^2J_{P,C}$ = 17 Hz, *C*H PPh$_2$), 135.21 (d, $^2J_{P,C}$ = 22 Hz, *C*H PPh$_2$), 136.38 (d, $^1J_{P,C}$ = 7 Hz, C_{ipso} PPh$_2$), 136.70 (C_{ipso} CH_2Ph), 138.42 (d, $^1J_{P,C}$ = 7 Hz, C_{ipso} PPh$_2$), 170.22 (d, $^3J_{P,C}$ = 4 Hz, CONH), 172.05 (*C*O$_2$Me) ppm. ^{31}P{^{1}H} NMR ($CDCl_3$): δ = –20.5 (s) ppm. IR (neat): $\tilde{\nu}_{max}$ = 3300 (w, ν_{NH}), 1743 (vs., ν_{CO}), 1651 (vs., amide I), 1522 (vs., amide II), 1436 (s), 1276 (m), 1218 (m), 1178 (m), 1107 (w), 1028 (w), 1002 (w), 911 (w), 822 (m), 748 (vs), 699 (vs), 666 (w), 548 (w), 485 (s) cm^{-1}. FAB MS : *m*/*z* (%) = 576 (100) [M + H]$^{+\cdot}$, 544 (4) [M – OMe]$^+$, 510 (14) [M – C_5H_5]$^+$, 498 (9), 481 (7), 450 (5), 412 (13) [M – CH(CH_2Ph)CO_2Me]$^+$, 397 (29) [M – NHCH(CH_2Ph)CO_2Me]$^+$, 346 (9), 277 (15), 226 (11), 201 (6) [Ph_2PO]$^+$, 183 (24) [Ph_2P – 2 H]$^+$, 170 (12), 154 (17), 136 (21), 121 (18) [Fe(C_5H_5)]$^+$, 105 (9), 91 (19), 77 (16), 69 (13), 55 (24). HR MS (FAB): calcd. for $C_{33}H_{31}NO_3PFe$ [M + H]$^+$ 576.1391; found 576.1401.

(S_p)-1-({[2-(Diphenylphosphanyl)-1-ferrocenyl]carbonyl}oxy)-1*H*-benzotriazole [(S_p)-10]: The active ester (S_p)-**10** was isolated from amidation reactions between (S_p)-**1** and (*R*)-amino acid methyl esters in the presence of HOBt/EDC as an orange solid after column chromatography on silica gel with dichloromethane/methanol (50:1) as the eluent. $[a]_D$ = –209 (*c* = 0.5, $CHCl_3$). ^{1}H NMR ($CDCl_3$): δ = 4.02 (ddd, *J* = 0.9, 1.6, 2.5 Hz, 1 H, C_5H_3), 4.46 (s, 5 H, C_5H_5), 4.73 (dt, *J* = 0.6, 2.7 Hz, 1 H, C_5H_3), 5.36 (ddd, *J* = 0.9, 1.6, 2.6 Hz, 1 H, C_5H_3), 6.96 (dt, *J* = 1.1, 8.1 Hz, 1 H, C_6H_4), 7.20–7.55 (m, 10 H, PPh$_2$), 7.35–7.40 (m, 2 H, C_6H_4), 8.02 (dt, *J* = 1.0, 8.3 Hz, 1 H, C_6H_4) ppm. ^{13}C{^{1}H} NMR ($CDCl_3$): δ = 68.08 (d, $^2J_{P,C}$ = 16 Hz, *C*CONH C_5H_3), 72.04 (*C*H C_5H_5), 73.76 (*C*H C_5H_3), 74.60 (*C*H C_5H_3), 77.24 (d, $J_{P,C}$ = 5 Hz, *C*H C_5H_3), 81.90 (d, $^1J_{P,C}$ = 20 Hz, *C*P C_5H_3), 108.32 (*C*H C_6H_4), 120.27 (*C*H C_6H_4), 124.54 (*C*H C_6H_4), 128.40 (*C*H C_6H_4), 128.42 (2 × d, $^3J_{P,C}$ = 5 Hz, *C*H PPh$_2$), 128.47 (*C*H PPh$_2$), 128.74 (*C* C_6H_4), 129.42 (*C*H PPh$_2$), 132.44 (d, $^2J_{P,C}$ = 20 Hz, *C*H PPh$_2$), 134.85 (d, $^2J_{P,C}$ = 21 Hz, *C*H PPh$_2$), 137.03 (d, $^1J_{P,C}$ = 13 Hz, C_{ipso} PPh$_2$), 138.61 (d, $^1J_{P,C}$ = 13 Hz, C_{ipso} PPh$_2$), 143.41 (*C* C_6H_4), 167.97 (d, $^3J_{P,C}$ = 4 Hz, CO) ppm. ^{31}P{^{1}H} NMR ($CDCl_3$): δ = –17.5 (s) ppm. IR (Nujol): $\tilde{\nu}_{max}$ = 1777 (vs., ν_{CO}), 1321 (w), 1247 (m), 1237 (m), 1155 (w), 1107 (w), 1086 (s), 1019 (m), 926 (m), 905 (m), 829 (w), 741 (vs), 697 (s), 500 (m), 484 (m), 464 (m) cm^{-1}. FAB MS: *m*/*z* (%) = 532 (20) [M + H]$^{+\cdot}$, 521 (5), 446 (5), 429 (15), 414 (12), 397 (25) [M – OBt]$^+$, 369 (3) [M – CO_2Bt]$^+$, 277 (11), 257 (6), 226 (5), 215 (12), 201 (18) [Ph_2PO]$^+$, 185 (55), 183 (9) [Ph_2P – 2 H]$^+$, 149 (5), 121 (5) [Fe(C_5H_5)]$^+$, 110 (27), 93 (100), 75 (22), 57 (25). ESI MS: *m*/*z* (%) = 554 [M + Na]$^+$, 570 [M + K]$^+$. HR MS (FAB): calcd. for $C_{29}H_{23}N_3O_2PFe$ [M + H]$^+$ 532.0877; found 532.0888.

Catalytic Tests: The ligand (18 μmol) and the copper salt (15 μmol of Cu) were mixed with dry dichloromethane (3 mL) and stirred at room temperature for 20 min. The mixture was cooled in ice, and (*E*)-1,3-diphenylprop-2-en-1-one (**11a**; 104 mg, 0.50 mmol) was added. After the mixture had been stirred for another 10 min, a solution of Et_2Zn in heptane (0.75 mL of 1 M solution, 0.75 mmol) was introduced, and the stirring was continued at 0 °C for 4 h. The reaction mixture was washed with saturated aqueous NH_4Cl (2 × 5 mL) and extracted with diethyl ether. The organic layers were dried ($MgSO_4$) and concentrated under vacuum. Subsequent purification by column chromatography (silica gel; hexane/diethyl ether, 1:1) afforded the alkylation product **12a** or, in cases of incomplete conversion, its mixture with unreacted substrate. Levels of conversion were determined from ^{1}H NMR spectra. Enantiomeric excesses were established by HPLC analysis: Daicel Chiralcel OD-H column (250 mm × 4.6 mm), hexane/*i*PrOH (99:1), flow rate 0.75 mL min^{-1}; t_R[(*R*)-**12a**] = 20.3, t_R[(*S*)-**12a**] = 23.0 min. Spectroscopic data for the alkylation product were in accordance with literature. The configuration was assigned on the basis of optical rotation.[26] Reactions with the substituted chalcones **11b**–**g** were performed similarly. The products were analysed by NMR spectroscopy and HPLC[20b,20e] (see the Supporting Information).

Model Complexation Experiments: Ligand **2** (6.6 mg/13.5 μmol or 14.6 mg/30 μmol) and $(CuOTf)_2$·PhMe (3.9 mg, 15 μmol Cu) were mixed with CD_2Cl_2 (1 mL). The mixture was sonicated for ca. 5 min and filtered through a pad of Celite to eliminate traces of paramagnetic Cu^{II}, and the filtrate was analysed by NMR spectroscopy. The crystalline complex **14** resulted when the reagents [15 μmol of **2** and 7.5 μmol of $(CuOTf)_2$·PhMe] were mixed in chloroform (ca. 1 mL), and the solution was layered with hexane. Analytical data for **14** are available in the Supporting Information.

X-ray Crystallography

Crystallographic Data for (S,S_p)-9: $C_{33}H_{30}FeNO_3P$, *M* = 575.40, orange prism, 0.40 × 0.55 × 0.55 mm; orthorhombic, space group $P2_12_12_1$, *a* = 11.6754(1), *b* = 11.7822(1), *c* = 20.1930(2) Å; *V* = 2777.79(4) Å^3, *Z* = 4. Diffraction data were collected with a Nonius KappaCCD instrument (Mo-K_α radiation, λ = 0.71073 Å) at 150(2) K and were corrected for absorption [μ(Mo-K_α) = 0.636 mm^{-1}; transmission factors: 0.718–0.835]. A total of 48591 diffractions was measured (θ_{max} = 27.5°), of which 6361 were unique (R_{int} = 4.2%) and 6068 observed with $I > 2\sigma(I)$. The structure was solved by direct methods (SIR97[27]) and refined by full-matrix least squares on F^2 (SHELXL97[28]). Non-hydrogen atoms were refined with anisotropic displacement parameters. Hydrogen atoms, except for the amide hydrogen atom, were placed in their calculated positions and refined as riding atoms with U_{iso}(H) assigned to a multiple of U_{eq} of their bonding carbon atom. The amide hydrogen atom, H1N, was identified on a difference Fourier map and refined similarly. The refinement converged ($\Delta/\sigma_{max} \leq$ 0.001, 354 parameters) to *R* = 2.37% for observed, and *R* = 2.61%, *wR* = 6.21%, GOF = 1.053 for all diffractions; $\Delta\rho$ = 0.51, –0.23 e·Å^{-3}. The Flack enantiomorph parameter[29] was determined to be –0.012(8).

Crystallographic Data for 14: $C_{55}H_{50}Cl_6CuF_3Fe_2N_2O_9P_2S$, *M* = 1421.91, yellow prism, 0.20 × 0.23 × 0.35 mm; triclinic, space group $P\bar{1}$, *a* = 13.0920(3), *b* = 14.4847(3), *c* = 17.6069(4) Å; α = 97.023(1), β = 97.085(1), γ = 112.233(1)°; *V* = 3014.2(1) Å^3, *Z* = 2. Diffraction data were collected as described above; absorption was neglected [μ(Mo-K_α) = 1.243 mm^{-1}]. A total of 59208 diffractions was measured (θ_{max} = 27.5°), of which 13796 were unique (R_{int} = 4.2%)

and 9588 observed with $I > 2\sigma(I)$. The structure was solved and refined as described for (S,S_p)-**9**, except that one of the phenyl rings (C62–C67), the triflate anion and one chloroform molecule had to be refined over two positions due to disorder. The refinement converged ($\Delta/\sigma_{max} \leq 0.001$, 734 parameters) to $R = 5.23\%$ for observed, and $R = 8.42\%$, $wR = 14.8\%$, GOF = 1.065 for all diffractions; $\Delta\rho = 1.12$, -1.20 e Å^{-3}.

CCDC-767197 [(S,S_p)-**9**] and -767199 (**14**) contain the supplementary crystallographic data for this paper. These data can be obtained free of charge from The Cambridge Crystallographic Data Centre via www.ccdc.cam.ac.uk/data_request/cif.

Supporting Information (see footnote on the first page of this article): Details on the preparation of the starting amino acid methyl ester hydrochlorides, the crystal structure of **13**, a full view of the crystal structure of **14**, characterisation data for the complex [Cu(**2**)$_2$](TfO), and analytical data for the alkylation products **12a**–**g**.

Acknowledgments

This work was financially supported by the Grant Agency of Charles University in Prague (project no. 58009) and by the Ministry of Education of the Czech Republic (nos. LC06070 and MSM0021620857).

[1] Selected reviews: a) B. E. Rossiter, N. M. Swingle, *Chem. Rev.* **1992**, *92*, 771–806; b) M. P. Sibi, S. Manyem, *Tetrahedron* **2000**, *56*, 8033–8061; c) N. Krause, A. Hoffmann-Röder, *Synthesis* **2001**, 171–196; d) B. L. Feringa, R. Naasz, R. Imbos, L. A. Arnold in *Modern Organocopper Chemistry* (Ed.: N. Krause), Wiley-VCH, Weinheim, **2002**, chapter 7, pp. 224–258; e) A. Alexakis, C. Benhaim, *Eur. J. Org. Chem.* **2002**, 3221–3236; f) F. López, A. J. Minnaard, B. L. Feringa, *Acc. Chem. Res.* **2007**, *40*, 179–188; g) J. Christoffers, G. Koripelly, A. Rosiak, M. Rössle, *Synthesis* **2007**, 1279–1300; h) A. Alexakis, J. E. Bäckvall, N. Krause, O. Pàmies, M. Diéguez, *Chem. Rev.* **2008**, *108*, 2796–2823; i) S. R. Harutyunyan, T. den Hartog, K. Geurts, A. J. Minnaard, B. L. Feringa, *Chem. Rev.* **2008**, *108*, 2824–2852; j) T. Jerphagnon, M. G. Pizzuti, A. J. Minnaard, B. L. Feringa, *Chem. Soc. Rev.* **2009**, *38*, 1039–1075.

[2] a) A. Alexakis, J. Frutos, P. Mangeney, *Tetrahedron: Asymmetry* **1993**, *4*, 2427–2430; b) A. Alexakis, S. Mutti, J. F. Normant, *J. Am. Chem. Soc.* **1991**, *113*, 6332–6334.

[3] P. Knochel, R. D. Singer, *Chem. Rev.* **1993**, *93*, 2117–2188.

[4] a) J. Tauchman, I. Císařová, P. Štěpnička, *Organometallics* **2009**, *28*, 3288–3302; b) J. Schulz, I. Císařová, P. Štěpnička, *J. Organomet. Chem.* **2009**, *694*, 2519–2530; c) M. Lamač, I. Císařová, P. Štěpnička, *New J. Chem.* **2009**, *33*, 1549–1562; d) P. Štěpnička, M. Krupa, M. Lamač, I. Císařová, *J. Organomet. Chem.* **2009**, *694*, 2987–2993; e) J. Kühnert, I. Císařová, M. Lamač, P. Štěpnička, *Dalton Trans.* **2008**, 2454–2464; f) J. Kühnert, M. Lamač, J. Demel, A. Nicolai, H. Lang, P. Štěpnička, *J. Mol. Catal. A* **2008**, *285*, 41–47; g) M. Lamač, J. Tauchman, I. Císařová, P. Štěpnička, *Organometallics* **2007**, *26*, 5042–5049; h) J. Kühnert, M. Dušek, J. Demel, H. Lang, P. Štěpnička, *Dalton Trans.* **2007**, 2802–2811; i) P. Štěpnička, J. Schulz, I. Císařová, K. Fejfarová, *Collect. Czech. Chem. Commun.* **2007**, *72*, 453–467; j) M. Lamač, I. Císařová, P. Štěpnička, *Eur. J. Inorg. Chem.* **2007**, 2274–2287; k) M. Lamač, J. Tauchman, S. Dietrich, I. Císařová, H. Lang, P. Štěpnička, *Appl. Organomet. Chem.* **2010**, *24*, 326–331.

[5] Other examples of phosphanylferrocenecarboxamides: a) W. Zhang, T. Shimanuki, T. Kida, Y. Nakatsuji, I. Ikeda, *J. Org. Chem.* **1999**, *64*, 6247–6251; b) J. M. Longmire, B. Wang, X. Zhang, *J. Am. Chem. Soc.* **2002**, *124*, 13400–13401; c) S.-L. You, X.-L. Hou, L.-X. Dai, *J. Organomet. Chem.* **2001**, *637–639*, 762–766; d) J. M. Longmire, B. Wang, X. Zhang, *Tetrahedron Lett.* **2000**, *41*, 5435–5439; e) S.-L. You, X.-L. Hou, L.-X. Dai, B.-X. Cao, J. Sun, *Chem. Commun.* **2000**, 1933–1934; f) M. Tsukazaki, M. Tinkl, A. Roglans, B. J. Chapell, N. J. Taylor, V. Snieckus, *J. Am. Chem. Soc.* **1996**, *118*, 685–686; g) H. Jendralla, E. Paulus, *Synlett* **1997**, 471–472.

[6] B. L. Feringa, R. Badorrey, D. Peña, S. R. Harutyunyan, A. J. Minnaard, *Proc. Natl. Acad. Sci. USA* **2004**, *101*, 5834–5838.

[7] a) T. Morimoto, Y. Yamaguchi, M. Suzuki, A. Saitoh, *Tetrahedron Lett.* **2000**, *41*, 10025–10029; b) A. V. Malkov, J. B. Hand, P. Kočovský, *Chem. Commun.* **2003**, 1948–1949; c) X. Hu, H. Chen, X. Zhang, *Angew. Chem. Int. Ed.* **1999**, *38*, 3518–3521; d) Y. Liang, S. Gao, H. Wan, Y. Hu, H. Chen, Z. Zheng, X. Hu, *Tetrahedron: Asymmetry* **2003**, *14*, 3211–3217. For a related ferrocene derivative, see: e) J. F. Jensen, I. Søtofte, H. O. Sørensen, M. Johannsen, *J. Org. Chem.* **2003**, *68*, 1258–1265.

[8] a) G. Helmchen, A. Pfaltz, *Acc. Chem. Res.* **2000**, *33*, 336–345 and refs. therein; b) E. L. Stangeland, T. Sammakia, *Tetrahedron* **1997**, *53*, 16503–16510; c) R. Shintani, G. C. Fu, *Org. Lett.* **2002**, *4*, 3699–3702.

[9] a) A. W. Hird, A. H. Hoveyda, *Angew. Chem. Int. Ed.* **2003**, *42*, 1276–1279; b) B. Breit, A. C. Laungani, *Tetrahedron: Asymmetry* **2003**, *14*, 3823–3826; c) R. R. Cesati III, J. de Armas, A. H. Hoveyda, *J. Am. Chem. Soc.* **2004**, *126*, 96–101.

[10] Proline-based phosphanyl carboxamides: a) M. Kanai, Y. Nakagawa, K. Tomioka, *Tetrahedron* **1999**, *55*, 3843–3854; b) M. Kanai, K. Tomioka, *Tetrahedron Lett.* **1995**, *36*, 4275–4278.

[11] Representative examples: a) M. T. Reetz, A. Gosberg, D. Moulin, *Tetrahedron Lett.* **2002**, *43*, 1189–1191; b) F. López, S. R. Harutyunyan, A. J. Minnaard, B. L. Feringa, *J. Am. Chem. Soc.* **2004**, *126*, 12784–12785; c) F. López, S. R. Harutyunyan, A. Meetsma, A. J. Minnaard, B. L. Feringa, *Angew. Chem. Int. Ed.* **2005**, *44*, 2752–2756; d) V. E. Albrow, A. J. Blake, R. Fryatt, C. Wilson, S. Woodward, *Eur. J. Org. Chem.* **2006**, 2549–2557; e) L.-T. Liu, M.-C. Wang, W.-X. Zhao, Y.-L. Zhou, X.-D. Wang, *Tetrahedron: Asymmetry* **2006**, *17*, 136–141; f) D.-Y. Zou, Z.-C. Duan, X.-P. Hu, Z. Zheng, *Tetrahedron: Asymmetry* **2009**, *20*, 235–239.

[12] a) J. Podlaha, P. Štěpnička, J. Ludvík, I. Císařová, *Organometallics* **1996**, *15*, 543–550; b) P. Štěpnička, *Eur. J. Inorg. Chem.* **2005**, 3787–3803.

[13] a) P. Štěpnička, *New J. Chem.* **2002**, *26*, 567–575; b) B. Breit, D. Breuninger, *Synthesis* **2005**, 2782–2786.

[14] This route is commonly used in the preparation of ferrocene–amino acid conjugates: a) H.-B. Kraatz, *J. Inorg. Organomet. Polym. Mater.* **2005**, *15*, 83–106; b) N. Metzler-Nolte, M. Salmain in *Ferrocenes: Ligands, Materials and Biomolecules* (Ed.: P. Štěpnička), Wiley, Chichester, **2008**, chapter 13, pp. 499–639. For examples concerning the preparation of amides from of Hdpf and (S_p)-**1**, see ref.[4]

[15] a) See, e.g.: D. R. Scott, R. S. Becker, *J. Chem. Phys.* **1961**, *35*, 516; b) cf. λ_{max} = 443 nm for Hdpf (ref.[12a]).

[16] The amide hydrogen atom probably forms an intramolecular hydrogen bond with the phosphorus lone pair: N···P 3.193(1) Å, H1N···P 2.46 Å, N–H1N···P 143°.

[17] A. L. Spek, *J. Appl. Crystallogr.* **2003**, *36*, 7–13.

[18] G. Delapierre, T. Constantieux, J. M. Brunel, G. Buono, *Eur. J. Org. Chem.* **2000**, 2507–2511.

[19] At low temperatures the system is less prone to decomposition, as indicated by suppressed darkening of the reaction mixture.

[20] a) Y. Hu, X. Liang, J. Wang, Z. Zheng, X. Hu, *J. Org. Chem.* **2003**, *68*, 4542–4545; b) H. Wan, Y. Hu, Y. Liang, S. Gao, J. Wang, Z. Zheng, X. Hu, *J. Org. Chem.* **2003**, *68*, 8277–8280; c) Y. Hu, X. Liang, J. Wang, Z. Zheng, X. Hu, *Tetrahedron: Asymmetry* **2003**, *14*, 3907–3915; d) X. Luo, Y. Hu, X. Hu, *Tetrahedron: Asymmetry* **2006**, *16*, 1227–1231; e) J. Escorihuela, M. I. Burguete, S. V. Luis, *Tetrahedron Lett.* **2008**, *49*, 6885–6888; see also ref.[7d,11e]

[21] X.-X. Han, L.-H. Weng, X.-B. Leng, Z.-Z. Zhang, *Polyhedron* **2001**, *20*, 1881–1884.
[22] M. G. Miles, G. Doyle, R. P. Cooney, R. S. Tobias, *Spectrochim. Acta Part A* **1969**, *25*, 1515–1526.
[23] D. M. Pore, U. V. Desai, T. S. Thopate, P. P. Wadgaonkar, *Russ. J. Org. Chem.* **2007**, *43*, 1088–1089.
[24] M. Brenner, W. Huber, *Helv. Chim. Acta* **1953**, *36*, 1109–1115.
[25] N. Cramer, S. Laschat, A. Baro, *Organometallics* **2006**, *25*, 2284–2291.
[26] A. Hajra, N. Yoshikai, E. Nakamura, *Org. Lett.* **2006**, *8*, 4153–4155.
[27] A. Altomare, M. C. Burla, M. Camalli, G. L. Cascarano, C. Giacovazzo, A. Guagliardi, A. G. G. Moliterni, G. Polidori, R. Spagna, *J. Appl. Crystallogr.* **1999**, *32*, 115–119.
[28] G. M. Sheldrick, *SHELXL97, Program for Crystal Structure Refinement from Diffraction Data*, University of Göttingen, Germany, **1997**.
[29] H. D. Flack, *Acta Crystallogr., Sect. A: Fundam. Crystallogr.* **1983**, *39*, 876–881.

Received: April 8, 2010
Published Online: June 11, 2010

10.2 Appendix 2

J. Tauchman, I. Císařová, P. Štěpnička: "Chiral phosphinoferrocene carboxamides with amino acid substituents as ligands for Pd-catalysed asymmetric allylic substitutions. Synthesis and structural characterisation of catalytically relevant Pd complexes." *Dalton Trans.* **2011**, *40*, 11748.

Dalton
Transactions

Cite this: *Dalton Trans.*, 2011, **40**, 11748

www.rsc.org/dalton

PAPER

Chiral phosphinoferrocene carboxamides with amino acid substituents as ligands for Pd-catalysed asymmetric allylic substitutions. Synthesis and structural characterisation of catalytically relevant Pd complexes†

Jiří Tauchman, Ivana Císařová and Petr Štěpnička*

Received 28th June 2011, Accepted 16th August 2011
DOI: 10.1039/c1dt11230a

An extensive series of chiral amino acid amides prepared from 1′-(diphenylphosphino)ferrocene-1-carboxylic acid (Hdpf) or its planar-chiral isomer, 2-(diphenylphosphino)ferrocene-1-carboxylic acid, have been tested as ligands for Pd-catalysed asymmetric allylic substitution reactions. In alkylation of 1,3-diphenylallyl acetate as a model substrate with dimethyl malonate the ligands performed well in terms of both reaction rate and enantioselectivity, achieving up to 98% ee. In contrast, the reactions of the same substrate with other nucleophiles proceeded either slowly and with poor ee's (amination with benzylamine) or not at all (etherification with benzyl alcohol). In order to rationalise the influence of the ligand structure on the reaction course, three model complexes, *viz*. [(η^3-methallyl)PdCl(L-κ*P*)], [(η^3-methallyl)Pd(L-κ^2*O*,*P*)]ClO_4 and [(η^3-methallyl)Pd(L-κ*P*)$_2$]ClO_4 have been prepared from the achiral amide $Ph_2PfcCONHCH_2CO_2Me$ (L; fc = ferrocene-1,1′-diyl) and structurally characterised. The coordination study showed that the amido-phosphines readily form 1 : 1 complexes as O,P-chelates where the amino acid chirality is brought close to the Pd atom. At higher ligand-to-metal ratios, however, simple P-monodentate coordination prevails, minimising the influence of the chiral amino acid pendant.

Introduction

Palladium-catalysed asymmetric allylic substitution is a powerful synthetic tool allowing for stereoselective construction of C–C and C-heteratom bonds from a range of substrates.[1] Functional group tolerance and wide applicability in the synthesis of various chiral molecules led to a search for efficient ligands for this reaction, which meanwhile turned into a benchmark test for chiral donors. Particularly attractive proved to be donor-unsymmetric bidentate, potentially chelating ligands which electronically differentiate allylic termini in (η^3-allyl)palladium intermediates and thus provide the necessary bias for the reaction to proceed selectively.[1,2]

During the last few decades, numerous chiral, ferrocene-based donors of this kind have been developed and tested in allylic substitutions. As illustrious examples[1g–h,3] may serve ferrocene diphosphines and the related mixed-donor ligands (mostly P,N- and P,O-donors), 2-ferrocenyl-4,5-dihydrooxazoles (oxazolines) and diphosphine diamides analogous to Trost's ligands.[1,4]

In our previous work, we focused on catalytic utilisation of phosphinoferrocene carboxamides in Suzuki-Miyaura and Heck reactions[5] and in asymmetric allylic alkylation.[6] The favourable catalytic properties and easy synthesis led us to extend our studies towards amides prepared from ferrocene phosphinocarboxylic acids and *amino acid* esters as a readily available chiral pool.[7] Although similar ligands with organic backbones are known,[8] this concept did not yet pervade the chemistry of ferrocene ligands.

This contribution details catalytic results obtained with a series of chiral phosphinoferrocene carboxamides bearing amino acid pendants (Scheme 1) in Pd-catalysed asymmetric allylic substitution reactions. Also reported are the preparation and structural characterisation of several (η^3-allyl)Pd(II) complexes as models for the plausible reaction intermediates.

Results

The preparation of amino acid amides **1–4** and **7–10** was reported elsewhere.[7] Two new ligands included in this study, (*S*)-**5** and (*S*,*S*)-**6**, were obtained in an analogous manner by amide coupling of 1′-(diphenylphosphino)ferrocene-1-carboxylic acid (Hdpf) with amino acid methyl esters formed *in situ* from the respective hydrochlorides and triethylamine.

Chiral phosphine-amide ligands **2–10** (Scheme 1) were tested in palladium-catalysed asymmetric allylic alkylation using the common model reaction system comprising 1,3-diphenylallyl acetate (**11a**) as the allylic substrate and an 'instant' nucleophile[9] generated from dimethyl malonate and *N*,*O*-bis(trimethylsilyl)-acetamide (BSA; Scheme 2). The pre-catalyst was formed

Department of Inorganic Chemistry, Faculty of Science, Charles University in Prague, Hlavova 2030, 12840, Prague, Czech Republic. E-mail: stepnic@natur.cuni.cz

† CCDC reference numbers 823874–823876. For crystallographic data in CIF or other electronic format see DOI: 10.1039/c1dt11230a

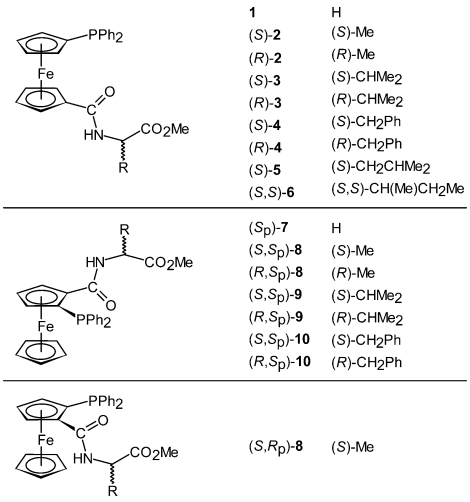

	1	H
	(*S*)-**2**	(*S*)-Me
	(*R*)-**2**	(*R*)-Me
	(*S*)-**3**	(*S*)-CHMe$_2$
	(*R*)-**3**	(*R*)-CHMe$_2$
	(*S*)-**4**	(*S*)-CH$_2$Ph
	(*R*)-**4**	(*R*)-CH$_2$Ph
	(*S*)-**5**	(*S*)-CH$_2$CHMe$_2$
	(*S*,*S*)-**6**	(*S*,*S*)-CH(Me)CH$_2$Me
	(S_p)-**7**	H
	(*S*,S_p)-**8**	(*S*)-Me
	(*R*,S_p)-**8**	(*R*)-Me
	(*S*,S_p)-**9**	(*S*)-CHMe$_2$
	(*R*,S_p)-**9**	(*R*)-CHMe$_2$
	(*S*,S_p)-**10**	(*S*)-CH$_2$Ph
	(*R*,S_p)-**10**	(*R*)-CH$_2$Ph
	(*S*,R_p)-**8**	(*S*)-Me

Scheme 1 Chiral phosphine-amide ligands tested in this study.

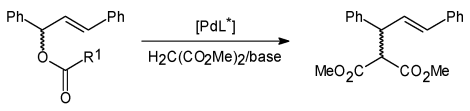

11 [R^1 = Me (**a**), OEt (**b**)] **12**

Scheme 2

in situ from [Pd(μ-Cl)(η^3-C_3H_5)]$_2$ and the respective ligand. Initial catalytic tests were carried out with ligands (S_p)-**7** and (*S*)-**2** as the representatives (Table 1).

The first catalytic tests with the planar-chiral ligand (S_p)-**7** (Table 1, entries 1–8) already showed that the reaction proceeds with reasonable conversions and good ee's. Subsequent attempts to improve the reaction outcome by addition of catalytic amounts of alkali metal acetates (10% with respect to the allylic substrate) failed, the addition resulting in lower conversions and ee's. In contrast, cooling the reaction system containing only BSA to 0 °C considerably increased the enantioselectivity (ee 98%!), albeit on account of the reaction rate (10% conversion after 24 h; entry 7). Addition of NaOAc as a base additive slightly improved the conversion at 0 °C but the ee dramatically decreased (entry 8).

A similar reaction with catalyst based on ligand (*S*)-**2** featuring chirality only in the amino acid side chain was faster, affording complete conversion within 24 h (entries 9–16 in Table 1). Notably, however, the catalyst based on (*S*)-**2** produced the alkylation product with the same degree of asymmetric induction as for (S_p)-**7** but with an inverted ratio of the enantiomers ((*S*)-**12** dominant; *cf*. entries 1 and 9). Similarly to (S_p)-**7**, the addition of alkali metal acetates to (*S*)-**2**/Pd system did not improve the catalytic performance, resulting in lower ee's while the conversions either remained virtually unchanged (Na and Cs) or decreased (Li, K and Rb). A decrease in the conversion *and* ee's was surprisingly noted also when the reaction temperature was lowered to 0 °C (entries 15 and 16).

Upon testing different solvents or bases (entries 17–27) it was found that the reaction becomes slower and less selective in THF and DMF, and stops entirely in dioxane or toluene. In acetonitrile, the conversion remained high but selectivity decreased (conversion 100% after 24 h, ee = –77% with (*S*)-**2**). The use of bases other than BSA also resulted in lower conversions and markedly decreased the enantioselectivity. Finally, changing the reaction partners (entries 28–31) had a detrimental effect on the reaction outcome. The reaction with **11a** and di-*tert*-butyl malonate as a more bulky nucleophile did not proceed while carbonate **11b** and dimethyl malonate afforded the alkylation product still quantitatively but with a relatively lower selectivity.

Additional experiments with ligand (*S*)-**2** revealed that the reaction outcome depends strongly on the ligand-to-metal ratio (results not tabulated). Whereas the conversions achieved with (*S*)-**2** remained practically complete in all cases (98–100% after 24 h), the enantioselectivity decreased from ee –85% at L : Pd ratio 1 : 1 to –71% at L : Pd = 1 : 1.2 and –62% at L : Pd = 1 : 1.5 and, finally, to *zero* at L : Pd = 2 : 1. A similar but less pronounced trend was noted also in reactions with ligand (S_p)-**7**, which afforded the alkylation product with 81% conversion and 85% ee at L : Pd ratio 1 : 1 and with an 82% conversion and 77% ee at L : Pd ratio 2 : 1.

After surveying the reaction parameters, the whole series of ligands was assessed under optimised conditions (BSA without any added alkali metal acetate, dichloromethane, room temperature). The results are summarised in Table 2.

Table 1 Summary of catalytic results obtained with ligands (*S*)-**2** and (S_p)-**7** in asymmetric allylic alkylation[a]

Entry	Ligand	Solvent	Base/additive	Conv./%	ee/% [config][f]
1	(S_p)-**7**	CH_2Cl_2	BSA/none	81	85 [*R*]
2	(S_p)-**7**	CH_2Cl_2	BSA/LiOAc	79	61 [*R*]
3	(S_p)-**7**	CH_2Cl_2	BSA/NaOAc	80	81 [*R*]
4	(S_p)-**7**	CH_2Cl_2	BSA/KOAc	54	55 [*R*]
5	(S_p)-**7**	CH_2Cl_2	BSA/RbOAc	47	61 [*R*]
6	(S_p)-**7**	CH_2Cl_2	BSA/CsOAc	75	64 [*R*]
7[b]	(S_p)-**7**	CH_2Cl_2	BSA/none	10	98 [*R*]
8[b]	(S_p)-**7**	CH_2Cl_2	BSA/NaOAc	24	37 [*R*]
9	(*S*)-**2**	CH_2Cl_2	BSA/none	100	–85 [*S*]
10	(*S*)-**2**	CH_2Cl_2	BSA/LiOAc	90	–67 [*S*]
11	(*S*)-**2**	CH_2Cl_2	BSA/NaOAc	100	–65 [*S*]
12	(*S*)-**2**	CH_2Cl_2	BSA/KOAc	80	–50 [*S*]
13	(*S*)-**2**	CH_2Cl_2	BSA/RbOAc	84	–41 [*S*]
14	(*S*)-**2**	CH_2Cl_2	BSA/CsOAc	100	–70 [*S*]
15[b]	(*S*)-**2**	CH_2Cl_2	BSA/none	10	–40 [*S*]
16[b]	(*S*)-**2**	CH_2Cl_2	BSA/NaOAc	90	–58 [*S*]
17	(*S*)-**2**	THF	BSA/none	56	–45 [*S*]
18	(*S*)-**2**	dioxane	BSA/none	0	—
19	(*S*)-**2**	toluene	BSA/none	0	—
20	(*S*)-**2**	MeCN	BSA/none	100	–77 [*S*]
21	(*S*)-**2**	DMF	BSA/none	67	–74 [*S*]
22	(*S*)-**2**	CH_2Cl_2	NaN(SiMe$_3$)$_2$	49	–26 [*S*]
23	(*S*)-**2**	CH_2Cl_2	KN(SiMe$_3$)$_2$	11	–20 [*S*]
24	(*S*)-**2**	CH_2Cl_2	KO*t*-Bu	72	–4 [*S*]
25	(*S*)-**2**	CH_2Cl_2	K_2CO_3	5	—
26	(*S*)-**2**	CH_2Cl_2	K_3PO_4	37	0
27	(*S*)-**2**	CH_2Cl_2	DBU[e]	82	–6 [*S*]
28[c]	(*S*)-**2**	CH_2Cl_2	BSA/none	0	—
29[c]	(*S*)-**2**	CH_2Cl_2	BSA/NaOAc	0	—
30[d]	(*S*)-**2**	CH_2Cl_2	BSA/none	100	–78 [*S*]
31[d]	(*S*)-**2**	CH_2Cl_2	BSA/NaOAc	100	–61 [*S*]

[a] Reaction of **11a** with 3 equiv. of dimethyl malonate and 3 equiv. of BSA in the presence of 5 mol.% of Pd catalyst generated *in situ* from [Pd(μ-Cl)(η-C_3H_5)]$_2$ and a ligand (Pd : L = 1 : 1) in 3 mL of solvent at room temperature for 24 h. [b] Reaction performed at 0 °C. [c] Reaction with di-*tert*-butyl malonate. [d] Reaction with **11b** as the substrate. [e] DBU = 1,8-diazabicyclo[5.4.0]undec-7-ene. [f] ee = ([*R*] – [*S*])/([*R*] + [*S*]).

Table 2 Survey of the ligands in the Pd-catalysed allylic alkylation[a]

Amino acid	Hdpf			(S_p)-Hpfc		
	Ligand	Conv./%	ee/%	Ligand	Conv./%	ee/%
Gly	**1**	—	—	(S_p)-**7**	81	85 [*R*]
(*S*)-Ala	(*S*)-**2**	100	−85 [*S*]	(S,S_p)-**8**	55	52 [*R*]
(*R*)-Ala	(*R*)-**2**	100	84 [*R*]	(R,S_p)-**8**[b]	34	83 [*R*]
(*S*)-Val	(*S*)-**3**	23	−24 [*S*]	(S,S_p)-**9**	80	60 [*R*]
(*R*)-Val	(*R*)-**3**	25	26 [*R*]	(R,S_p)-**9**	12	57 [*R*]
(*S*)-Leu	(*S*)-**5**	93	−65 [*S*]	—	—	—
(*S*,*S*)-Ile	(*S*,*S*)-**6**	53	−11 [*S*]	—	—	—
(*S*)-Phe	(*S*)-**4**	56	−67 [*S*]	(S,S_p)-**10**	51	65 [*R*]
(*R*)-Phe	(*R*)-**4**	92	66 [*R*]	(R,S_p)-**10**	15	58 [*R*]

[a] For conditions, see Table 1, footnote *a*. Data for compounds (*S*)-**2** and (S_p)-**7** are included from Table 1 for a comparison. [b] The enantiomeric ligand (S,R_p)-**8** gave **12** with 43% conversion and −85% ee.

In general, the reaction rate (conversion) and stereoselectivity varied greatly with the ligand structure. Reactions with ligands derived from achiral Hdpf and (*S*)-amino acid esters produced the alkylation product enriched in (*S*)-**12**, while the enantiomeric ligands expectedly favoured the formation of (*R*)-**12**. Among donors obtained from (*S*)-amino acids, which constitute a more extensive set, the best conversion and ee were achieved with (*S*)-**2** as a ligand possessing the smallest substituent in the amino acid residue. Increasing the steric bulk of the amino acid substituent significantly decreased the enantioselectivity. For instance, (*S*)-**5** featuring an amino acid residue branched in γ-position and the ligand obtained from (*S*)-phenylalanine afforded the alkylation product with a lower, *ca.* 65–67% ee. The more sterically encumbered ligands branched in β-position ((*S*)-**3** and (*S*,*S*)-**6**) performed even worse (Table 2).

Trends among ligands derived from planar-chiral 2-(diphenylphosphino)ferrocene-1-carboxylic acid (Hpfc) are less obvious, probably because of an interplay of the two chirality elements. Yet again, the best results were obtained with ligand (S_p)-**7** containing the least sterically demanding glycine pendant.

Ligand (*S*)-**2** was chosen for further testing in allylation of model N- and O-nucleophiles. Amination performed with **11a** and benzylamine in the presence of BSA as a base (Scheme 3, Table 3) afforded only racemic **13** (96% conversion after 2 days with 5% mol.% of Pd catalyst). Similar reactions without any additive proceeded much slower and with only a poor enantioselectivity (Table 3). An analogous etherification of **11a** with benzyl alcohol (Scheme 4) in the presence of 5 mol.% of the same Pd-catalyst and BSA or Cs_2CO_3 as the base (3 equiv.) did not proceed at all.

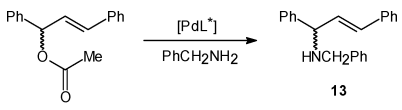

11a **13**

Scheme 3

Table 3 Summary of catalytic results obtained in allylic amination[a]

Entry	Base	*t*/h	Conv. (ee)/%
1	BSA	24	62 (0)
2	BSA	48	96 (0)
3	none	24	20 (12) [*R*]
4	none	48	29 (13) [*R*]

[a] Conditions: 5 mol.% Pd catalyst prepared *in situ* from [Pd(μ-Cl)(η^3-C_3H_5)]$_2$ and (*S*)-**2** (L : Pd = 1 : 1); $PhCH_2NH_2$ (3 equiv.), BSA (3 equiv.) in CH_2Cl_2 (3 mL), room temperature.

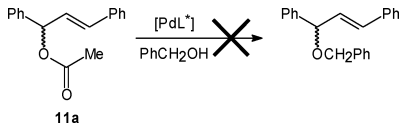

11a

Scheme 4

Coordination study

In order to gain an insight into the nature of putative reaction intermediates and structural factors governing the reaction course, we decided to synthesise and *structurally* characterise some model (η^3-allyl)palladium(II) complexes. Unfortunately, repeated attempts to prepare any well-defined (solid) samples of the most catalytically relevant (η^3-1,3-diphenylallyl)palladium complexes with (*S*)-**2** failed.[10] Therefore, we turned to similar reactions with achiral donor **1**.[11]

Indeed, the reaction of [(η^3-$Ph_2C_3H_3$)$PdCl]_2$ and **1** produced an orange solid, which showed a signal due to [(η^3-$Ph_2C_3H_3$)Pd(**1**)]$^+$ (*m*/*z* 784) in ESI mass spectra and contained one dominant and two very minor species according to ^{1}H (ref.)[12] and ^{31}P NMR analysis. The NMR spectra suggested that the PPh_2 group is coordinated in all cases (δ_P 14.8 major, 15.5 and 16.0 minor). Considering the high conformational flexibility of (η^3-$Ph_2C_3H_3$)Pd moiety and similarity of the ^{31}P NMR chemical shifts, the minor components are most probably isomers to the major component differing in the overall molecular conformation. However, other species resulting by, *e.g.*, self-ionisation ([(η^3-$Ph_2C_3H_3$)PdCl(**1**)] → [(η^3-$Ph_2C_3H_3$)Pd(**1**)]Cl), cannot simply be excluded.

When $AgClO_4$ (1 equiv.) was added to *in situ* formed [(η^3-$Ph_2C_3H_3$)PdCl(**1**)], the chloride complex was cleanly converted to a new compound, which showed one broad, low-field shifted signal in its ^{31}P NMR spectrum (δ_P 19.5). The ^{1}H NMR spectrum displayed *very* broad resonances, suggesting some dynamic equilibria. The ESI mass spectrum expectedly showed a peak at *m*/*z* 784 ([(η^3-$Ph_2C_3H_3$)Pd(**1**)]$^+$).

Because our subsequent attempts at obtaining crystalline materials from [(η^3-$Ph_2C_3H_3$)PdCl(**1**)] and [(η^3-$Ph_2C_3H_3$)Pd(**1**)]ClO_4 met with no success, we ultimately turned to η^3-methallyl complexes with non-chiral ligand **1** as even simpler (an potentially better crystallising) compounds (Scheme 5). Thus, the dipalladium complex **14** reacted smoothly with **1** yielding the bridge-cleavage product **16** in which the ferrocene ligand coordinates as a P-monodentate donor. The reactions of **1** with complex **15**, which was obtained from **14** *via* halogen abstraction with $AgClO_4$,[13] proceeded under displacement of the coordinated acetonitrile ligands to afford complex **17** featuring the amidophosphine as an O,P-chelate donor or bis-phosphine complex **18** depending on the Pd/**1** molar ratio. According to NMR analysis of the reaction mixtures, the complexation reactions proceed cleanly, affording only the products specified.

Complexes **16** and **17** are highly soluble in common organic solvents and were therefore isolated by precipitation as yellow air-stable solids showing a high tendency to hold solvent residua. The

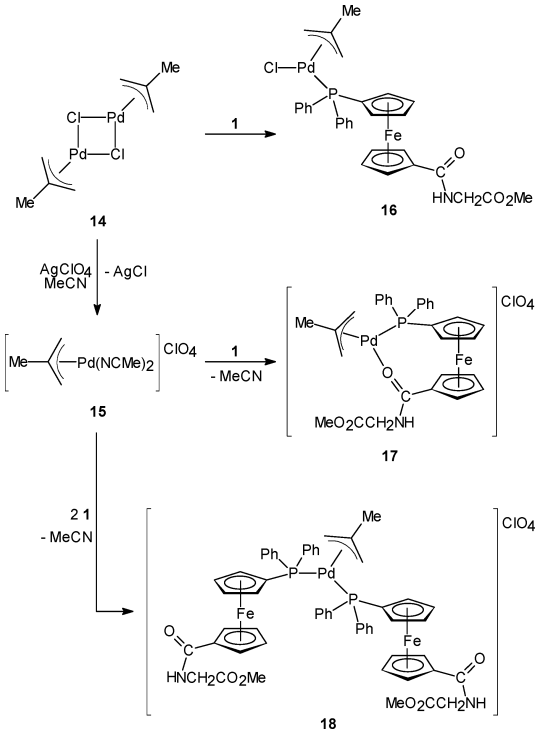

Scheme 5 Preparation of (η^3-methallyl)palladium complexes.

solubility of complex **18** is relatively lower. It is noteworthy that complex **16** did not appreciably react with BSA, $NaN(SiMe)_3$ or KO*t*-Bu (2 equiv.; reactions in CH_2Cl_2 at room temperature for *ca.* 20 h). In contrast, addition of NaH and stirring overnight caused extensive decomposition.

Complexes **16–18** exhibit single resonances in their $^{31}P\{^1H\}$ NMR spectra, shifted markedly to lower fields *versus* free **1** due to P-coordination of the ferrocene ligand (*cf.* **16**: $\delta_P = 11.6$, **17**: $\delta_P = 20.8$, **18**: $\delta_P = 18.2$; **1**: $\delta_P = -16.9$). Coordination of the amide oxygen in **17** is manifested by a shift of the associated ^{13}C NMR resonance to lower fields (*cf*. δ_C(CONH) *ca.* 170 for **16** and **18**, and *ca.* 174 for **17**) and further in IR spectra, where the amide I band (largely $\nu_{C=O}$) moves to lower energies (1652/1655 cm^{-1} for **16**/**18** *vs.* 1596 cm^{-1} for **17**) while the amide II band shifts in the opposite direction (1538/1536 cm^{-1} for **16**/**18** and 1558 cm^{-1} for **17**).[6b,7a] The response of the terminal ester group, which is not involved in coordination, remains practically unaffected ($\nu_{C=O} \approx 1750$ cm^{-1}, $\delta_C \approx 170$).

The non-equivalent allylic CH_2 groups in **16** and **17** give rise to two pairs of signals ($H^{syn/anti}$) in the ^1H NMR and two separate signals in the $^{13}C\{^1H\}$ NMR spectra. For both compounds, the low-field ^{13}C NMR signals show splitting with ^{31}P (δ_C 78.65 for **16**, 83.34 for **17**; $^2J_{PC}$ *ca.* 30 Hz) and can thus be attributed to the CH_2 groups located *trans* to the phosphorus donor atom. The signals due to CH_2 *trans* to Cl or O appear as singlets at higher fields (δ_C 64.13 for **16**, and 55.44 for **17**). It is noteworthy that a larger difference in the ^{13}C chemical shifts in this case corresponds to a larger difference in *trans*-influence of the respective donor groups ($\Delta_{P/Cl} < \Delta_{P/O}$) and also in the lengths of the Pd–CH_2 bonds (see below).

Allylic CH_2 groups in complex **18** are equivalent, being observed as a pair of signals in the ^1H NMR spectrum and one ^{13}C NMR resonance which overlaps with the solvent signal ($\delta_C \approx 76.6$). Owing to the presence of two identical phosphine groups in **18**, the $^{13}C\{^1H\}$ NMR signals due to carbons within the Ph_2P-substituted cyclopentadienyl and phenyl rings (except for CH_{para}) and signal of the allylic C_{ipso} carbon are seen as characteristic non-binomial triplets typical of virtually coupled ABX spin systems of the type ^{12}C–$^{31}P(A)$–M–$^{31}P(B)$–$^{13}C(X)$ (M = metal).[14] Similar features were observed in the spectra of bis-phosphine complexes with other 1′-functionalised (diphenylphoshino)ferrocene ligands, *trans*-[$PdCl_2(Ph_2PfcX$-κ*P*$)_2$] (X = a functional group)[15] and *trans*-[$W(CO)_4(Ph_2PfcCH{=}CH_2$-κ*P*$)_2$].[16]

Crystal structures. Complex **15** (Fig. 1) crystallises in the monoclinic space group $P2_1/m$ so that both ions constituting the structure reside on the crystallographic mirror planes, similar to [Pd(η^3-C_3H_5)$(MeCN)_2]_2(B_{10}H_{10})\cdot C_6H_6$.[17] Similarly to other π-allyl complexes,[18] the allyl plane is tilted with respect to the plane defined by palladium and its ligating nitrogen atoms, {Pd, N, N′}, at the dihedral angle of 117.4(2)°. The Pd–$C_{terminal}$ distance in **15** is by *ca.* 0.04 Å shorter than the Pd–C_{meso} bond and the methyl group in *meso* position is displaced from the allyl plane {C1, C2, C1′} towards the Pd atom by 0.301(3) Å. The geometry of the Pd-NCMe moiety in **15** compares well with that in the mentioned η^3-C_3H_5 complex. In the crystal, the ions constituting the structure of **15** are interconnected *via* C–H···O interactions[19] into layers oriented parallel to the *ab* plane.

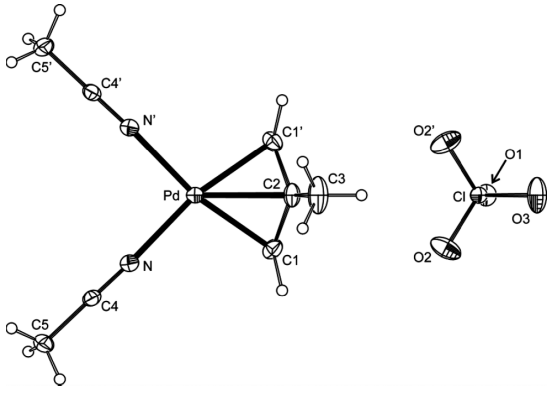

Fig. 1 PLATON plot of the molecular structure of **15** (30% probability level). Primed atoms are generated by the (x, $\frac{1}{2} - y$, z) symmetry operation. Selected distances and angles (in Å and deg): Pd–N 2.079(1), N–C4 1.131(2), C4–C5 1.454(2), Pd–N–C4 176.8(1), N–C4–C5 179.6(3); Pd–C1 2.103(2), Pd–C2 2.144(2), C1–C2 1.402(2), C2–C3 1.501(4), C1–C2–C1′ 114.7(2); Cl–O 1.429(2)–1.439(2), O–Cl–O 109.03(9)–109.8(1).

The molecular structures of **16**·H_2O and **17** are presented in Fig. 2 and 3. Selected distances and angles are given in Table 4. The Pd-donor (Cl, O, P, and allyl carbons) distances in **16**·H_2O and **17** are unexceptional in view of the data reported for [(η^3-methallyl)PdCl(L-κ*P*)] (L = PPh_3[20] or Hdpf[21]) and the O,P-chelate complexes [(μ-O,P:O′,P′-L^1)$Pd_2(\eta^3$-$C_3H_5)_2$](OTf)$_2$ (L^1 = (*R*,*R*)-1,2-(2-$Ph_2PC_6H_4CONH)C_6H_{10}$; Trost's ligand),[22] and [Pd(η^3-1,3-$Ph_2C_3H_5$)(L^2-κ^2*O*,*P*)] (L^2 = [Fe(η^5-C_5H_3-1-PPh_2-2-$CONHCH_2Ph$)(η^5-C_5H_5)].[6b] The allyl unit in **16**·H_2O extends away from the

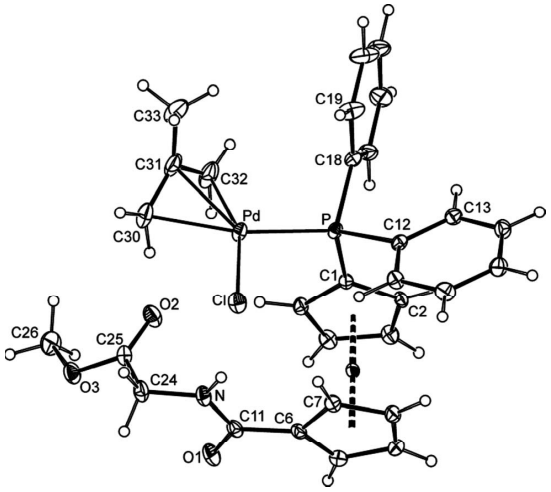

Fig. 2 PLATON plot of the complex molecule (major contributing part) in **16**·H_2O. Displacement ellipsoids enclose the 30% probability level.

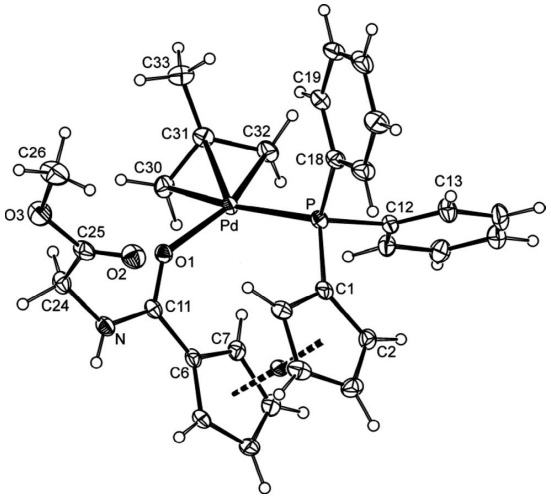

Fig. 3 PLATON plot of the complex cation the crystal structure of **17**. Displacement ellipsoids enclose the 30% probability level.

ferrocene unit and above the amino acid residue whereas in **17** it is embedded within a donor pocket created by the chelate ligand.[23] The allyl planes are tilted with respect to the plane defined by the Pd and the σ-donor atoms (the dihedral angles are 115.5(3)° for **16**·H_2O and 112.1(5)° for **17**) and the methyl substituent is inclined towards palladium (the distances of the methyl carbon from the allyl planes are 0.271(5) Å for **16**·H_2O and 0.248(6) Å for **17**). In both structures, the Pd–C(allyl) bond lengths gradually decrease from C30 to C32. A smaller absolute difference in **16**·H_2O (*cf*. *ca.* 0.09 Å for **16**·H_2O and *ca.* 0.12 Å for **17**) corresponds with the nature of donors in *trans* positions (*trans*-influence: PR_3 > Cl > O).[24] The allylic C–C bond lengths follow a similar though less pronounced trend.

Change in the mode of coordination such in **16**·H_2O and **17** obviously alters the geometry of the ferrocene ligand. The

Table 4 Selected geometric data (in Å and °) for **16**·H_2O and **17**[a]

Parameter	**16**·H_2O (X = Cl)[d]	**17** (X = O1)
Pd–X	2.3730(8)	2.142(3)
Pd–P	2.3163(7)	2.313(1)
Pd–C30	2.198(3)	2.210(5)
Pd–C31	2.173(3)	2.173(4)
Pd–C32	2.110(3)	2.087(4)
X–Pd–P	106.09(3)	101.76(8)
X–Pd–C30	93.35(9)	94.2(1)
P–Pd–C32	93.56(9)	97.4(1)
C30–Pd–C32	66.7(1)	67.0(2)
C30–C31	1.394(4)	1.388(6)
C31–C32	1.425(4)	1.428(6)
C31–C33	1.485(5)	1.497(6)
C30–C31–C32	114.4(3)	114.9(4)
C30/C32–C31–C33	122.0(3)/122.4(3)	122.3(4)/121.9(4)
C11–O1	1.235(3)	1.249(5)
C11–N	1.340(3)	1.326(4)
O1–C11–N	121.6(2)	120.1(3)
O1–C11–N–C24	0.5(4)	3.3(6)
φ[b]	6.3(3)	21.8(5)
C25–O2	1.198(4)	1.190(6)
C25–O3	1.328(4)	1.335(5)
O2–C25–O3	124.8(3)	124.9(4)
Fe–Cg1	1.647(1)	1.645(2)
Fe–Cg2	1.650(1)	1.649(2)
∠Cp1,Cp2	3.4(2)	5.9(3)
τ[c]	85	63

[a] Definition of the ring planes: Cp1 = C(1–5), Cp2 = C(6–10). Cg1/2 denote the respective ring centroids. [b] Dihedral angle subtended by the amide {C11,O1,N} and Cp2 ring planes. [c] Torsion angle C1–Cg1–Cg2–C6. [d] Data for the major contributing part (see Experimental).

closure of the O,P-chelate ring requires reorientation of the cyclopentadienyl (Cp) rings and rotation of the amide plane from an arrangement coplanar with its parent cyclopentadienyl ring. The amide moieties $C(O)NHCH_2$ in both structures are practically planar (see the O1–C11–N–C24 torsion angles in Table 4) but assume mutually opposite orientations. In **16**·H_2O, the amide plane is oriented with its N atom to the side of the phosphorus substituent while in **17** the amide oxygen is closer to PPh_2 due to chelation. Furthermore, the coordination results in a slight elongation of the C=O and shortening of the C–N amide bonds (uniformly by ±0.014 Å). Similar changes can be detected in the structures of the mentioned bis[(allyl)palladium] complex featuring Trost's ligand[22] and in Pd(II) complexes with phosphinoferrocene carboxamides.[6b,7a]

It also is noteworthy that complex **16** isolated from the reaction mixture is amorphous and does not crystallise under anhydrous conditions. The crystallisation commences readily once some adventitious water is present, affording the stoichiometric solvate **16**·H_2O. The reason for such behaviour becomes evident upon inspection of the crystal assembly. The water molecules in **16**·H_2O behave as molecular clips, connecting two adjacent molecules of the complex into a centrosymmetric array *via* hydrogen bonds to carbonyl oxygen as a bifurcate H-bond acceptor (Fig. 4). The amide NH group oriented towards the (allyl)Pd unit forms an intramolecular hydrogen bond with the Pd-bound chloride. On the other hand, the solid-state packing of non-solvated **17** is dominated by hydrogen bonds between NH[25] and CH protons as H-bond donors and perchlorate oxygen atoms as acceptors.

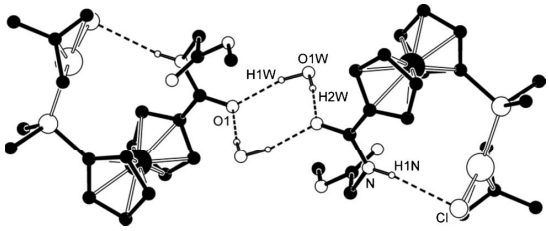

Fig. 4 Hydrogen bonding interactions (dashed lines) in the structure of **16**·H_2O. For clarity, only relevant hydrogen atoms and pivotal carbons of the phenyl rings are shown. H-bond parameters are as follows: O1W–H1W···O1, O1W···O1 = 2.863(3) Å, angle at H1W = 167°; O1W–H2W···O1, O1W···O1 = 2.895(3) Å, angle at H2W = 172°; N1–H1N···Cl, N1···Cl = 3.292(2) Å, angle at H1N = 158°.

Discussion and conclusion

Unlike many other chiral phosphinoferrocene ligands obtained by multi-step procedures, the chiral amides prepared by conjugation of ferrocene phosphinocarboxylic acids with amino acid esters are readily accessible in good yields and purity and, above all, are highly structurally versatile. The results collected indicate that these amides are efficient ligands for Pd-catalysed asymmetric allylic alkylation. In the model reaction of dimethyl malonate with in the presence of BSA, they produce the alkylation product with up to 98% ee under optimised reaction conditions. On the other hand, the ligands perform only poorly in the corresponding amination and etherification reactions.

The model coordination study expectedly demonstrated that the phosphine-amide ligands coordinate the soft palladium(II) ion[26] preferentially *via* their soft P-donor site. At 1 : 1 metal-to-ligand ratio, however, they form chelates. Although this has not been proven *in situ* (*i.e.*, under conditions mimicking exactly the reaction mixture), the formation of chelated Pd(II) intermediates appears to be the only plausible explanation for the observed reaction outcome. Regardless of whether O,P- (neutral ligand) or P,N-chelates (deprotonated ligand) are formed as catalytically active intermediates, the chelation brings the chirality inherent in the amino acid into a vicinity of the catalytic centre. The catalysed reaction (conversion *and* ee) is then controlled largely by spatial properties of the amino acid substituent. Besides, the coordination of two different donor atoms leads to an electronic differentiation of allylic termini in (η^3-allyl)palladium(II) reaction intermediates (see structural data above), which then react with relatively different rates with the incoming nucleophile (preferentially at the site opposite to the donor with a larger *trans*-influence).[1,27]

Increasing the Pd-to-ligand ratio to 1 : 2 results in the formation of bis(phosphine) complexes, where the amino acid chirality is located rather far from the catalytic centre. This particularly holds true for ligands obtained from achiral Hdpf, with which only racemic alkylation product was obtained at the Pd : L ratio of 1 : 2.

The situation becomes more complicated (and less predictable) upon introduction of planar chirality into the system mostly because the chirality elements may combine in a matched or a mismatched manner (*cf*. the catalytic performance of (S,S_p)- and (R,S_p)-**8**). In addition, the donor groups attached in positions 1 and 2 of the ferrocene moiety are closer to each other than in the Hdpf-based ligands, which may result in sterically crowded intermediates and a diminished preference for a single reaction intermediate.

Experimental

Materials and methods

All syntheses were performed under an argon atmosphere with exclusion of the direct daylight. Solvents used in the syntheses and catalytic tests were dried over by appropriate drying agents and distilled under argon: dichloromethane (K_2CO_3), 1,4-dioxane, toluene and tetrahydrofuran (sodium metal). Anhydrous acetonitrile and *N*,*N*-dimethylformamide were purchased from Fluka. Methanol was distilled from MeONa. Benzylamine and benzyl alcohol were distilled under vacuum. Amino acid methyl ester hydrochlorides [$H_3NCH(R)CO_2Me$]Cl (R = (S)-CH_2CHMe_2 and (S,S)-$CHMeCH_2Me$) were prepared by reactions of the respective amino acids with thionyl chloride in dry methanol.[28] Hdpf,[29] ligand **1**[7a] and its chiral analogues (**2–4**, **7–10**),[7b] *rac*-1,3-diphenylprop-2-en-1-yl acetate (**11a**),[30] *rac*-ethyl-(1,3-diphenylprop-2-en-1-yl) carbonate (**11b**),[31] *rac*-*N*-benzyl-(1,3-diphenylprop-2-en-1-yl)amine (**13**),[32] and [Pd(μ-Cl)(η^3-MeC_3H_4)]$_2$ (**14**)[33] were prepared according to literature procedures. Other chemicals (Aldrich, Fluka) and solvents used for crystallisations and in chromatography (Lach-Ner) were used as received.

NMR spectra were recorded with a Varian UNITY Inova 400 spectrometer (^{1}H, 399.95 MHz, ^{13}C, 100.58 MHz; and ^{31}P, 161.90 MHz) at 298 K. Chemical shifts (δ (ppm)) are given relative to internal $SiMe_4$ (^{1}H and ^{13}C) or to external 85% aqueous H_3PO_4 (^{31}P). IR spectra were obtained with an FT IR Nicolet Magna 760 instrument. High resolution electrospray ionisation mass spectra (ESI MS) were obtained with an LTQ Orbitrap XL spectrometer (Thermo Fisher Scientific). Optical rotations were determined with an automatic polarimeter Autopol III (Rudolph Research) at room temperature.

Safety Note. **Caution**! Although we have not encountered any problems it should be noted that perchlorate salts of metal complexes with organic ligands are potentially explosive and should be handled only in small quantities and with care.

Syntheses and catalytic tests

***N*-[(1*S*)-1-methoxycarbonyl-3-methylbutyl] [1′-(diphenylphosphino)ferrocene-1-carboxamide] ((*S*)-5).** Hdpf (207 mg, 0.50 mmol) and 1-hydroxybenzotriazole (81 mg, 0.60 mmol) were mixed with dry dichloromethane (10 mL). The suspension was cooled in an ice bath and treated with 1-(3-dimethylaminopropyl)-3-ethylcarbodiimide (0.1 mL, 0.6 mmol). The resultant mixture was stirred at 0 °C for 15 min, whereupon the solids dissolved to give a clear orange-red solution. A mixture of (S)-[$H_3NCH(CH_2CHMe_2)CO_2Me$]Cl (127 mg, 0.70 mmol), triethylamine (0.1 mL, 0.8 mmol) and dichloromethane (20 mL) prepared separately was introduced and the resulting mixture was stirred at room temperature overnight. Then, it was washed successively with 10% aqueous citric acid (25 mL), saturated aqueous $NaHCO_3$ (2× 25 mL), and brine (25 mL). The organic phase was dried ($MgSO_4$), evaporated under vacuum, and the

orange residue was purified by column chromatography over silica gel using dichloromethane/methanol (10 : 1, v/v) as the eluent. A single orange band was collected and evaporated to afford analytically pure (*S*)-**5** as an orange solid (262 mg, 97%).

^{1}H NMR NMR ($CDCl_3$): δ 0.96 (d, $^3J_{HH}$ = 6.4 Hz, 3 H, CH*Me*$_2$), 0.97 (d, $^3J_{HH}$ = 6.4 Hz, 3 H, CH*Me*$_2$), 1.59–1.79 (m, 3 H, C*H*$_2$C*H*Me$_2$), 3.72 (s, 3 H, OMe), 4.08 (dq, *J* = 1.2, 3.1 Hz, 1 H, fc), 4.21 (dt, *J* = 1.3, 2.4 Hz, 1 H, fc), 4.23 (dt, *J* = 1.2, 2.4 Hz, 1 H, fc), 4.26 (dq, *J* = 1.2, 3.4 Hz, 1 H, fc), 4.43 (dt, *J* = 1.3, 2.5 Hz, 1 H, fc), 4.48 (dt, *J* = 1.2, 2.4 Hz, 1 H, fc), 4.53 (dt, *J* = 1.3, 2.6 Hz, 1 H, fc), 4.62 (dt, *J* = 1.3, 2.5 Hz, 1 H, fc), 4.72 (ddd, $^3J_{HH}$ = 5.0, 8.6, 9.1 Hz, 1 H, NHC*H*), 6.16 (d, $^3J_{HH}$ = 8.3 Hz, 1 H, NH), 7.29–7.40 (m, 10 H, PPh$_2$). ^{13}C{^{1}H} NMR ($CDCl_3$): δ 21.82 (CH*Me*$_2$), 22.95 (CH*Me*$_2$), 25.00 (*C*HMe$_2$), 41.53 (CH$_2$), 50.70 (NHCH), 52.25 (OMe), 69.53 (*C*H fc), 69.65 (d, J_{PC} = 1 Hz, *C*H fc), 71.76 (*C*H fc), 71.82 (d, J_{PC} = 1 Hz, *C*H fc), 72.91 (d, J_{PC} = 4 Hz, *C*H fc), 73.15 (d, J_{PC} = 4 Hz, *C*H fc), 74.13 (d, J_{PC} = 13 Hz, *C*H fc), 74.60 (d, J_{PC} = 15 Hz, *C*H fc), 76.06 (*C*-CONH fc), 128.29 (2× d, $^3J_{PC}$ = 7 Hz, *C*H PPh$_2$), 128.78 (*C*H PPh$_2$), 128.84 (*C*H PPh$_2$), 133.35 (d, $^2J_{PC}$ = 9 Hz, *C*H PPh$_2$), 133.54 (d, $^2J_{PC}$ = 10 Hz, *C*H PPh$_2$), 137.96 (d, $^1J_{PC}$ = 8 Hz, C_{ipso} PPh$_2$), 138.21 (d, $^1J_{PC}$ = 8 Hz, C_{ipso} PPh$_2$), 169.86 (CONH), 173.69 (*C*O$_2$Me). The signal due to *C*-P of fc was not found. ^{31}P{^{1}H} NMR ($CDCl_3$): δ −16.9 (s). IR (Nujol): ν_{NH} 3287 m, ν_{CO} 1731 vs, amide I 1622 vs, amide II 1539 vs; 1435 s, 1301 m, 1251 w, 1181 w, 1163 w, 1096 w, 1027 m, 997 w, 837 m, 744 s, 697 s, 497 m, 454 w cm^{-1}. HR MS (ESI+) calc. for $C_{30}H_{33}NO_3PFe$ [M + H]$^+$ 542.1547, found 542.1542. $[\alpha_D]^{25\,°C}$ +2 (*c* 0.5, $CHCl_3$).

***N*-[(1*S*,2*S*)-1-methoxycarbonyl-2-methylbutyl] [1′-(diphenylphosphino)ferrocene-1-carboxamide] ((*S*,*S*)-6).** Amide (*S*,*S*)-**6** was prepared similarly to (*S*)-**5**, starting with Hdpf (207 mg, 0.50 mmol), 1-hydroxybenzotriazole (81 mg, 0.60 mmol), 1-(3-dimethylaminopropyl)-3-ethylcarbodiimide (0.1 mL, 0.6 mmol), (*S*,*S*)-[H$_3$NCH(CHMeCH$_2$Me)CO$_2$Me]Cl (127 mg, 0.7 mmol) and triethylamine (0.1 mL, 0.8 mmol). Isolation as described above afforded (*S*,*S*)-**6** as an orange oil (255 mg, 94%).

^{1}H NMR NMR ($CDCl_3$): δ 0.95 (t, $^3J_{HH}$ = 7.4 Hz, 3 H, CH$_2$*Me*), 0.96 (d, $^3J_{HH}$ = 6.8 Hz, 3 H, CH*Me*), 1.25 (m, 1 H, CH$_2$), 1.50 (m, 1H, CH$_2$), 1.96 (m, 1 H, C*H*Me), 3.72 (s, 3 H, OMe), 4.10 (dq, *J* = 1.1, 3.0 Hz, 1 H, fc), 4.22 (m, 3 H, fc), 4.42 (dt, *J* = 1.2, 2.4 Hz, 1 H, fc), 4.47 (dt, *J* = 1.2, 2.4 Hz, 1 H, fc), 4.54 (dt, *J* = 1.5, 2.5 Hz, 1 H, fc), 4.60 (dt, *J* = 1.3, 2.4 Hz, 1 H, fc), 4.69 (dd, $^3J_{HH}$ = 5.0, 8.7 Hz, 1 H, NHC*H*), 6.16 (d, $^3J_{HH}$ = 8.7 Hz, 1 H, NH), 7.28–7.40 (m, 10 H, PPh$_2$). ^{13}C{^{1}H} NMR ($CDCl_3$): δ 11.60 (CH$_2$*Me*), 15.74 (CH*Me*), 25.36 (CH$_2$), 37.87 (*C*HMe), 52.08 (OMe), 56.38 (NHCH), 69.30 (*C*H fc), 69.65 (d, J_{PC} = 1 Hz, *C*H fc), 71.79 (*C*H fc), 71.83 (d, J_{PC} = 1 Hz, *C*H fc), 72.93 (d, J_{PC} = 4 Hz, *C*H fc), 73.09 (d, J_{PC} = 4 Hz, *C*H fc), 74.15 (d, J_{PC} = 13 Hz, *C*H fc), 74.41 (d, J_{PC} = 15 Hz, *C*H fc), 76.24 (*C*-CONH fc), 128.24 (2× d, $^3J_{PC}$ = 7 Hz, *C*H PPh$_2$), 128.66 (*C*H PPh$_2$), 128.72 (*C*H PPh$_2$), 133.35 (d, $^2J_{PC}$ = 6 Hz, *C*H PPh$_2$), 133.54 (d, $^2J_{PC}$ = 7 Hz, *C*H PPh$_2$), 138.36 (d, $^1J_{PC}$ = 9 Hz, C_{ipso} PPh$_2$), 138.52 (d, $^1J_{PC}$ = 10 Hz, C_{ipso} PPh$_2$), 169.84 (CONH), 172.71 (*C*O$_2$Me). The signal due to *C*-P of fc was not found. ^{31}P{^{1}H} NMR ($CDCl_3$): δ −17.0 (s). IR (neat): ν_{NH} 3334 m, ν_{CO} 1743 vs, amide I 1652 vs, amide II 1520 vs; 1435 s, 1299 m, 1201 w, 1179 m, 1163 s, 1094 w, 1027 m, 998 w, 833 m, 746 s, 699 s, 497 s, 451 w cm^{-1}. HR MS (ESI+) calc. for $C_{30}H_{33}NO_3PFe$ [M + H]$^+$ 542.1547, found 542.1541. $[\alpha_D]^{25\,°C}$ −2 (*c* 0.5, $CHCl_3$).

Asymmetric allylic alkylation. General procedure. Ligand (12.5 μmol), [Pd(μ-Cl)(η^3-C$_3$H$_5$)]$_2$ (2.3 mg, 6.3 μmol) and alkali metal acetate (25 μmol; if appropriate) were mixed with dry dichloromethane (3 mL) and the mixture was stirred at room temperature for 20 min. Allylic substrate (0.25 mmol; 63.1 mg of acetate **11a** or 70.6 mg of carbonate **11b**) was added and, after stirring for another 5 min, malonate ester (0.75 mmol; 0.09 mL of dimethyl malonate or 0.17 mL of di-*tert*-butyl malonate) and *N*,*O*-bis(trimethylsillyl)acetamide (BSA; 0.75 mmol, 0.19 mL) were introduced successively. The resulting mixture was stirred for 24 h at reaction temperature (see Table 1), and then diluted with dichloromethane (3 mL) and washed with saturated aqueous NH_4Cl (2 × 5 mL). The organic layer was separated, dried over $MgSO_4$, and evaporated under vacuum. Subsequent purification by column chromatography (silica gel; hexane-ethyl acetate, 3 : 1 v/v) afforded the alkylation product **12** (or its mixture with **11a** in the case of incomplete conversions).

Conversions were determined by ^{1}H NMR spectroscopy. Enantiomeric excesses were established from ^{1}H NMR spectra recorded in C_6D_6 in the presence of the chiral lanthanide shift reagent tris(3-trifluoroacetyl-*d*-camphorato)europium(III). The configuration of the major component was assigned on the basis of optical rotation.[34]

Asymmetric allylic amination. General procedure. Ligand (*S*)-**2** (6.2 mg, 12.5 μmol) and [Pd(μ-Cl)(η^3-C$_3$H$_5$)]$_2$ (2.3 mg, 6.3 μmol) were mixed with dry dichloromethane (3 mL) and the mixture was stirred at room temperature for 20 min. Acetate **11a** (0.25 mmol, 63.1 mg was introduced and, after stirring for another 5 min, benzylamine (0.75 mmol, 0.08 mL) and *N*,*O*-bis(trimethylsillyl)acetamide (BSA; 0.75 mmol, 0.19 mL) were added successively. The resulting mixture was stirred for 24 h or 48 h at room temperature, diluted with diethyl ether (5 mL) and washed with saturated aqueous NH_4Cl (2× 5 mL). The organic layer was separated, dried over $MgSO_4$, and concentrated under vacuum. Subsequent purification by column chromatography (silica gel; hexane-ethyl acetate, 3 : 1 v/v) afforded the alkylation product (or its mixture with **11a** in the case of incomplete conversions).

Conversions were determined by ^{1}H NMR spectroscopy. Enantiomeric excesses were established by HPLC analysis using Daicel Chiralcel OD-H column and hexane/2-propanol 99 : 1 (v/v) as the eluent; t_R((*R*)-**13**) = 18.4, t_R((*S*)-**13**) = 19.8 min at a flow rate of 0.50 mL min^{-1}. The configuration was assigned on the basis of optical rotation. Spectroscopic data of the product were in accordance with the literature.[35]

Asymmetric allylic etherification. General procedure. Ligand (*S*)-**2** (6.2 mg, 12.5 μmol) and [Pd(μ-Cl)(η^3-C$_3$H$_5$)]$_2$ (2.3 mg, 6.3 μmol) were mixed with dry dichloromethane (3 mL) and the mixture was stirred for 20 min. Then, acetate **11a** (0.25 mmol, 63.1 mg was added and, after stirring for another 5 min, neat benzyl alcohol (0.75 mmol, 0.08 mL) and a base (0.75 mmol; 0.19 mL of *N*,*O*-bis(trimethylsilyl)acetamide or 244 mg of Cs_2CO_3) were added successively. The resulting mixture was stirred at room temperature for 24 h or 48 h, diluted with diethyl ether (5 mL) and washed with saturated aqueous NH_4Cl (2× 5 mL). The organic layer was separated, dried over $MgSO_4$, and evaporated under reduced pressure. Purification by column chromatography (conditions as above) recovered only **11a**.

Preparation of palladium(II) complexes

[Pd(MeCN)$_2$(η^3-C$_3$H$_4$Me)]ClO$_4$ (15). A solution of AgClO$_4$ (415 mg, 2.0 mmol) in acetonitrile (5 mL) was added to a dichloromethane solution of **14** (394 mg, 1.0 mmol in 10 mL). An off-white precipitate formed immediately and the yellow colour due to the starting Pd complex disappeared. The mixture was stirred for 10 min in the dark and filtered. The colourless filtrate was evaporated to an oil, which was taken up with acetonitrile (5 mL). The solution was precipitated with diethyl ether (35 mL), yielding an oil, which quickly crystallised. The separated product was filtered off, washed with diethyl ether and dried under vacuum. Yield: 542 mg (79%), white powdery solid. Note: The product is quite stable in the air but deposits Pd(0) upon prolonged standing. It appropriate, it can be purified by dissolving in acetonitrile, filtration and precipitation with diethyl ether.

^{1}H NMR (CDCl$_3$): δ 2.16 (s, 3 H, Me allyl), 2.41 (s, 6 H, MeCN), 3.04 and 4.41 (2× br s, 2 H, CH$_2$ allyl). ^{13}C{^{1}H} NMR (CDCl$_3$): δ 3.13 (*Me*CN), 22.81 (Me allyl), 63.04 (CH$_2$ allyl), 121.92 (Me*C*N), 134.41 (C$_{ipso}$ allyl). IR (Nujol): 2318 m, 2292 m, ν_3(ClO$_4$) 1098/1082 vs composite, ν_1(ClO$_4$) 931 w, 961 m, 839 m, ν_4(ClO$_4$) 624 s cm^{-1}. Anal. calc. for C$_8$H$_{13}$ClNO$_4$Pd: C 28.01, H 3.82, N 8.17%. Found: C 28.23, H 3.95, N 8.24%.

[(η^3-C$_3$H$_4$Me)PdCl(1-κ*P*)] (16). A solution of **1** (146 mg, 0.30 mmol) in chloroform (3 mL) was added to solid [Pd(μ-Cl)(η^3-C$_3$H$_4$Me)]$_2$ (**14**; 59 mg, 0.15 mmol). The reaction mixture was stirred at room temperature for 1 h and then poured into pentane (30 mL). After standing at −18 °C overnight, the precipitated product was filtered off, washed thoroughly with pentane and dried under vacuum. Yield: 195 mg (95%), yellow solid.

^{1}H NMR NMR (CDCl$_3$): δ 1.89 (s, 3 H, Me allyl), 2.47 (s, 1 H, CH$_2$ allyl), 2.81 (s, 1 H, CH$_2$ allyl), 3.51 (d, $^2J_{HH}$ = 10 Hz, 1 H, CH$_2$ allyl), 4.29 (m, 1 H, C–C$_5H_4$), 3.72 (s, 3 H, OMe), 3.90 (m, 1 H, C–C$_5H_4$), 3.94 (dd, $^2J_{HH}$ = 17.5 Hz, $^3J_{HH}$ = 5.8 Hz, 1 H, CH_2NH), 4.21 (dd, $^2J_{HH}$ = 17.5 Hz, $^3J_{HH}$ = 6.4 Hz, 1 H, CH_2NH), 4.29 (m, 1 H, P–C$_5H_4$), 4.44 (dd, $^2J_{HH}$ = 6.8 Hz, $^3J_{PH}$ = 3.0 Hz, 1 H, CH$_2$ allyl), 4.61 (m, 1 H, P–C$_5H_4$), 4.70 (m, 1 H, P–C$_5H_4$), 4.81 (m, 1 H, P–C$_5H_4$), 5.02 (m, 1 H, C–C$_5H_4$), 5.31 (m, 1 H, C–C$_5H_4$), 7.31–7.54 (m, 8 H, PPh$_2$), 7.79–7.86 (m, 2 H, PPh$_2$), 7.92 (t, $^3J_{HH}$ = 5.9 Hz, 1 H, NH). ^{13}C{^{1}H} NMR (CDCl$_3$): δ 23.12 (Me allyl), 41.05 (CH$_2$N), 51.96 (OMe), 64.13 (CH$_2$ allyl), 70.07 (CH C–C$_5$H$_4$), 70.32 (CH C–C$_5$H$_4$), 71.94 (2C, CH C–C$_5$H$_4$), 73.37 (d, J_{PC} = 10 Hz, CH P–C$_5$H$_4$), 73.55 (d, J_{PC} = 6 Hz, CH P–C$_5$H$_4$), 74.25 (d, J_{PC} = 46 Hz, C$_{ipso}$ P–C$_5$H$_4$), 74.41 (d, J_{PC} = 9 Hz, CH P–C$_5$H$_4$), 76.90 (C$_{ipso}$ C–C$_5$H$_4$), 78.65 (d, $^2J_{PC}$ = 32 Hz, CH$_2$ allyl), 128.29 (d, $^3J_{PC}$ = 10 Hz, CH$_{meta}$ PPh$_2$, 4C), 129.77 (d, $^4J_{PC}$ = 1 Hz, CH$_{para}$ PPh$_2$), 130.26 (d, $^4J_{PC}$ = 2 Hz, CH$_{para}$ PPh$_2$), 132.27 (d, $^2J_{PC}$ = 12 Hz, CH$_{ortho}$ PPh$_2$), 133.37 (d, $^2J_{PC}$ = 5 Hz, C$_{ipso}$ allyl), 133.69 (d, $^2J_{PC}$ = 12 Hz, CH$_{ortho}$ PPh$_2$), 135.06 (d, $^1J_{PC}$ = 43 Hz, C$_{ipso}$ PPh$_2$), 137.56 (d, $^1J_{PC}$ = 44 Hz, C$_{ipso}$ PPh$_2$), 170.05 (CONH), 170.82 (*C*O$_2$Me). A resonance due to one CH of P–C$_5$H$_4$ is obscured by the solvent signal. ^{31}P{^{1}H} NMR (CDCl$_3$): δ 11.6 (s). IR (Nujol): ν_{NH} 3305 m, ν_{CO} 1750 vs, amide I 1652 vs, amide II 1538 vs, 1436 vs, 1304 m, 1211 s, 1196 s, 1178 s, 1098 m, 1172 w, 1030 m, 979 w, 837 m, 750 s, 697 vs, 629 w, 617 w, 519 m, 497 w, 471 w cm^{-1}. ESI MS: *m*/*z* 646 ([M − Cl]$^+$). Anal. calc. for C$_{30}$H$_{31}$ClFeNO$_3$PPd ·0.15 CH$_2$Cl$_2$: C 52.10, H 4.54, N 2.02%. Found: C 52.19, H 4.54, N 1.79%. The amount of solvent was confirmed by NMR.

[(η^3-C$_3$H$_4$Me)Pd(1-κ^2*O*,*P*)]ClO$_4$ (17). A solution of **1** (43 mg, 0.09 mmol) in chloroform (2 mL) was added to solid [Pd(MeCN)$_2$(η^3-C$_3$H$_4$Me)]ClO$_4$ (**15**; 30 mg, 0.09 mmol). The resulting mixture was stirred at room temperature for 1 h and then poured into pentane (30 mL). After standing overnight at −18 °C, the precipitated product was filtered off, washed with pentane and dried under vacuum. Yield: 63 mg (96%), yellow solid.

^{1}H NMR NMR (CDCl$_3$): δ 2.18 (s, 3 H, Me allyl), 2.94 (br d, $^3J_{HH}$ = 2.0 Hz, 1 H, CH$_2$ allyl), 3.10 (br q, $^3J_{HH} \approx$ 2.6 Hz, 1 H, CH$_2$ allyl), 3.68 (s, 3 H, OMe), 4.06 (d, $^2J_{HH}$ = 9.3 Hz, 1 H, CH$_2$ allyl), 4.08 (br m, 1 H, P–C$_5H_4$), 4.16 (d, $^3J_{HH}$ = 6.0 Hz, 2 H, CH_2NH), 4.29 (br m, 1 H, P–C$_5H_4$), 4.39 (br dt, $^3J_{HH}$ = 1.3, 2.6 Hz, 1 H, C–C$_5H_4$), 4.44 (br dt, $^3J_{HH}$ = 1.3, 2.6 Hz, 1 H, C–C$_5H_4$), 4.64 (br m, 1 H, P–C$_5H_4$), 4.71–4.76 (br m, 2 H, CH$_2$ allyl + P–C$_5H_4$), 5.16 (br dt, $^3J_{HH}$ = 1.3, 2.6 Hz, 1 H, C–C$_5H_4$), 5.32 (br dt, $^3J_{HH}$ = 1.3, 2.6 Hz, 1 H, C–C$_5H_4$), 7.41–7.54 (m, 10 H, PPh$_2$), 8.07 (t, $^3J_{HH}$ = 5.9 Hz, 1 H, NH). ^{13}C{^{1}H} NMR (CDCl$_3$): δ 23.23 (Me allyl), 42.04 (CH$_2$N), 52.16 (OMe), 55.44 (CH$_2$ allyl), 71.56 (d, J_{PC} = 49 Hz, C$_{ipso}$ P–C$_5$H$_4$), 71.73 (CH C–C$_5$H$_4$), 71.96 (CH C–C$_5$H$_4$), 72.71 (CH C–C$_5$H$_4$), 72.96 (CH C–C$_5$H$_4$), 73.85 (d, J_{PC} = 7 Hz, CH P–C$_5$H$_4$), 74.27 (d, J_{PC} = 7 Hz, CH P–C$_5$H$_4$), 74.35 (C$_{ipso}$ C–C$_5$H$_4$), 75.00 (d, J_{PC} = 10 Hz, CH P–C$_5$H$_4$), 75.76 (d, J_{PC} = 12 Hz, CH P–C$_5$H$_4$), 83.34 (d, $^2J_{PC}$ = 27 Hz, CH$_2$ allyl), 129.01 (d, $^3J_{PC}$ = 10 Hz, CH$_{meta}$ PPh$_2$), 129.07 (d, $^3J_{PC}$ = 10 Hz, CH$_{meta}$ PPh$_2$), 131.19 (d, $^4J_{PC}$ = 2 Hz, CH$_{para}$ PPh$_2$), 131.29 (d, $^4J_{PC}$ = 2 Hz, CH$_{para}$ PPh$_2$), 132.00 (d, $^1J_{PC}$ = 45 Hz, C$_{ipso}$ PPh$_2$), 132.77 (d, $^2J_{PC}$ = 13 Hz, CH$_{ortho}$ PPh$_2$), 133.01 (d, $^2J_{PC}$ = 14 Hz, CH$_{ortho}$ PPh$_2$), 136.09 (d, $^2J_{PC}$ = 5 Hz, C$_{ipso}$ allyl), 169.51 (CO$_2$Me), 174.12 (CONH). ^{31}P{^{1}H} NMR (CDCl$_3$): δ 20.8 (s). IR (Nujol): ν_{NH} 3350 m, ν_{CO} 1754 vs, 1652 m, amide I 1596 vs, amide II 1558 vs, 1436 vs, 1311 m, 1213 s, 1198 s, 1169 s, ν_3(ClO$_4$) 1097 br vs, ν_1(ClO$_4$) 930 w, 908 w, 837 m, 750 s, 697 vs, ν_4(ClO$_4$) 624 vs, 471 *vs.* cm^{-1}. ESI MS: *m*/*z* 646 ([M − ClO$_4$]$^+$; *i.e.*, the cation). Anal. calc. for C$_{30}$H$_{31}$ClFeNO$_7$PPd·0.25C$_5$H$_{12}$: C 49.27, H 4.53, N 1.82%. Found: C 49.27, H 4.68, N 2.02%. The amount of solvent was verified by NMR.

[(η^3-C$_3$H$_4$Me)Pd(1-κ*P*)$_2$]ClO$_4$ (18) was prepared and isolated similarly to **17**, using **14** (34 mg, 0.10 mmol) and **1** (97 mg, 0.20 mmol). Yield: 119 mg (97%), yellow powder.

^{1}H NMR NMR (CDCl$_3$): δ 1.84 (s, 3 H, Me allyl), 3.47 (m, 2 H, CH$_2$ allyl), 3.69 (dt, $^3J_{HH}$ = 1.3, 2.6 Hz, 2 H, C–C$_5H_4$), 3.73 (s, 8 H, OMe and CH$_2$ allyl), 3.78 (dt, $^3J_{HH}$ = 1.3, 2.6 Hz, 2 H, C–C$_5H_4$), 4.09–4.13 (m, 6 H, CH_2NH and P–C$_5H_4$), 4.19 (br s, 2 H, P–C$_5H_4$), 4.61 (m, 2 H, P–C$_5H_4$), 4.63 (dt, $^3J_{HH}$ = 1.2, 2.6 Hz, 2 H, P–C$_5H_4$), 4.64 (m, 2 H, C–C$_5H_4$), 4.68 (dt, $^3J_{HH}$ = 1.3, 2.6 Hz, 2 H, C–C$_5H_4$), 7.04 (t, $^3J_{HH}$ = 5.9 Hz, 2 H, NH), 7.24–7.51 (m, 20 H, PPh$_2$). ^{13}C{^{1}H} NMR (CDCl$_3$): δ 23.48 (Me allyl), 41.25 (CH$_2$NH), 52.12 (OMe), 69.66 (CH C–C$_5$H$_4$), 69.95 (CH C–C$_5$H$_4$), 72.13 (CH C–C$_5$H$_4$), 72.36 (CH C–C$_5$H$_4$), 73.69 (t, J' = 6 Hz, CH P–C$_5$H$_4$), 73.93 (t, J' = 4 Hz, CH P–C$_5$H$_4$), 74.08 (t, J' = 4 Hz, CH P–C$_5$H$_4$), 74.58 (t, J' = 7 Hz, CH P–C$_5$H$_4$), *ca.* 76.6 (CH$_2$ allyl; partly obscured by the solvent signal), 78.25 (t, J' = 23 Hz, C$_{ipso}$ P–C$_5$H$_4$), 128.70 (t, J' = 5 Hz, CH$_{meta}$ PPh$_2$), 128.78 (t, J' = 5 Hz, CH$_{meta}$ PPh$_2$), 130.94 (CH$_{para}$ PPh$_2$), 131.29 (CH$_{para}$ PPh$_2$), 131.40 (d, J' = 23 Hz, C$_{ipso}$ PPh$_2$), 132.08 (d, J' = 23 Hz, C$_{ipso}$ PPh$_2$), 132.85 (t, J' = 6 Hz, CH$_{ortho}$ PPh$_2$), 133.20 (t, J' = 7 Hz, CH PPh$_2$), 137.70 (t, J' = 5 Hz, C$_{ipso}$ allyl), 169.68 (CONH), 170.59 (*C*O$_2$Me). The resonance due to C$_{ipso}$ of C–C$_5$H$_4$ overlaps with the signal of solvent. ^{31}P{^{1}H} NMR (CDCl$_3$): δ 18.2 (s). IR

Table 5 Summary of crystallographic parameters, data collection and structure refinement parameters for **15**, **16**·H_2O and **17**[a]

Compound	**15**	**16**·H_2O	**17**
Formula	$C_9H_{13}ClN_2O_4Pd$	$C_{30}H_{33}ClFeNO_4PPd$	$C_{30}H_{31}ClFeNO_7PPd$
M	343.05	700.24	746.23
Crystal system	Monoclinic	Monoclinic	Monoclinic
Space group	$P2_1/m$ (no. 14)	$P2_1/c$ (no. 14)	$P2_1/n$ (no. 14)
a/Å	7.3756(2)	10.0468(7)	14.4397(6)
b/Å	10.4597(3)	30.550(2)	15.1067(6)
c/Å	8.3592(2)	9.7502(7)	15.0910(7)
β (°)	95.8421(17)	105.252(4)	112.494(1)
U/Å^3	641.53(3)	2887.2(3)	3041.4(2)
Z	2	4	4
μ(Mo-Kα)/mm^{-1}	1.655	1.310	1.256
T[b]	0.654–0.750	0.603–0.711	0.641–0.746
Diffrns collected	8315	28502	26854
Unique diffrns	1543	6639	6962
Obsd[c] diffrns	1505	5960	4760
R_{int}[d]/%	2.78	2.65	3.96
R[d] obsd diffrns/%	1.76	3.22	3.86
R, wR[d] all data/%	1.80, 4.45	3.77, 7.47	7.69, 10.3
$\Delta\rho$/e Å^{-3}	0.41, –0.46	0.54 –0.46	2.02,[e] –1.15
CCDC entry	823874	823875	823876

[a] Common details: T = 150(2)K. [b] The range of transmission factors. [c] Observed diffractions with $I > 2\sigma(I)$. [d] $R_{int} = \sum|F_o^2 - F_o^2(\text{mean})|/\sum F_o^2$, where F_o^2(mean) is the average intensity of symmetry-equivalent diffractions. $R = \sum\|F_o| - |F_c\|/\sum|F_o|$, $wR = [\sum\{(wF_o^2 - F_c^2)^2\}/\sum(wF_o^2)^2]^{1/2}$. [e] Residual electron density in vicinity of the Pd atom.

(Nujol): ν_{NH} 3385 m, ν_{CO} 1753 vs, amide I 1655 vs, amide II 1536 vs, 1437 vs, 1303 m, 1211 s, 1196 s, 1177 s, 1164 m, 1101 vs, 1037 m, 1000 w, 839 w, 748 m, 697 s, 624 m, 484 s cm^{-1}. MS (ESI+): m/z 1131 ([$(C_3H_4Me)Pd(\mathbf{1})_2$]$^+$), 938, 646 ([$(C_3H_4Me)Pd(\mathbf{1})$]$^+$). Anal. calc. for $C_{56}H_{55}ClFe_2N_2O_{10}P_2Pd\cdot0.15C_5H_{12}$: C 54.86, H 4.61, N 2.26%. Found: C 54.87, H 4.90, N 2.00%. The presence of solvent was verified by NMR.

X-Ray crystallography

Single crystals suitable for X-ray diffraction analysis were grown by liquid-phase diffusion from dichloromethane-hexane (**15**: colourless block, 0.18 × 0.25 × 0.35 mm^3), toluene-hexane (**16**·H_2O: orange prism, 0.28 × 0.34 × 0.43 mm^3) and ethyl acetate-hexane (**17**: orange bar, 0.21 × 0.24 × 0.29 mm^3).

Full-set diffraction data ($\pm h \pm k \pm l$, $2\theta_{max}$ = 55°, completeness ≥ 98.7%) were collected with a Buker Apex2 (**16**·H_2O, **17**) or a Nonius KappaCCD (**15**) diffractometers equipped with Oxford Cryosystem cooling device. The measurements were performed at 150(2) K using with graphite-monochromated Mo-Kα radiation (λ = 0.71073 Å) and the data were corrected for absorption. Further details are presented in Table 5.

The structures were solved by direct methods (SHEXLS-97[36] or SIR-97[37]) and refined by full-matrix least-squares based on F^2 (SHELXL97[38]). All non-hydrogen atoms were refined with anisotropic displacement parameters. The amide (NH) hydrogen in **17** and allylic hydrogens in **15** were located on difference electron density maps and refined as riding atoms. All other hydrogen atoms were included in their calculated positions and refined as riding atoms. The PdCl(η^3-MeC_3H_4) moiety in the structure of **16**·H_2O appears to be disordered over two positions. However, because of the low contribution of the less populated orientation and overlaps, only the Pd atom could be refined over two positions (the refined occupancies were *ca.* 96.6 : 3.4). All geometric calculations were performed with a recent version of PLATON[39,40] program.

Acknowledgements

This work was supported by the Grant Agency of Charles University in Prague (project no. 58009) and by the Ministry of Education of the Czech Republic (project nos. LC06070 and MSM0021620857).

References

1 (*a*) G. Consiglio and R. M. Waymouth, *Chem. Rev.*, 1989, **89**, 257; (*b*) B. M. Trost and D. L. Van Vranken, *Chem. Rev.*, 1996, **96**, 395; (*c*) B. M. Trost and M. L. Crawley, *Chem. Rev.*, 2003, **103**, 2921; (*d*) T. Graening and H.-G. Schmalz, *Angew. Chem., Int. Ed.*, 2003, **42**, 2580; (*e*) B. M. Trost, *J. Org. Chem.*, 2004, **69**, 5813; (*f*) B. M. Trost, T. Zhang and J. D. Sieber, *Chem. Sci.*, 2010, **1**, 427; (*g*) T. Hayashi in *Catalytic Asymmetric Synthesis* (Ed.: I. Ojima), chapter 7.1, pp. 325-365, VCH, New York 1993; (*h*) I. G. Rios, A. Rosas-Hernandez and E. Martin, *Molecules*, 2011, **16**, 970.

2 B. M. Trost, M. R. Machacek and A. Aponick, *Acc. Chem. Res.*, 2006, **39**, 747.

3 (*a*) T. Hayashi in *Ferrocenes: Homogeneous Catalysis, Organic Synthesis, Materials Science* (Ed.: A. Togni and T. Hayashi), chapter 2, pp. 105-142, VCH, Weinheim, 1995; (*b*) H.-U. Blaser, W. Chen, F. Camponovo and A. Togni in *Ferrocenes: Ligands, Materials and Biomolecules* (Ed. P. Štěpnička), chapter 6, pp. 205-235, Wiley, Chichester 2008; (*c*) P. Štěpnička and M. Lamač in *Ferrocenes: Ligands, Materials and Biomolecules* (Ed. P. Štěpnička), chapter 7, pp. 237-277, Wiley, Chichester 2008; (*d*) C. J. Richards and A. J. Locke, *Tetrahedron: Asymmetry*, 1998, **9**, 2377; (*e*) T. J. Colacot, *Chem. Rev.*, 2003, **103**, 3101; (*f*) O. B. Sutcliffe and M. R. Bryce, *Tetrahedron: Asymmetry*, 2003, **14**, 2297; (*g*) L.-X. Dai, T. Tu, S.-L. You, W.-P. Deng and X.-L. Hou, *Acc. Chem. Res.*, 2003, **36**, 659; (*h*) R. C. J. Atkinson, V. C. Gibson and N. J. Long, *Chem. Soc. Rev.*, 2004, **33**, 313; (*i*) X. L. Hou, S. L. You, T. Tu, W. P. Deng, X. W. Wu, M. Li, K. Yuan, T. Z. Zhang and L. X. Dai, *Top. Catal.*, 2005, **35**, 87; (*j*) S. P. Flanagan and P. J. Guiry, *J. Organomet. Chem.*, 2006, **691**, 2125.

4 B. M. Trost, B. Breit, S. Peukert, J. Zambrano and J. W. Ziller, *Angew. Chem., Int. Ed. Engl.*, 1995, **34**, 2386.

5 (*a*) P. Štěpnička, J. Schulz, I. Císařová and K. Fejfarová, *Collect. Czech. Chem. Commun.*, 2007, **72**, 453; (*b*) J. Kühnert, M. Dušek, J. Demel, H. Lang and P. Štěpnička, *Dalton Trans.*, 2007, 2802; (*c*) J. Kühnert, M.

Lamač, J. Demel, A. Nicolai, H. Lang and P. Štěpnička, *J. Mol. Catal. A: Chem.*, 2008, **285**, 41; (*d*) J. Schulz, I. Císařová and P. Štěpnička, *J. Organomet. Chem.*, 2009, **694**, 2519; (*e*) P. Štěpnička, M. Krupa, M. Lamač and I. Císařová, *J. Organomet. Chem.*, 2009, **694**, 2987.
6 (*a*) M. Lamač, I. Císařová and P. Štěpnička, *Eur. J. Inorg. Chem.*, 2007, 2274; (*b*) M. Lamač, J. Tauchman, I. Císařová and P. Štěpnička, *Organometallics*, 2007, **26**, 5042; (*c*) M. Lamač, I. Císařová and P. Štěpnička, *New J. Chem.*, 2009, **33**, 1549; (*d*) M. Lamač, J. Tauchman, S. Dietrich, I. Císařová, H. Lang and P. Štěpnička, *Appl. Organomet. Chem.*, 2010, **24**, 326.
7 (*a*) J. Tauchman, I. Císařová and P. Štěpnička, *Organometallics*, 2009, **28**, 3288; (*b*) J. Tauchman, I. Cisařová and P. Štěpnička, *Eur. J. Org. Chem.*, 2010, 4276.
8 For a review, see: P. J. Deuss, R. den Heeten, W. Laan and P. C. J. Kamer, *Chem.–Eur. J.*, 2011, **17**, 4680.
9 (*a*) B. M. Trost and D. J. Murphy, *Organometallics*, 1985, **4**, 1143; (*b*) M. T. El Gihani and H. Heaney, *Synthesis*, 1998, 357.
10 Similarly to reactions with **1**, the bridge cleavage reaction of [(η^3-allyl)PdCl]$_2$ afforded [(η^3-allyl)PdCl{(*S*)-**2**}]. However, in further reactions, this complex yielded only a material showing extremely broad NMR signals (reaction with 1 equiv. of $AgClO_4$), or a complex reaction mixture (reaction with 4 equiv. BSA).
11 [(η^3-allyl)PdCl(**1**)]: A solution of **1** (0.03 mmol) in chloroform (2 mL) was added to solid [(η^3-allyl)PdCl]$_2$ (0.015 mmol). After stirring for 45 min, the resulting yellow-orange solution was filtered and evaporated under vacuum. [(η^3-allyl)Pd(**1**)]ClO_4: To a solution of [(η^3-allyl)PdCl(**1**)] prepared as described above was added $AgClO_4$ (0.03 mmol) dissolved in dry MeCN (0.5 mL) and the mixture was stirred in the dark for 10 min. The AgCl formed was filtered off and the filtrate was evaporated to dryness yielding the product as an orange-brown solid.
12 Selected ^{1}H NMR data for the major product (in $CDCl_3$): δ 3.92 (s, OCH_3); 3.19 and 3.99 (two partly obscured dd, 1 H each, CH_2NH), 8.09 (br unresolved t, 1 H, CH_2NH); 4.09 (m), 5.61 (dd, $J \approx 10$ and 13 Hz) and 6.37 (dd, $J \approx 11$ and 13 Hz) (3 × 1 H, allylic protons); 3.93 (2 H), 3.96, 4.45, 4.62, 4.83, 4.98 and 5.50 (multiplets attributed to fc protons).
13 For an early example, see: D. J. Mabbott, B. E. Mann and P. M. Maitlis, *J. Chem. Soc., Dalton Trans.*, 1977, 294.
14 (*a*) P. S. Pregosin and R. W. Kunz in *NMR Basic Principles and Progress*, (Ed.: P. Diehl, E. Fluck and R. Kosfeld), vol. 16, sect. E, p. 65 and references cited therein. Springer, Berlin 1979; (*b*) W. H. Hersch, *J. Chem. Educ.*, 1997, **74**, 1485.
15 (*a*) X = CO_2H: P. Štěpnička, J. Podlaha, R. Gyepes and M. Polášek, *J. Organomet. Chem.*, 1998, **552**, 293; (*b*) X = PO_3Et_2: P. Štěpnička, I. Císařová and R. Gyepes, *Eur. J. Inorg. Chem.*, 2006, 926; (*c*) X = $CONH(CH_2)_nPy$ (n = 1, 2; Py = pyrid-2-yl): ref. 5b; (*d*) X = $CONHCH_2CO_2Me$: ref. 7a; (*e*) X = $CH{=}CH_2$: P. Štěpnička and I. Císařová, *Collect. Czech. Chem. Commun.*, 2006, **71**, 215; (*f*) X = Py or CH_2Py: P. Štěpnička, J. Schulz, T. Klemann, U. Siemeling and I. Císařová, *Organometallics*, 2010, **29**, 3187.
16 P. Štěpnička, *J. Organomet. Chem.*, 2008, **693**, 297.
17 G. A. Kukina, V. S. Sergienko, Yu. L. Gaft, I. A. Zakharova and M. A. Porai-Koshits, *Inorg. Chim. Acta*, 1980, **45**, L257.
18 Ch. Elschenbroich and A. Salzer, *Organometallics, A Concise Introduction*, 2nd edn, sect. 15.3, pp. 280–287, VCH, Weinheim 1992.
19 C–H···O interactions: (1) C1–H1B···O2^i, C1···O2 = 3.453(2) Å, angle at H1B = 153°; (2) C5–H5A···O2^{ii}, C5···O2 = 3.513(3) Å, angle at H5A = 175°; (3) C5–H5C···O3^{iii}, C5···O3 = 3.395(3) Å, angle at H5C = 141°; *i*. 1 − *x*, −*y*, 1 − *z*; *ii*. −*x*, −*y*, 1 − *z*; *iii*. 1 − *x*, $-\frac{1}{2}$ + *y*, 1 − *z*.
20 J. W. Faller, C. Blankenship, B. Whitmore and S. Sena, *Inorg. Chem.*, 1985, **24**, 4483.
21 P. Štěpnička and I. Císařová, *Collect. Czech. Chem. Commun.*, 2006, **71**, 279.
22 C. P. Butts, J. Crosby, G. C. Lloyd-Jones and S. C. Stephen, *Chem. Commun.*, 1999, 1707.
23 As the result, the Pd···Fe separation is considerably shorter in **17** (4.0226(7) Å) than in **16**·H_2O (4.5985(7) Å).
24 T. G. Appleton, H. C. Clark and L. E. Manzer, *Coord. Chem. Rev.*, 1973, **10**, 335.
25 Hydrogen bond parameter are as follows; N–H1N···O4^{iv}: N···O = 3.018(5) Å, angle at H1N = 175°; *iv*. 1 − *x*, $-\frac{1}{2}$ + *y*, $\frac{1}{2}$ − *z*.
26 (*a*) R. G. Pearson, *J. Am. Chem. Soc.*, 1963, **85**, 3533; (*b*) F. R. Hartley, *The Chemistry of Platinum and Palladium*, Applied Science, London 1973.
27 (*a*) H. Kurosawa, *J. Organomet. Chem.*, 1987, **334**, 243; (*b*) D. J. Cárdenas and A. M. Echavarren, *New J. Chem.*, 2004, **28**, 338.
28 M. Brenner and W. Huber, *Helv. Chim. Acta*, 1953, **36**, 1109.
29 J. Podlaha, P. Štěpnička, J. Ludvík and I. Císařová, *Organometallics*, 1996, **15**, 543.
30 I. D. G. Watson, S. A. Styler and A. K. Yudin, *J. Am. Chem. Soc.*, 2004, **126**, 5086.
31 F. Ferioli, C. Fiorelli, G. Martelli, M. Monari, D. Savoia and P. Tobaldin, *Eur. J. Org. Chem.*, 2005, 1416.
32 M. Toffano, J.-Y. Legros and J.-C. Fiaud, *Tetrahedron Lett.*, 1997, **38**, 77.
33 W. T. Dent, R. Long and A. J. Wilkinson, *J. Chem. Soc.*, 1964, 1585.
34 T. Hayashi, A. Yamamoto, T. Hagihara and Y. Ito, *Tetrahedron Lett.*, 1986, **27**, 191.
35 T. Ohta, H. Sasayama, O. Nakajima, N. Kurahashi, T. Fujii and I. Furukawa, *Tetrahedron: Asymmetry*, 2003, **14**, 537.
36 G. M. Sheldrick, *SHELXS-97. Program for Crystal Structure Solution from Diffraction Data*, University of Göttingen, Germany, 1997.
37 A. Altomare, M. C. Burla, M. Camalli, G. L. Cascarano, C. Giacovazzo, A. Guagliardi, A. G. G. Moliterni, G. Polidori and R. Spagna, *J. Appl. Crystallogr.*, 1999, **32**, 115.
38 G. M. Sheldrick, *SHELXL-97. Program for Crystal Structure Refinement from Diffraction Data*, *University of Göttingen*, Germany, 1997.
39 A. L. Spek, *PLATON-A Multipurpose Crystallographic Tool*, Utrecht University, Utrecht, The Netherlands, 2003 and updates. For a reference, see: A. L. Spek, *J. Appl. Crystallogr.*, 2003, **36**, 7.
40 All numerical values are rounded with respect to their estimated standard deviations (esd's) given with one decimal. Parameters concerning atoms in fixed positions (hydrogens) are given without esd's.

10.3 Appendix 3

J. Tauchman, B. Therrien, G. Süss-Fink, P. Štěpnička: "Heterodinuclear Arene Ruthenium Complexes Containing a Glycine-Derived Phosphinoferrocene Carboxamide: Synthesis, Molecular Structure, Electrochemistry, and Catalytic Oxidation Activity in Aqueous Media." *Organometallics* **2012**, *31*, 3985.

ORGANOMETALLICS

Article

pubs.acs.org/Organometallics

Heterodinuclear Arene Ruthenium Complexes Containing a Glycine-Derived Phosphinoferrocene Carboxamide: Synthesis, Molecular Structure, Electrochemistry, and Catalytic Oxidation Activity in Aqueous Media

Jiří Tauchman,[†] Bruno Therrien,[‡] Georg Süss-Fink,*[,‡] and Petr Štěpnička*[,†]

[†]Department of Inorganic Chemistry, Faculty of Science, Charles University in Prague, Hlavova 2030, CZ-12840 Prague 2, Czech Republic

[‡]Institut de Chimie, Université de Neuchâtel, Avenue de Bellevaux 51, CH-2000 Neuchâtel, Switzerland

Supporting Information

ABSTRACT: Three series of heterodinuclear ruthenium–iron complexes have been synthesized from (η^6-arene)ruthenium dichloride dimers and phosphinoferrocene ligands containing glycine-based carboxamido substituents. The neutral complexes [(η^6-arene)RuCl$_2$(Ph$_2$PfcCONHCH$_2$CO$_2$Me-κP)] (**4**, arene = benzene (**a**), *p*-cymene (**b**), hexamethylbenzene (**c**); fc = ferrocene-1,1′-diyl) were obtained by the bridge cleavage reaction of [(η^6-arene)RuCl$_2$]$_2$ with Ph$_2$PfcCONHCH$_2$CO$_2$Me (**1**) in chloroform solution. The complex [(η^6-*p*-cymene)-RuCl$_2$(Ph$_2$PfcCONHCH$_2$CONH$_2$-κP)] (**6b**) was synthesized in the same way from Ph$_2$PfcCONHCH$_2$CONH$_2$ (**3**); the preparation of [(η^6-*p*-cymene)RuCl$_2$(Ph$_2$PfcCONHCH$_2$CO$_2$H-κP)] (**5b**), featuring the ferrocene ligand in the free acid form (**2**), failed due to side reactions and isolation problems. The salts [(η^6-arene)RuCl(MeCN)(**1**-κP)][PF$_6$] (**7a–c**) and [(η^6-arene)Ru(MeCN)$_2$(**1**-κP)][PF$_6$]$_2$ (**8a–c**) were prepared from **1** and the acetonitrile precursors [(η^6-arene)RuCl(MeCN)$_2$][PF$_6$] and from **4a–c** via halide removal with Ag[PF$_6$] in acetonitrile solution, respectively. Alternative synthetic routes to **7b** and **8b** were also studied. The compounds were fully characterized by elemental analysis, multinuclear NMR, IR, and electrospray ionization mass spectra, and their electrochemical properties were studied by cyclic voltammetry at a Pt-disk electrode. The single-crystal X-ray analyses of two representatives (**4b** and **8b**) revealed a pseudotetrahedral coordination geometry at the ruthenium centers and eclipsed conformations of the ferrocene moieties, with the substituents at the two cyclopentadienyl rings being anti with respect to each other. All complexes showed high activity for the catalytic oxidation of secondary alcohols with *tert*-butyl hydroperoxide to give ketones in aqueous media. The most active catalyst was obtained from the neutral *p*-cymene complex **4b**, showing a catalytic turnover frequency of 13 200 h^{-1} at room temperature for the oxidation of 1-phenylethanol at a substrate/catalyst ratio of 100 000.

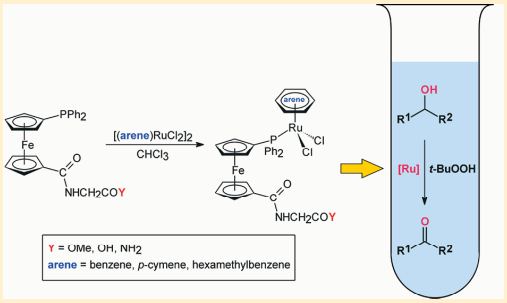

INTRODUCTION

Ligands obtained by "conjugation" of phosphinocarboxylic acids with amino acids have received considerable attention in the recent past, owing to their rich coordination chemistry and manifold catalytic applications.[1,2] Indeed, these compounds represent attractive targets for ligand design, being synthesized readily in good yields by conventional amide coupling reactions and are thus accessible in many variants, differing in the overall structure and substitution patterns.

Stimulated by our investigation into the chemistry of 1′-(diphenylphosphino)ferrocene-1-carboxamides with simple[3] and functional substituents at the amide nitrogen (type **A** in Scheme 1; e.g., compounds bearing pyridyl,[4] hydroxyalkyl,[5] and sulfonatoalkyl[6] groups), we have recently turned also to analogous donors prepared from amino acids. So far, we have synthesized and catalytically tested several such ligands obtained from 1′-(diphenylphosphino)ferrocene-1-carboxylic acid (Hdpf) or its planar-chiral 1,2-isomer and from both achiral glycine (compounds **1–3** in Scheme 1)[7] and various chiral amino acids.[8] We have also demonstrated that these ligands are easily modified at their amide substituent. For instance, compound **1**, resulting from Hdpf and glycine methyl ester hydrochloride, was readily converted to the corresponding acid **2** (by hydrolysis) or amide **3** (by reaction with liquid ammonia).[7] These changes naturally affect both the coordination and physicochemical properties (e.g., solubility) of these donors and can be thus used to fine tune the catalytic performance of complexes prepared thereof.

Received: March 14, 2012
Published: April 30, 2012

dx.doi.org/10.1021/om3002087 | *Organometallics* 2012, 31, 3985–3994

Scheme 1. Hdpf Derivatives

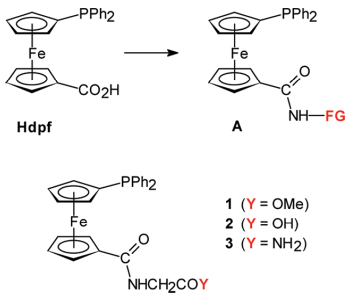

In the search for other potentially useful synthetic transformations in which Hdpf–amino acid conjugates could be used, we turned to transition-metal-catalyzed *oxidation* reactions. Phosphinoferrocene ligands have been used only rarely in such reactions, presumably due to their possible decomposition following oxidation of the ferrocene unit.[9] In this contribution, we describe the preparation, structural characterization, and electrochemistry of three series of (η^6-arene)Ru complexes with glycine-based amidophosphine ligands **1**–**3**. We also report the catalytic performance of these ruthenium–iron complexes in the selective oxidation of secondary alcohols with *tert*-butyl hydroperoxide to give the corresponding ketones.

RESULTS AND DISCUSSION

Synthesis and Structural Characterization of the Ruthenium–Iron Compounds. Three series of (η^6-arene)Ru complexes containing **1** as a P-monodentate ligand were prepared (Scheme 2); viz., the neutral complexes of the type [(η^6-arene)$RuCl_2$(**1**-κP)] as well as two series of cationic complexes resulting from the substitution of chloro by acetonitrile ligands, which were isolated as PF_6^- salts. The neutral complexes **4a**–**c** were obtained by a bridge cleavage reaction from the respective dimeric precursor [(η^6-arene)-$RuCl_2$]$_2$ and **1** in chloroform. The related complex **6b** was synthesized similarly from the amide **3**. In contrast, attempts to prepare [(η^6-*p*-cymene)$RuCl_2$(**2**-κP)] (**5b**) from the free acid **2** were unsuccessful due to side reactions;[10] in our hands it was not possible to isolate **5b** (detected by NMR) from the reaction mixture.

Removal of the chloro ligands from **4a**–**c** with 2 equiv of Ag[PF_6] in acetonitrile produced the bis-acetonitrile complexes as hexafluorophosphate salts **8a**–**c**. The formally intermediary monoacetonitrile compounds **7a**–**c** were obtained by replacement of one acetonitrile ligand in the precursors [(η^6-arene)$RuCl(MeCN)_2$][PF_6] with a stoichiometric amount of ligand **1**.

Additional reactivity studies showed that the cationic complexes **7b** and **8b** are accessible either in a direct way from [(*p*-cymene)$RuCl(MeCN)_2$]$^+$ or [(*p*-cymene)Ru-$(MeCN)_3$]$^{2+}$ via substitution of the acetonitrile ligands with **1** or, alternatively, by sequential removal of the chloro ligands from the dichlororuthenium complex **4b**. These interconversions are schematically shown in Scheme 3 and described in detail in the Supporting Information.

The compounds were characterized by combustion analyses, ^{1}H, ^{31}P{^{1}H}, and ^{19}F NMR spectroscopy, IR spectroscopy, and

Scheme 2. Preparation of Ruthenium–Iron Complexes 4–8

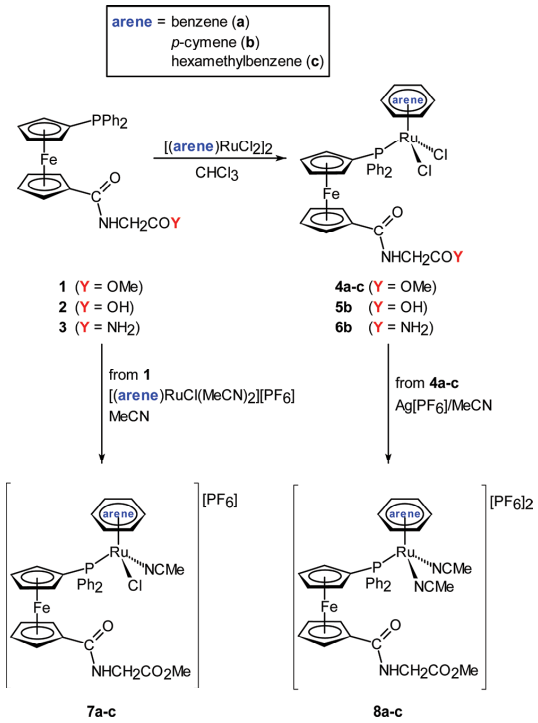

ESI mass spectrometry. The molecular structures of **4b** and **8b** were determined by single-crystal X-ray diffraction analysis.

The proton NMR spectra of **4a**–**c**, **5b**, and **8a**–**c** display characteristic signals of the arene ligand and four resonances attributable to the 1,1′-disubstituted ferrocene moiety. In the case of **7**, possessing a stereogenic Ru atom, the originally degenerate signals become diastereotopic and anisochronic. For instance, four CH resonances of the cymene CH groups and eight signals for the ferrocene protons are seen in the ^{1}H NMR spectrum of **7b**. The spectra further comprise signals due to the glycine pendant, namely the singlet of the terminal methyl group at δ_H ca. 3.7–3.8 and NH-coupled ($^3J_{HH} \approx 6$ Hz) doublet of the methylene group at δ_H 4.0–4.1. The spectrum of **6b** shows the expected three signals for the nonequivalent NH protons. The ^{31}P{^{1}H} NMR spectra of neutral complexes **4a**–**c** and **5b** display one singlet resonance in the range δ_P 15–19. This signal shifts to lower fields in the spectra of mono- and dicationic complexes (**7a**–**c**, δ_P 28–30; **8a**–**c**, δ_P 33–35 ppm). The presence of the hexafluorophosphate ion is manifested via a characteristic septet in the ^{31}P NMR spectrum (δ_P −145) and a doublet in the ^{19}F NMR spectrum (δ_F −73; $^1J_{PF}$ = 706 Hz).

The presence of amide and ester groups are clearly reflected in IR spectra showing intense bands due to ν_{NH} (ca. 3375 cm^{-1}), $\nu_{C=O}$ (1747–1751 cm^{-1}), amide I (1638–1653 cm^{-1}), and amide II (1530–1553 cm^{-1}) vibrations. The ester band is missing from the IR spectrum of **5b**, which on the other hand shows further bands due to the secondary and terminal primary amide groups. IR spectra of cationic complexes **7a**–**c** and **8a**–**c** further indicate the presence of coordinated MeCN ($\nu_{C\equiv N}$ 2293–2330 cm^{-1}) and the PF_6^- counterion (a strong band at 835–847 cm^{-1}). Positive-ion electrospray ionization (ESI)

dx.doi.org/10.1021/om3002087 | *Organometallics* 2012, 31, 3985–3994

Scheme 3. Mutual Interconversions and Alternative Preparations of (η^6-*p*-cymene)ruthenium(II) Complexes with Ligand 1[a]

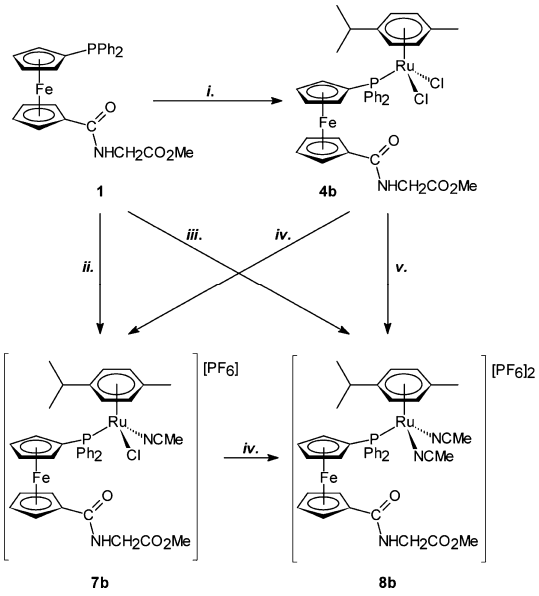

[a]Legend: (i) $[(p\text{-cymene})RuCl_2]_2$; (ii) $[(p\text{-cymene})RuCl(MeCN)_2]$-$[PF_6]$; (iii) $[(p\text{-cymene})Ru(MeCN)_3][PF_6]_2$; (iv) $Ag[PF_6]$; (v) 2 $Ag[PF_6]$. Reaction (i) was carried out in $CHCl_3$. All other reactions were performed in acetonitrile. For a complete description of the experiments, see the Supporting Information.

mass spectra of the neutral complexes **4a–c** and **5b** show ions corresponding to $[M + Na]^+$ or $[M - Cl]^+$. The spectra of the monocationic complexes **7a–c** display ions resulting via elimination of acetonitrile from their cations ($[M - MeCN - PF_6]^+$), while **8a–c** give rise to ions of the type $[(arene)Ru(\mathbf{1} - H)]^+$ or $[M - PF_6]^+$.

Description of the Crystal Structures. Single crystals suitable for X-ray diffraction analysis were obtained from diffusion of diethyl ether into a solution in methanol (**4b**·$2CH_3OH$) or acetonitrile (**8b**). Molecular structures of the complex molecule in the solvate **4b**·$2CH_3OH$ and the cation in the structure of **8b** are presented in Figure 1. Selected geometric data are given in Table 1.

The overall structures of both complex species are rather similar: the axis of the cymene ligand is oriented roughly parallel to the vector connecting the simple ligands (Cl1/Cl2 or N2/N3), and the arene ring is practically parallel to the basal plane of the three-legged piano-stool structure.[11] The ferrocene units are rotated with respect to the (η^6-*p*-cymene)Ru^{II} unit, as evidenced by the dihedral angles of planes of the Ru-bound arene and the phosphinylated cyclopentadienyl rings being 79.2(3)° for **4b**·$2CH_3OH$ and 69.2(4)° for **8b**. Notably, the Cg3–Ru1–donor angles (see Table 1 for defniinitions) in both compounds are rather similar (124.95(9)–130.37(9)° for **4b**·$2CH_3OH$, 126.0(2)–129.7(2)° for **8b**), which rules out any significant deformation of the coordination sphere around Ru resulting from different steric demands of the two-electron donors (Cl and CH_3CN vs the relatively bulkier phosphine). Otherwise, the Ru–donor distances and the overall geometry are unexceptional and compare well with the data reported previously for $[(\eta^6\text{-}p\text{-cymene})RuCl_2(Hdpf\text{-}\kappa P)]$[12] and $[(\eta^6\text{-benzene})Ru(MeCN)_2(PPh_3)](CF_3SO_3)_2$.[13]

The geometry of coordinated **1** does not differ much from that found for free $Ph_2PfcCONHCH_2CO_2Bu\text{-}t$.[7] The 1,1′-disubstituted ferrocene moieties in **4b**·$2CH_3OH$ and **8b** assume

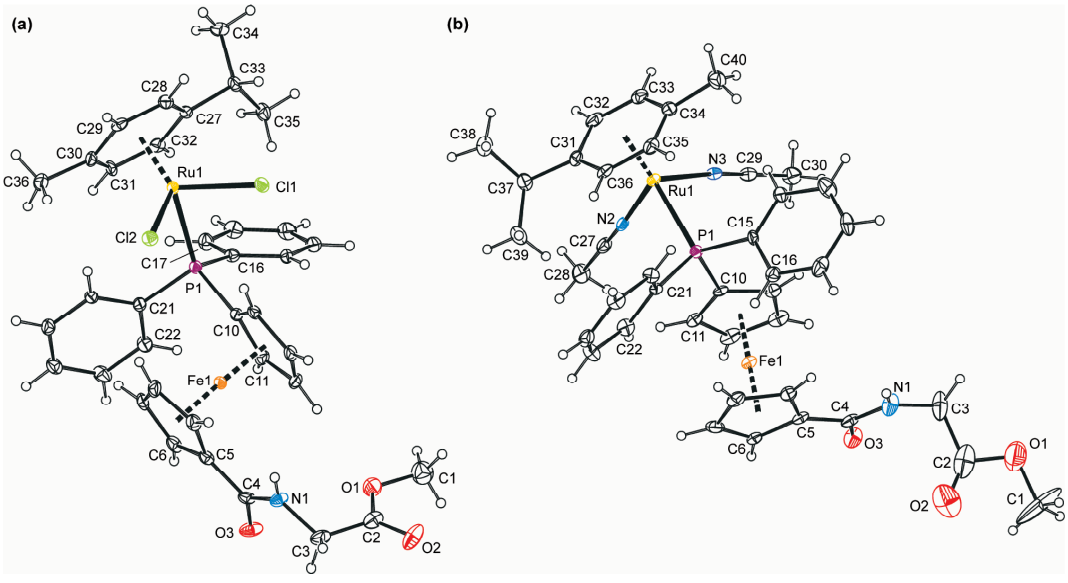

Figure 1. Views of (a) the complex molecule in **4b**·$2CH_3OH$ and (b) the cation in the structure of compound **8b**. Displacement ellipsoids correspond to the 30% probability level.

dx.doi.org/10.1021/om3002087 | *Organometallics* 2012, 31, 3985–3994

Table 1. Selected Distances (Å) and Angles (deg) for Compounds 4b·2CH$_3$OH and 8b[a]

param	**4b**·2CH$_3$OH (X = Cl1, Z = Cl2)	**8b**[b] (X = N2, Z = N3)
Ru1–P1	2.380(1)	2.369(2)
Ru1–X	2.422(1)	2.062(6)
Ru1–Z	2.431(1)	2.056(6)
Ru–Cg3	1.718(2)	1.731(3)
P1–Ru1–X	86.75(5)	88.9(2)
P1–Ru1–Z	87.65(5)	84.8(2)
X–Ru1–Z	88.99(5)	84.9(2)
Fe1–Cg1	1.654(3)	1.656(4)
Fe1–Cg2	1.647(3)	1.654(4)
∠Cp1,Cp2	3.8(4)	3.2(5)
τ	156	137
φ	9.2(7)	8(1)
C4–O3	1.238(7)	1.229(9)
C4–N1	1.343(8)	1.339(9)
O3–C4–N1	121.1(6)	122.4(7)
C2–O1	1.326(8)	1.40(2)
C2–O2	1.215(8)	1.24(2)
O1–C2–O2	123.6(6)	122(1)

[a]Definitions: Cp1 = C(5–9), Cp2 = C(10–14), arene = benzene ring of the π-coordinated *p*-cymene (i.e., C(27–32) for **4b**, and C(31–36) for **8b**). Cg1, Cg2, and Cg3 denote the centroids of the Cp1, Cp2, and arene rings, respectively. τ = torsion angle C5–Cg1–Cg2–C10. φ = dihedral angle subtended by the plane Cp1 and the amide unit [C4, O3, N1]. [b]Further data: N2–C27 = 1.14(1) Å, N2–C27–C28 = 178.9(9)°, N3–C29 = 1.144(9) Å, N3–C29–C30 = 179.1(7)°.

intermediate conformations close to anti-eclipsed (compare the τ angles in Table 1 with the ideal value of 144°) and exert regular geometries with tilt angles of ca. 3–4° and individual Fe–C distances falling into narrow ranges (2.036(6)–2.061(6) and 2.033(8)–2.066(9) Å for **4b**·2CH$_3$OH and **8b**, respectively). The planes of the amide moieties are rotated only by ca. 8–9° from the planes of their parent cyclopentadienyl rings (Cp1), and the whole amido-ester pendants extend away from the ferrocene and the (η^6-arene)Ru units.

Electrochemistry. The electrochemical properties of complexes **4a–c**, **5b**, **7a–c**, and **8a–c** were studied by cyclic voltammetry at a platinum-disk electrode. The measurements were performed on ca. 0.5 mM acetonitrile solutions containing 0.1 M [Bu$_4$N][PF$_6$] as the supporting electrolyte using ferrocene/ferrocenium as an internal reference. The pertinent data are summarized in Table 2.

When the external potential is increased in cyclic voltammetry, complexes **4a–c** undergo first a reversible one-electron redox change centered very likely at the ferrocene unit (Figure 2).[14] The separation of the anodic and cathodic peaks in cyclic voltammograms of these compounds was ca. 70–75 mV, similar to that of ferrocene/ferrocenium under the same experimental conditions. The ratios of the anodic and cathodic peak currents were close to unity, and the peak currents of this wave increased with the square root of the scan rate, indicating that the redox process is controlled by diffusion. Because of electron density transfer upon coordination, the redox potentials were more positive than that of free ligand **1** ($E^{\circ\prime}$ = 0.26 V in CH$_2$Cl$_2$).[7] Furthermore, the potentials decreased upon increasing the number of alkyl substituents at the Ru-bound arene ligand (i.e., with increasing donor ability of the η^6-arene donor).

A second redox event in **4a–c** observed at higher potentials is electrochemically irreversible and multielectron in nature

Table 2. Summary of Electrochemical Data for 4a–c, 5b, 7a–c, and 8a–c[a]

compd	$E^{\circ\prime}$(Fe$^{II/III}$) (V)	E_{pa}(Ru) (V)
4a	0.315	0.935
4b	0.285	0.850
4c[b]	0.245	0.710
5b	0.260	0.850
7a	0.430	n.d.
7b	0.410	n.d.
7c	0.385	n.d.
8a	0.540	n.d.
8b	0.530	n.d.
8c	0.510	n.d.

[a]The potentials are quoted relative to ferrocene/ferrocenium. $E^{\circ\prime}$ = $^1/_2(E_{pa} + E_{pc})$, where E_{pa} (E_{pc}) is the anodic (cathodic) peak potential in cyclic voltammetry. n.d. = not determined. [b]This compound shows a more complicated redox response (see text).

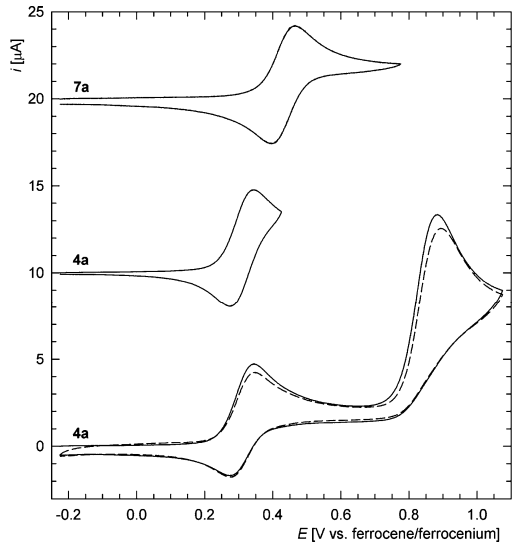

Figure 2. Cyclic voltammograms of complexes **4a** (full and partial) and **7a**, as recorded at a Pt-disk electrode on dichloromethane solutions (scan rate 100 mV s^{-1}). For clarity, the second scan is shown by a dashed line (for the full voltammogram of **4a**) and the voltammograms are shifted by +10 and +20 μA to avoid overlaps.

(Figure 2). The anodic peak potential (E_{pa}) of the second wave decreased significantly with an increasing number of arene substituents, suggesting the second redox change to occur predominantly at the (η^6-arene)Ru moiety. In the case of **4c**, an additional pair of redox waves was seen between the redox waves, probably due to adsorption. On the other hand, the redox response of compound **5b** did not differ from that of **4b**: the first wave appeared shifted slightly to lower potentials, while the redox potential of the second oxidation remained the same, which supports the assignment of the redox processes.

Replacement of the anionic chloro ligands by the neutral solvent molecules as in complexes **7** and **8** produces positively charged species, which could be expected to be more difficult to oxidize. Indeed, the cyclic voltammograms of **7a–c** displayed only one electrochemically reversible redox wave, attributable to the ferrocene/ferrocenium couple shifted to higher

dx.doi.org/10.1021/om3002087 | *Organometallics* 2012, 31, 3985–3994

potentials as compared with that in the respective complexes **4a–c** (Figure 2). As for the parent neutral complexes, the compounds bearing more alkylated arene ligands became oxidized more easily ($E^{\circ\prime}$: **7c** < **7b** < **7a**). In the case of **8a–c**, this redox wave was shifted even further but was much less affected by the substituents at the arene ring. The second oxidations of **7** and **8** were probably located outside the accessible potential range.

Catalytic Reactions. Metal-catalyzed oxidation of alcohols to give carbonyl compounds such as aldehydes, ketones, and carboxylic acids is an important transformation both for organic synthesis and for industrial manufacturing.[15] There are many reports concerning this reaction using molecular oxygen[16] and hydrogen peroxide[17] as oxidants, the problem very often being the activity and selectivity of the catalyst. As far as this reaction in aqueous media is concerned, the oxidation of alcohols with H_2O_2 under phase-transfer conditions has been proposed.[18] Noyori reported a combined system composed of Na_2WO_4 and $[CH_3(n\text{-}C_8H_{17})_3N][HSO_4]$ as a phase-transfer catalyst, which efficiently catalyzes the oxidation of alcohols to the corresponding carbonyl compounds with high yields.[19] Trakarnpruk[20] and Punniyamurthy[21] compared the oxidation activity of hydrogen peroxide and *tert*-butyl hydroperoxide, another cheap and easy to use peroxide. A number of catalysts for the use of *t*-BuOOH have been reported to date.[22] Watanabe[23] and Muharashi[24] used the ruthenium complex $[RuCl_2(PPh_3)_3]$, which catalyzes the oxidation with high conversion (>92%). Recently, Singh used arene ruthenium complexes of the type $[(\eta^6\text{-arene})RuCl(L)][PF_6]$ (arene = *p*-cymene, benzene; L = *N*-[2-(arylchalcogeno)ethyl]morpholines with aryl = Ph, 2-pyridyl (for S), Ph (for Se), 4-$MeOC_6H_4$ (for Te)) as catalysts for alcohol oxidation, using *N*-methylmorpholine *N*-oxide (NMO), *t*-BuOOH, $NaIO_4$, and NaOCl as the oxidants.[25] We recently reported on the use of ruthenium arene bis-saccharinato complexes as alcohol oxidation catalysts that work efficiently in aqueous solution.[26]

All ruthenium–iron compounds reported above were tested as defined precatalysts in the oxidation of secondary alcohols to ketones. Complex **4b** obtained in a straightforward manner from the most easily accessible and cheapest Ru precursor was tested first in the oxidation of 1-phenylethanol as a model substrate with *t*-BuOOH in pure water (Scheme 4; for complete results in a tabulated form, see the Supporting Information, Table S1). Indeed, the oxidation reaction in the presence of 0.1 mol % of **4b** proceeded cleanly to produce acetophenone with complete conversion within 3 h (at room temperature). When the catalyst amount was lowered to 0.01 mol %, the conversion achieved in 3 h was only 83% but the reaction reached completion within 5 h. Decreasing the catalyst loading further to 0.001 mol % expectedly decreased the reaction rate (30% and 66% conversion in 3 and 5 h, respectively). Even in this case, however, complete conversion to acetophenone was achieved in 24 h. No reaction was seen without the Ru complex.

Scheme 4. Oxidation of 1-Phenylethanol to Acetophenone

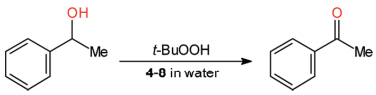

A possible influence of the catalyst structure and reaction conditions on the course of the oxidation process was studied next. The results obtained with all defined (η^6-arene)Ru complexes in the model oxidation reaction at a substrate to catalyst ratio of 100 000:1, summarized in Table 3, clearly show the superior performance of compound **4b** at short reaction times. Only slightly worse results were obtained with the monocationic complexes **7a,c**. On the other hand, all catalysts tested gave complete or practically complete conversions in 24 h. This observation may indicate that the differences in performance observed at relatively shorter reaction times could reflect the ease of conversion of the defined precatalysts into the catalytically active species, presumably an aqua complex. This assumption is supported by our previous studies[25] and, indirectly, also by the observed dependence of turnover number on the pH of the reaction mixture (Figure 3). The best results were obtained at pH ca. 5.5–7.0. The aquation reaction, representing the likely catalyst activation step, is probably hindered at lower pH, while reactions at higher pH can lead to hydroxo complexes.[27] Otherwise, however, the

Table 3. Catalytic Activity of Complexes 4a–c, 6b, 7a–c, and 8a–c in the Oxidation of 1-Phenylethanol with *t*-BuOOH[a]

entry	cat.	conversn[b] after 5 h/24 h (%)	TON[c] after 24 h	TOF[d] after 5 h (h^{-1})
1	**4a**	30/99	99 000	6 000
2	**4b**	66/100	100 000	13 200
3	**4c**	45/100	100 000	9 000
4	**6b**	41/99	99 000	8 200
5	**7a**	61/100	100 000	12 200
6	**7b**	53/99	99 000	10 600
7	**7c**	61/100	100 000	12 200
8	**8a**	35/100	100 000	7 000
9	**8b**	38/99	99 000	7 600
10	**8c**	28/100	100 000	5 600
11	none	0/0	0	0

[a]Reaction conditions: alcohol (1.0 mmol) and *t*-BuOOH (4.0 mmol) in 4 mL of water, substrate/catalyst = 100 000, room temperature, reaction time 5 or 24 h. [b]Determined by ^{1}H NMR spectroscopy. [c]Turnover number: mol product/mol catalyst – after 24 h. [d]Turnover frequency: mol product/(mol catalyst × reaction time) – after 5 h.

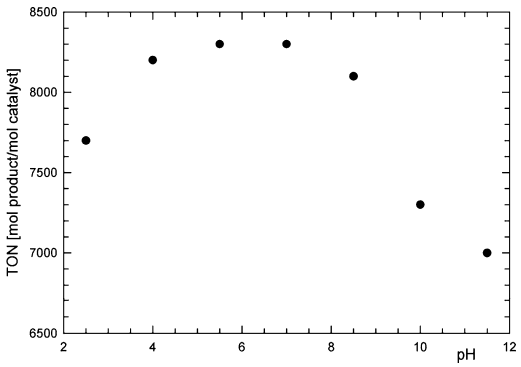

Figure 3. pH dependence of the turnover number (TON) for oxidation of 1-phenylethanol with *t*-BuOOH mediated by complex **4b** (0.01 mol %) at room temperature after 3 h. For tabulated results, see the Supporting Information (Table S1).

dx.doi.org/10.1021/om3002087 | *Organometallics* 2012, 31, 3985–3994

reaction proceeded with no significant induction period and does not depart much from the exponential dependence expected for (pseudo) first-order kinetics (Figure 4).

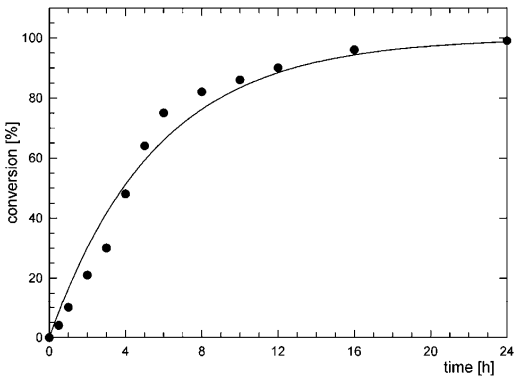

Figure 4. Kinetic profile for oxidation of 1-phenylethanol with *t*-BuOOH mediated by complex **4b** (0.01 mol %) at room temperature. The solid line represents an ideal kinetic fit: conversion = $a(1 - \exp[-bt])$. Parameters of the fit: a = 100(5)%, b = 0.18(2) h^{-1}, R^2 = 0.973.

Upon replacing pure water as the reaction mixture with organic solvents (hexane, diethyl ether, toluene, dichloromethane) or their biphasic aqueous mixtures, the oxidation reaction became considerably slower and did not reach completion even after 24 h (with 0.001 mol % catalyst; see the Supporting Information, Table S3). Also, when *t*-BuOOH was replaced with sodium perchlorate or sodium periodate (4 equiv), the conversions dropped to 9 and 62%, respectively, after 3 h (Supporting Information, Table S1). Other oxidants tested (aqueous hydrogen peroxide, benzoyl peroxide, 3-chloroperoxybenozic acid, oxone, or *N*-methylmorpholine *N*-oxide; 4 equiv vs the substrate) resulted in conversions not exceeding 3%. Bubbling air through the reaction mixture also did not induce any oxidation over 3 h.

A survey of various substrates (Table 4) showed that complex **4a** at 0.001 mol % loading promotes efficiently and cleanly the oxidation of 1-phenylethanol derivatives substituted at the benzene ring (entries 2−8), the exception being the 4-methoxyphenyl and 2-bromophenyl derivatives. The naphthyl analogue diphenylmethanol and even cyclic secondary alcohols with fused benzene rings were also efficiently oxidized (entries 9 and 11−13). On the other hand, 1-cyclohexylethanol and aliphatic secondary alcohols (entries 10, 14, and 15) gave only moderate conversions.

Water is the best reaction medium for this catalytic reaction, and the neutral dichloro complexes are more active than their monocationic monochloro acetonitrile and dicationic bis(acetontrile) counterparts. Together with a pronounced pH dependence of the reaction course, this suggests that aquation of the chloro ligands plays an important role and that an aqua complex may be the real entry to the catalytic cycle. A mechanism based on this observation, in accordance with our earlier findings,[25] is shown in Scheme 5. Since we did not detect any oxoruthenium(IV) intermediates during our catalytic reactions, this mechanistic scheme remains only a plausible working hypothesis. The involvement of Ru−OOH species formed in situ (probably via an intermediate Ru aqua complex) cannot be ruled out at this point (see alternative route in Scheme 5).[28]

CONCLUSION

Heterobimetallic Fe^{II}−Ru^{II} complexes **4**−**8** are easily prepared from the common (η^6-arene)Ru^{II} precursors and phosphinoferrocene carboxamides with amino acid pendant chains, either in a direct way or in a convergent manner. Electrochemical studies revealed electronic communication between the $Ru^{II/III}$ and $Fe^{II/III}$ redox centers present in these compounds, typically manifested through changes in the redox potentials of both redox couples observed upon modification of only one of them. The stable compounds **4**−**8** give rise to highly active catalysts for the Ru-catalyzed oxidation of secondary alcohols to ketones. The oxidations are advantageously performed in water at room temperature and proceed cleanly and rapidly even at catalyst to substrate ratios as low as 1:100 000. Surprisingly, the presence of oxidation-sensitive ferrocene-based ligands does not seem to

Table 4. Oxidation of Various Secondary Alcohols in the Presence of Catalyst 4b[a]

entry	substrate	product	conversn[b] after 5 h/24 h (%)	isolated yield after 24 h (%)
1	1-phenylethanol	acetophenone	66/100	93
2	1-(4-fluorophenyl)ethanol	4′-fluoroacetophenone	46/99	92
3	1-(4-chlorophenyl)ethanol	4′-chloroacetophenone	53/100	90
4	1-(4-bromophenyl)ethanol	4′-bromoacetophenone	67/100	91
5	1-(4-methylphenyl)ethanol	4′-methylacetophenone	62/99	90
6	1-(4-methoxyphenyl)ethanol	4′-methoxyacetophenone	44/70	n.d.
7	1-(3-bromophenyl)ethanol	3′-bromoacetophenone	47/99	92
8	1-(2-bromophenyl)ethanol	2′-bromoacetophenone	8/35	n.d.
9	1-(2-naphthyl)ethanol	2′-acetonaphthone	53/100	91
10	1-cyclohexylethanol	hexahydroacetophenone	13/36	n.d.
11	diphenylmethanol	benzophenone	77/100	94
12	1-indanol	1-indanone	67/99	90
13	1-tetralol	1-tetralone	61/99	89
14	cyclohexanol	cyclohexanone	14/55	n.d.
15	2-butanol	2-butanone	8/29	n.d.

[a]Reaction conditions: alcohol (1.0 mmol) and *t*-BuOOH (4.0 mmol) in 4 mL of water, substrate/catalyst =100 000, room temperature, reaction time 5 or 24 h. [b]Determined by ^{1}H NMR spectroscopy.

dx.doi.org/10.1021/om3002087 | *Organometallics* 2012, 31, 3985−3994

Scheme 5. Plausible Mechanistic Alternatives for the Ru-Catalyzed Oxidation of Alcohols with Peroxides[a]

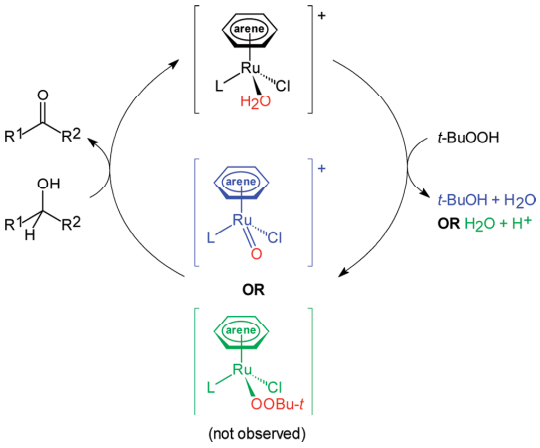

[a]L is the P-coordinated amidophosphine **1**.

impose any limitations on the catalyst stability and performance.

EXPERIMENTAL SECTION

Materials and Methods. All (η^6-arene)Ru complexes were synthesized under a nitrogen atmosphere and with the exclusion of direct daylight. No such precautions were applied to the catalytic tests. The compounds $[(\eta^6\text{-arene})RuCl_2]_2$ (arene = benzene, *p*-cymene),[29] $[(\eta^6\text{-}C_6Me_6)RuCl_2]_2$,[30] and $[(\eta^6\text{-arene})Ru(MeCN)_2Cl][PF_6]$[31] and ligands $Ph_2PfcC(O)NHCH_2COY$ (Y = OMe (**1**), OH (**2**), NH_2 (**3**))[7] were prepared according to the literature procedures. Solvents used in the syntheses and catalytic experiments were dried by standing over appropriate drying agents and distilled under nitrogen (dichloromethane, chloroform, and acetonitrile with CaH_2; hexane, diethyl ether, and toluene over sodium metal). Other chemicals and solvents used for crystallizations and in chromatography were used without further purification.

NMR spectra were recorded on a Bruker 400 MHz spectrometer (^{1}H, 400.13 MHz; ^{31}P, 161.98 MHz; ^{19}F, 376.50 MHz) at 296 K unless noted otherwise. Chemical shifts (δ/ppm) are given relative to the residual peak of the solvent (^{1}H; CD_3CN, δ_H = 1.94; $CDCl_3$, δ_H = 7.26), to 85% aqueous H_3PO_4 (^{31}P) or to neat $CFCl_3$ (^{19}F). Infrared spectra were recorded on KBr pellets with a Perkin–Elmer FTIR 1720-X spectrometer. Electrospray ionization (ESI) mass spectra were obtained in positive-ion mode with an LCQ Finnigan mass spectrometer.

Electrochemical measurements were performed with a computer-controlled multipurpose μAUTOLAB III potentiostat (Eco Chemie) at room temperature using a standard three-electrode cell equipped with a platinum-disk (AUTOLAB RDE, 3 mm diameter) working electrode, platinum-sheet auxiliary electrode, and double-junction Ag/AgCl (3 M KCl) reference electrode. Samples were dissolved in acetonitrile (Sigma-Aldrich, absolute) to give a solution containing ca. 0.5 mM of the analyte and 0.1 M $[Bu_4N][PF_6]$ (Fluka, purissimum for electrochemistry). The solutions were deaerated by bubbling with argon before the measurements and then kept under an argon blanket. The potentials are given relative to ferrocene/ferrocenium reference. The redox potential of the ferrocene/ferrocenium couple was 0.425 V vs Ag/AgCl (3 M KCl).

General Procedure for the Synthesis of Complexes $[(\eta^6\text{-arene})RuCl_2(1\text{-}\kappa P)]$ (4). A solution of ligand **1** (1.0 equiv) in $CHCl_3$ (5 mL per 0.2 mmol of the ligand) was added to the solid dimer $[(\eta^6\text{-arene})RuCl_2]_2$ (0.5 equiv). After the mixture was stirred at room temperature for 3 h, the solvent was evaporated under vacuum and the residue was purified by column chromatography on silica gel using chloroform/acetone (5/1 v/v) as the eluent.

Complex ***4a***. Starting from **1** (194 mg, 0.4 mmol) and $[(\eta^6\text{-benzene})RuCl_2]_2$ (100 mg, 0.2 mmol), the general procedure afforded **4a** as an orange foam. Yield: 274 mg (84%). ^{1}H NMR ($CDCl_3$, 50 °C): δ 3.36 (br s, 2 H, fc), 3.82 (s, 3 H, OMe), 4.13 (d, $^3J_{HH}$ = 6.1 Hz, 2 H, NHCH_2), 4.59 (br s, 2 H, fc), 4.69 (unresolved q, 2 H, fc), 4.72 (vt, 2 H, fc), 5.32 (s, 6 H, η^6-C_6H_6), 7.34–7.46 (m, 6 H, PPh_2), 7.70–7.82 (m, 4 H, PPh_2), 7.83 (t, $^3J_{HH}$ = 6.2 Hz, 1 H, NHCH$_2$). ^{31}P{^{1}H} NMR ($CDCl_3$, 50 °C): δ 15.2 (s). IR (KBr): ν_{NH} 3306 m, ν_{CO} 1747 vs, amide I 1651 vs, amide II 1553 vs cm^{-1}. MS (ESI+): *m*/*z* 758 ([M + Na]$^+$), 700 ([M − Cl]$^+$). Anal. Calcd for $C_{32}H_{30}NO_3PCl_2FeRu\cdot0.65CHCl_3$: C, 48.24; H, 3.80; N, 1.72. Found: C, 48.29; H, 3.80; N, 1.62.

Complex ***4b***. Starting from **1** (146 mg, 0.3 mmol) and $[(\eta^6\text{-}p\text{-cymene})RuCl_2]_2$ (92 mg, 0.15 mmol), the general procedure gave **4b** as an orange solid. Yield: 225 mg (94%). ^{1}H NMR ($CDCl_3$): δ 0.99 (d, $^3J_{HH}$ = 7.0 Hz, 6 H, CHMe_2), 1.70 (s, 3 H, η^6-C_6H_4Me), 2.44 (sept, $^3J_{HH}$ = 6.9 Hz, 1 H, $CHMe_2$), 3.27 (br s, 2 H, fc), 3.78 (s, 3 H, OMe), 4.09 (d, $^3J_{HH}$ = 6.1 Hz, 2 H, NHCH_2), 4.49 (vt, 2 H, fc), 4.55 (br s, 2 H, fc), 4.58 (unresolved q, 2 H, fc), 5.12 (d, $^3J_{HH}$ = 5.5 Hz, 2 H, η^6-C_6H_4), 5.19 (d, $^3J_{HH}$ = 6.1 Hz, 2 H, η^6-C_6H_4), 7.36–7.46 (m, 6 H, PPh_2), 7.59 (t, $^3J_{HH}$ = 6.0 Hz, 1 H, NHCH$_2$), 7.75–7.85 (m, 4 H, PPh_2). ^{31}P{^{1}H} NMR ($CDCl_3$): δ 17.2 (s). IR (KBr): ν_{NH} 3315 m, ν_{CO} 1750 vs, amide I 1648 vs, amide II 1530 vs cm^{-1}. MS (ESI+): *m*/*z* 814 ([M + Na]$^+$), 756 ([M − Cl]$^+$). Anal. Calcd for $C_{36}H_{38}NO_3PCl_2FeRu\cdot0.05CHCl_3$: C, 54.30; H, 4.81; N, 1.76. Found: C, 54.20; H, 4.78; N, 1.66.

Complex ***4c***. Starting with ligand **1** (146 mg, 0.3 mmol) and $[(\eta^6\text{-}C_6Me_6)RuCl_2]_2$ (100 mg, 0.15 mmol), the general procedure gave **4c** as a red solid. Yield: 228 mg (91%). ^{1}H NMR ($CDCl_3$, 50 °C): δ 1.67 (s, 18 H, η^6-C_6Me_6), 3.35 (br s, 2 H, fc), 3.79 (s, 3 H, OMe), 4.10 (d, $^3J_{HH}$ = 5.9 Hz, 2 H, NHCH_2), 4.41 (br s, 2 H, fc), 4.51 (br s, 2 H, fc), 4.57 (br s, 2 H, fc), 7.28–7.43 (m, 6 H, PPh_2), 7.69–7.92 (br s, 4 H of PPh_2 and 1 H of NHCH$_2$). ^{31}P{^{1}H} NMR ($CDCl_3$, 50 °C): δ 18.9 (s). IR (KBr): ν_{NH} 3312 m, ν_{CO} 1751 vs, amide I 1651 vs, amide II 1534 vs cm^{-1}. MS (ESI+): *m*/*z* 784 ([M − Cl]$^+$). Anal. Calcd for $C_{38}H_{42}NO_3PCl_2FeRu\cdot0.15CHCl_3$: C, 54.71; H, 5.07; N, 1.67. Found: C, 54.61; H, 4.94; N, 1.61.

Attempted Preparation of $[(\eta^6\text{-}p\text{-cymene})RuCl_2(2\text{-}\kappa P)]$ (5b). The reaction of acid **2** with $[(\eta^6\text{-}p\text{-cymene})RuCl_2]_2$ (general procedure) afforded a complicated mixture containing several soluble products (complexes). The composition of the crude reaction mixture changed with reaction time. Repeated attempts to isolate any defined material by column chromatography or crystallization failed.

Preparation of $[(\eta^6\text{-}p\text{-cymene})RuCl_2(3\text{-}\kappa P)]$ (6b). This compound was obtained similarly to complexes **4** from diamide **3** (94 mg, 0.2 mmol) and $[(\eta^6\text{-}p\text{-cymene})RuCl_2]_2$ (61 mg, 0.1 mmol). Yield of **6b**: 155 mg (88%), red solid. ^{1}H NMR ($CDCl_3$): δ 0.97 (d, $^3J_{HH}$ = 6.9 Hz, 6 H, CHMe_2), 1.78 (s, 3 H, η^6-C_6H_4Me), 2.49 (sept, $^3J_{HH}$ = 6.9 Hz, 1 H, $CHMe_2$), 3.29 (br s, 2 H, fc), 4.04 (d, $^3J_{HH}$ = 6.1 Hz, 2 H, NHCH_2), 4.50 (m, 4 H, fc), 4.53 (vt, 2 H, fc), 5.16 (m, 4 H, η^6-C_6H_4), 5.53 (br s, 1 H, CONH$_2$), 6.59 (br s, 1 H, CONH$_2$), 7.38–7.48 (m, 6 H, PPh_2), 7.72–7.86 (m, 4 H of PPh_2 and 1 H of NHCH$_2$). ^{31}P{^{1}H} NMR ($CDCl_3$): δ 17.0 (s). IR (KBr): ν_{NH} 3389 s, ν_{NH} 3319 s, amide I 1683 vs, amide I 1647 vs, amide II 1529 s cm^{-1}. MS (ESI+): *m*/*z* 799 ([M + Na]$^+$), 741 ([M − Cl]$^+$). Anal. Calcd for $C_{35}H_{37}N_2O_2PCl_2FeRu\cdot0.85CHCl_3$: C, 49.04; H, 4.35; N, 3.19. Found: C, 49.08; H, 4.28; N, 3.04.

General Procedure for the Preparation of Compounds $[(\eta^6\text{-arene})RuCl(MeCN)(1\text{-}\kappa P)][PF_6]$ (7). A solution of **1** (97 mg, 0.2 mmol) in acetonitrile (10 mL) was added to the solid solvento complex $[(\eta^6\text{-arene})Ru(MeCN)_2Cl][PF_6]$ (0.2 mmol). The resulting mixture was stirred at room temperature for 4 h and then evaporated under vacuum. Preparative thin-layer chromatography on silica gel plates with chloroform/acetonitrile (4/1 v/v) afforded the products as yellow solids.

Compound ***7a***. Following the general procedure, $[(\eta^6\text{-}C_6H_6)Ru(MeCN)_2Cl][PF_6]$ (88 mg, 0.2 mmol) and **1** (97 mg, 0.2 mmol) afforded **7a** as a yellow solid. Yield: 99 mg (51%). ^{1}H NMR

dx.doi.org/10.1021/om3002087 | *Organometallics* 2012, 31, 3985–3994

(CD_3CN): δ 2.22 (s, 3 H, MeCN), 3.71 (s, 3 H, OMe), 3.94 (dt, $J \approx$ 1.3, 2.5 Hz, 1 H, fc), 3.96 (d, $^3J_{HH}$ = 6.1 Hz, 1 H, NHCH_2), 3.98 (d, $^3J_{HH}$ = 6.1 Hz, 1 H, NHCH_2), 4.06 (dt, $J \approx$ 1.3, 2.5 Hz, 1 H, fc), 4.14 (m, 1 H, fc), 4.60 (dt, $J \approx$ 1.3, 2.6 Hz, 1 H, fc), 4.66 (m, 2 H, fc), 4.72 (m, 1 H, fc), 4.82 (m, 1 H, fc), 5.64 (s, 6 H, η^6-C_6H_6), 6.99 (t, $^3J_{HH}$ = 6.0 Hz, 1 H, N*H*CH$_2$), 7.51–7.83 (m, 10 H, PPh_2). $^{31}P\{^1H\}$ NMR (CD_3CN): δ −144.6 (sept, $^1J_{PF}$ = 706 Hz, PF_6), 28.1 (s, PPh_2). $^{19}F\{^1H\}$ NMR (CD_3CN): δ −72.9 (d, $^1J_{PF}$ = 706 Hz, PF_6). IR (KBr): ν_{NH} 3442 m, $\nu_{C\equiv N}$ 2296 w, ν_{CO} 1748 vs, amide I 1651 vs, amide II 1534 vs, ν_{PF} 842 vs cm^{-1}. MS (ESI+): m/z 700 ([M − MeCN − PF_6]$^+$). Anal. Calcd for $C_{34}H_{33}N_2O_3F_6P_2ClFeRu\cdot 0.75CHCl_3$: C, 42.79; H, 3.49; N, 2.87. Found: C, 42.84; H, 3.48; N, 2.91.

Compound ***7b***. This compound was prepared similarly from [(η^6-*p*-cymene)Ru(MeCN)$_2$Cl][PF_6] (100 mg, 0.2 mmol) and **1** (97 mg, 0.2 mmol). Yield: 132 mg (65%), yellow solid. ^1H NMR (CD_3CN): δ 0.99 (d, $^3J_{HH}$ = 6.9 Hz, 3 H, CHMe_2), 1.00 (d, $^3J_{HH}$ = 6.9 Hz, 3 H, CHMe_2), 1.90 (s, 3 H, η^6-C_6H_4Me), 2.15 (s, 3 H, MeCN), 2.35 (sept, $^3J_{HH}$ = 7.0 Hz, 1 H, C*H*Me$_2$), 3.70 (s, 3 H, OMe), 3.85 (dt, $J \approx$ 1.3, 2.5 Hz, 1 H, fc), 3.93 (dt, $J \approx$ 1.3, 2.6 Hz, 1 H, fc), 3.95 (d, $^3J_{HH}$ = 6.1 Hz, 2 H, NHCH_2), 4.00 (m, 1 H, fc), 4.47 (dt, $J \approx$ 1.4, 2.6 Hz, 1 H, fc), 4.61 (dt, $J \approx$ 1.3, 2.6 Hz, 1 H, fc), 4.63 (m, 1 H, fc), 4.73 (m, 2 H, fc), 5.17 (d, J_{HH} = 6.1 Hz, 1 H, η^6-C_6H_4), 5.43 (dt, J_{HH} = 6.2, 1.4 Hz, 1 H, η^6-C_6H_4), 5.50 (d, J_{HH} = 6.5 Hz, 1 H, η^6-C_6H_4), 5.74 (dd, J_{HH} = 6.4, 1.0 Hz, 1 H, η^6-C_6H_4), 6.89 (t, $^3J_{HH}$ = 6.1 Hz, 1 H, N*H*CH$_2$), 7.55–7.94 (m, 10 H, PPh_2). $^{31}P\{^1H\}$ NMR (CD_3CN): δ −144.6 (sept, $^1J_{PF}$ = 706 Hz, PF_6), 27.7 (s, PPh_2). $^{19}F\{^1H\}$ NMR (CD_3CN): δ −72.9 (d, $^1J_{PF}$ = 706 Hz, PF_6). IR (KBr): ν_{NH} 3418 s, $\nu_{C\equiv N}$ 2293 w, ν_{CO} 1750 s, amide I 1651 s, amide II 1533 s, ν_{PF} 840 vs cm^{-1}. MS (ESI+): m/z 756 ([M − MeCN − PF_6]$^+$). Anal. Calcd for $C_{38}H_{41}N_2O_3F_6P_2ClFeRu\cdot 0.55CHCl_3$: C, 45.95; H, 4.16; N, 2.78. Found: C, 55.97; H, 4.11; N, 2.70.

Compound ***7c***. Starting with [(η^6-hexamethylbenzene)Ru(MeCN)$_2$Cl][PF_6] (105 mg, 0.2 mmol) and **1** (97 mg, 0.2 mmol), the general procedure afforded **7c** as a yellow solid. Yield: 150 mg (70%). ^1H NMR (CD_3CN): δ 1.76 (s, 18 H, η^6-C_6Me_6), 2.16 (s, 3 H, MeCN), 3.68 (m, 1 H, fc), 3.70 (s, 3 H, OMe), 3.75 (m, 1 H, fc), 3.96 (br d, $^3J_{HH}$ = 6.1 Hz, 2 H, NHCH_2), 4.28 (br s, 1 H, fc), 4.62 (m, 1 H, fc), 4.50 (m, 2 H, fc), 4.64 (m, 1 H, fc), 4.72 (m, 1 H, fc), 6.92 (t, $^3J_{HH}$ = 5.9 Hz, 1 H, N*H*CH$_2$), 7.50–7.85 (m, 10 H, PPh_2). $^{31}P\{^1H\}$ NMR (CD_3CN): δ −144.6 (sept, $^1J_{PF}$ = 706 Hz, PF_6), 29.7 (s, PPh_2). $^{19}F\{^1H\}$ NMR (CD_3CN): δ −72.9 (d, $^1J_{PF}$ = 706 Hz, PF_6). IR (KBr): ν_{NH} 3440 m, $\nu_{C\equiv N}$ 2289 w, ν_{CO} 1749 vs, amide I 1653 vs, amide II 1534 vs, ν_{PF} 847 vs cm^{-1}. MS (ESI+): m/z 784 ([M − MeCN − PF_6]$^+$). Anal. Calcd for $C_{40}H_{45}N_2O_3F_6P_2ClFeRu\cdot 0.9CHCl_3$: C, 45.59; H, 4.29; N, 2.60. Found: C, 45.48; H, 4.28; N, 2.75.

General Procedure for the Synthesis of Compounds [(η^6-arene)Ru(MeCN)$_2$(1-κP)][PF_6]$_2$ (8). A solution of the respective complex [(η^6-arene)RuCl_2(**1**-κP)] (**4**; 1 equiv) in acetonitrile (2 mL per 0.1 mmol of Ru complex) was treated with the stoichiometric amount of Ag[PF_6] (2 equiv) dissolved in acetonitrile (3 mL per 0.2 mmol of Ag salt). The resulting yellow-orange reaction mixture was stirred at room temperature for 3 h, the precipitated solid (AgCl) was removed by filtration through a PTFE filter, and the filtrate was evaporated under vacuum. The residue was purified by preparative thin-layer chromatography on SiO_2 with $CHCl_3$/acetonitrile (2/1 v/v) as the eluent. When they are analyzed by conventional elemental analysis, the bis(acetonitrile) complexes **8** notoriously give erratic results, very likely due to incomplete combustion.

Compound ***8a***. Starting from **4a** (147 mg, 0.2 mmol) and Ag[PF_6] (101 mg, 0.4 mmol), the general procedure afforded **8a** as a yellow solid. Yield: 92 mg, 44%. ^1H NMR (CD_3CN): δ 2.23 (s, 6 H, MeCN), 3.70 (s, 3 H, OMe), 3.98 (d, $^3J_{HH}$ = 6.1 Hz, 2 H, NHCH_2), 4.21 (vt, 2 H, fc), 4.36 (vq, 2 H, fc), 4.73 (vt, 2 H, fc), 4.90 (vq, 2 H, fc), 5.94 (s, 6 H, η^6-C_6H_6), 6.95 (t, $^3J_{HH}$ = 6.0 Hz, 1 H, N*H*CH$_2$), 7.60–7.77 (m, 10 H, PPh_2). $^{31}P\{^1H\}$ NMR (CD_3CN): δ −144.6 (sept, $^1J_{PF}$ = 707 Hz, PF_6), 33.7 (s, PPh_2). $^{19}F\{^1H\}$ NMR (CD_3CN): δ −72.8 (d, $^1J_{PF}$ = 706 Hz, PF_6). IR (KBr): ν_{NH} 3417 m, $\nu_{C\equiv N}$ 2330 w and 2302 w, ν_{CO} 1748 s, amide I 1639 s, amide II 1542 s, ν_{PF} 836 vs cm^{-1}. MS (ESI+): m/z 586 ([(C_6H_6)Ru(**1** − H)]$^+$).

Compound ***8b***. This compound was prepared similarly from **4b** (158 mg, 0.2 mmol) and Ag[PF_6] (101 mg, 0.4 mmol) and isolated as a yellow solid. Yield: 122 mg (56%). ^1H NMR (CD_3CN): δ 1.07 (d, $^3J_{HH}$ = 6.9 Hz, 6 H, CHMe_2), 1.93 (s, 3 H, η^6-C_6H_4Me), 2.29 (s, 6 H, MeCN), 2.49 (sept, $^3J_{HH}$ = 6.9 Hz, 1 H, C*H*Me$_2$), 3.70 (s, 3 H, OMe), 3.97 (d, $^3J_{HH}$ = 6.1 Hz, 2 H, NHCH_2), 4.12 (vt, 2 H, fc), 4.31 (vq, 2 H, fc), 4.67 (vt, 2 H, fc), 4.85 (vq, 2 H, fc), 5.65 (d, $^3J_{HH}$ = 6.5 Hz, 2 H, η^6-C_6H_4), 5.81 (d, $^3J_{HH}$ = 6.5 Hz, 2 H, η^6-C_6H_4), 6.91 (t, $^3J_{HH}$ = 6.0 Hz, 1 H, N*H*CH$_2$), 7.65–7.81 (m, 10 H, PPh_2). $^{31}P\{^1H\}$ NMR (CD_3CN): δ −144.6 (sept, $^1J_{PF}$ = 707 Hz, PF_6), 33.0 (s, PPh_2). $^{19}F\{^1H\}$ NMR (CD_3CN): δ −72.8 (d, $^1J_{PF}$ = 707 Hz, PF_6). IR (KBr): ν_{NH} 3414 m, $\nu_{C\equiv N}$ 2329 w and 2299 w, ν_{CO} 1747 s, amide I 1638 vs, amide II 1542 s, ν_{PF} 835 vs cm^{-1}. MS (ESI+): m/z 948 ([M − PF_6]$^+$).

Compound ***8c***. Following the general procedure, **4c** (164 mg, 0.2 mmol) and Ag[PF_6] (101 mg, 0.4 mmol) afforded **8c** as a yellow solid. Yield: 123 mg, 55%. ^1H NMR (CD_3CN): δ 1.87 (s, 18 H, η^6-C_6Me_6), 2.35 (s, 6 H, MeCN), 3.70 (s, 3 H, OMe), 3.96 (vt, 2 H, fc), 3.97 (d, $^3J_{HH}$ = 6.1 Hz, 2 H, NHCH_2), 4.41 (vq, 2 H, fc), 4.63 (vt, 2 H, fc), 4.83 (vq, 2 H, fc), 6.90 (t, $^3J_{HH}$ = 6.1 Hz, 1 H, N*H*CH$_2$), 7.63–7.78 (m, 10 H, PPh_2). $^{31}P\{^1H\}$ NMR (CD_3CN): δ −144.6 (sept, $^1J_{PF}$ = 707 Hz, PF_6), 34.6 (s, PPh_2). $^{19}F\{^1H\}$ NMR (CD_3CN): δ −72.9 (d, $^1J_{PF}$ = 706 Hz, PF_6). IR (KBr): ν_{NH} 3444 m, $\nu_{C\equiv N}$ 2327 w and 2295 w, ν_{CO} 1747 vs, amide I 1639 vs, amide II 1542 vs, ν_{PF} 839 vs cm^{-1}. MS (ESI+): m/z 976 ([M − PF_6]$^+$), 748 ([(C_6Me_6)Ru(**1** − H)]$^+$).

X-ray Crystallography. The diffraction data were collected with a Stoe image plate diffraction system equipped with a ϕ circle goniometer, using Mo Kα graphite-monochromated radiation (λ = 0.710 73 Å; ϕ range 0–200°, 2θ range from 3.0 to 59°, $D_{max} - D_{min}$ = 12.45–0.81 Å). The structures were solved by direct methods using the program SHELXS-97.[32] Refinement and all further calculations were carried out using SHELXL-97.[32] Examination of the structures with PLATON[33] reveals in **4b** additional disordered solvent molecules, while in **8b** voids between anions and cations are observed. Therefore, new data sets corresponding to omission of the missing solvent molecules were generated with the SQUEEZE algorithm[34] and the structures were refined to full convergence. In both structures, the hydrogen atoms were included in their calculated positions and treated as riding atoms using the SHELXL default parameters. The non-hydrogen atoms were refined anisotropically, using weighted full-matrix least squares based on F^2. Crystallographic details are available as Supporting Information (Table S4). The figures were drawn with the PLATON program. The same program was used to perform all geometric calculations.

CCDC-866729 (**4b**·2CH_3OH) and CCDC-866730 (**8b**) contain the supplementary crystallographic data for this paper. These data can be obtained free of charge at www.ccdc.cam.ac.uk/conts/retrieving.html (or from the Cambridge Crystallographic Data Centre, 12, Union Road, Cambridge CB2 1EZ, U.K.; fax, (internat.) +44-1223/336-033; e-mail, deposit@ccdc.cam.ac.uk).

General Procedure for the Oxidation of Secondary Alcohols. The appropriate quantities of the catalyst and alcohol (1 mmol) were mixed with water (4 mL) in an open vial. The oxidizing agent (4 mmol) was added slowly, and the resulting mixture was stirred at room temperature for the given reaction time. Then, it was extracted with diethyl ether (2 × 5 mL) and dried over anhydrous $MgSO_4$. A small aliquot was analyzed by ^1H NMR spectroscopy to determine the conversion. In the case of complete conversion, the extracts were evaporated and the crude product was isolated by flash column chromatography over silica using a hexane/diethyl ether mixture to give pure ketones following evaporation.

Characterization Data of the Oxidation Products. Acetophenone:[35] ^1H NMR ($CDCl_3$) δ 2.61 (s, 3 H, Me), 7.43–7.50 (m, 2 H, C_6H_5), 7.52–7.61 (m, 1 H, C_6H_5), 7.93–7.98 (m, 2 H, C_6H_5). 4′-Fluoroacetophenone:[34] ^1H NMR ($CDCl_3$) δ 2.59 (s, 3 H, Me), 7.09–7.16 (m, 2 H, C_6H_4), 7.96–8.01 (m, 2 H, C_6H_4). 4′-Chloroacetophenone:[34] ^1H NMR ($CDCl_3$) δ 2.59 (s, 3 H, Me), 7.41–7.47 (m, 2 H, C_6H_4), 7.88–7.92 (m, 2 H, C_6H_4). 4′-Bromoacetophenone (ref.[34]): ^1H NMR ($CDCl_3$) δ 2.58 (s, 3 H, Me), 7.58–7.62 (m, 2 H, C_6H_4), 7.79–7.84 (m, 2 H, C_6H_4). 4′-Methylacetophenone:[34] ^1H NMR ($CDCl_3$) δ 2.42 (s, 3 H, *Me*C_6H_4), 2.59 (s, 3 H, Me), 7.23–7.28 (m, 2 H, C_6H_4),

7.83−7.88 (m, 2 H, C_6H_4). 3′-Bromoacetophenone:[36] ^{1}H NMR ($CDCl_3$) δ 2.60 (s, 3 H, Me), 7.35 (t, J_{HH} = 7.9 Hz, 1 H, C_6H_4), 7.69 (dd, J_{HH} = 1.0, 7.9 Hz, 1 H, C_6H_4), 7.88 (d, J_{HH} = 7.8 Hz, 1 H, C_6H_4), 8.09 (br s, 1 H, C_6H_4). 2′-Acetonaphthone:[34] ^{1}H NMR ($CDCl_3$) δ 2.72 (s, 3 H, Me), 7.53 (dt, J_{HH} = 1.1, 6.8 Hz, 1 H, Ar), 7.60 (dt, J_{HH} = 1.2, 6.8 Hz, 1 H, Ar), 7.87 (d, J_{HH} = 6.0 Hz, 1 H, Ar), 7.89 (d, J_{HH} = 8.2 Hz, 1 H, Ar), 7.96 (d, J_{HH} = 8.0 Hz, 1 H, Ar), 8.03 (dd, J_{HH} = 1.7, 8.6 Hz, 1 H, Ar), 8.46 (br s, 1 H, Ar). Benzophenone:[35] ^{1}H NMR ($CDCl_3$) δ 7.46−7.52 (m, 4 H, Ar), 7.57−7.64 (m, 2 H, Ar), 7.78−7.83 (m, 4 H, Ar). 1-Indanone:[37] ^{1}H NMR ($CDCl_3$): δ 2.67−2.72 (m, 2 H, CH_2), 3.12−3.17 (m, 2 H, CH_2), 7.37 (t, J_{HH} = 7.4 Hz, 1 H, Ar), 7.48 (d, J_{HH} = 7.7 Hz, 1 H, Ar), 7.59 (dt, J_{HH} = 1.1, 7.4 Hz, 1 H, Ar), 7.76 (d, J_{HH} = 7.7 Hz, 1H, Ar). 1-Tetralone:[38] ^{1}H NMR ($CDCl_3$) δ 2.10−2.18 (m, 2 H, CH_2), 2.66 (t, J_{HH} = 6.6 Hz, 2 H, CH_2), 2.97 (t, J_{HH} = 6.1 Hz, 2 H, CH_2), 7.25 (d, J_{HH} = 8.2 Hz, 1 H, Ar), 7.31 (t, J_{HH} = 7.5 Hz, 1 H, Ar), 7.47 (dt, J_{HH} = 1.3, 3.7 Hz, 1 H, Ar), 8.04 (dd, J_{HH} = 1.0, 7.8 Hz, 1H, Ar).

■ ASSOCIATED CONTENT

Supporting Information

Text giving alternative syntheses of compounds **7b** and **8b**, tables summarizing complete catalytic results (Tables S1−S3) and relevant crystallographic data (Table S4), and CIF files giving crystal data for **4b**·2CH_3OH and **8b**. This material is available free of charge via the Internet at http://pubs.acs.org.

■ AUTHOR INFORMATION

Corresponding Author

*E-mail: georg.suess-fink@unine.ch (G.S.-F.); stepnic@natur.cuni.cz (P.S.).

Notes

The authors declare no competing financial interest.

■ ACKNOWLEDGMENTS

Results presented in this paper were obtained during cooperation within the framework of the bilateral Swiss-Czech Scientific Exchange Program (Sciex) NMS-CH (Project No. 10.133) and is a part of the long-term research project of the Faculty of Science, Charles University in Prague, supported by the Ministry of Education, Youth and Sports of the Czech Republic (Project No. MSM 0021620857).

■ REFERENCES

(1) Representative examples: (a) Joó, F.; Trócsányi, E. *J. Organomet. Chem.* **1982**, *231*, 63. (b) Breit, B.; Laungani, A. C. *Tetrahedron: Asymmetry* **2003**, *14*, 3823. (c) Hird, A. W.; Hoveyda, A. H. *Angew. Chem., Int. Ed.* **2003**, *42*, 1276. (d) Laungani, A. C.; Breit, B. *Chem. Commun.* **2008**, 844. (e) Laungani, A. C.; Slattery, J. M.; Krossing, I.; Breit, B. *Chem. Eur. J.* **2008**, *14*, 4488. (f) Laungani, A. C.; Keller, M.; Slattery, J. M.; Krossing, I.; Breit, B. *Chem. Eur. J.* **2009**, *15*, 10405. (g) Mino, T.; Kashihara, K.; Yamashita, M. *Tetrahedron: Asymmetry* **2001**, *12*, 287. (h) Marinho, V. R.; Rodrigues, A. I.; Burke, A. J. *Tetrahedron: Asymmetry* **2008**, *19*, 454. (i) Lee, Y.-H.; Kim, Y. K.; Son, J.-H.; Ahn, K. H. *Bull. Korean Chem. Soc.* **2003**, *24*, 225.

(2) Štěpnička, P. *Chem. Soc. Rev.* **2012**, DOI: 10.1039/C2CS00001F.

(3) (a) Štěpnička, P.; Schulz, J.; Císařová, I.; Fejfarová, K. *Collect. Czech. Chem. Commun.* **2007**, *72*, 453. (b) Lamač, M.; Císařová, I.; Štěpnička, P. *Eur. J. Inorg. Chem.* **2007**, 2274. (c) Lamač, M.; Tauchman, J.; Císařová, I.; Štěpnička, P. *Organometallics* **2007**, *26*, 5042. (d) Kühnert, J.; Lamač, M.; Demel, J.; Nicolai, A.; Lang, H.; Štěpnička, P. *J. Mol. Catal. A: Chem.* **2008**, *285*, 41. (e) Lamač, M.; Císařová, I.; Štěpnička, P. *New J. Chem.* **2009**, *33*, 1549. (f) Štěpnička, P.; Krupa, M.; Lamač, M.; Císařová, I. *J. Organomet. Chem.* **2009**, *694*, 2987. (g) Štěpnička, P.; Solařová, H.; Lamač, M.; Císařová, I. *J. Organomet. Chem.* **2010**, *695*, 2423. (h) Štěpnička, P.; Solařová, H.; Císařová, I. *J. Organomet. Chem.* **2011**, *696*, 3727.

(4) (a) Kühnert, J.; Dušek, M.; Demel, J.; Lang, H.; Štěpnička, P. *Dalton Trans.* **2007**, 2802. (b) Kühnert, J.; Císařová, I.; Lamač, M.; Štěpnička, P. *Dalton Trans.* **2008**, 2454.

(5) (a) Schulz, J.; Císařová, I.; Štěpnička, P. *J. Organomet. Chem.* **2009**, *694*, 2519. (b) Schulz, J.; Renfrew, A. K.; Císařová, I.; Dyson, P. J.; Štěpnička, P. *Appl. Organomet. Chem.* **2010**, *24*, 392. For an example from another laboratory, see: Zhang, W.; Shimanuki, T.; Kida, T.; Nakatsuji, Y.; Ikeda, I. *J. Org. Chem.* **1999**, *64*, 6247.

(6) Schulz, J.; Císařová, I.; Štěpnička, P. *Organometallics* **2012**, *31*, 729.

(7) Tauchman, J.; Císařová, I.; Štěpnička, P. *Organometallics* **2009**, *28*, 3288.

(8) (a) Tauchman, J.; Císařová, I.; Štěpnička, P. *Eur. J. Org. Chem.* **2010**, 4276. (b) Tauchman, J.; Císařová, I.; Štěpnička, P. *Dalton Trans.* **2011**, *40*, 11748.

(9) (a) Baratta, W.; Bossi, G.; Putignano, E.; Rigo, P. *Chem. Eur. J.* **2011**, *17*, 3474. (b) Schley, N. D.; Dobereiner, G. E.; Crabtree, R. H. *Organometallics* **2011**, *30*, 4174. (c) For a related article, see: Torres, J.; Sepúlveda, F.; Carrión, M. C.; Jalón, F. A.; Manzano, B. R.; Rodriguez, A. M.; Zirakzadeh, A.; Weissensteiner, W.; Mucientes, A. E.; de la Peña, M. A. *Organometallics* **2011**, *30*, 3490.

(10) NMR spectra recorded shortly after mixing [(η^6-*p*-cymene)$RuCl_2$]$_2$ with **2** in $CDCl_3$ revealed dominant signals due to complex **5b** as the expected bridge-cleavage product and several additional resonances due to unidentified side products (e.g., a P,O chelate or P,O-bridged multinuclear complex). Upon prolonged standing in solution, the amount of the side products increased. Attempts to purify the crude reaction mixture failed.

(11) In the case of **4b**·2CH_3OH, the dihedral angle of planes C(27−32) and [Cl1, Cl2, P1] is 2.0(2)°. The dihedral angle subtended by the C(31−36) and [N2, N3, P1] planes in **8b** is 4.1(3)°.

(12) Štěpnička, P.; Demel, J.; Čejka, J. *J. Mol. Catal. A: Chem.* **2004**, *224*, 161.

(13) Lackner, W.; Standfest-Hauser, C. M.; Mereiter, K.; Schmid, R.; Kirchner, K. *Inorg. Chim. Acta* **2004**, *357*, 2721.

(14) (a) Štěpnička, P.; Gyepes, R.; Lavastre, O.; Dixneuf, P. H. *Organometallics* **1997**, *16*, 5089. (b) Therrien, B.; Vieille-Petit, L.; Jeanneret-Gris, J.; Štěpnička, P.; Süss-Fink, G. *J. Organomet. Chem.* **2004**, *689*, 2456. (c) Sixt, T.; Sieger, M.; Krafft, M. J.; Bubrin, D.; Fiedler, J.; Kaim, W. *Organometallics* **2010**, *29*, 5511.

(15) Larock, R. C. In *Comprehensive Organic Transformations*; VCH: New York, 1999.

(16) (a) Wang, G.-Z.; Andreasson, U.; Bäckvall, J.-E. *J. Chem. Soc., Chem. Commun.* **1994**, 1037. (b) Bäckvall, J.-E.; Chowdhury, R. L.; Karlsson, U. *J. Chem. Soc., Chem. Commun.* **1991**, 473. (c) Buffin, B. P.; Clarkson, J. P.; Belitz, N. L.; Kundu, A. *J. Mol. Catal. A: Chem.* **2005**, *225*, 111. (d) Liu, L.; Yu, M.; Wayland, B. B.; Fu, X. *Chem. Commun.* **2010**, *46*, 6353. (e) ten Brink, G.-J.; Arends, I. W. C. E.; Sheldon, R. A. *Science* **2000**, *287*, 1636.

(17) (a) Jacobson, S. E.; Muccigrosso, D. A.; Mares, F. *J. Org. Chem.* **1979**, *44*, 921. (b) Trost, B. M.; Masuyama, Y. *Tetrahedron Lett.* **1984**, *25*, 173. (c) Venturello, C.; Ricci, M. *J. Org. Chem.* **1986**, *51*, 1599. (d) Bortolini, O.; Campestrini, S.; Di Furia, F.; Modena, G. *J. Org. Chem.* **1987**, *52*, 5467. (e) Ishii, Y.; Yamawaki, K.; Yoshida, T.; Ura, T.; Ogawa, M. *J. Org. Chem.* **1987**, *52*, 1868. (f) Campestrini, S.; Carraro, M.; Ciriminna, R.; Pagliaro, M.; Tonellato, U. *Tetrahedron Lett.* **2004**, *45*, 7283. (g) Shul'pina, L. S.; Veghini, D.; Kudinov, A. R.; Shul'pin, G. B. *React. Kinet. Catal. Lett.* **2006**, *88*, 157. (h) Joseph, J. K.; Jain, S. L.; Sain, B. *Eur. J. Org. Chem.* **2006**, 590. (i) Neumann, R.; Gara, M. *J. Am. Chem. Soc.* **1995**, *117*, 5066. (j) Velusamy, S.; Punniyamurthy, T. *Eur. J. Org. Chem.* **2003**, 3913. (k) Sloboda-Rozner, D.; Alsters, P. L.; Neumann, R. *J. Am. Chem. Soc.* **2003**, *125*, 5280. (l) Gharnati, L.; Döring, M.; Arnold, U. *Curr. Org. Synth.* **2009**, *6*, 342.

(18) (a) Bortolini, O.; Conte, V.; Di Furia, F.; Modena, G. *J. Org. Chem.* **1986**, *51*, 2661. (b) Barak, G.; Dakka, J.; Sasson, Y. *J. Org. Chem.* **1988**, *53*, 3553. (c) Ishii, Y.; Yamawaki, K.; Ura, T.; Yamada, H.; Yoshida, T.; Ogawa, M. *J. Org. Chem.* **1988**, *53*, 3587. (d) Venturello, C.; Gambaro, M. *J. Org. Chem.* **1991**, *56*, 5924.

(19) (a) Noyori, R.; Aoki, M.; Sato, K. *Chem. Commun.* **2003**, 1977. (b) Sato, K.; Aoki, M.; Takagi, J.; Noyori, R. *J. Am. Chem. Soc.* **1997**, *119*, 12386. (c) Sato, K.; Takagi, J.; Aoki, M.; Noyori, R. *Tetrahedron Lett.* **1998**, *39*, 7549. (d) Sato, K.; Aoki, M.; Takagi, J.; Zimmermann, K.; Noyori, R. *Bull. Chem. Soc. Jpn.* **1999**, *72*, 2287.
(20) Trakarnpruk, W.; Kanjina, W. *Ind. Eng. Chem. Res.* **2008**, *47*, 964.
(21) Rout, L.; Nath, P.; Punniyamurthy, T. *Adv. Synth. Catal.* **2007**, *349*, 846.
(22) (a) Shimizu, M.; Kuwajima, I. *Tetrahedron Lett.* **1979**, *20*, 2801. (b) Kuwajima, I.; Shimizu, M.; Urabe, H. *J. Org. Chem.* **1982**, *47*, 837. (c) Takai, K.; Oshima, K.; Nozaki, H. *Tetrahedron Lett.* **1980**, *21*, 1657. (d) Kaneda, K.; Kawanishi, Y.; Jitsukawa, K.; Teranishi, S. *Tetrahedron Lett.* **1983**, *24*, 5009. (e) Jitsukawa, K.; Kaneda, K.; Teranishi, S. *J. Org. Chem.* **1984**, *49*, 199. (f) Masuyama, Y.; Takahashi, M.; Kurusu, Y. *Tetrahedron Lett.* **1984**, *25*, 4417. (g) Kaneda, K.; Kawanishi, Y.; Teranishi, S. *Chem. Lett.* **1984**, 1481. (h) Rong, M; Liu, C.; Han, J.; Sheng, W.; Zhang, Y.; Wang, H. *Catal. Lett.* **2008**, *125*, 52. (i) Sarmah, P.; Barman, R. K.; Purkayashta, P.; Bora, S. J.; Phukan, P.; Das, B. K. *Indian J. Chem.* **2009**, *48A*, 637. (j) Kurusu, Y. *J. Inorg. Org. Polym.* **2000**, *10*, 127. (k) Choudhary, V. R.; Dumbre, D. K.; Narkhede, V. S.; Jana, S. K. *Catal. Lett.* **2003**, *86*, 229. (l) Muzart, J. *Chem. Rev.* **1992**, *92*, 113. (m) Muzart, J.; Ajjou, A. N'A. *Synthesis* **1993**, 785.
(23) Tsuji, Y.; Ohta, T.; Ido, T.; Minbu, H.; Watanabe, Y. *J. Organomet. Chem.* **1984**, *270*, 333.
(24) Murahashi, S.-I.; Naota, T. *Synthesis* **1993**, 433.
(25) (a) Singh, P.; Singh, A. K. *Eur. J. Inorg. Chem.* **2010**, 4187. (b) Singh, P.; Singh, A. K. *Organometallics* **2010**, *29*, 6433.
(26) Thai, T.-T.; Therrien, B.; Süss-Fink, G. *J. Organomet. Chem.* **2011**, *696*, 3285.
(27) Dougan, S. J.; Sadler, P. J. *Chimia* **2007**, *61*, 704.
(28) See, for instance: Fung, W.-H.; Yu, W.-Y.; Che, C.-M. *J. Org. Chem.* **1998**, *63*, 2873.
(29) Zelonka, R. A.; Baird, M. C. *Can. J. Chem.* **1972**, *50*, 3063.
(30) Bennett, M. A.; Huang, T.-N.; Matheson, T. W.; Smith, A. K. *Inorg. Synth.* **1982**, *21*, 74.
(31) Jensen, S. B.; Rodger, S. J.; Spicer, M. D. *J. Organomet. Chem.* **1998**, *556*, 151.
(32) Sheldrick, G. M. *Acta Crystallogr.* **2008**, *A64*, 112.
(33) Spek, A. L. *J. Appl. Crystallogr.* **2003**, *36*, 7.
(34) van der Sluis, P.; Spek, A. L. *Acta Crystallogr.* **1990**, *A46*, 194.
(35) Ruan, J.; Li, X.; Saidi, O.; Xiao, J. *J. Am. Chem. Soc.* **2008**, *130*, 2424.
(36) Levy, R.; Azerraf, C.; Gelman, D.; Rueck-Braun, K.; Kapoor, P. N. *Catal. Commun.* **2009**, *11*, 298.
(37) Kumar, K. A.; Maheswari, C. U.; Ghantasala, S.; Jyothi, C.; Reddy, K. R. *Adv. Synth. Catal.* **2011**, *353*, 401.
(38) Zhang, G.; Wen, X.; Wang, Y.; Mo, W.; Ding, C. *J. Org. Chem.* **2011**, *76*, 4665.

■ NOTE ADDED AFTER ASAP PUBLICATION

This paper was published ASAP on April 30, 2012. A correction has been made in the fourth paragraph in the Catalytic Reactions section of the Results and Discussion. The revised version was posted on May 7, 2012.

10.4 Appendix 4

J. Tauchman, P. Štěpnička: "Preparation and structural characterisation of a novel ferrocene–amino acid conjugate." *Inorg. Chem. Commun.* **2010**, *13*, 14.

Inorganic Chemistry Communications 13 (2010) 149–152

Contents lists available at ScienceDirect

Inorganic Chemistry Communications

journal homepage: www.elsevier.com/locate/inoche

Preparation and structural characterisation of a novel ferrocene–amino acid conjugate

Jiří Tauchman, Petr Štěpnička *

Department of Inorganic Chemistry, Faculty of Science, Charles University in Prague, Hlavova 2030, 12840 Prague, Czech Republic

ARTICLE INFO

Article history:
Received 8 September 2009
Accepted 27 October 2009
Available online 30 October 2009

Keywords:
Ferrocene
Glycine
Ferrocenophane
Structure elucidation
Cyclic voltammetry

ABSTRACT

A new type of ferrocene–amino acid conjugate, 2-[(methoxycarbonyl)methyl]-2-aza[3]ferrocenophane (**1**), was obtained in a rather low yield via condensation reaction of 1,1′-bis(hydroxymethyl)ferrocene and glycine methyl ester in the presence of $[RuCl_2(PPh_3)_3]$ as a catalyst. The compound was characterised by combustion analysis and by spectroscopic method, and its solid-state structure was established by single-crystal X-ray diffraction analysis. Compound **1** is reluctant towards alkylation with MeI but readily forms a stable picrate salt. Cyclic voltammetry experiments on **1** (in CH_3CN at Pt electrode) revealed the compound to undergo a one-electron reversible oxidation attributable to ferrocene/ferrocenium couple ($E^{o\prime}$ = −5 mV vs. ferrocene itself), which shifts towards more positive potentials upon protonation with HCl.

Ferrocenylated amino acids and peptides have been intensely studied in the recent past mainly due to their attractiveness as redox-active biomolecular probes and structural models for peptides [1]. Most typically such compounds have been obtained by condensation between an appropriate organometallic reagent (usually ferrocenecarboxylic acid or its derivative) and free (terminal) amino group of an amino acid or a peptide chain to give the respective *N*-ferrocenecarbonyl derivative (type **I** in Scheme 1). By contrast, other methods including ferrocenylmethylation at the N-terminus or preparation of amino acids bearing the ferrocenyl moiety in the side chain (structures **II** and **III** in Scheme 1, respectively) remain considerably less explored [1].

While seeking for an alternative "ferrocenylation" method applicable to amino acids, we became inspired with ferrocenophane amines of the type **IV** (Scheme 2). Such compounds have been originally synthesised by condensation of 1,1′-bis(hydroxymethyl)ferrocene with isocyantes (**IV**: R = C_6H_4X-4, where X = H, OMe, NO_2 [2]), by twofold alkylation of an amine (RNH_2) with 1,1′-bis(bromomethyl)ferrocene (**IV**: R = $C_6H_4NO_2$-4 [3]) or 1,1′-bis(*N*-pyridiummethyl)ferrocene dichloride (**IV**: R = Me [4]) and, finally, by reductive ammination of ferrocene-1,1′-dicarbaldehyde (**IV**: R = ω-[(7-chloro-4-quinolyl)amino]alkyl [5]). More recently, Osakada and co-workers devised a practical synthetic route to ferrocenophanes **IV** based on Ru-catalysed condensation of 1,1′-bis(hydroxymethyl)ferrocene with amines [6]. We decided to make use of this approach in the preparation of a novel ferrocene–glycine conjugate **1** (Scheme 2) [7].

Compound **1** was prepared [8] by following the literature method consisting in thermally induced condensation of 1,1′-bis(hydroxymethyl)ferrocene [10] with glycine methyl ester [11] at 170 °C in the presence of $[RuCl_2(PPh_3)_3]$ (3.5 mol.%) using *N*-methylpyrrolidone as the solvent (Scheme 3). Isolation by column chromatography afforded analytically pure **1** as an air-stable orange crystalline solid in 10% yield. Apart from for **1**, only small amount of 2-oxa[3]ferrocenophane, which is evidently the product of dehydration of the starting diol, was isolated from the crude reaction mixtures. Attempts at improving the yield of **1** failed probably because of competitive decomposition pathways operating under the relatively harsh reaction conditions.

Compound **1** was characterised by the conventional spectroscopic methods and by combustion analysis [12]. In ^{1}H NMR spectra, it showed a pair of apparent triplets due to symmetrically 1,1′-disubstituted ferrocene moiety (i.e., due to two identical AA′BB′ spin systems) and resonances attributable to the modifying substituent, namely a singlet for the equivalent, ferrocene-bound CH_2 groups (δ_H 3.10) and two additional singlets for the glycine residue (δ_H 3.66 and 3.75 for CH_2 and CH_3 group, respectively). ^{13}C NMR spectra were also in accordance with the formulation, displaying two ferrocene CH resonances and one down-field shifted C_{ipso} signal (δ_C 83.15) as it is typical for alkyl-substituted ferrocenes. Signals of the amino acid moiety were observed in the expected region (δ_C 58.77 and 51.42 for CH_2 and CH_3 groups, respectively); the glycine C=O was found at δ_C 171.65. Finally, IR spectra of **1** confirmed the presence of the terminal ester group, showing a strong $\nu_{C=O}$ band at 1739 cm^{-1}.

Solid-state structure of **1** was determined by single-crystal X-ray diffraction [13]. A view of the molecular structure is presented

* Corresponding author. Fax: +420 221 951 253.
E-mail address: stepnic@natur.cuni.cz (P. Štěpnička).

1387-7003/$ - see front matter © 2009 Elsevier B.V. All rights reserved.
doi:10.1016/j.inoche.2009.10.038

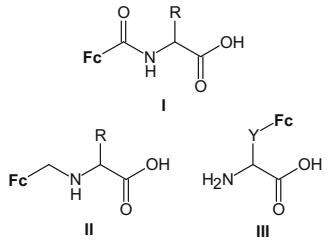

Scheme 1. Selected examples of ferrocenylated amino acids (Fc = ferrocenyl, Y = an organic spacer).

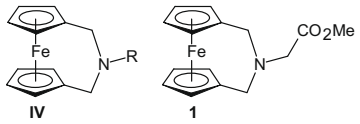

Scheme 2. [3]Ferrocenophane amines (**IV**) and the amino acid derivative under study (**1**).

in Fig. 1 together with selected distances and angles. The bridged cyclopentadienyl rings in the molecule of **1** are mutually eclipsed and symmetrically tilted by ca. 12° (the variation in the Fe-ring centroid distances being statistically insignificant), and the geometry of the ferrocenophane part does not differ much from the structural data reported for the N-methyl analogue (**IV**, R = Me [4]). The CNC bridge in **1** is bent at the nitrogen atom with the C11–N–C12 angle being 113.8(1)°, and symmetrically incorporates the glycine unit (the C11/C12–N–C13 angles differ by only 1°). However, the pendant moiety it is slightly twisted at the C13–C14 bond (N–C13–C14–O1 = 9.1(3)°), which lowers the overall molecular symmetry. As a consequence, the {C13, C14, O1, O2, C15} plane [16] is practically perpendicular to the {C11, N, C12} plane (dihedral angle = 83.6(2)°) but, simultaneously, inclined towards the Cp2 ring as evidenced by the dihedral angles of the {C13, C14, O1, O2, C15} plane and the Cp1/Cp2 rings being 4.5(1)/15.8(1)° (Fig. 2).

Alkylation of **1** with an excess of methyl iodide [17] met with no success, leading only to a complete recovery of unchanged **1**. On the other hand, treatment of **1** with 2,4,6-trinitrophenol in ethyl acetate and subsequent crystallisation [18] yielded picrate **2** as a red crystalline solid (Scheme 3), which was characterised by melting point and by spectroscopic methods [19]. Ions constituting salt **2** were clearly seen in electrospray mass spectra. Likewise, the ^{1}H NMR spectrum of **2** showed signals attributable to cation [**1**H]$^+$ and characteristic resonance due to the picrate protons at δ_H 8.94. The presence of the picrate anion was further manifested in IR spectra via the diagnostic bands at 1556/1567 ($\nu_{as}NO_2$), 1321/1364 (ν_sNO_2), 1615/1629 (ν_{C-C}), and at 1270 cm^{-1} (phenoxide ν_{C-O}) [20]. A band due to glycine C=O group ($\nu_{C=O}$) was observed at 1751 cm^{-1}, shifted by 12 cm^{-1} to higher energies compared to **1**.

Cyclic voltammogram of compound **1** recorded in acetonitrile at a platinum electrode [21] displayed a diffusion-controlled, one-electron reversible oxidation [22] at $E^{o\prime}$ = –0.005 V vs. ferrocene/ferrocenium reference (Fig. 3). Addition of MeI (10 equiv., 30 min) to the analysed solution left the redox response unchanged which is, indeed, in line with the observed reluctance of **1** towards alkylation. On the other hand, addition of HCl (as a methanol solution) led to immediate protonation at the nitrogen atom, which in turn resulted in a pronounced shift of the ferrocene/ferrocenium wave towards more positive potentials (ca. 275 mV with 5 equiv., and ca. 300 mV with 10 equiv. of added HCl), while not affecting its overall reversibility (Fig. 3) [23].

In summary, we have succeeded in preparing of a new type of ferrocene–amino acid conjugate starting from simple precursors

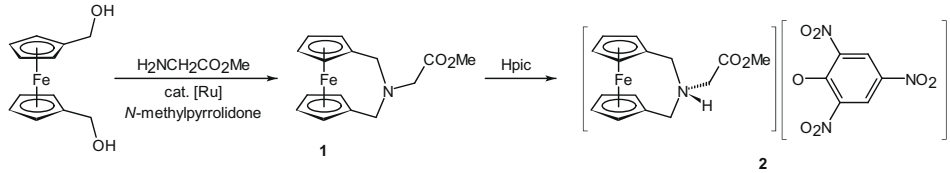

Scheme 3. Preparation of ferrocenophane **1** and its picrate salt **2** (Hpic = 2,4,6-trinitrophenol).

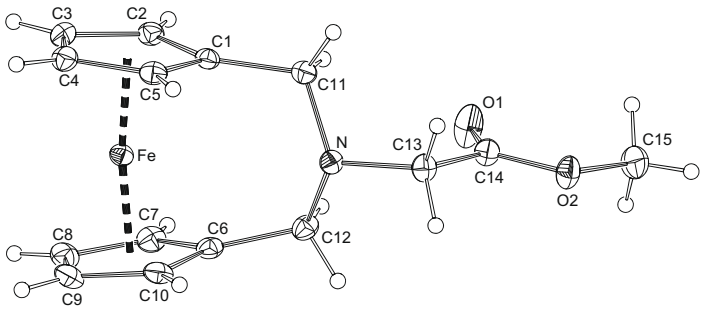

Fig. 1. View of the molecule of **1** showing displacement ellipsoids at the 30% probability level. Selected distances and angles: Fe–Cg1 1.6370(7), Fe–Cg2 1.6353(8), C1–C11 1.499(2), C6–C12 1.496(2), N–C11 1.471(2), N–C12 1.475(2), N–C13 1.454(2), C13–C14 1.518(2), C14–O1 1.201(2), C14–O2 1.332(2), O2–C15 1.445(2); ∠Cp1, Cp2 11.9(1), C11–N–C12 113.8(1), N–C13–C14 116.7(1), O1–C14–O2 123.5(2), C14–O2–C15 116.0(1). Definition of ring planes: Cp1 = C(1–5), Cp2 = C(6–10); Cg1 and Cg2 are the respective centroids.

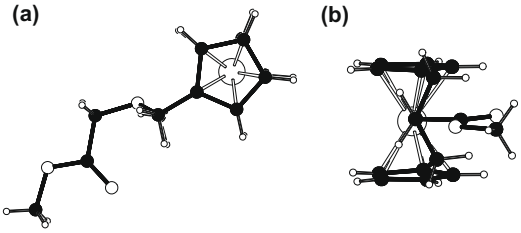

Fig. 2. Projections of the molecule of **1** along (a) the C1–C6 vector, and (b) the C13–N bond (for atom labelling, see Fig. 1).

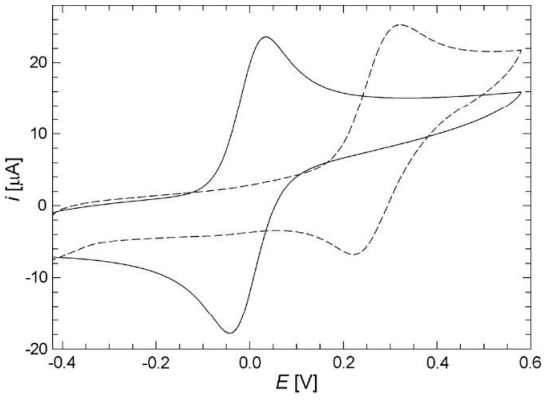

Fig. 3. Cyclic voltammograms of **1** before (solid line) and after (dashed line) addition of 5 equiv. of HCl (recorded in acetonitrile on Pt electrode, 100 mV s^{-1} scan rate).

and using the known synthetic protocol. Although validated only for glycine, this method most likely represents a general approach to structurally unique amino acid derivatives that contain the redox-active ferrocene moiety.

Ferrocenophane **1**, was characterised by a combination of combustion analysis and common spectroscopic methods, and its formulation was corroborated by X-ray crystallography. Cyclic voltammetry measurements have shown the compound to undergo one-electron reversible electron oxidation, presumably at the ferrocene moiety. Upon protonation, this oxidation expectedly becomes more difficult, which is reflected by a shift of the associated redox wave towards more positive potentials. In the case of the related N-methyl derivative (**IV**, R = Me), a shift +380 mV was noted for the ferrocene/ferrocenium wave upon protonation with $H[BF_4]$ in the same solvent [4].

Supplementary material

CCDC 746701 contains the supplementary crystallographic data for this paper. These data can be obtained free of charge from The Cambridge Crystallographic Data Centre via www.ccdc.cam.ac.uk/data_request/cif.

Acknowledgements

The authors are grateful to Dr. I. Císařová for recording the X-ray diffraction data. This work was financially supported by the Grant Agency of Charles University in Prague (Project No. 58009) and is a part of long-term research projects supported by the Ministry of Education, Youth and Sports of the Czech Republic (Project Nos. MSM 0021620857 and LC 06070).

References

[1] (a) N. Metzler-Nolte, M. Salmain, The bioorganometallic chemistry of ferrocene, in: P. Štěpnička (Ed.), Ferrocenes: Ligands, Materials and Biomolecules, Wiley, Chichester, 2008, pp. 499–639 (Chapter 13);
(b) T. Moriuchi, T. Hirao, Top. Organomet. Chem. 17 (2006) 143;
(c) H.-B. Kraatz, J. Inorg. Organomet. Polym. Mater. 15 (2005) 83;
(d) D.R. van Staveren, N. Metzler-Nolte, Chem. Rev. 104 (2004) 5931;
(e) T. Moriuchi, T. Hirao, Chem. Soc. Rev. 33 (2004) 294.
[2] H.-J. Lorkowski, P. Kieselack, Chem. Ber. 99 (1966) 3619.
[3] A.S. Georgopoulou, D.M.P. Mingos, A.J.P. White, D.J. Williams, B.R. Horrocks, A. Houlton, J. Chem. Soc., Dalton Trans. (2000) 2969.
[4] H. Plenio, J. Yang, R. Diodone, J. Heinze, Inorg. Chem. 33 (1994) 4098.
[5] C.M. N'Diaye, L.A. Maciejewski, J.S. Brocard, C. Biot, Tetrahedron Lett. 42 (2001) 7221.
[6] K. Osakada, T. Sakano, M. Horie, Y. Suzaki, Coord. Chem. Rev. 250 (2006) 1012. and references cited therein.
[7] Synthesis of a ferrocenophane-based γ-amino acid has been recently communicated by Erker and coworkers: L. Tebben, K. Bussmann, M. Hegemann, G. Kehr, R. Fröhlich, G. Erker, Organometallics 27 (2008) 4269.
[8] A solution of $[RuCl_2(PPh_3)_3]$ (27 mg, 0.03 mmol, 3.5 mol.%) in dry 1-methyl-2-pyrrolidone (1.5 mL) was added to solid 1,1-bis(hydroxymethyl)ferrocene (200 mg, 0.81 mmol) and $[H_3NCH_2CO_2Me]Cl$ (110 mg, 0.88 mmol). After stirring at room temperature under Ar atmosphere for 5 min, triethylamine (0.2 mL, 1.76 mmol) was introduced and the mixture was heated at 170 °C in the dark for 24 h. Then, the volatiles were removed under vacuum and the dark residue was extracted with ethyl acetate. Some insoluble by-products were separated by filtration and the extract was purified by column chromatography (silica gel, hexane:ethyl acetate, 5:1 v/v). The second band was collected and evaporated to afford analytically pure **1** as a yellow solid (24 mg, 10%). The first minor band contains mostly 2-oxa[3]ferrocenophane according to NMR spectra [9].
[9] M.A. Carroll, A.J.P. White, D.A. Widdowson, D.J. Williams, J. Chem. Soc., Perkin Trans. 1 (2000) 1551.
[10] V.K. Aggarwal, D. Jones, M.L. Turner, H. Adams, J. Organomet. Chem. 524 (1996) 263.
[11] Glycine methyl ester is formed *in situ* from glycine methyl ester hydrochloride and triethylamine.
[12] *Analytical data for* **1**: ^{1}H NMR ($CDCl_3$, 400 MHz, $SiMe_4$): δ 3.10 (s, 4H, $C_5H_4CH_2$), 3.66 (s, 2H, CH_2CO_2Me), 3.75 (s, 3H, OMe), 4.09 and 4.12 (2 × apparent t, $J' \approx 1.8$ Hz, 4H, C_5H_4). $^{13}C\{^1H\}$ NMR ($CDCl_3$, 101 MHz, $SiMe_4$): δ 51.20 ($C_5H_4CH_2$), 51.42 (OMe), 58.77 (CH_2CO_2Me), 69.27 and 69.95 (CH of C_5H_4); 83.15 (C_{ipso} of C_5H_4), 171.65 (CO_2Me). IR (Nujol): ν_{CH} 3101 w, 3094 w, 3080 m; $\nu_{C=O}$ 1739 vs; 1299 m, 1287 w, 1229 w, 1197 vs, 1174 vs, 1144 vs, 1113 m, 1039 s, 1026 s, 996 s, 931 m, 854 s, 849 s, 819 w, 812 w, 801 s, 773 s, 688 m, 569 m, 540 m, 510 vs cm^{-1}. ESI + MS: *m*/*z* 300 ($[M + H]^+$), 322 ($[M + Na]^+$). Anal. Calc. for $C_{15}H_{17}FeNO_2$: C, 60.22; H, 5.73; N, 4.68%. Found: C, 60.00; H, 5.61; N, 4.57%.
[13] Orange prism from hot heptane (0.05 × 0.25 × 0.25 mm^3). The diffraction data were collected with a Nonius KappaCCD diffractometer (Mo Kα radiation, $\lambda = 0.71073$ Å; $\theta_{max} = 27.5°$) at 150(2) K. Crystallographic data: $C_{15}H_{17}FeNO_2$, $M = 299.15$ g mol^{-1}, orthorhombic, space group *Pccn* (no. 56), $a = 12.1391(2)$ Å, $b = 20.8244(3)$ Å, $c = 10.4905(3)$ Å; $V = 2651.9(1)$ $Å^3$, $Z = 8$, Total 36709 diffractions of which 3041 were unique ($R_{int} = 4.6\%$) and 2598 observed according to $I_o > 2\sigma(I_o)$ criterion. The structure was solved by direct methods (SIR97 [14]) and refined on F^2 (SHELXL-97 [15]). All non-hydrogen atoms were refined with anisotropic displacement parameters; the hydrogens were included in their calculated positions. Refinement parameters: *R* (observed diffractions) = 2.93%, *R* (all data) = 3.72%, *wR* (all data) = 7.35%, residual electron density: 0.38, −0.37 e $Å^{-3}$.
[14] A. Altomare, M.C. Burla, M. Camalli, G.L. Cascarano, C. Giacovazzo, A. Guagliardi, A.G.G. Moliterni, G. Polidori, R. Spagna, J. Appl. Crystallogr. 32 (1999) 115.
[15] G.M. Sheldrick, SHELXL97, Program for Crystal Structure Refinement from Diffraction Data, University of Göttingen, Germany, 1997.
[16] Atoms defining the {C13, C14, O1, O2, C15} plane are coplanar within 0.01 Å.
[17] Unchanged **1** was recovered after reacting with an excess of MeI in acetonitrile overnight (5 mg (17 μmol) of **1** and 14 mg (0.1 mmol) of MeI in 1 mL of dry solvent).
[18] Compound **1** (5 mg, 17 μmol) and 2,4,6-trinitrophenol (Hpic; 4.5 mg, 20 μmol) were dissolved in ethyl acetate (1 mL). The mixture was layered with hexane (2 mL) and allowed to crystallise at room temperature. The separated deep red crystalline picrate **2** was filtered off, washed with pentane and dried under vacuum. The yield was not determined.
[19] M.p. 170–172 °C (ethyl acetate–hexane). ^{1}H NMR ($CDCl_3$, 400 MHz, $SiMe_4$): δ 3.85 (s, 3H, OMe), 4.01 (br s, 4H, $C_5H_4CH_2$ or C_5H_4), 4.21 (s, 2H, CH_2CO_2Me), 4.28 (br apparent t, $J' \approx 1.8$ Hz, 4H, C_5H_4), 4.45 (br s, 4H, $C_5H_4CH_2$ or C_5H_4), 8.94 (s, 2H, $OC_6H_2(NO_2)_3$). ESI MS (methanol): *m*/*z* 300 ($[\mathbf{1} + H]^+$), 322 ($[\mathbf{1} + Na]^+$); 228 (pic^-), 479 ($[(pic)_2Na]^-$), 730 ($[(pic)_3Na_2]^-$). IR (neat; diffuse reflectance): ν 3115 w, 3096 w, 3085 m, 3078 w, 3007 m, 2995 w, 2970 w, 2947 m, ca.

2850–2599 composite m, 1866 w, 1751 s, 1629 s, 1615 s, 1567 s, 1556 s, 1521 m, 1493 s, 1457 m, 1447 w, 1432 s, 1364 m, 1321 vs, 1270 s, 1242/1235 m, 1212 m, 1161 s, 1075 s, 1044 m, 993 m, 964 m, 940 w, 931 s, 909 m, 865 w, 851 m, 811 m, 790 m, 747 m, 711 s cm^{-1}.

[20] For recent references dealing with IR spectra of amino acid picrates, see: (a) M.B. Mary, V. Sasirekha, V. Ramakrishnan, Spectrochim. Acta Part A 65 (2006) 414;
(b) S. Senthilkumar, M.B. Mary, V. Ramakrishnan, J. Raman Spectrosc. 38 (2007) 288.

[21] Electrochemical measurements were performed with a multipurpose potentiostat μAUTOLAB III (Eco Chemie) at room temperature using a standard three-electrode cell (platinum disc working electrode, platinum sheet auxiliary electrode, and saturated calomel reference electrode) and acetonitrile solutions (Aldrich, absolute) containing 1 mM of the analyte and 0.1 M $Bu_4N[PF_6]$ (Fluka, puriss. for electrochemistry). The solutions were deaerated with argon prior to the measurement and then kept under an argon blanket. The redox potentials are given relative to ferrocene/ferrocenium reference. Reactions with HCl and MeI were performed directly in the cell. The reagents were added to the analysed solution (0.7 M HCl in MeOH, neat MeI) and the mixture was stirred for 5 (HCl) or 30 min (MeI) to ensure complete reaction.

[22] The ratio of the anodic and cathodic peak currents (i_{pa}/i_{pc}) remained close to unity at scan rates (v) in the range 0.05–1 V s^{-1}, and the anodic peak current increased with the square root of the scan rate ($i_{pa} \propto v^{1/2}$). The observed separation of the anodic and cathodic peaks (ΔE_p = 75 mV at 100 mV s^{-1}) was close to that of ferrocene itself under the same conditions (ca. 70 mV).

[23] Some ill-defined peaks were observed in the cathodic region of the voltammogram.